THE WATER ACCEPTANCE OF WRAPPED SUBSURFACE DRAINS

Promotor: dr. ir. W.H. van der Molen
Emeritus-hoogleraar in de Agrohydrologie

L.C.P.M. Stuyt

THE WATER ACCEPTANCE OF WRAPPED SUBSURFACE DRAINS

Proefschrift
ter verkrijging van de graad van doctor
in de landbouw- en milieuwetenschappen
op gezag van de rector magnificus,
dr. H.C. van der Plas,
in het openbaar te verdedigen
op vrijdag 24 januari 1992
des namiddags te vier uur in de Aula
van de Landbouwuniversiteit te Wageningen.

ABSTRACT

Stuyt, L.C.P.M. 1992. The water acceptance of wrapped subsurface drains. Doctoral thesis. Wageningen Agricultural University, Wageningen, The Netherlands, (X) + 314 pp.

The water acceptance of subsurface, agricultural pipe drains is largely determined by the hydraulic conductivity of the surrounding zone. If this zone consists of soil with a poor structural stability, such drains must be wrapped with an envelope to control the rate of pipe sedimentation while safeguarding easy access of water. The studies were made to elicidate the effects of envelope specifications on these requirements.

Envelope response was observed in analogue models, for cohesionless, and weakly cohesive, very fine sandy soils. Cohesionless soils were stabilised best by "thin" envelopes. Water access was easy and was not a factor of importance in design. In weakly-cohesive soils, the capability of envelopes to meet the requirements was quantified using an "Envelope Suitability Index" (ESI). Both soil type and envelope type had a significant effect on ESI. Nevertheless, analogue model tests were of limited value because the findings could not be compared with field observations.

A field survey was made of grade lines of 184 drains and of soil invasion and sedimentation patterns, root penetration and other phenomena in these drains. They were wrapped with various envelope types and installed in weakly-cohesive, very fine sandy soils in three experimental fields in The Netherlands. Over 9600 m of drain length were inspected. The rate of pipe sedimentation differed significantly between the experimental fields. The particle retention capability of envelopes was associated with the effective opening size of their pores, "O_{90}". The mechanisms of soil invasion into drains and the observed sedimentation rates differed from those predicted in analogue models. Generally, envelope specification had no significant effect on drainage resistance; only in cases where drains were also used for subirrigation did "voluminous" envelopes have significantly lower drainage resistances than "thin" ones.

Cores, containing wrapped drain sections with the surrounding soil were sampled at 45 locations. All sections had been functioning in weakly-cohesive, fine-sandy soils for a period of 5 years. The effect of soil and envelope specification on the flow of soil particles near the drains was investigated by microgranulometric analysis. Generally, the finest soil particles were found to be concentrated near the soil/envelope interface. This tendency was largely accounted for by the particle size distribution of the soil. A "natural soil filter" had only developed in a few instances. The envelopes improve stability through supporting the soils rather than through acting as filters. The cores were also examined by x-ray computerised tomography (CT) through 50 adjacent slices. This yielded three dimensional (3D) mappings of the most permeable areas inside the drain envelopes and surrounding soils that convey most of the water to the drains. A finite element model was used to study the effect of radial soil heterogeneity around a subsurface drain on the water table height. Water flow and envelope clogging were found to be quite heterogeneous and were mainly determined by soil structural features. Soil structural stability is therefore the main determinant of the service life of wrapped drains. The physical effect of an envelope on physical soil/envelope interactions is less important than is generally assumed. On the contrary, soil properties are crucial.

Additional index words: agricultural drainage, envelope materials, geotextiles, drain filters, mineral clogging, core sampling, computerised tomography, image processing.

NN08201, 1468

STELLINGEN

I

Terecht stelde de Jager reeds in 1965: "De invloed van de doorlaatfactor van de grond in de onmiddellijke omgeving van een drainbuis is van grotere betekenis voor de toestroming van het water dan de geometrie van perforaties of stootvoegen bij verschillende typen buizen. Dit stelt speciale eisen aan de uitvoering van drainages." In het onderzoek is, en bij het leggen van drainages wordt met deze stelling te weinig rekening gehouden.

(Stelling No. XI, behorend bij het proefschrift van A.W. de Jager, getiteld: "Hoge afvoeren van enige Nederlandse stroomgebieden." Landbouwhogeschool, Wageningen, 1965.)

Dit Proefschrift.

II

De waterstroming in de onmiddellijke omgeving van draineerbuizen die zijn geïnstalleerd in zwak-cohesieve gronden wordt grotendeels bepaald door de structuur van de grond rondom zulke buizen en is heterogeen. Daarom is het "klassieke" concept van de intreeweerstand die het water nabij deze buizen ondervindt in dergelijke gronden niet of slechts gedeeltelijk geldig.

Dit proefschrift.

III

Het functioneren van omhullingsmaterialen in zwak-cohesieve gronden kan niet worden voorspeld door middel van analoge modelproeven in een laboratorium.

Dit proefschrift.

IV

Met betrekking tot het grondkerend vermogen van omhullingsmaterialen voor draineerbuizen is de karakteristieke poriegrootte ("O_{90}") de enige parameter waarvan de significantie is aangetoond.

Dit Proefschrift.

V

De dikte van een omhullingsmateriaal heeft in de praktijk meestal geen effect op de drainageweerstand. Alleen indien sprake is van microbiologische en/of ijzerverstopping verdienen "volumineuze" materialen de voorkeur.

Dit Proefschrift.

VI

Rondom vooromhulde draineerbuizen is slechts bij uitzondering sprake van "natuurlijke filteropbouw" in de omringende, zwak-cohesieve grond. Meestal verstopt deze grond met gesuspendeerd bodemmateriaal. De textuur van de grond speelt hierbij een rol; specificaties van het omhullingsmateriaal niet.

Dit proefschrift.

VII

Het bedrijfsleven levert omhullingsmaterialen voor draineerbuizen. Aannemers bepalen echter de eigenschappen van het belangrijkste filtermateriaal, zijnde de grond in de onmiddellijke omgeving van zulke buizen.

Dit proefschrift.

VIII

Vrijwel alle in de literatuur gerapporteerde proefnemingen zijn gelukt.

IX

Omdat de effecten van het "doorspuiten" van draineerbuizen op de drainageweerstand en de slibhoogte in deze buizen slechts incidenteel en gebrekkig zijn vastgesteld en ondeskundig "doorspuiten" soms nadelige gevolgen heeft voor de werking van drainage is het niet verstandig om zonder meer tot "doorspuiten" over te gaan.

X

De kwaliteit van manuscripten wordt nadelig beïnvloed door het gebruik van tekstverwerkers.

Mendelson, E. 1991. How computers can damage your prose. Times Literary Supplement, 22-2-91.

XI

De macht der feiten is groter dan alle wettelijke theorie, leerde Thorbecke reeds. Dit geldt niet alleen in het staatsbestel maar ook in de hydrologie. Bij theorievorming spelen computers een grote rol; van de feiten stelt men zich op de hoogte door het doen van waarnemingen. Niet aan een computerscherm, maar in het veld. Dit laatste wordt wordt nog wel eens vergeten.

XII

Bij de hydrologische systeemanalyse en de ontwikkeling van modellen ten behoeve van ecohydrologie en regionaal waterbeheer is "3D Computer Vision" een nuttig hulpmiddel om het realiteitsgehalte van modellen te verifiëren.

XIII

De kennis, opgedaan in verdrogende natuurterreinen is niet zonder meer toepasbaar in vernattingsstudies.

Steenvoorden, J.H.A.M. et al. 1991. Van verdrogen naar vernatten. Verkennende studie naar huidige kennis en wenselijk onderzoek, uitgevoerd door het Staring Centrum. NRLO Rapport No. 91/10.

XIV

Het is onjuist dat zwangerschapsverlof wordt geregistreerd als ziekteverlof.

XV

Elke braio is een aio maar niet elke braio is een braio terwijl sommige aio's braio's zijn.

"College wil nieuwe braio-ronde"; Wagenings Universiteitsblad 6(28):9.

Stellingen behorend bij het proefschrift van L.C.P.M. Stuyt:
"The water acceptance of subsurface wrapped drains".
Wageningen, 24 januari 1992

Dedicated to my wonderful wife

To my parents

The studies presented in this thesis were performed at

DLO The Winand Staring Centre for Integrated Land, Soil and Water Research (SC-DLO)

Marijkeweg 11/22
P.O. Box 125, NL-6700 AC Wageningen
The Netherlands

sc-dlo

Parts of these studies were financially supported by the following Companies and Institutions: the Big 'O' filters U.K. Ltd (United Kingdom), Draka Polva (The Netherlands), Du Pont de Nemours International S.A. (Switzerland), ENKA BV (The Netherlands), Geotechnics Holland BV (The Netherlands), Griendtsveen Turfstrooisel Maatschappij BV (The Netherlands), Heidemij Materials (The Netherlands), Horman Drainagefilter BV (The Netherlands), KOMO (The Netherlands), Landinrichtingsdienst (The Netherlands), Oltmanns Ziegel und Kunststoffe GmbH (Germany), BV Polvom (The Netherlands), Rijksdienst voor de IJsselmeerpolders (The Netherlands) and Wavin KLS BV (The Netherlands).

Printed by Krips Repro Meppel, The Netherlands

TEN GELEIDE

Dit proefschrift kon alleen worden voltooid dankzij de steun van de mij dierbaren en de hulp van vele anderen. Als eerste wil ik mijn ouders noemen die mij de kans gaven om te studeren en die mij, soms bezorgd, maar altijd enthousiast, hebben bemoedigd tijdens mijn promotieonderzoek en de voltooiïng van het proefschrift. Vervolgens wil ik mijn promotor, Prof. Dr. W.H. van der Molen noemen. Het was een bijzonder voorrecht om met hem te mogen werken. Ik heb grote bewondering voor zijn eenvoud en scherpzinnigheid, alsook voor zijn vermogen mij in staat te stellen me op mijn eigen wijze te ontplooien, maar mij toch de grondregels voor het doen van onderzoek mee te geven. "Concepts without percepts are empty, percepts without concepts are blind" (Immanuel Kant). Het vak leerde ik van Dr. J. (Jans) Wesseling, die me tijdens mijn afstudeerfase al begeleidde en mij uitnodigde om op het toenmalige Instituut voor Cultuurtechniek en Waterhuishouding (ICW) te komen werken. Ik heb aan Dr. Wesseling, een pionier op het gebied van drainage, veel te danken. Dat geldt ook voor Dr. W. (Willy) Dierickx (Rijksstation voor de Landbouwtechniek, Merelbeke, België), Ir. C.L. (Cor) van Someren (ILRI), Ing. H.J. Meijer (ICW), Ing. W.H. (Wim) Naarding en Ing. T.E.J. (Ton) van Zeijts (beiden Landinrichtingsdienst) die mij vertrouwd maakten met de discrepantie tussen theorie en praktijk.

Het onderzoek is grotendeels verricht binnen de muren van het Staringgebouw te Wageningen. Alle betrokkenen wil ik bedanken voor hun inspanningen. In het bijzonder ben ik H.P. (Hans) Spits erkentelijk voor zijn enthousiasme en de kundigheid waarmee hij steeds weer mijn ideeën vorm gaf en realiseerde. Mevr. G.A. (Atie) Valk, Ing. A.J. (Arie) Oosten en Ing. D.M. (Derk) Bakker voerden vele bewerkelijke laboratoriumproeven uit. Zonder de belangstelling en actieve betrokkenheid van Dr. E.B.A. (Evert) Bisdom en Dr. J.F.Th. (Job) Schoute was de hoeksteen van dit werk niet gerealiseerd. Vele problemen op het gebied van de informatica werden opgelost door Ing. E.C. (Edgar) Vos. Dankzij de expertise van Dr. T. (Thomas) Zissis (University of Thessaloniki), die tijdelijk op het Staring Centrum verbleef, konden de resultaten beter worden onderbouwd. Drs. J.H. (Jan) Oude Voshaar (GLW-DLO) assisteerde bij het statistisch bewerken van gegevens. Het geduld van de directeur van DLO-Staring Centrum, Ir. G.A. Oosterbaan, is lange tijd op de proef gesteld. Ik ben hem erkentelijk voor zijn consideratie.

Sommige, veelal cruciale bijdragen zijn van elders afkomstig. Drs. J.W. (Job) Baretta (NIOZ, Texel) introduceerde de 'Elzone' particle counter. Ir. V. (Victor)

Roos (TFDL) gaf waardevolle adviezen op het terrein van de informatica. Mevr. Drs. J. (Jacqueline) de Lange (TFDL-DLO) ontwikkelde programmatuur. J. (Johannes) van den Ende (BV Drainagebedrijf Scaldis, Borssele) stelde glasvezelkabels ter beschikking. Ir. D. (Douwe) van der Kooy (Horman Drainagefilter BV, 's Gravendeel) assisteerde bij het opsporen van drains. T. (Teunis) Rozenveld (Landinrichtingsdienst Drenthe) was actief betrokken bij de eerste bemonsteringen van drainsecties. Ing. H. Kremer en J.A.J. (Jan) Koenraadt (beiden Landinrichtingsdienst) en de families van Wieringen te Uithuizermeeden, Meyer (Valthermond) en Dane (Willemstad) waren behulpzaam bij zaken betreffende de proefvelden van de Landinrichtingsdienst. Dr. H. (Henk) Venema en Dr. B. (Ben) Verbeeten jr. (beiden Academisch Medisch Centrum, Amsterdam) speelden een beslissende rol bij de introductie en de toepassing van de CT-scanner. Dr. J. Timmer (Philips Medical Systems, Best) verbeterde de CT-beelden. J. (Jan) van Dijk, beroepsfotograaf te 's-Gravenhage, verzorgde de anaglyphen (stereoscopische afbeeldingen). Dr. G. Boom (Rijksuniversiteit Groningen) maakte me vertrouwd met stereoscopische projectietechnieken.

Prof. Dr. G. (Gordon) Spoor (Silsoe College, Silsoe, U.K.) made many amendments to the installments of the manuscript. He also made quite a few useful suggestions. His assistance is highly appreciated.

Ik stel er prijs op ook het werk van de leden van de promotiecommissie te memoreren. Aan hen mijn verontschuldigingen voor het (te) lijvige manuscript, dat voortkwam uit het omvangrijke bestand aan zeer uiteenlopende waarnemingen.

Naast het doen van het wetenschappelijke werk heeft ook het verschijnen van dit geschrift vele voeten in de aarde gehad. Ik wil de hulp en de waardevolle adviezen van met name M.C. (Rien) van Son en P. (Piet) Slootweg (video-ondersteuning en illustraties) en Ir. L.M. (Chiel) Fernig (illustraties) niet onvermeld laten.

Aan alle betrokkenen - hetzij vermeld, hetzij onvermeld - mijn hartelijke dank.

Maurits, jij was nog te klein om te begrijpen waar papa zo lang mee bezig was. Gelukkig is voor jou, Alexander, de periode dat "papa op kantoor woonde", voorgoed voorbij. Gezinsuitbreiding en tijdverslindend promotieonderzoek accorderen slecht. Yolanda zorgde ervoor dat het huishouden niet volledig gesurmenageerd raakte. Mijn dank aan haar betreft echter meer.

CONTENTS

1 INTRODUCTION

1 Introduction

Design of drain filters for soils
of low structural stability

In any subsurface drainage system, all the water discharged must pass through the soil surrounding the drain and in many cases through a filter placed between the soil and the drain pipe. In addition, the major portion of the available hydraulic head will be dissipated near the drain. The zone around a drain pipe therefore needs careful design, particularly if the structural stability of the soil to be drained is poor.

Drainage system design is based on a water flow analysis into drains, which is usually approximated to a case of two-dimensional steady groundwater flow. This problem is solved using the differential equation of Laplace with appropriate boundary conditions, usually in a vertical cross-section through the drains. Simplifying assumptions are made concerning the media involved, i.e. the soil near the drain and the drain filter or envelope, thus presuming idealized flow media. Such idealized flow media are usually considered as isotropic and homogeneous throughout.

Cohesionless and weakly-cohesive soils

With the exception of cohesionless soils and those with well-graded granular filters, natural soils and other drain filters may be very much different to these idealized media. In fact, the heterogeneous composition of both soil and filter may be the principal factor which controls the flow of water to subsurface drains. Any theories which are based on idealized flow conditions cannot resolve the effects on drain functioning of irregularities caused by layered soils, backfill aggregates, macropores, cracks, soil structure deterioration etc.. This is particularly so if the physical dimensions of the heterogeneities are relatively large as compared to the dimensions of the flow area under consideration. Therefore, whereas soil heterogeneity may not be so important to an analysis on a field scale, in the small flow area near drains it is crucial. This fact may impose severe restrictions to efforts to investigate properties of drain filters, notably in weakly-cohesive soils.

Envelope materials as the weak link in drainage engineering

In The Netherlands, about 80% of all laterals are pre-wrapped pipes; a measure of the high percentage of unstable soils. Due to the drag force of the water, soil particles or aggregates may be carried through the wrapping material (often referred to as "envelope" or "drain filter") into the pipe via its perforations. This process can never be prevented completely, but envelopes may substantially slow it down. In doing so, however, the envelope itself (or its transition with the surrounding soil) may become clogged by trapped sediment.

From an engineering standpoint, design and use of traditional filters is not a major problem. Such filters, consisting of gravel, broken shells or loose organic materials like peat litter are quite voluminous and have proved satisfactory under most circumstances. Reliable and unambiguous design criteria for traditional granular drain filters (gravels and very coarse sands) are available and have been applied successfully in practice (Terzaghi, 1961). This category of filters is beyond the scope of this study. Since traditional granular filters were comparatively expensive, the use of cheaper (and often less reliable) alternatives became widespread. These materials were usually composed of organic fibres such as found in crop residues. Peat filters, already mentioned, were applied successfully for many years although problems arose with straw. Straw is prone to microbiological decomposition and may develop impermeable crusts. Reed gave more satisfactory results than chopped flax.

Installing drains by manual labour cannot be done under adverse ("poor") conditions such as shallow groundwater tables or general wetness. This ensured a long service life for the installed systems. Since the introduction of mechanisation however, introduced in 1954, installation speed has risen drastically and control of the quality of the work (e.g. grade line accuracy) has become more difficult, particularly after the introduction of the flexible corrugated pipe. Installation under poor conditions also became possible and proved hard to prevent, due to the high fixed costs of machinery.

In further attempts to bring down the cost of drainage systems and to increase installation capacities, loose organic materials were gradually replaced by cover materials in strip form: a roll of such a strip could be carried on a trencher and rolled out over the pipe as it was being installed. The first materials produced in strip-form were fibrous peat, flax straw and coconut fibres. In the 1960s, strips of glass fibre sheet were also used, being affordable and easy to handle. Meanwhile, high quality peat litter, a traditional filter, became scarce, prompting a search for alternatives.

Soon after the introduction of corrugated pipes in 1962 the use of cover materials in strip-form was abandoned and fibrous envelopes were developed which could be wrapped around corrugated pipes prior to installation. Pipe and filter could now be installed as a composite, wrapped drain, reducing the installation costs by roughly 50%.

Wrapped drains may be installed with chain diggers ("trenchers") as well as with trenchless installation machines. Quality control of drains, installed with the latter type of machine is even more problematic, because it is impossible to monitor the installation process which is hidden to the eye and inaccessible.

Following the introduction of these new types of drain envelopes, hitherto infrequently occurring problems like mineral, chemical and microbiological (iron ochre) clogging of envelopes and pipes have become widespread. In this study, only mineral clogging will be considered.

In contrast to the traditional voluminous filters like gravel, the physical dimensions of new pipe envelopes are now "approaching the limit" in this respect. Pipe envelopes or filters are required to retain an as yet unknown number of soil aggregates, whilst safeguarding proper drainage by not loosing permeability through excessive mineral envelope- and pipe clogging. Particularly in the temperate climatic zones, groundwater drainage has become considerably cheaper over the past decades. Envelope research is therefore prompted by economic as well as technical factors. Notably in arid areas, where drainage systems are mainly installed for salinity control, the need to replace potentially excellent but expensive gravel filters by affordable synthetic alternatives is urgent. Experience, however, proves that it is difficult to develop reliable envelopes for use in weakly-cohesive soils, at marginal cost.

Progress in research

Much has been written about the flow of water through porous media into drains, but these theories cannot provide generally valid recommendations for the design of affordable envelope materials and well-established, universal guidelines for their application. Existing empirical guidelines, though often applied successfully, are only regionally applicable. Mineral clogging near the interface between envelopes and weakly-cohesive soils has always been difficult to analyze theoretically because (a) the complicated nature of this process is underestimated, (b) unambiguous analogue simulation in a laboratory has proved to be very difficult, and (c) the process itself is inaccessible to direct monitoring, either in the field, or in a laboratory, due to fundamental limitations of existing research tools.

In The Netherlands, many field and laboratory tests have been made. Field research is however expensive and time consuming, and the results are non-transferable and often contradictory. On the other hand, attempts to develop a standard laboratory test for envelopes have not been very successful. Research into drain envelopes is therefore restricted to monitoring the response of "promising" materials in terms of their sand-tightness and hydraulic conductivity in laboratory tests, and monitoring the drainage resistance of laterals in experimental fields. As a result, the role of envelopes in the process of mineral clogging is still not well understood, a rational approach to envelope design has not been developed, and the data emerging from experience and tests is difficult to apply in drainage engineering practice.

Two main categories of drain envelope research have been reported: one that seeks to simulate and understand the process of mineral envelope clogging and another dealing with the effect of assumed mineral clogging rates on the hydraulic functioning of a drainage system. In the first category, efforts are made to observe changes in hydraulic and filtering properties of envelopes with time. This is done using analogue laboratory models as well as experimental fields. In the second category, mathematical as well as analogue models are used to simulate discharge through wrapped drains. The practical approach used in both these categories is as follows.

1. Simulation of mineral clogging

1.1 Analogue simulation: soil tank models

The physical process of envelope clogging is simulated in laboratory arrangements like permeameters or soil tank models. A sample of an envelope and a soil are installed in the laboratory test apparatus, saturated with water and subjected to a continuous flow of water for a restricted period of time (Stuyt, 1982). Mineral clogging rates and hydraulic conductivities are recorded. Results have limited, regional applicability and are often ambiguous. The assumption that knowledge of physical properties of envelopes on the one hand and soil texture data on the other will provide conclusive answers concerning applicability of these envelopes in those soils, has proved to be too optimistic.

1.2 Research in experimental fields

Drains, wrapped with several envelope types are installed in the field. Soil texture is determined at several locations. Drain outflow rates and water table elevations are frequently recorded, drainage resistances of laterals are investigated with time and attempts are made to correlate drainage resistances to envelope types. Excavations are made to check drain clogging rates and microbiological decomposition of organic envelopes (Scholten, 1988).

2. Models to simulate discharge

2.1 Mathematical models

Radial flow towards a drain through a soil and an envelope is simulated by solving the Laplace equation. This is done either analytically, through complex transformation of the two-dimensional flow domain (Nieuwenhuis and Wesseling, 1979), or numerically. Discharge rates and hydraulic gradients are computed as related to hydraulic conductivities and geometric boundary conditions.

2.2 Analogue models

The analogy of water flow in porous media and electric current in conductive media is the basis of electric analogue models. A model, representing a wrapped drain, is immersed in electrolytic fluid and acts as an electrode. A copper cylinder wall, placed around the drain electrode forms the outside flow boundary. Electric current flows from the cylinder wall electrode through the envelope and the drain. The three-dimensional voltage distribution in the electrolyte is recorded with a sensing probe. Voltage distributions are analogous to the distribution of hydraulic heads around drains and the effect of assumed hydraulic conductivities, envelope geometries and pipe perforation patterns on the head distribution is investigated (Dierickx, 1980).

3. Other investigations

Several investigations have been made into the heterogeneity in and near drain envelopes. Drain sections have been sampled and preserved in resin after which two-dimensional cross-sections could be examined. Through this procedure, soil density variations, contact erosion patterns and mineral clogging rates can be qualitatively analysed (Gourc, 1982). The highly complex three dimensional structure of these phenomena is however neither visualized nor quantified, yet this structure governs the functioning of drain envelopes in the field.

It is important to realize that the ongoing inability to monitor contact erosion and mineral clogging at soil/envelope interfaces and, as a consequence, recognition and quantification of inherent mechanisms, blocks further progress in improving drain envelope design. More quantative data are urgently needed to advance beyond the current point of stagnation. The ongoing increase in computational power, combined with sophisticated display techniques have recently enabled the application of x-ray computerised tomography or CT, an existing medical diagnostic tool, in soil science (Petrovic et al., 1982). CT allows nondestructive and non-invasive quantitative analysis of geometrically complex soil particle movement patterns and soil structure components, in three-dimensional space. It is used in this study to examine common drain filters and their local soil environment under various conditions, after a service life of at least five years.

Contents of this study

This study provides factual information concerning (a) mineral clogging of pipes and hydraulic conductivities of soil- and envelope samples as investigated in laboratory permeameter flow tests, (b) rates and patterns of sedimentation in drain pipes, related to envelope material and grade line accuracy as recorded in experimental fields, (c) macro-morphological heterogeneities in drain envelopes and in the surrounding soil due to internal erosion and mineral clogging processes around drains, (d) the flow of soil particles and -aggregates in the immediate vicinity of wrapped drains, and (e) an attempt to model water flow into drains using a numerical solution of the Laplace equation. All but the first phenomenon were investigated on lateral drains which had been functioning for at least five years. Research is focused on agricultural drainage systems in the temperate humid climate of The Netherlands.

In *Chapter 2*, laboratory experiments on mineral clogging of drains and envelopes are described. Two tests were made; one with cohesionless soil samples and another with weakly-structured soils. In both tests, two main categories of envelopes were examined: envelopes with a thickness less than 1 mm ("thin" or "sheet" envelopes) and "voluminous" envelopes. The testing procedure proved very sensitive to soil sample configuration or "structure". After briefly discussing the test results and their consequences, subsequent work in three experimental fields is described in the following chapters. In *Chapter 3*, the findings of a field survey into sedimentation patterns and other phenomena in 184 lateral drains are presented. The effects of grade line inaccuracies of these drains, wrapped with various envelope types, are also discussed. The survey was made with a miniature video camera inspection system and special grade line recording equipment. On the basis of the acquired data, 45 locations were selected at which undisturbed drain sections were sampled. Determination of sample dimension and -geometry, sampling criteria and the field sampling procedure are the main topics in *Chapter 4*. The variability of soil texture (=particle size distribution of soils) near drains was measured with a computerised particle size analysis instrument. The result of this analysis is presented in *Chapter 5*. All samples were exposed to a non-disturbing and non-invasive x-ray CT scanning system. The CT data were used for two purposes: (a) to analyze the radial heterogeneity of the soil around drains, and (b) to quantify and visualize three-dimensional features in envelopes and soils. In *Chapter 6*, the effect of radial heterogeneity of the soil on the mid-drain water table elevation was assessed using a two-dimensional numerical ("finite element") simulation model for saturated groundwater flow. The results of the three-dimensional analysis provide hitherto unknown information regarding soil structure, contact erosion and mineral clogging patterns at soil/envelope interfaces and clogging patterns inside envelopes. They are reported and discussed in *Chapter 7*. In the final chapter, results of the various research components are summarized and discussed. The water acceptance of drains as related to soils and envelope -specifications is assessed and conclusions are drawn. *Chapter 8* concludes with recommendations for the selection and installation of envelope materials in agricultural drainage engineering.

□

REFERENCES

Dierickx, W. 1980. Electrolytic analogue study of the effect of openings and surrounds of various permeabilities on the performance of field drainage pipes. Comm. of the Nat. Inst. for Agr. Eng. (Med. Rijksstation voor Landbouwtechniek) 77. Merelbeke (Belgium).

Gourc, J.P. 1982. Quelques aspects du comportement des Geotextiles en Mecanique des sols (Some aspects of the behaviour of geotextiles with respect to soil mechanics). Thèse, Université scientifique et médicale / Institut National Polytechnique, Grenoble, France (in French).

Nieuwenhuis, G.J.A. and J. Wesseling. 1979. Effect of perforation and filter material on entrance resistance and effective diameter of plastic drain pipes. Agric. Water Managem. 2, 1: 1-9.

Petrovic, A.M., J.E. Siebert and P.E. Rieke. 1982. Soil bulk density analysis in three dimensions by computed tomography scanning. Soil Sci. Soc. Amer. Journ. 46(3): 445-450.

Scholten, J. 1988. Vijfentwintig jaar drainagematerialenonderzoek bij de Rijksdienst voor de IJsselmeerpolders (Twenty-five years of drain envelope research by the Dutch Polder Development Authority). Flevobericht nr. 291, Ministerie van verkeer en Waterstaat. ISBN 90 369 1040 4 (in Dutch).

Stuyt, L.C.P.M. 1982. Drainage envelope research in The Netherlands. Proc. 2nd Int. Drain. Workshop, Washington DC. Ed. CPTA, Carmel, Indiana U.S.A.:106-123.

Terzaghi, K. and R.B. Peck. 1961. Die Bodenmechanik in der Baupraxis. (Soil mechanics in building construction). Springer, Berlin, Germany (in German).

2 ANALOGUE SIMULATION OF MINERAL ENVELOPE CLOGGING

2 Analogue simulation of mineral envelope clogging

ABSTRACT

The suitability of envelopes to prevent excessive sedimentation in agricultural drains, yet promoting easy access of water, was examined in two configurations of an analogue laboratory model. The model apparatus consists of an upright plexiglass pipe section in which an envelope sample disc and an abutting soil sample are mechanically supported by a flattened portion of corrugated drain while loaded by weights or a spring. The assembly was exposed to one-dimensional vertical water flow, discharging through the corrugated disc. Tests were made with cohesionless, and with weakly-cohesive, very fine sands. Cohesionless soil samples favour reproducible results but their resemblance to field conditions is poor. The reverse is true when using weakly-cohesive samples. Cohesionless soils stabilized most satisfactorily by thin envelopes. Most entrance resistances were low and were not a factor of importance in design. In weakly-cohesive soils, the suitability of envelopes was assessed from their hydraulic properties and their soil particle retention capabilities, which were integrated in one parameter, the "Envelope Suitability Index" (ESI). Permeameter flow tests are of limited value if results cannot be compared with field observations. The assumption that moisture retention curves of envelopes are identical to pore size distributions is unsound.

1 INTRODUCTION

Although there is an obvious need to define general and valid design specifications for, and application possibilities of moderately priced envelope materials in weakly-cohesive soils, attempts to tackle this problem have never been very successful. The inability is due to superficial knowledge of the flow of water and particles in the immediate vicinity of drain pipes, installed in weakly cohesive soils, and the functioning of envelopes. Many types of analogue models and testing procedures, designed to simulate mineral envelope clogging in laboratories, have been proposed, mainly in Europe and in the USA. Research in the Netherlands is reviewed here.

In the Netherlands, the use of fibrous peat litter as a cover layer for drain tiles was common practice for decades, and lasted until the end of the 1950s. On a much smaller scale, tiles were covered with chopped flax, straw from cereal crops, wood chips, sawdust, heather bushes and shells. These materials were not always available in the required quantities and their handling was often laborious. The use of straw has not been successful because it often decomposed into low-permeable cakes.

Glass fibre sheet, a mineral fibre nonwoven envelope, was introduced in the early 1960s and standards for this material were formulated in 1964. Due to rumours of mineral clogging its use declined soon afterward (Cultuurtechnische Dienst, 1964). In fact, it was the pipe material, not the envelope that caused the problems. The glass fibre sheet was wrapped around (40 mm outside diameter) smooth plastic pipes with sawn slots; corrugated pipes had not been introduced at that time. The area of the membrane, involved in the water flow, coincided with the very limited area of these slots (Fig. 1a). When using this membrane with a corrugated pipe, this area is much larger because of the voids between the envelope and the valleys of the corrugations (Fig. 1b). This greatly facilitates the water acceptance of the drain. Due to this incident, reluctance to apply sheet envelopes persists even today. Other problems arose because drains were installed in unstable soils in areas where drainage experience was limited. In addition, the change to mechanized installation made it possible to install drains in wet soils. Hence, hitherto unknown problems were created like poor functioning of laterals due to soil structure deterioration near drains. These and other incidents have stimulated research into drain envelopes.

Analogue modelling of water flow near subsurface drains was introduced in the Netherlands by Hooghoudt in the 1930s (Meijer, personal communication[1]). He built a concrete tank, 25 m long by 5 m wide to verify his mathematical solutions of flow towards drains. Much smaller analogue models reappeared in the mid 1950s. These models were used to verify solutions for flow in the immediate vicinity of drains, considering radial flow resistance and resistance due to flow which converges towards the perforations ("entrance resistance"). De Jager (1960a, 1960b) used a large sand tank model for making rapid comparisons between various types of plastic strips which were applied when draining soils by plastic lined mole channels and various types of newly introduced plastic pipes (Fig. 2). Radial flow towards drains could not be simulated in this large tank due to its rectangular, interior geometry. A similar model was developed by Wesseling and used by Wesseling and Homma at the Institute for Land and Water Management Research (ICW) in Wageningen. This model was 3 m long, 0.4 m wide and 1.60

[1]Retired from the former Institute for Land and Water Management Research (ICW), Wageningen, The Netherlands.

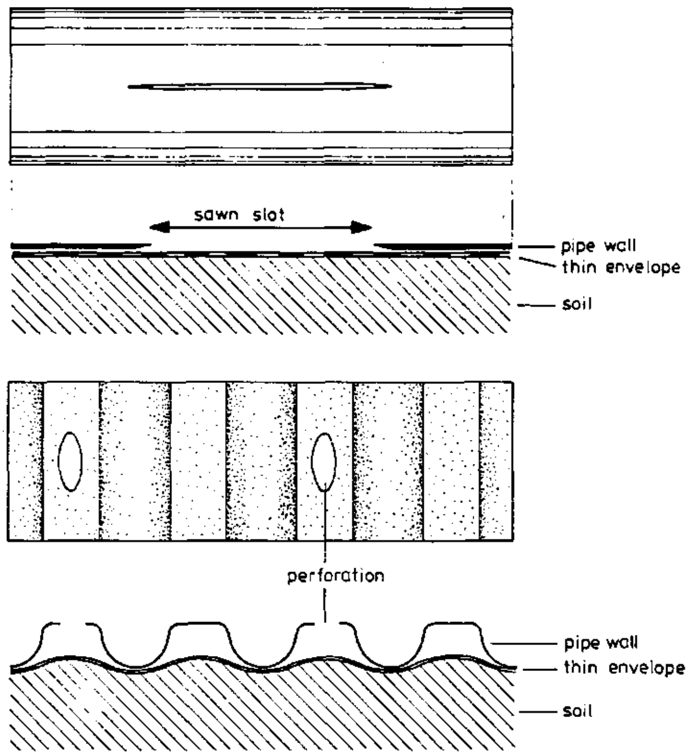

Figure 1. **a. Details of a smooth drain pipe. b. Details of a corrugated drain pipe. Reprinted with permission (Landinrichtingsdienst).**

m high. Its front was partly manufactured from glass, allowing flow lines to be observed by using dye tracers (Homma, personal communication[2]). The experiments with this "Wesseling" model allowed comparisons between newly introduced drain pipes and envelope materials with old established tile drains. The model was filled with "stuifzand", an eolic sand with 80-85% of the particles in the size range 100-300 µm. Water was supplied through a sprinkler system. The experiments compared discharges from pipes at various rates of water supply. The model was originally designed to investigate the effect of various perforation patterns in bare pipes. It was less suitable for routine measurements because

[2]Retired from the Institute for Land and Water Management Research (ICW), Wageningen, The Netherlands

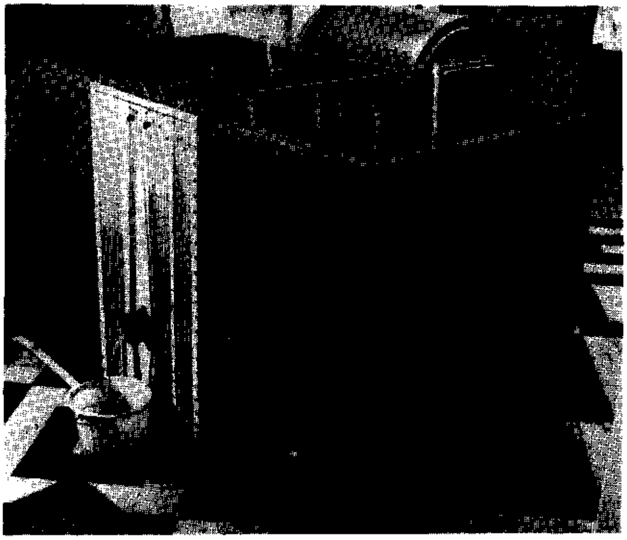

Figure 2. Sand tank as used by de Jager and Cavelaars. Its dimensions are 2 (W) x 1.2 (H) x 1 (D) m. Its central section was filled with soil as "trench backfill". The remainder of the soil in the tank remained in place. From Cavelaars (1965).

(a) model preparation was time and labour consuming, and (b) due to its large capacity the model needed much time to reach equilibrium. The model was therefore replaced by a smaller, cylindrical model.

From 1960 onwards, Cavelaars continued the research of de Jager in the large model tank. An important finding gained with this model was the poor reproducibility of the experiments: the results were highly sensitive to the initial soil moisture content and the manipulation of soil samples. Hence, Cavelaars concluded that installation conditions might be of paramount importance for the service life of drains (Cavelaars, 1965; Willet, 1962). This tank model was abandoned later for two reasons: the laborious testing procedure and the settling of soil underneath the drain, which created cavities and unrealistic flow conditions (Cavelaars, personal communication[3]).

The model was replaced by a new generation of cylindrical models. In these models, a drain section was installed in an upright position in its centre. Simultaneously, models of this type were developed by Cavelaars (1965) (Fig. 3),

[3]Retired from Heidemij, The Netherlands.

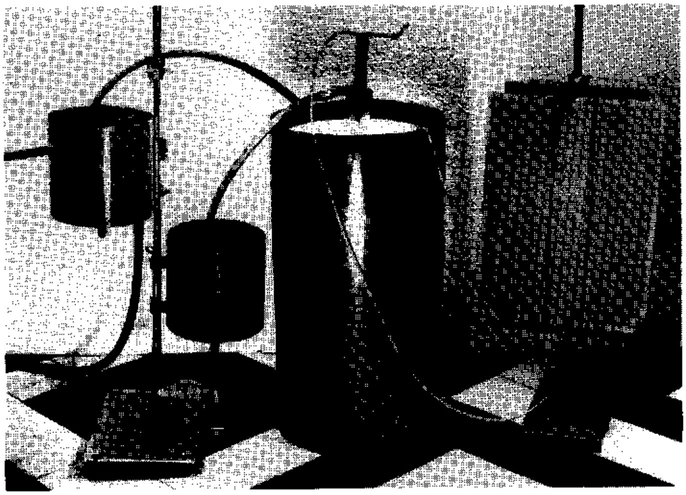

Figure 3. **The cylindrical drain test model, developed by Cavelaars. Reprinted with permission from Cavelaars (1965).**

Boumans (1963) and Wesseling & Homma (1965). The common idea was to observe properties of envelopes only, not to simulate field conditions. Results were to be "translated" to field conditions at a later stage. Boumans used a rubber sealing on top of the sand, creating confined flow with horizontal, radial flow lines, allowing simple formulae to be used to describe the flow conditions. He stressed the importance of model preparation, the modelling results being very dependent on the way the sand tank was filled. Boumans insisted on the use of structureless soil samples to ensure homogeneity and isotropy, resulting in reproducible experiments, yet he regarded the absence of structure in soil samples to be in conflict with field conditions. Entrapped air, too, caused considerable problems because it reduced the effective pore space of the soil. Boumans therefore recommended the model to be filled with sand and water simultaneously but acknowledged that air may also dissolve from the flowing water during a test. Following his observations, Boumans suggested that an envelope may promote the washing out of fine soil particles near the interface between envelope and soil (development of a "natural soil filter"). The model designed by Cavelaars was largely identical; instead of using rubber sealing on top of the soil, he used a plastic sheet which was kept in place by ponded water. Wesseling & Homma (1965) used oil barrels (capacity 30 litres) that were modified to sand tank models

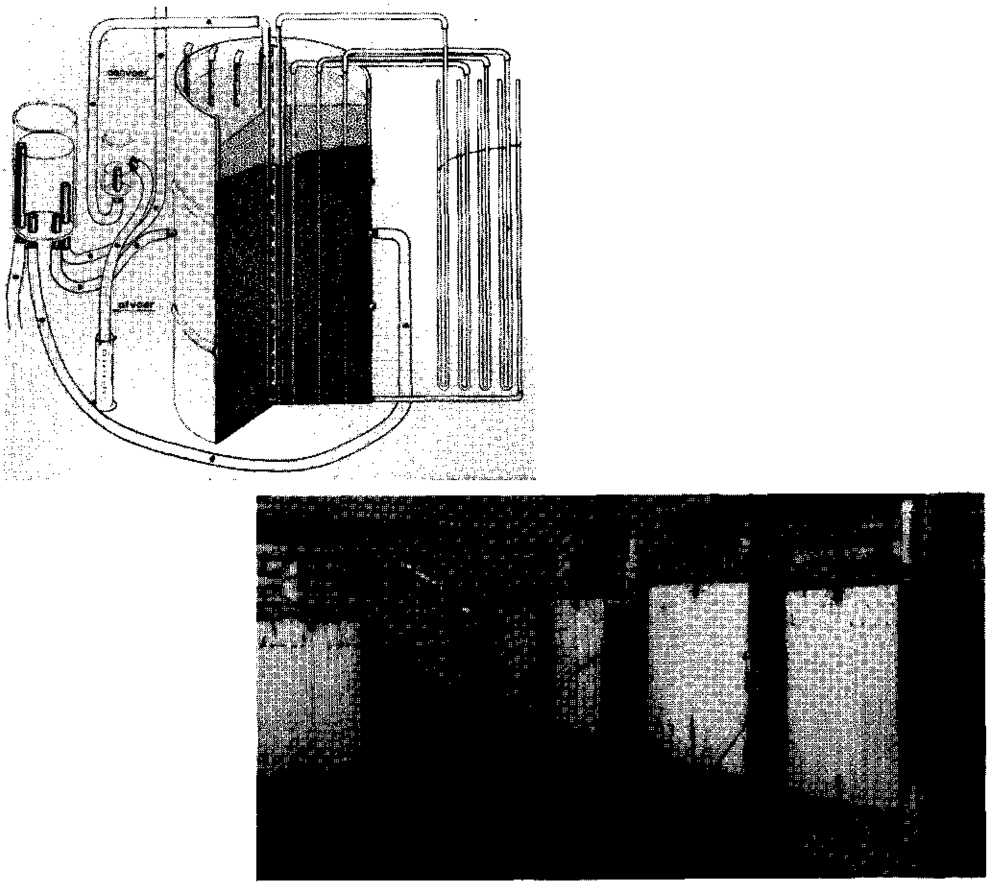

Figure 4. **Barrels, used as sand tank models by Wesseling and Homma: water supply and manometer system (top); laboratory view (bottom).**

(Fig. 4). They measured the effect of various envelopes on the entrance resistance of drains. Contrary to the cylindrical models of Boumans and Cavelaars, the sand on top was not sealed off and flow towards the drain was equivalent to free surface flow from the outer perimeter of the drum to its centre. Entrance resistances of combinations of pipes and envelopes were found by comparing the head losses due to this flow with those found for flow towards a fully permeable well according to Thiem's equation. Homogeneous sand was used to obtain reproducible and consistent results. Entrance resistances were found to be inversely proportional to envelope thickness. It was acknowledged that field results were likely to be less favourable due to clogging by mineral particles and ochre deposition. At a later stage, the barrel was replaced by a plastic container, the

"ICW model" because its small diameter (360 mm) probably caused considerable data spread (Wesseling & Homma, 1967). The "ICW model" had a diameter of 660 mm and contained a 600 mm long drain section. Feddes (1966) tested peat varieties and some synthetic granular waste materials in this model. Wrapped pipes were installed in upright position, (Fig. 5). His results confirmed earlier findings though it was recognized that the soil load, acting on horizontally installed laterals in the field but absent in the laboratory container, might invalidate the results for design purposes. Meijer (1972, 1974) continued testing with this container, using eolic sand, sampled at Kootwijk, The Netherlands. All kinds of envelope materials were examined, including shredded car tyres and coffee grounds. The main conclusion of this work was that envelope pores must not be too small in order to allow a limited number of soil fines to be evacuated into the pipe, promoting enhanced hydraulic conductivities in the soil around drains (i.e. the development of a "natural soil filter") (Meijer & Feddes, 1972). Awareness of the structural stability of a soil as a crucial parameter was awakening but the link with envelope functioning was not yet made. Wesseling & van Someren (1972) reported on the experience gained in the Netherlands at that date.

At the end of the 1960s, coconut fibres were introduced as a material for envelopes. Being comparatively cheap, "cocos" soon dominated the market because high quality peat litter became scarce and expensive (Meijer, 1973). At a later stage it was discovered that coconut fibres were often subject to microbiological decay (Meijer & Knops, 1977, Antheunisse, 1979, 1980, 1981), stimulating the drive to replace organic substances with synthetic alternatives. It was argued that, contrary to "organic" envelopes, "synthetic" ones could be manufactured according to design criteria which could be established in a laboratory test.

At the beginning of the 1970s, a newly installed drainage system at "de Drieban" in the Province of Noord-Holland, largely failed. A minor part was installed in August and functioned satisfactorily. The remainder was installed during the subsequent winter under wet conditions and failed. The area was redrained successfully two years later (van Someren, personal communication[4]). Following this experience, Homma (1973) investigated the influence of installation conditions on drainage efficiency in an analogue laboratory model. He found that drainage under wet conditions may reduce the hydraulic conductivity of the trench backfill by a factor 100.

By 1975, a Dutch working group of agricultural drainage specialists, "Drainage Studie Groep" (DSG) concluded that the results of laboratory tests were

[4]Retired from the International Institute for Land Reclamation and Improvement (ILRI), Wageningen, The Netherlands.

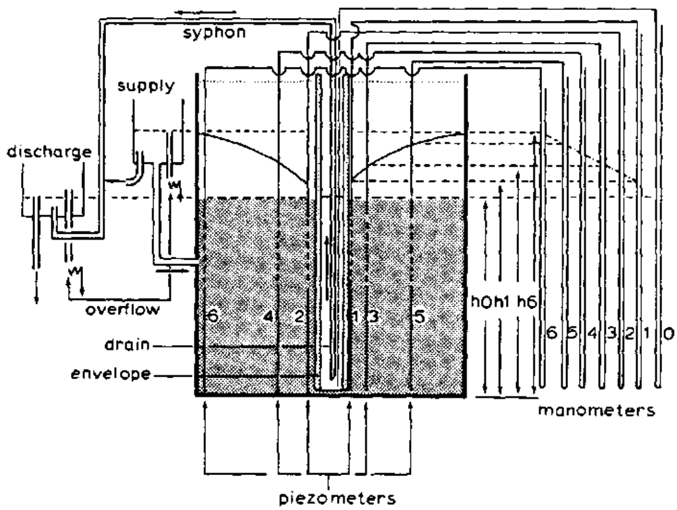

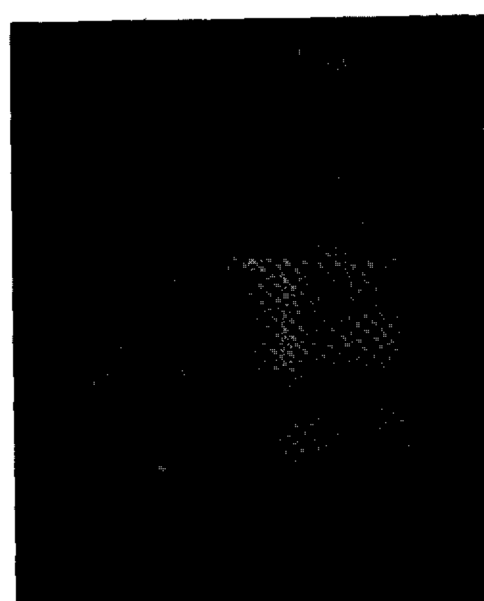

Figure 5. **Vertical cylindrical sand tanks, used by Feddes (1966) and Meijer (1972): water supply and manometer system (top); laboratory view (bottom).**

ambiguous. They could neither provide sound design criteria for the envelopes themselves, nor valid recommendations for their installation in various soil types. Despite these conclusions another laboratory project was initiated because field research was considered too expensive while the results were not convincing either (Jonkers & Miedema, 1975). Boers (1975) reviewed five Dutch analogue models for testing (wrapped) drains with emphasis on the "ICW model". Attention was focussed on the influence of disturbing factors like a seepage surface at the drain wall, the effect of air in soil pores and soil compaction on flow hydraulics. The influence of such factors could be minimized if several rules were strictly obeyed with respect to discharge, test duration, etc.. No attention was devoted however to soil particle movement near the drain.

Emerging from discussions in the DSG, Wesseling (1975) summarized the Dutch experience, gained with laboratory testing so far. A major disadvantage of existing tests was the fact that mineral clogging was inadequately simulated due to the upright position of the drain. Sand tanks with horizontal drains were considered more reliable but too laborious, hence he suggested using a small container with flat envelope sample discs (envelope + pipe material) installed at the bottom. In a new project, a standard applicability test for envelopes was to be developed. This test should (a) be a tool to quantify design parameters for envelopes, (b) be reproducible and (c) include major factors which affect mineral clogging. It was not intended to simulate field conditions, and the results were to be linked to field observations at a later stage.

Knops and Eskes introduced a laboratory testing system consisting of upright cylindrical permeameters as recommended by the DSG (Eskes, 1977). As the reproducibility was considered very important, artificial, cohesionless soil fractions were used instead of natural soils. They developed an apparatus to determine pore size distributions of envelopes by means of a suction method and established relationships between envelope pore sizes and their filtering and hydraulic properties. Although physical properties of envelopes could be determined, the results could not be unequivocally transferred to field conditions because the properties of cohesionless, artificial soil fractions differed from the ill-defined and uncertain behaviour of natural, weakly-cohesive soils. Although the results were not conclusive it was decided to continue this type of test, provided that cooperation could be established with soil scientists.

Concurrently, similar research was carried out elsewhere. Van Someren and Boers (1977) used the sand tank model, developed by Boumans in 1963, to test drain envelopes in Pakistan. A sand tank model study was made in Belgium

(Dierickx, personal communication[5]), followed by field experiments (Dierickx & Leyman, 1978). Zuidema and Scholten (1979) measured entrance resistances of wrapped drains in a large sand tank with a horizontally oriented drain section (Fig. 6). They used cohesionless soil samples from the newly reclaimed Dutch IJssellake polders. No attempts were made to explain the process of mineral clogging of envelopes (Scholten, 1988). Preparation and operation of these tests was time consuming but agreement with results from field experiments was fair.

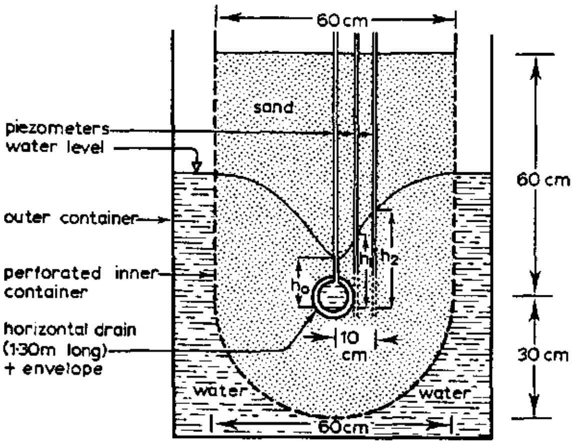

Figure 6. **Cross-section of horizontal sand tank model, used by Zuidema and Scholten (1979).**

Meanwhile, mathematical and analogue models were developed and used to quantify the influence of envelope permeability and -thickness on the entrance resistance of drains. These models assumed that the envelope, the soil and regions of comparatively low hydraulic conductivity (e.g. due to mineral clogging) were homogeneous and isotropic. As such, they were a further development of previous work by Widmoser (1968). Major contributions were made by Nieuwenhuis & Wesseling (1979) who developed a mathematical model, and Dierickx (1980) who used an electrolytic analogue model.

Kumova (1979) used the sand tank models of Wesseling & Homma and Boumans for comparative envelope tests with "Blokzijl" sand and "Almere sand",

[5]Research Officer, Agricultural Research Centre, Research Station for Agricultural Engineering, B-9820 Merelbeke, Belgium.

very fine sandy marine deposits from the IJssellake Polder area in the Netherlands. She concluded that thin envelopes could only be successfully applied in moderate to coarse sandy soils. The influence of unfavourable (wet) installation conditions, discussed by Willet (1962), Cavelaars (1965, 1966, 1967, 1970) and van Someren & Naarding (1965), and not covered by this test, were considered to be a serious challenge to the validity of the results.

Meanwhile, Knops (1979) reviewed the progress in research. He concluded that field experiments were too expensive for the results obtained and suggested emphasis to be placed on laboratory testing once more, testing promising envelope materials further under field conditions. In addition, Knops published guidelines for the selection of appropriate envelopes, in cooperation with other Dutch drainage experts (Knops & Zuidema, 1977; Knops et al., 1979).

The work of Knops and Eskes was continued by Seijger (1978, 1980). He modified the laboratory apparatus and measured the thickness, pore size distribution, hydraulic conductivity and the particle retention capability of various envelopes. The particle retention capability of envelopes was examined with cohesionless soil fractions. The test was therefore a tool to quantify design parameters of envelopes as suggested by Wesseling (1975) but did not simulate mineral clogging under field conditions. The earlier awareness that soil structure was a factor of significance in mineral clogging of envelopes and pipes receded. From Seijger's work, some qualitative conclusions could be drawn. Soil load has a significant influence on the pore size distribution of voluminous envelopes (thickness > 1 mm). Voluminous envelopes have a better particle retention capability than thin ones. The latter have relatively narrow pore size distributions and are prone to mineral clogging. Voluminous ones have wide pore size distributions, larger pores and higher residual hydraulic conductivities. Coconut fibre envelopes were not recommended because of their poor particle retention capability. The number of experiments was insufficient to observe significant trends in hydraulic and filtering properties of envelopes. No effort could be made to link the results to data from field experiments, simply because such data were not available. In Belgium, properties of envelopes were observed in a similar laboratory apparatus, using sieved aggregates to represent weakly-cohesive soils (Dierickx & Yüncüoglu, 1982).

In 1980, the Dutch Foundation KOMO (Quality Declarations Organisation for Building Materials and Components) initiated and sponsored a laboratory research project at ICW[6] in Wageningen, The Netherlands. The research was also sponsored by Dutch Governmental Institutions and Dutch and foreign

[6]The former Institute for Land and Water Management Research.

manufacturers of pipe and envelope materials. Through this initiative, the laboratory work of Seijger could be continued (Stuyt, 1981a, 1981b, 1982b, 1984a, 1985, 1986a; Stuyt & Cestre, 1986). Envelopes were examined in two subsequent projects which are described in this Chapter.

The first project was guided by a working group of drainage specialists. Although former efforts to link results from laboratory tests to field data had failed, the working group again decided to simulate mineral clogging with cohesionless soil samples on the assumption that design and application specifications for envelopes could emerge from laboratory observations only. Results were qualitative but - contrary to general opinion - sheet envelopes performed remarkably well (Stuyt, 1984b; Stuyt & Oosten, 1986). As a result of these observations the "Landinrichtingsdienst" (= Dutch Governmental Service for Land and Water Use) set up three new field trials, designed to compare the hydraulic and filtering properties of sheet envelopes with those of voluminous ones.

In *the second project*, new procedures were followed so that more accurate observations could be made. The major modification was the nature of the soil samples. Instead of structureless materials, weakly-cohesive soil samples were used, having a structural stability similar to those encountered in the field (Stuyt, 1987, 1988a, 1988b, 1988c; Stuyt & Bakker, 1987).

2 THE FIRST PROJECT

2.1 Experimental Procedures

2.1.1 Determination of the pore size distribution of envelope materials

Moisture retention curves of voluminous envelopes were determined and converted into equivalent pore size distributions using the Hagan-Poiseuille equation. Assuming that water in voluminous envelopes is retained by capillary forces and that all pores have cylindrical shapes, water suction h [L] is related to pore radius r [L] as

$$h = (2 \cdot s \cdot \cos \alpha) / (\rho \cdot g \cdot r) \qquad (m) \qquad (1)$$

where	h = water suction	(m)
	s = surface tension of water	($kg.s^{-2}$)
	α = liquid/solid contact angle	(-)
	ρ = density of water	($kg.m^{-3}$)
	g = acceleration of gravity	($m.s^{-2}$)
	r = pore radius	(m)

Usually, envelope fibres are assumed to exhibit a contact angle $\alpha = 0$ although α is known to be different for various materials. Data must therefore be interpreted with caution. Measuring accuracy is estimated to be ±15%, depending on pore size (Eskes, 1977).

Procedure. A 100 mm diameter envelope sample disc was placed on a sintered glass plate with a median pore diameter of 14 µm and covered by a cut portion of corrugated drain, a perforated plexiglass disc and a plexiglass ring (Fig. 7a). While subjecting the sample to a static pressure equivalent to the soil overburden pressure at one metre drain depth, the ring was fixed. Air was removed under vacuum and the saturated sample was installed in the laboratory apparatus (Fig. 7b) whereby the funnel-shaped outlets at the bottoms of the plexiglass rings were connected to burettes through T-joints. At saturation, the level of these T-joints coincided with that of the envelope sample discs. From saturation, the water

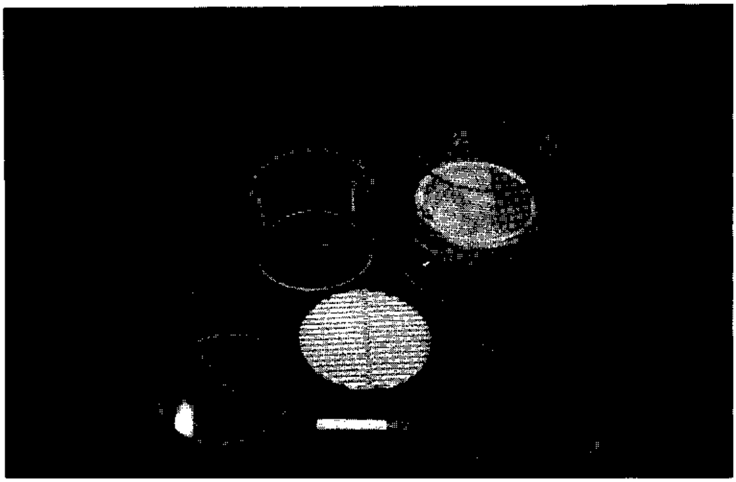

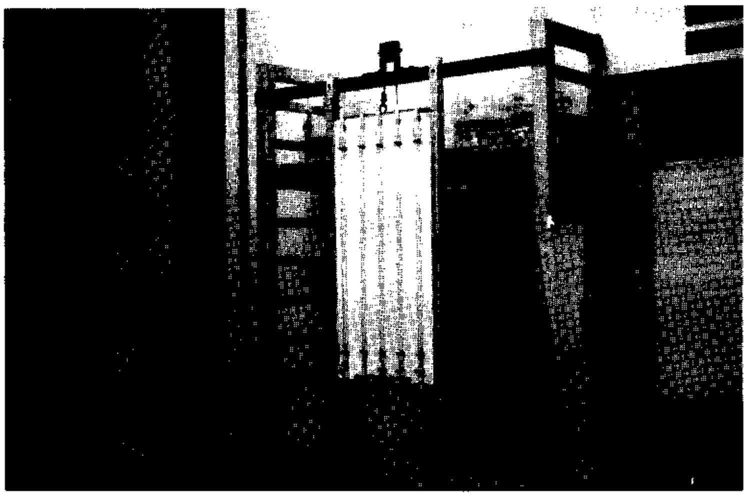

Figure 7. **Apparatus for determination of a moisture retention curve of a voluminous envelope: envelope sample disc and components of sample holder (top) and the laboratory apparatus (four samples installed) (bottom).**

suction was increased in 12 discrete steps by lowering the burettes. The outflowing volumes of water, released after each suction increase were recorded. Downward burette travel distances were 21, 25, 35, 49, 71, 99, 141, 197, 282, 395, 590 and 1000 mm, draining cylindrical pores with diameters up to 1410, 1200, 850, 600, 420, 300, 210, 150, 105, 75, 50 and 30 μm, respectively. The time required to reach equilibrium after each suction increase ranged from 2 hours (1410 μm) to 72 hours (30 μm). All measurements were replicated five times and moisture retention curves were successfully determined of 6 voluminous envelopes.

2.1.2 Determination of hydraulic and filtering properties of envelope materials

Hydraulic and filtering properties of envelopes were observed in an analogue model, designed to simulate mineral clogging.

Procedure. An air-tight model apparatus consisted of eight plexiglass cylinders ("permeameters"), mounted in an upright position, and connected to a closed circuit water supply system which included fastened, air-tight, single level, constant head tanks (Fig. 8, 9). Each permeameter, 150 mm inside diameter by 580 mm high, comprised three distinct sections (Fig. 10). The top section included a water inlet tube and an air release valve. It contained the soil sample, a gravel bed diffuser and a PVC container including steel weights simulating the soil load. Piezometers are installed at the following locations: one at the soil/envelope interface, 7 in the soil sample, at 15, 30, 42, 54, 66, 78 and 90 mm distance from this interface, and one in the gravel bed diffuser at 110 mm from the interface. The middle section contained the envelope material, a cut portion of corrugated pipe resting on a perforated template. Under it, another piezometer was installed. The lower section contained a funnel-shaped outlet, draining to a sediment trap. Flow rates were recorded with flowmeters. Nitrogen gas was supplied continuously to prevent ochre buildup. Details are given in Stuyt (1983b). The tests lasted 14 days and four replicates were made using "Almere" sand, a very fine marine deposit (Fig. 11). It was sampled near drain depth and prepared by drying at 105°C and subsequent aggregate crushing in order to create cohesionless soil samples. Preparation of the permeameters consisted of the following steps.

1. *Installation of sample discs*; the effect of binding strings around wrapped pipes was simulated using a steel ring with wires (Fig. 12).

2. *Filling with soil samples* (2½ kg) through a funnel with an extended outlet held just above the envelope sample to prevent soil stratification.

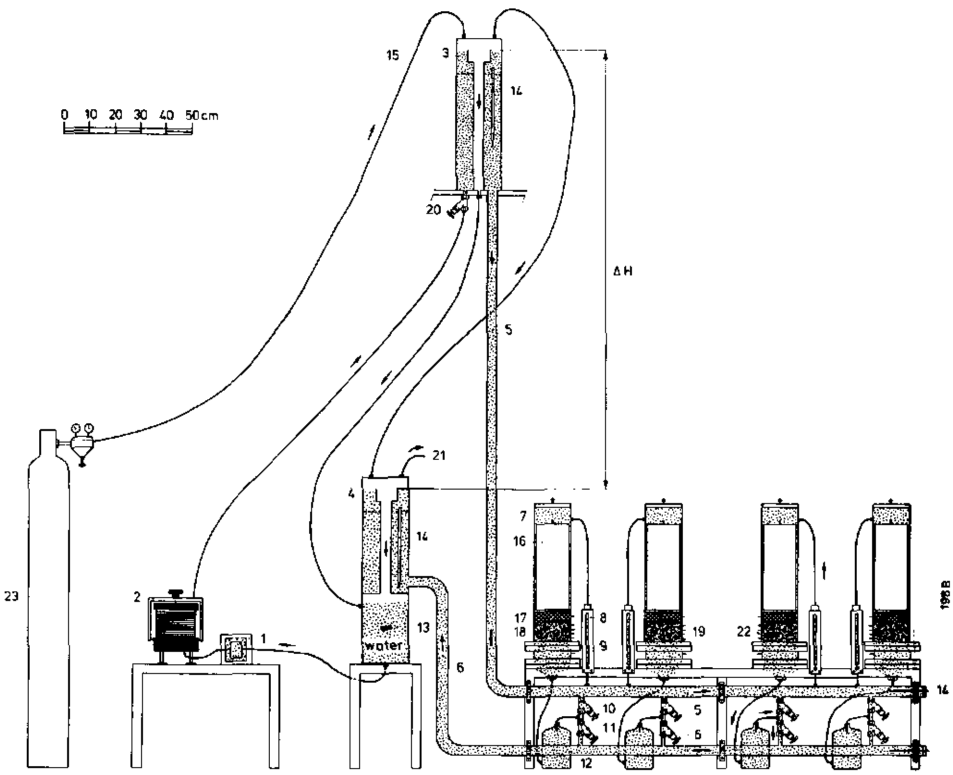

Figure 8. **Laboratory apparatus for testing the hydraulic- and filtering properties of envelopes. 1 = centrifugal pump, 2 = active carbon water filter, 3 = upper constant head tank, 4 = lower constant head and water supply tank, 5 = water supply tube, 6 = water discharge tube, 7 = cylindrical plexiglass tank, 8 = flow meter, 9 = needle valve, 10, 11 = taps, regulating flow directions, 12 = sediment trap, 13 = heating device, 14 = thermometer, 15 = supply valve for nitrogen gas, 16 = steel weights in PVC casing, 17 = gravel bed diffuser, 18 = soil sample, 19 = envelope sample, 20 = tap, regulating pump discharge, 21 = nitrogen gas outlet, 22 = piezometer (10 at each cylinder), 23 = nitrogen flask. Manometer boards are not depicted.**

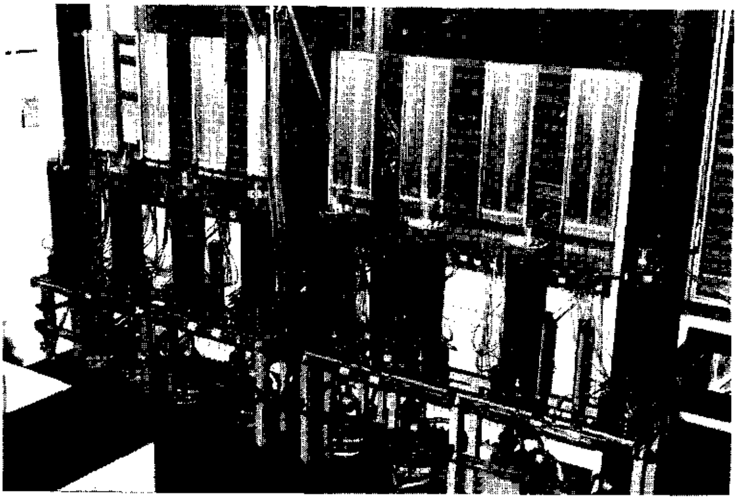

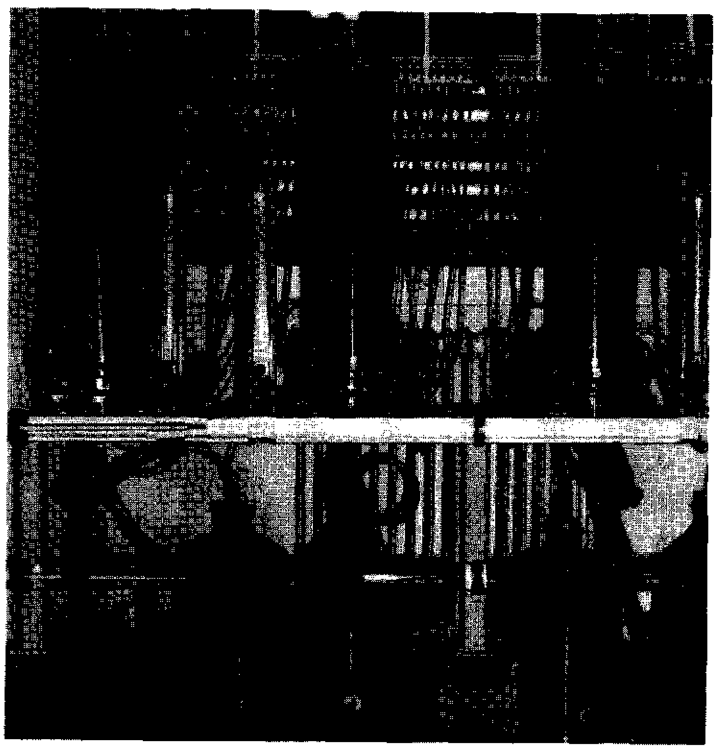

Figure 9. The laboratory apparatus, used during the first project: overall view (top) and detailed view (bottom).

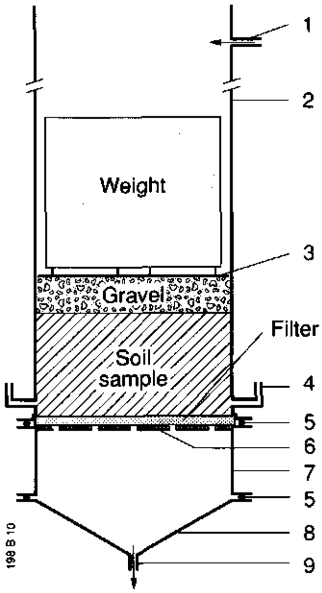

Figure 10. Cross sectional view of flow permeameter.

1 = water supply tube

2 = upper section of permeameter

3 = perforated template

4 = piezometer connection

5 = o-ring

6 = flattened portion of corrugated drain pipe, fixed onto a perforated template

7 = middle section of permeameter

8 = lower part of permeameter (funnel)

9 = water discharge tube

3. *Coverage of soil samples* with a gravel bed, a perforated lid and a container with steel weights.

4. *Gradual saturation* of the envelope sample disc and the soil sample from the bottom upwards, removing air pockets.

5. *Deaeration* of manometer tubes.

6. *Filling of top sections* of permeameters with water.

7. *Start* of water circulation.

Hydraulic heads were increased daily. This was done indirectly by adjusting needle valves. Each time when steady state was reached, flow rates and piezometric heads were recorded. The following parameters were observed and/or calculated:

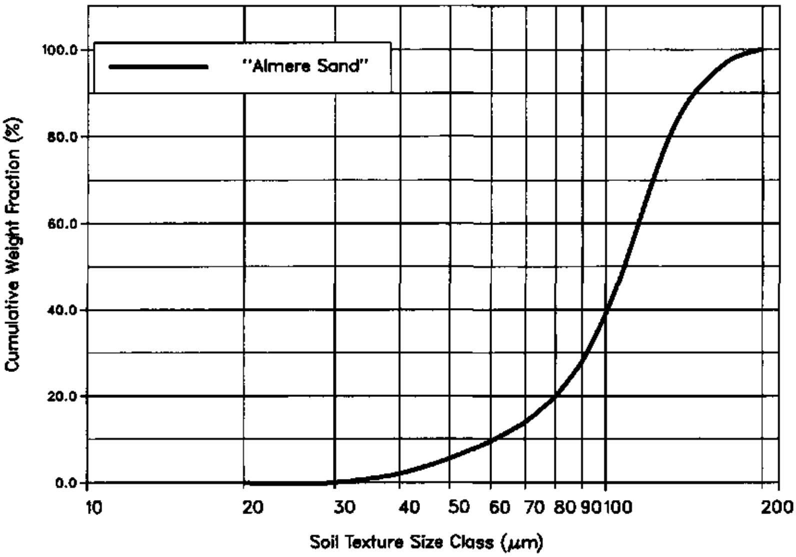

Figure 11. **The particle size distribution of "Almere Sand".**

1. **Pipe clogging rate** after completion of a flow test, expressed as sediment layer height in a 60 mm drain. The soil material in the sediment traps was weighed while wet. The equivalent sediment layer height was calculated as follows. The length of a 60 mm drain section having a wall area equal to the cut portion of corrugated pipe in the permeameters (ø = 150 mm) is

$$(1/4 \cdot \pi \cdot 150^2) / (57 \cdot \pi) = 22500/228 = 99 \text{ mm} \qquad (2)$$

assuming that the average inside diameter of a corrugated 60 mm outside diameter drain is 57 mm.

The average mass of wet soil, required to fill a 99 mm long pipe section completely was 0.52 kg (5 repetitions). The cross-sectional area A [L^2], filled by a quantity of sediment W [M] was calculated from

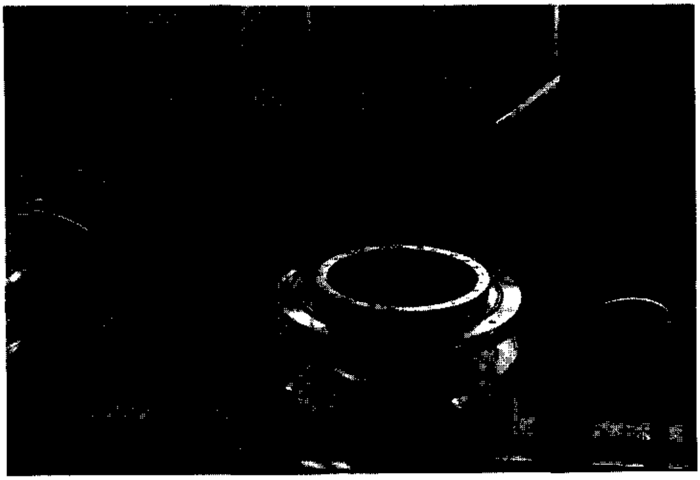

Figure 12. **A steel ring with wires simulates binding strings around pipe envelopes.**

$$A = (W/0.52) \cdot (\pi \cdot 0.057^2)/4 \cong 0.00491\ W \qquad (m^2) \quad (3)$$

where A = cross-sectional area of drain, filled with sediment (m^2)

W = mass of wet sediment, trapped after completion of a flow test (kg)

$W \leq 0.52$ (kg)

The height of a sediment layer h [L] having a cross-sectional area A [L^2] was calculated from

$$h = r - r \cos(\theta/2) \qquad (m) \quad (4)$$

where r = the radius of the drain (m). The angle θ is calculated from the cross-sectional area A [L] as

$$\theta - \sin\theta = 8A/0.06^2 \cong 2222\ A \qquad (rad) \quad (5)$$

cf. (Fig. 13).

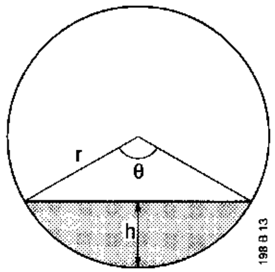

Figure 13. **Cross-sectional area of drain with sediment layer; r = internal pipe diameter [L], h = height of pipe sediment [L], θ: see text.**

From these equations, the relationship between W, the mass of mineral deposit in a sediment trap [M] and h, the height of a sediment layer in a 60 mm drain, was calculated (Fig. 14). In the Netherlands, a layer of pipe sediment exceeding 15 mm in a 60 mm drain is considered unacceptable because the transport capacity of the drain is reduced too much. According to Fig. 14, 0.1 kg of sediment in a sediment trap is equivalent to this threshold level. The height of the computed pipe sediment layer was used as a criterion to conclude whether or not the particle retention capability of envelopes was adequate.

2. Average saturated **hydraulic conductivities** of successive soil layers and their changes, with time.

3. **Rates of discharge** from a hypothetical field drainage system, equivalent to average flow rates observed in the model apparatus. They were calculated by approximation.

A typical Dutch drainage system consists of 60 mm pipe laterals with a drain spacing L = 15 m. Assuming horizontal and radial flow resistances in the soil to be such that the drains are flowing half full, the equivalent steady-state outflow rate from a drainage system, q $[L.T^{-1}]$, is computed from the permeameter discharge Q $[L^3.T^{-1}]$ as:

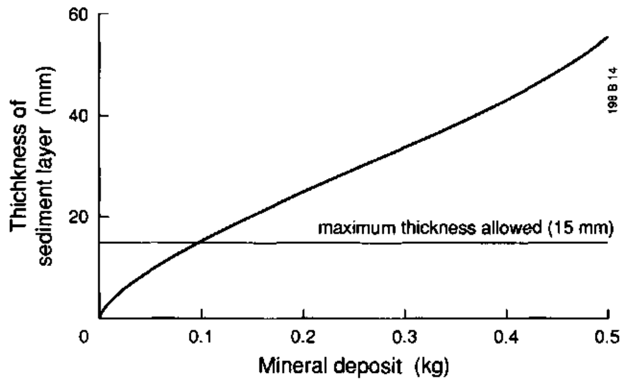

Figure 14. **Relation between the weight of mineral deposit in a sediment trap and the corresponding thickness of a sediment layer in a 60 mm drain pipe.**

$$q = (Q/A) \cdot (10000/L) \cdot (\pi \cdot d/2) \qquad (m.d^{-1})(6)$$

where

q = outflow rate $(m.d^{-1})$

Q = permeameter discharge $(m^3.d^{-1})$

A = surface area of permeameter bottom plate (m^2)

L = drain spacing (m)

d = pipe diameter (m)

Discharges were observed at laboratory temperature (20-23°C) and were converted to equivalent discharges at 10°C.

3. Average **entrance resistances** of envelopes with time.

Entrance resistances of envelope samples W_i [$T.L^{-1}$] were calculated from

$$W_i = \Delta h \cdot q_l^{-1} \qquad (d.m^{-1})$$

where Δh = head loss caused by water entry into the drain (m)

and q_l = discharge per running metre of drain [$L^2.T^{-1}$]:

$$q_l = (Q/A) \cdot (\pi \cdot d/2) \qquad (m^2.d^{-1})$$

The entrance resistance may also be expressed as a dimensionless entrance resistance factor α_i [-] which is the entrance resistance for a soil with a hydraulic conductivity equal to unity (Wesseling, 1979; Dierickx, 1980):

$$\alpha_i = W_i \cdot k \qquad (-) \qquad (9)$$

where k = the saturated hydraulic conductivity of the soil surrounding the drain ($m.d^{-1}$), i.e. the soil segment between 0 and 15 mm distance from the soil/envelope interface in a flow permeameter.

Values of α_i were computed to see if they are a factor of importance in design (i.e. drain spacing).

An assessment was made of the reproducibility of the testing conditions with attention focussed on soil samples which were likely to show greatest variability.

From November 1981 to March 1983, 20 envelope materials were subjected to flow tests. Two categories were distinguished: voluminous envelopes (thickness > 1 mm) and thin or sheet envelopes. Their characteristics are given in Table 1.

2.2 Results

Moisture retention curves of different envelopes are presented in Fig. 15. Major parameters of these curves are given in Table 2.

The hydraulic head ΔH [L], imposed on each composite envelope/soil sample,

Table 1. Characteristics of envelope materials

No.	raw material or brand name	composition and/or structure	category
1	Acrylic fibres	needlefelt fibres	voluminous
2	Coconut fibres	needlefelt fibres	voluminous
3	Coconut fibres	random fibres	voluminous
4	"Erolan 300"	needlepunched polyester filament nonwoven	voluminous
5	Peat fibres	random fibres	voluminous
6	Polypropylene fibres	needlefelt fibres 100 denier	voluminous
7	Polypropylene fibres	needlefelt fibres 200 denier	voluminous
8	Polypropylene fibres	needlefelt fibres 100/200 d.	voluminous
9	Polypropylene fibres	random fibres	voluminous
10	Polypropylene fibres	random fibres, class "A"	voluminous
11	Polypropylene fibres	random fibres, class "B"	voluminous
12	"PS-LDPE"	polystyrene beads, wrapped in perforated low-density polyethylene foil	voluminous
13	"Big 'O'" sock	polyamide fabric	thin/sheet
14	"Brentano" standard	polyamide fabric	thin/sheet
15	"Brentano" H	polyamide fabric	thin/sheet
16	"Cerex"	spunbonded polyamide filament nonwoven	thin/sheet
17	Glass fibre sheet	mineral nonwoven	thin/sheet
18	Glass fibre sheet Isover	mineral nonwoven	thin/sheet
19	"Typar" 68	heat bonded by component PE/PP filament nonwoven	thin/sheet
20	"Typar" 113	heat bonded by component PE/PP filament nonwoven	thin/sheet

was gradually increased to approximately 600 mm which is roughly equivalent to a hydraulic gradient $i = 6$ [-]. Occasionally, the maximum head could not be imposed because the capacity of the water supply system of the model apparatus was too small to cope with comparatively small flow resistances in the permeameters.

Quantities of soil, washed through the envelopes after completion of the flow tests and converted into equivalent sediment layer heights in 60 mm drains, entrance resistances and average equivalent discharges are given in Table 3.

Particle flow was a maximum during the first day of the test and decreased to negligible rates within a few days. Some clay size particles washed through all envelopes and remained in suspension for several days.

Table 2. Uniformity coefficients D_{60}/D_{10} and median pore sizes D_{50} of moisture retention curves of voluminous envelopes (averages of 5 repetitions).

Envelope material	D_{60}/D_{10}	D_{50}
Peat Fibres	5.51	178
Polypropylene random fibres	1.68	986
Polypropylene fibres 100 denier	1.54	746
Polypropylene fibres 200 denier	2.33	924
Polypropylene fibres 100/200 den.	1.57	888
"PS-LDPE" (polystyrene beads)	1.63	954

Table 3. Equivalent sediment layer heights in a 60 mm drain of soil quantities, washed through envelopes, entrance resistances W_i, entrance resistance factors α_i and average equivalent discharge rates at 10°C (drain spacing L=15 m). Figures are averages of four repetitions and are recorded at the end of the tests.

No.	Raw material (brand name)	Sediment layer height (mm)	Entrance Resistance W_i ($d.m^{-1}$)	α_i (-)	Equivalent discharge ($mm.d^{-1}$)
1	Acrylic fibres	0	.013	.10	45
2	Coconut fibres	43	.010	.14	24
3	Coconut fibres	54	.021	.07	40
4	"Erolan 300"	0	.025	.05	43
5	Peat fibres	0	.052	.20	29
6	Polypropylene fibres	33	.001	.01	32
7	Polypropylene fibres	53	.001	.02	40
8	Polypropylene fibres	31	.109	.70	45
9	Polypropylene fibres	>60	.010	.01	26
10	Polypropylene fibres	>60	.010	.02	27
11	Polypropylene fibres	12	.002	.02	47
12	"PS-LDPE"	22	.159	.84	37
13	"Big 'O'" fabric	4	.035	.08	40
14	"Brentano" standard	2	.114	.43	34
15	"Brentano" H	3	.063	.19	23
16	"Cerex"	12	.016	.04	28
17	Glass fibre sheet	2	.021	.06	30
18	Glass fibre sheet Isover	3	.040	.11	40
19	"Typar" 68	10	.019	.06	30
20	"Typar" 113	6	.169	.57	29

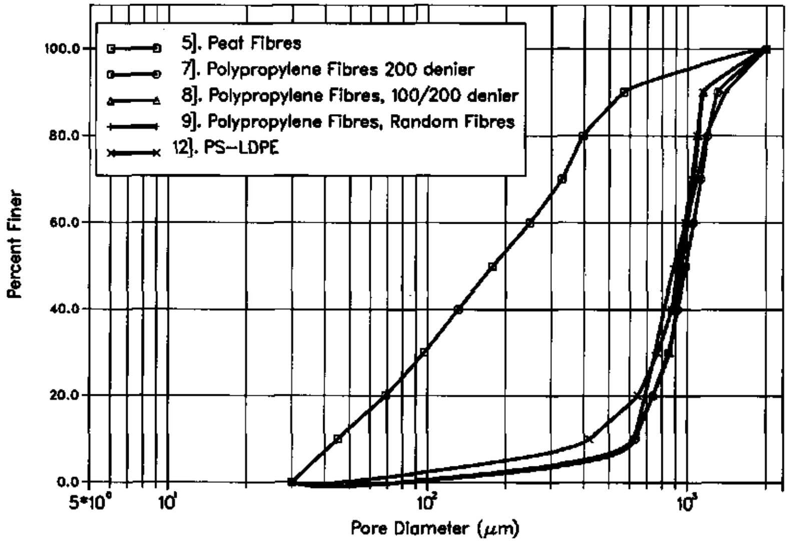

Figure 15. Moisture retention curves of several envelope materials. Figures are averages of five replicates.

2.3 Discussion

Except for the peat fibre envelope, the moisture retention curves of the voluminous envelopes have similar uniformity coefficients (D_{60}/D_{10}) and median pore sizes D_{50} (Fig. 15). The curves are very steep because much water was released within a narrow range of suctions. This result is questionable because of the large differences in length, thickness and shape of the basic components (fibres or beads) of the envelopes and their physical arrangement (fibre diameter, spatial geometry etc.).

While determining the moisture retention curve, drainage of an envelope pore is conditional on

1. the pore diameter in relation to the water suction applied,

2. the existence of a continuous air inlet path from a sample boundary to that pore, and

3. the existence of a continuous saturated water outlet path from that pore to

the porous support plate.

Conditions 2) and 3) are not necessarily met. If condition 2) is not fulfilled the pore is not drained, although it may be drained at some higher suction. If condition 3) is not obeyed a pore cannot be drained and it will continue to contain residual water. Both cases are likely to induce systematic differences between the actual pore size distribution of an envelope and the distribution derived from the moisture retention curve. This invalidates the suction method for the intended purpose. To prove the discrepancy between both types of distributions, determination of a moisture retention curve of a voluminous envelope was simulated by a simple computer model (Stuyt, 1982a). From a given input pore size distribution this model computed a corresponding moisture retention curve in a vertical, two-dimensional cross-section through an envelope sample. It is discussed in in more detail in Annex 1. The modelling results showed that moisture retention curves of envelopes are different from pore size distributions.

The particle retention capability of the envelopes was examined with cohesionless "Almere" sand. Thin or sheet envelopes were much better than voluminous ones, except for the fibrous peat envelope. All sheets satisfied the Dutch criterion ($\leq$15 mm sediment in a 60 mm drain) whereas most voluminous envelopes did not. In the latter cases, no significant correlations were found between mineral clogging rates and either average pore sizes D_{50} or uniformity coefficients D_{60}/D_{10} as determined from their moisture retention curves.

The average hydraulic conductivities of successive soil layers showed no changes with time (Stuyt, 1983a).

Most entrance resistances α_i did not markedly increase with time (i.e. with increasing hydraulic gradient) (Fig. 16) although some showed a rise, namely coconut fibres (No. 3), peat fibres (5), polypropylene fibres (8), both "Brentanos" (14 and 15) and "Typar" (20).

Entrance resistance causes a rise of the ground water table, not only near the drains, but also inbetween. Consequently, narrower spacing may be necessary to comply with design criteria (Wesseling, 1979; Dierickx, 1980). At the end of the flow tests, most entrance resistances are still quite low (Table 3). Wesseling (1979) concludes that in cases when α_i exceeds, on average, 0.3, it may influence design. Following this criterion, Polypropylene fibres (No. 8), "PS-LDPE" (12), "Brentano" standard (14) and "Typar" 113 (20) are the least promising. However, α_i-values published by Wesseling and van Someren (1972) indicate that entrance resistances, measured in the field, often exceed the values found in laboratory experiments, so other envelopes may give rise to problems as well.

Considering both particle retention capability and entrance resistance, the

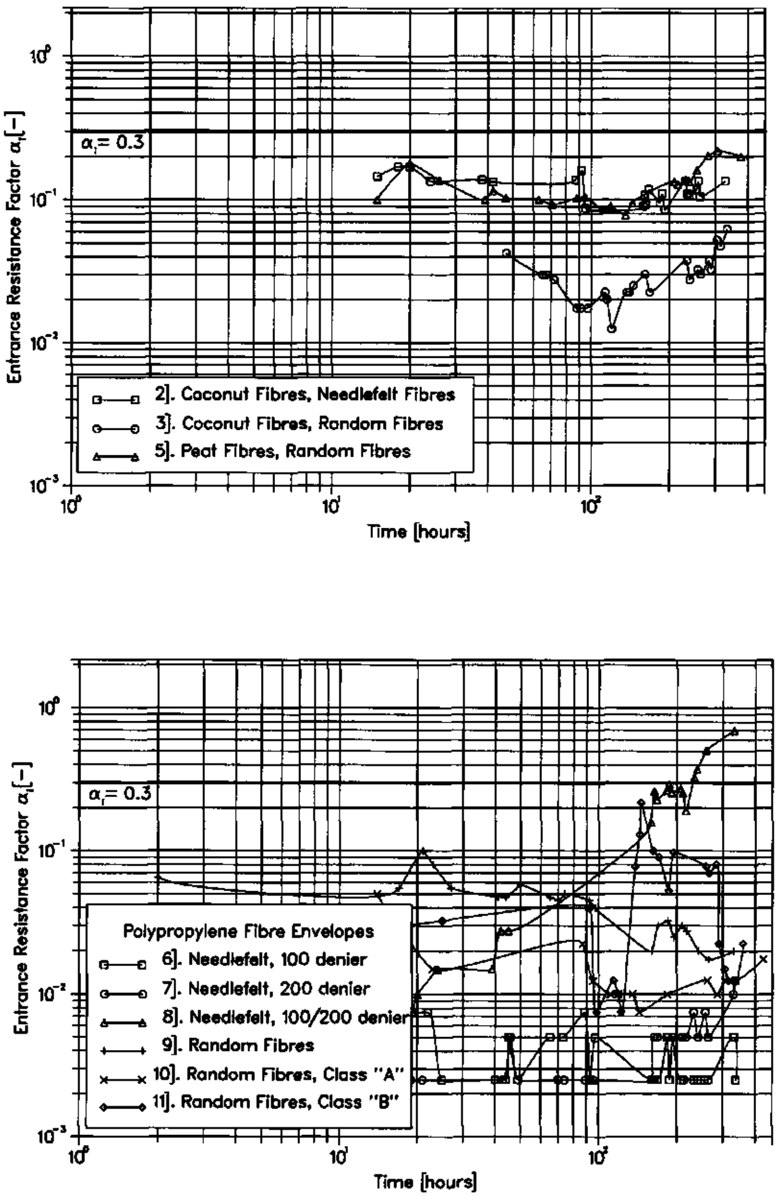

Figure 16. **Entrance resistance factors α_i, plotted with time. Figures are averages of four replicates.**

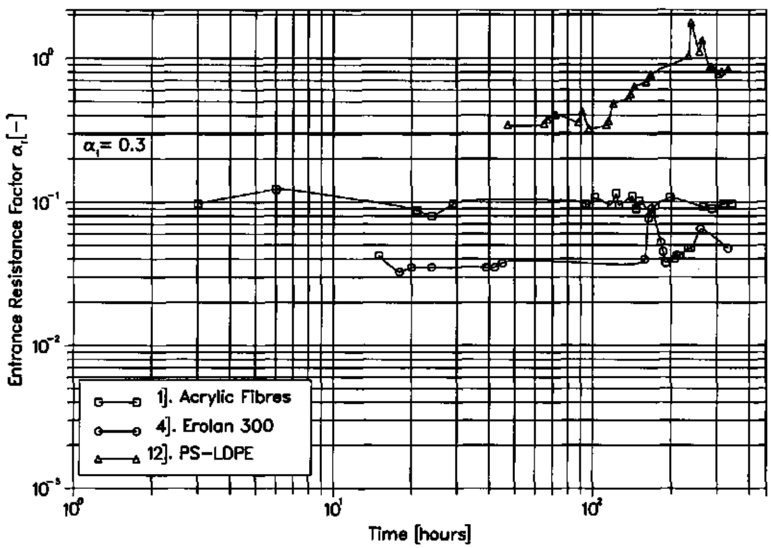

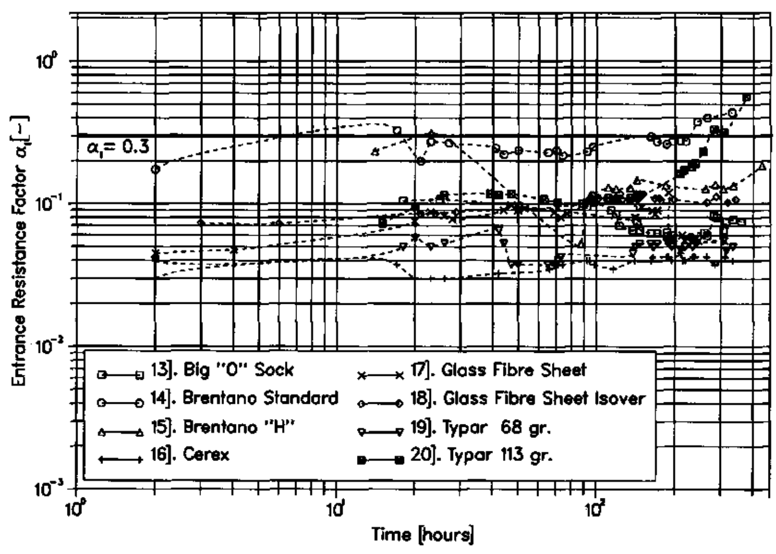

Figure 16 (continued). Entrance resistance factors α_i, plotted with time.

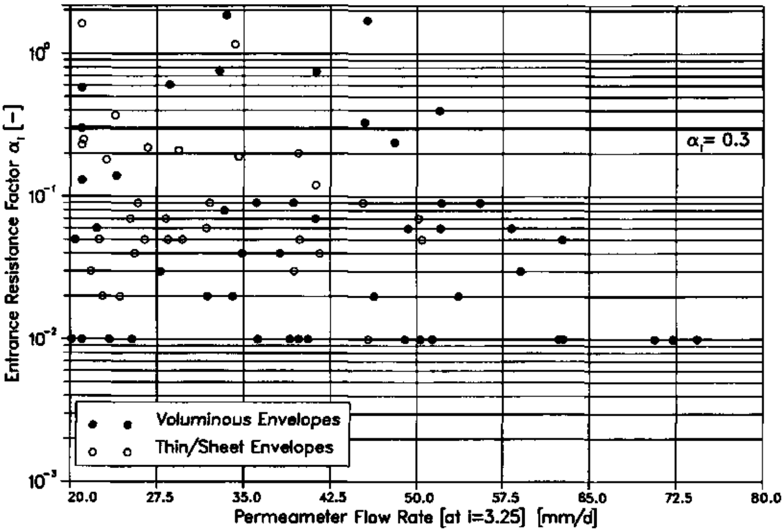

Figure 17. Relationship between permeameter discharges at the end of the flow tests at hydraulic gradient i = 3.25, and entrance resistance factors α_i, induced by envelopes.

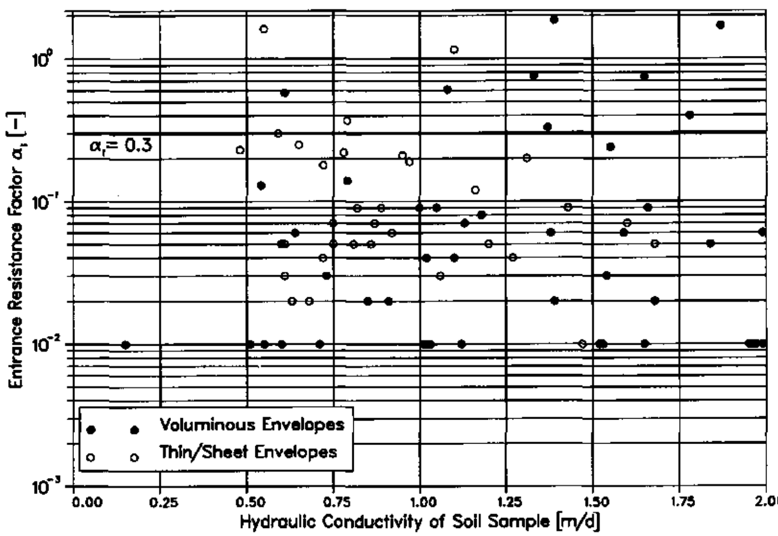

Figure 18. Average saturated hydraulic conductivities of the soil samples and entrance resistance factors α_i at the end of the flow tests.

following envelope materials have favourable properties: acrylic fibres (No. 1), "Erolan 300" (4), Peat fibres (5), Polypropylene fibres (11), "Big 'O'" fabric (13), Brentano "H" (15), "Cerex" (16), Glass fibre sheet (17), Glass fibre sheet Isover (18) and "Typar" 68 (19). Nevertheless, the significance of these properties for the functioning of envelopes in weakly-cohesive soils is ill-defined. Hence, these results are inadequate unless confirmed by field observations.

Assuming that Darcy's law holds (laminar flow), observed discharges from the permeameters at the end of the flow tests were converted to expected discharges at a hydraulic gradient $i = 3.25$ (=average of all replicates of all tests) (Fig. 17). Converted discharges largely exceeded a widely used Dutch steady-state design discharge (7 $mm.day^{-1}$ at 0.5 m watertable depth). The highest discharges were observed while testing voluminous envelopes.

Finally, an observation was made of the reproducibility of the permeameter flow tests on the basis of observed flow rates and head losses at the end of each test. The use of cohesionless soil samples enhanced the reproducibility. Moreover, the soil samples had been prepared with utmost care and may be assumed to have similar properties, e.g. hydraulic conductivities. In fact, the observed hydraulic conductivities were widely scattered, showing a tenfold difference in values (Fig. 18). In addition, the entrance resistance factors α_i were not related to the hydraulic conductivity of the soil samples (Fig. 18). Apparently, the hydraulic conductivity of the soil at the end of a flow test did not markedly influence the testing conditions.

These facts challenge the validity of the permeameter flow test, performed with cohesionless soil samples, as a reproducible tool for testing drain envelopes and determining their properties.

3 THE SECOND PROJECT

In this project, too, hydraulic and filtering properties of envelopes were observed in an analogue model. Previous attempts to "translate" such properties into recommendations for field applicability in weakly-cohesive soils had largely failed. The intention of this series of tests was therefore not to determine envelope properties as such but to try to create conditions more similar to those occurring in the field. This approach was also chosen for the following reason. Despite a persistent preference, in the Netherlands, for voluminous envelopes, thin envelopes are successfully applied, both in the Netherlands and elsewhere. A laboratory investigation into the functioning of thin envelopes under conditions which are reasonably close to field conditions was therefore necessary, particularly due to the fact that the entrance resistances of thin envelopes, as observed during the first laboratory project, appeared to be similar to those of voluminous ones. In this second series of experiments, envelopes were exposed to conditions, assumed to be similar to those existing in the field after installation in a comparatively dry soil. Weakly-cohesive soil samples were used. These samples are more representative for field conditions although they seriously challenge the reproducibility of the test. Poor reproducibility was unavoidable and had to be accepted.

Hydraulic conductivities and related parameters such as entrance resistances are rooted in the traditional concept of homogeneity and isotropy of porous media. In this project, however, the soil samples are heterogeneous and the flow of water and/or soil particles is preferential. With heterogeneous soil samples, hydraulic conductivities and entrance resistances can still be approximately determined if the dimensions of the porous media are large relative to those of the heterogeneous features (aggregates, macropores, voids etc.). In the available permeameters, the soil samples were too small to determine these parameters with confidence. Therefore, only the total head, dissipated by the composite sample, consisting of soil and envelope, was observed.

For these tests, the laboratory apparatus was redesiged. The single-level constant head tank was replaced by a fastened, air-tight, multi-level tank. Available heads were 0.05 - 1 m (0.05 m increments) and 1-2 m (0.25 m increments). Each permeameter, 150 mm inside diameter by 400 mm high, was built in three distinct sections (Fig. 19). The lower section included a water inlet tube, a spring which simulates the soil load, a 10 mm gravel bed diffuser and the soil sample (thickness 100 mm). A piezometer was inserted into the gravel bed diffuser. The middle section contained the envelope sample disc, a flattened portion of corrugated pipe and a perforated template. The top section contained a funnel-shaped outlet and

Table 4. Texture of soils, used in the analogue model.

Soil sample	Soil type	Clay (%)	Silt (%)	Median (μm)
Uithuizermeeden	silty sand	8	11	76
Lelystad	very fine sand	1	13	75
Valthermond	loamy sand	4	4	120
Willemstad	alkaline silt	9	26	69

the second piezometer. Flow rates were recorded with flowmeters. Water flowed through the permeameters in an upward direction. Details are given in Oosten & Stuyt (1986).

3.1 Test Procedure

Tests were made on four replicate samples and lasted 10 days on average. Soil, prone to mineral clogging, was sampled at four locations (Table 4).

Soil was sampled as deep as permitted by the actual ground water level, with moisture content near saturation. Average sampling depth was 0.70 m below the surface. The samples were installed in the permeameters within six hours after retrieval from the field. Large aggregates were crushed by hand, reducing the average aggregate diameter to approximately 10 mm. The permeameters were filled with a layer of 120 mm of soil and compacted with a steel weight, reducing the soil layer height to approximately 100 mm. Preparation of the permeameters was largely identical to the procedure which was followed in the first project. Details are given in Stuyt (1989). Hydraulic heads were increased daily. When steady state was reached, flow rates and piezometric heads were recorded. The following parameters were observed and/or calculated:

1. **Hydraulic conductivity** of the composite soil/envelope sample at the beginning of a flow test (initial hydraulic conductivity) as well as at the end (ultimate hydraulic conductivity). Due to the heterogeneity of the porous media the preferential flow was likely to be non-Darcyan. Nevertheless, hydraulic conductivities were calculated following Darcy's law and are rough indications rather than reliable determinations.

2. **Cumulative discharge**, CD [L], during a flow test. Discharges were estimated because the hydraulic conductivities could not be calculated with confidence.

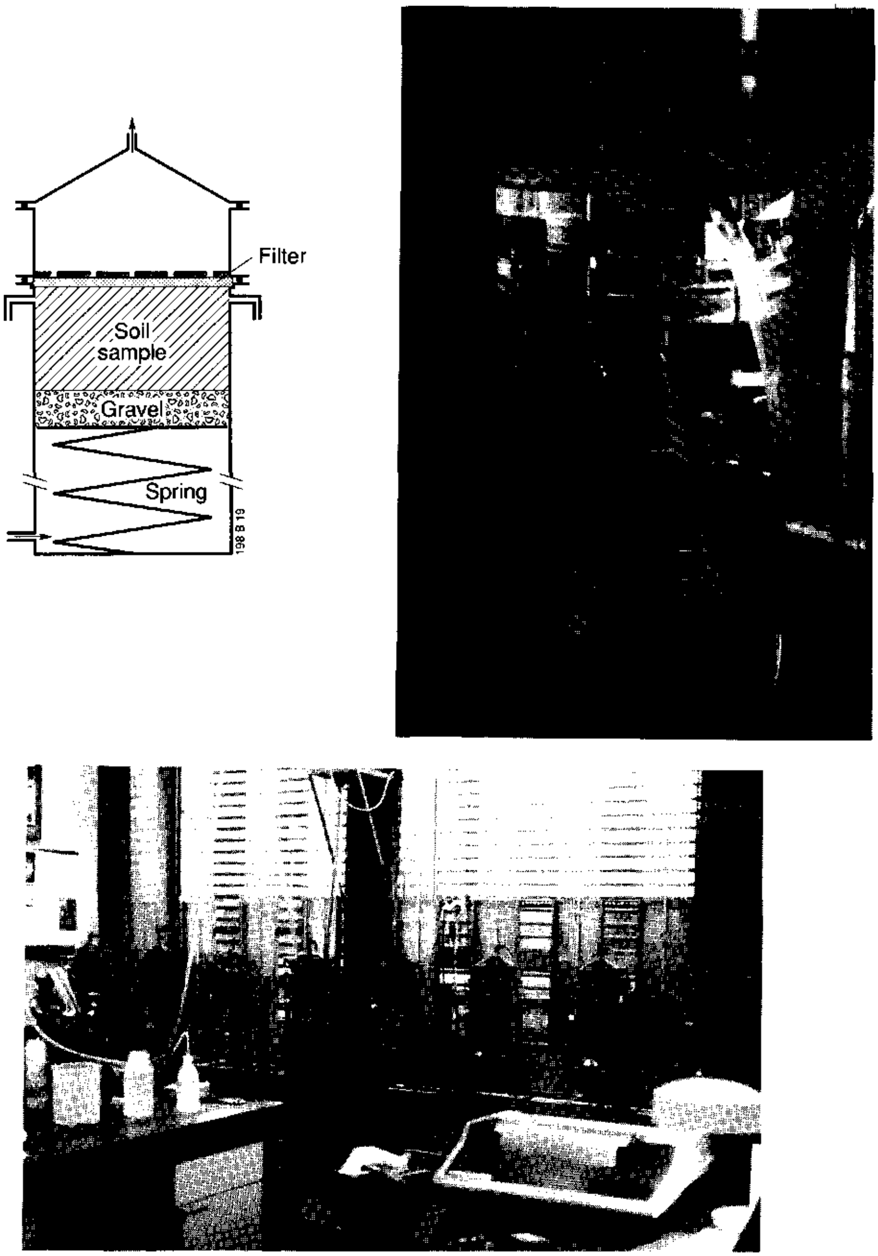

Figure 19. **The model apparatus, used for observation of hydraulic and filtering properties of envelopes in weakly-cohesive soils: cross-section of permeameter (top, left), detailed view of permeameter (top, right), laboratory view (bottom).**

The duration of the tests varied somewhat, but flows were accumulated for a maximum period of 240 hours. If a test was discontinued sooner, flow was assumed to have continued at the final rate.

3. **Pipe clogging rate**, PC [L], expressed as sediment layer height in a 60 mm pipe drain after completion of a flow test.

4. The "**Envelope Suitability Index**" (ESI), which is defined as:

$$ESI = {}^{10}\log CD - PC/\Delta h \qquad (-) \qquad (10)$$

where CD = the cumulative discharge from a permeameter apparatus during a flow test (mm), PC = pipe clogging rate (mm) and Δh = a constant, to be determined after completion of the laboratory experiments.

The ESI is a qualitative parameter in which the suitability of an envelope to convey water and to retain soil is expressed in an integrated manner. The idea behind ESI is the empirical experience that a limited rate of pipe sedimentation is tolerable or even desirable because it often promotes water flow into a drain. Excessive pipe sedimentation rates and limited water flow rates will cause the ESI to decrease.

5. Pore size distributions of the envelope materials were not determined, for four reasons:

   1. given the results obtained during the first project, pore size distributions of envelopes were within an, empirically determined, safe range (O_{90}[7] = 200 - 1200 μm) and were not found to be a factor of paramount importance,

   2. the suction method, used during the first project, does not yield reliable pore size distribution data,

   3. pore size distributions of several envelopes were known, either precisely or by approximation,

[7]The O_{90} or "effective opening size" of envelope pores is a design parameter; 90% of all envelope pores have a diameter equal to, or smaller than O_{90} (μm). It is a practical measure for the maximum pore diameter of an envelope and corresponds with the average particle diameter of a soil fraction of which 10% falls through an envelope during a sieving test.

4. neither staff, nor laboratory facilities were available to do the measurements.

6. The influence of soil properties an envelope category was established with linear regression. It was used to investigate the interaction between envelope type and soil sample type, by estimation of the resulting effect on CD (cumulative discharge), PC (pipe clogging rate) and ESI (Envelope Suitability Index). Preferably, the effect of each envelope type and each soil sample type on these parameters should have been assessed. Many interaction terms cannot however be estimated because the functioning of most envelopes could be observed with one soil sample type only, due to financial restrictions. As effects were expected to depend on envelope type, it was decided to regroup the envelopes into three categories: plain (no envelope), thin and voluminous. Hence, the regression models include two predictor factors, as follows:

$$CD = a_0 + a_1 x_{1i} + a_2 x_{2i} + e_i \tag{11a}$$

$$PC = a_0 + a_1 x_{1i} + a_2 x_{2i} + e_i \tag{11b}$$

$$ESI = a_0 + a_1 x_{1i} + a_2 x_{2i} + e_i \tag{11c}$$

where

x_1 = predictor factor 1: soil sample origin,

x_2 = predictor factor 2: envelope category.

The coefficients a_0, a_1 and a_2 were estimated for i = 1, 2, ..., 148 observations (37 permeameter flow tests with four replications); e_i is the residual of the model (unexplained variation). A selection procedure was used to find predictor variables which have a significant effect on CD, PC and ESI (Draper & Smith, 1981). The computations were made with the statistical program "Genstat" (Genstat 5 Committee, 1987).

From June 1985 to February 1988, 37 flow tests were made: 33 tests with envelopes and 4 without. 20 tests were made with a voluminous envelope and 13 with a thin or sheet envelope; see Table 5.

Table 5. Characteristics of envelope materials and origin of soil sample with which it was examined.

1. Plain tests (without envelope)

No. raw material or brand name	composition and/or structure	soil sample
1 plain	--	Lelystad
2 plain	--	Uithuizermeeden
3 plain	--	Valthermond
4 plain	--	Willemstad

2. Tests with voluminous envelopes (thickness ≥ 1 mm)

No. raw material or brand name	composition and/or structure	soil sample
5 Coconut fibres 750 gr/m^2	random fibres	Valthermond
6 Oltmanns P/C	polypropylene/coconut fibre mixture	Lelystad
7 Peat fibres "Fl 86"	random fibres	Valthermond
8 Peat Fibres "Garden"	random fibres	Uithuizermeeden
9 Peat fibres "Flevo F"	random fibres	Lelystad
10 Peat/Cocos mixture	random fibres	Uithuizermeeden
11 "Polva"	perforated polystyrene foil (4 abutting layers)	Uithuizermeeden
12 Polypropylene fibres	random fibres, O_{90} = 450 μm	Uithuizermeeden
13 Polypropylene fibres	random fibres, O_{90} = 700 μm	Valthermond
14 Polypropylene fibres	random fibres, O_{90} = 700 μm thickness = 5 mm	Valthermond
15 Polypropylene fibres	random fibres, class "A"	Lelystad
16 Polypropylene fibres	random fibres, class "B"	Lelystad
17 Polypropylene fibres	random fibres, class "C"	Valthermond
18 "PSL"	polystyrene beads, wrapped in plastic string netting	Lelystad
19 "PSL"	polystyrene beads, wrapped in plastic string netting	Valthermond
20 "PSL"	polystyrene beads, wrapped in plastic string netting	Willemstad
21 "PS-LDPE"	polystyrene beads, wrapped in perforated low-density polyethylene foil	Lelystad
22 "PS-LDPE" (winter 1986)	Polystyrene beads, wrapped in perforated low-density polyethylene foil	Valthermond
23 "PS-LDPE" (spring 1987)	Polystyrene beads, wrapped in perforated low-density polyethylene foil	Valthermond

Table 5 (continued).

No.	raw material or brand name	composition and/or structure	soil sample
24	"PS-LDPE"	Polystyrene beads, wrapped in perforated low-density polyethylene foil	Uithuizermeeden

3. Tests with thin or sheet envelopes (thickness < 1 mm)

No.	raw material or brand name	composition and/or structure	soil sample
25	Acrylic fibres	spunbonded filaments	Uithuizermeeden
26	"Big 'O'" standard 150 dtex	polyamide fabric	Valthermond
27	"Big 'O'" Heavy Pile #2	polyamide fabric	Uithuizermeeden
28	"Big 'O'" standard 150 dtex	polyamide fabric	Uithuizermeeden
29	"Cerex" (N-25)	spunbonded polyamide filament nonwoven	Willemstad
30	"Colback"	heat bonded by component PA/PET filament nonwoven	Lelystad
31	"Colbond" TSF 175	needlepunched polyester staple fibre nonwoven	Willemstad
32	"Coltron"	needlepunched polyester filament nonwoven	Uithuizermeeden
33	Glass fibre sheet "Isover"	mineral fibre nonwoven	Willemstad
34	"Romian" sock	polyamide fabric	Valthermond
35	"Typar" 3207	spunbonded polypropylene nonwoven	Valthermond
36	"Typar" 3267	spunbonded polypropylene nonwoven	Willemstad
37	"Typar" T-135	spunbonded polypropylene nonwoven	Lelystad

3.2 Results

The results were affected by problems in saturating the porous media. Due to the complicated pore geometry in the soil samples, not all pores were initially saturable, even when saturation was attempted at a very slow pace. During a flow test, trapped air was sometimes released due to the increasing hydraulic gradient. As a result, unexpected changes occurred in flow pattern, sedimentation rate and hydraulic properties. Sometimes, substantial quantities of air were released from interaggregate pores inside soil samples, and then trapped at the interface with the envelope. When such air was removed the flow rate increased.

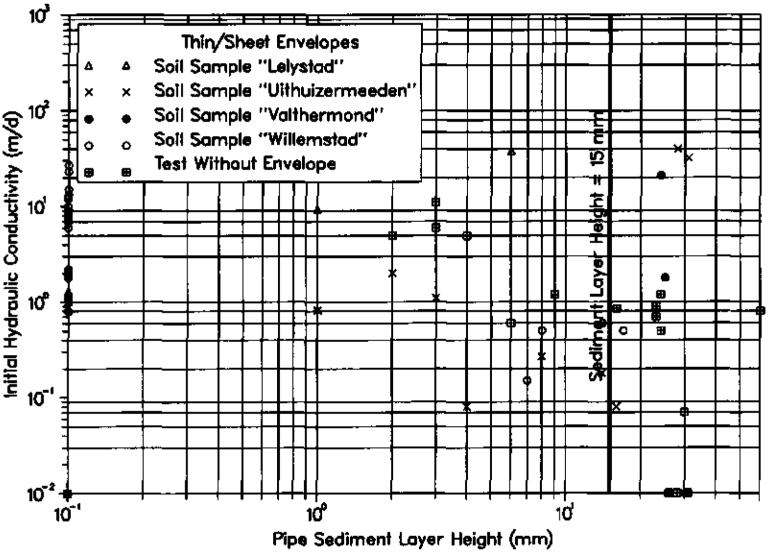

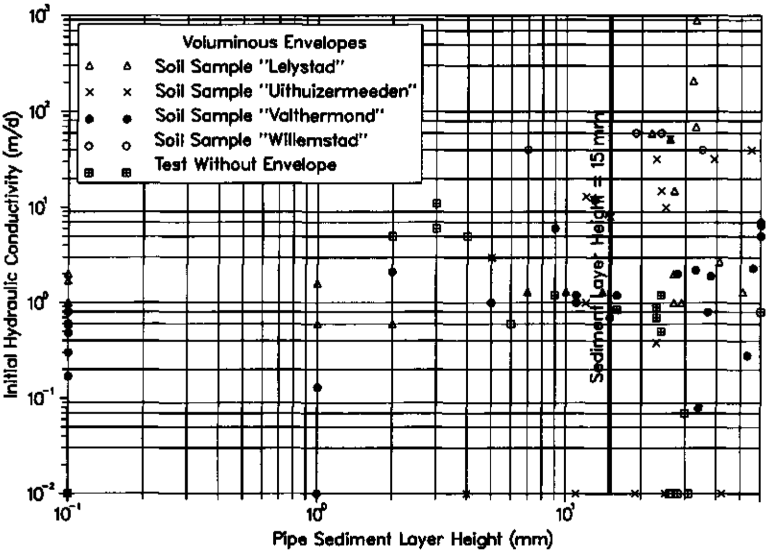

Figure 20. **Initial hydraulic conductivities and heights of sediment layers, observed in the permeameters.**

All observed and calculated parameter values are given in Annex 2 and include estimated initial and ultimate hydraulic conductivities [$L.T^{-1}$], cumulative discharges during the flow tests [L], equivalent sediment layer heights in a 60 mm drain after completion of the tests [L] and Envelope Suitability Indexes (ESI). Sediment layer heights [L] are plotted against the initial hydraulic conductivities [$L.T^{-1}$] in Fig. 20 and against changes in hydraulic conductivity (=ultimate K/initial K) [-] in Fig. 21. Cumulative discharges [L] are plotted against ultimate sediment layer heights [L] in Fig. 22, with reference to envelope category and soil sample origin, respectively. These plots were, more or less arbitrarily, segmented into areas which are bordered by lines with constant ESI (Fig. 23). Following this segmentation, Δh [L] in Eq. 10 was set to 36 mm, hence

$$ESI = {}^{10}\log CD - PC/36 \qquad (-) \qquad (12)$$

where CD = the cumulative discharge from a permeameter apparatus during a flow test (mm), and PC = pipe clogging rate (height of a sediment layer) (mm).

The result of the multiple linear regression analysis was as follows. The effect of each predictor factor, envelope category and soil sample origin, on cumulative discharge (CD) and pipe clogging rate (PC) was sometimes evident but not significant. Their effect on the Envelope Suitability Index (ESI) was however significant and so were some of the interactions between effects of CD and PC on ESI. Average ESI values are given in Table 6.

Table 6. Average values of ESI (Envelope Suitability Index) depending on soil sample type and envelope category (no envelope, voluminous or thin envelope).

Soil sample type	no envelope ESI	voluminous ESI	thin ESI
Lelystad	1.56	2.91	2.93
Uithuizermeeden	0.86	2.23	2.90
Valthermond	2.22	2.78	2.94
Willemstad	3.50	3.01	3.37

Most of the differences measured between envelope categories are significant. In addition, the differences depend on soil sample origin. With "Lelystad" and "Valthermond" soils, both voluminous and thin envelopes are better than no envelope. With "Uithuizermeeden" soil, thin envelopes are significantly better than voluminous ones which in turn are better than no envelope. With "Willemstad"

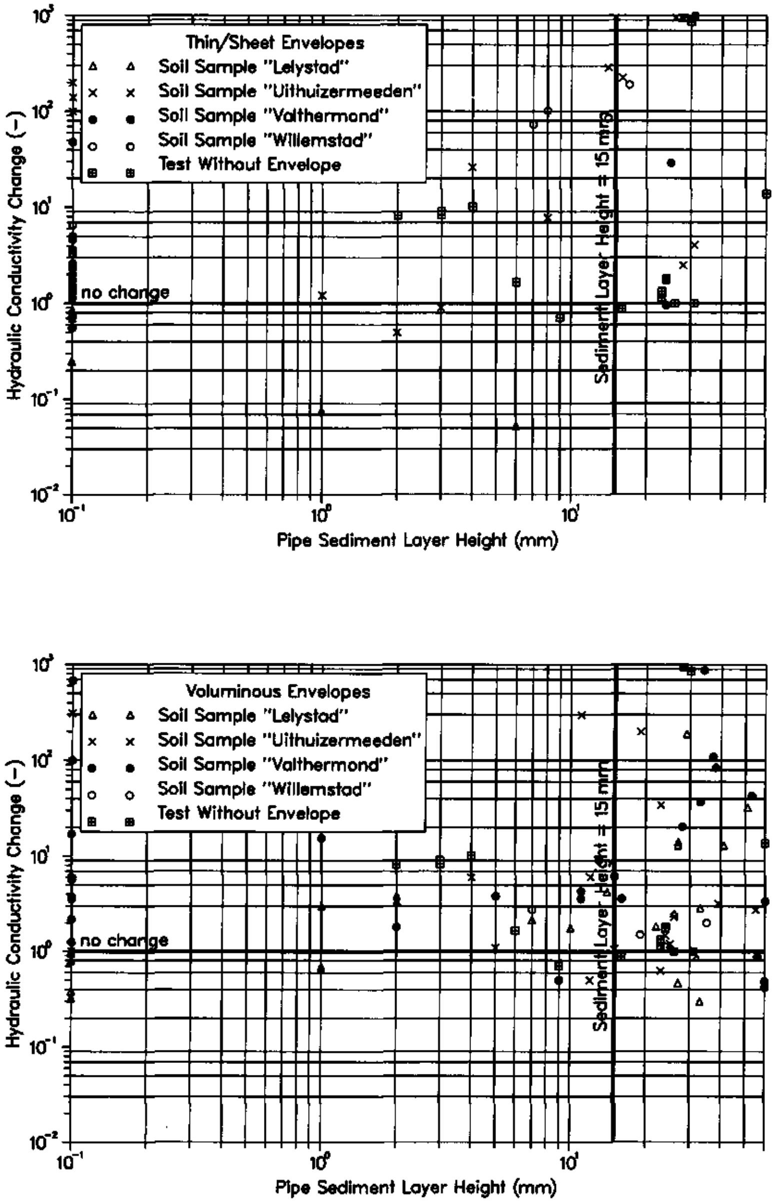

Figure 21. **Changes in hydraulic conductivity (=ultimate K/initial K) and sediment layer heights.**

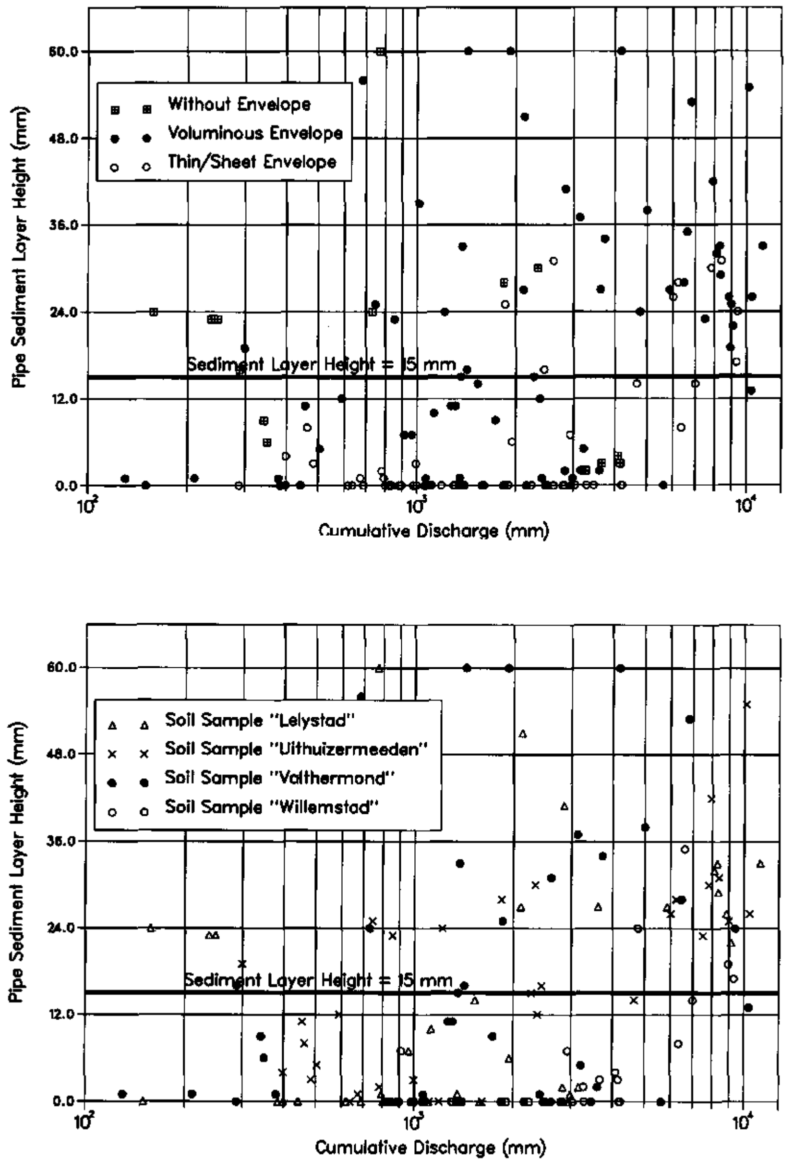

Figure 22. **Cumulative discharges and pipe sedimentation rates: (a) three categories: tests without envelope, voluminous envelopes and thin envelopes; (b) four categories: soil samples "Lelystad", "Uithuizermeeden", "Valthermond" and "Willemstad".**

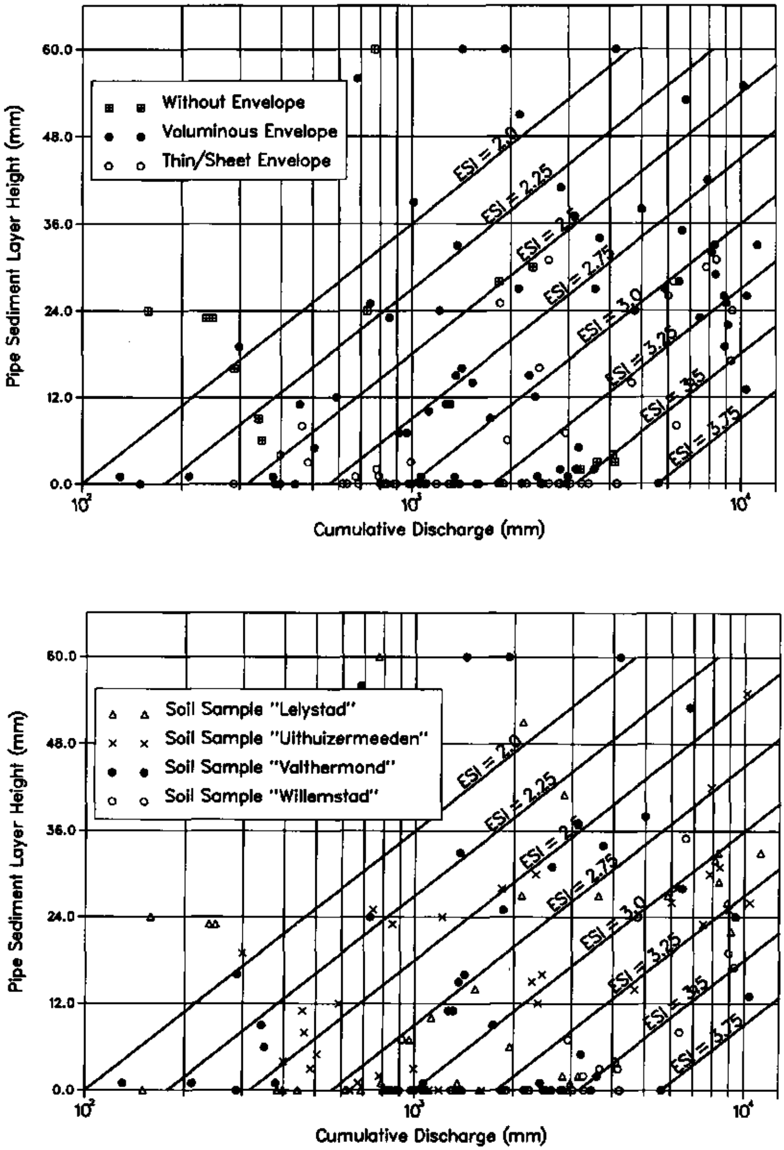

Figure 23. **Cumulative discharges, pipe sedimentation rates and Envelope Suitability Index (ESI): (a) three categories: tests without envelope, voluminous envelopes and thin envelopes; (b) four categories: soil samples "Lelystad", "Uithuizermeeden", "Valthermond" and "Willemstad".**

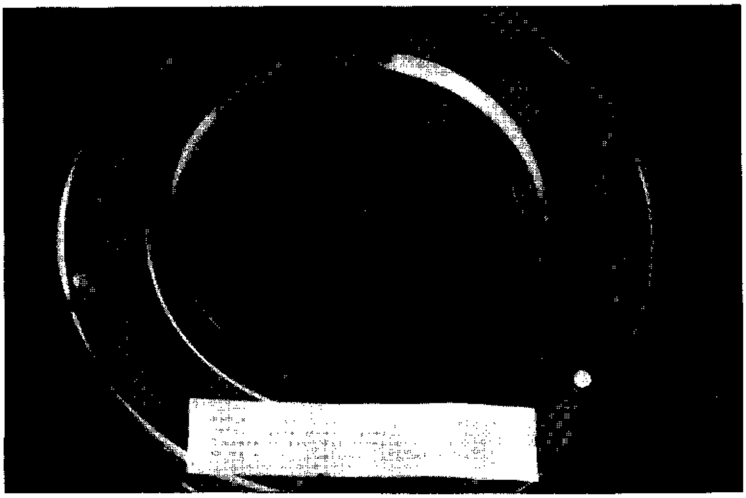

Figure 24. View of heterogeneous sedimentation of soil particles on a permeameter template after completion of a permeameter flow test.

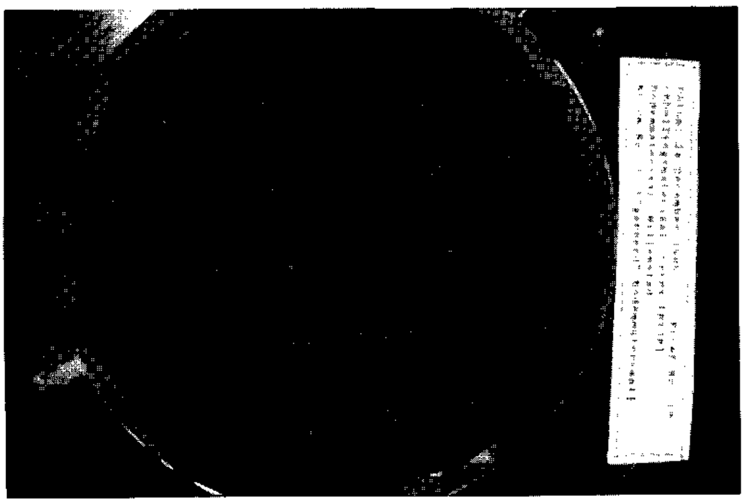

Figure 25. Contact erosion patterns in the soil at the soil/envelope interface, after completion of a flow test.

soil, no significant differences were found, though it appears that (a) drainage without an envelope may be considered, and (b) voluminous envelopes do slightly worse than thin ones.

After the completion of the tests, patterns of soil, washed through the envelopes and settled on top of the perforated support templates were photographed (Fig. 24). Mostly if not exclusively, heterogeneous sedimentation patterns were observed (Bakker, 1988). Following the careful removal of the envelope sample discs, contact erosion patterns were often recognized at the soil/envelope interface surface (Fig. 25).

3.3 Discussion

The cumulative discharges were widely scattered, both for the voluminous and thin envelopes. They were not clearly related to the effective opening sizes (O_{90}) of envelopes. For instance, when using "PSL" (O_{90} approx. 1000 µm) the cumulative discharge was quite variable, while substantial discharges were observed with Polypropylene fibres 450 (450 µm), (Annex 2, No. 12, 18, 19, 20). The hydraulic performance of thin envelopes was often satisfactory. With voluminous envelopes, initial hydraulic conductivities of the composite soil/envelope samples were generally higher than with thin ones (Fig. 20). During the flow tests, the cases where the hydraulic conductivity increased by far outnumber those with decreasing conductivity (Fig. 21).

Using voluminous envelopes, pipe sedimentation was proportional to the initial hydraulic conductivity of the composite soil/envelope sample. With thin ones, the trend appeared to be the reverse. The particle retention capability of voluminous envelopes was insufficient to cope with relatively loose, permeable and unstable backfill when the hydraulic gradient of the flowing water exceeded a critical value. The soil was no longer adequately supported by the envelope and beginnings of contact erosion introduced cavities at the interface between envelope and soil. This often lead to favourable hydraulic flow conditions, but at the expense of a substantial rate of pipe sedimentation. Thin envelopes gave a better protection against pipe sedimentation when the soil backfill was loose. In less permeable soils, pipe sedimentation would be substantial due to the development of critical hydraulic gradients. Still, the resulting hydraulic conductivity was generally lower than with voluminous envelopes. In general, it may be concluded that:

1. The *hydraulic conductivity* of porous media near a drain, wrapped with a voluminous envelope generally becomes higher than the conductivity near a drain, wrapped with a thin envelope;

2. The *particle retention capability* of voluminous envelopes is worse than the retention capability of thin envelopes;

3. A certain rate of *pipe sedimentation* is beneficial for the hydraulic conductivity of a soil/envelope combination, regardless of the type of envelope.

There is a weak but positive link between pipe sedimentation rate and cumulative discharge (Fig. 22). Voluminous envelopes give less protection against pipe sedimentation than sheet envelopes. The particle retention capability of voluminous envelopes is not clearly related to the effective opening size (O_{90}) of these envelopes. "PS-LDPE" (O_{90} approximately 1000 μm) conveys small as well as very large quantities of soil particles while protecting a similar sample (Annex 2, No. 22 and 23). Acceptable quantities pass through cocos envelopes (1200 μm) while those flowing through Polypropylene fibres 450 (450 μm) are sometimes too big (No. 5 and 12). In individual cases, substantial quantities of soil may pass through thin envelopes. Nevertheless, as a group, their particle retention capability is better than that of voluminous envelopes. This result is in accordance with

Table 7. Some envelopes with their hydraulic properties and particle retention capability. Figures are averages of four repetitions.

No.	envelope	0_{90} (μm)	layer thickness of pipe sediment (mm)	cumulative discharge (mm)
29	"Cerex" (N-25)	200	0	1234
33	Glass fibre sheet	250	0	2412
36	"Typar" 3267	320	0	3632
35	"Typar" 3207	340	8	2867
26	"Big 'O'" Stand. 150 dtex	400	13	3099
28	"Big 'O'" Stand. 150 dtex	400	3	734
12	PP 450	450	24	4513
10	Peat/cocos mixture	650	13	3435
14	PP 700 (5 mm)	700	31	3678
19	Polystyrene ("PSL")	1000	14	1339
20	Polystyrene ("PSL")	1000	22	7367
22	Polystyrene ("PS-LDPE")	1000	1	446
24	Polystyrene ("PS-LDPE")	1000	23	3045
5	Coconut fibres 750 gr/m^2	1200	9	3927

findings from the first project.

Effective opening sizes (O_{90}) of several envelopes were known. Table 7 gives pipe sedimentation rates and cumulative discharges, as observed with these envelopes. It can be seen that the particle retention capability of envelopes is poorly correlated with their effective opening size. Cumulative discharges are even more scattered.

Differences in performance between voluminous and thin envelopes are less pronounced than might be expected on the basis of theoretical model studies.

Based on the Envelope Suitability Index (ESI), the use of envelopes is recommended on all the soils, except for the "Willemstad" soil. "Willemstad" soil samples could not be taken at drain depth due to shallow groundwater tables. Instead, they were sampled at approximately 0.5 m depth below surface. The clay content of this soil decreases rapidly with depth and as a result, soil at drain depth (1.2 m) is less stable than soil at shallower depths.

Regrettably, it was not possible to compare these results with field observations made at the experimental fields "Uithuizermeeden", "Valthermond" and "Willemstad", because in these fields drainage resistances had been observed but almost no pipe sedimentation rates had been measured.

4 CONCLUSIONS

From 1982 to 1988, laboratory research was carried out with the intention of defining design specifications for drain envelopes to be used in weakly-cohesive soils.

During the **first project**, cohesionless soil samples were used with the intention of comparing the envelope properties, rather than simulating field conditions. Flow was one-dimensional through homogenized soil samples. The results were straightforward and confirmed earlier findings, but the reproducibility of the results was poor, the ultimate hydraulic conductivities of the soil samples being widely scattered, a factor which could not be controlled. Unfortunately, no sound data were available to compare the results with field observations. This is common practice in this area of research; it challenges the applicability of the results of this type of test, which essentially remains uncalibrated.

During the **second project**, untreated weakly-cohesive soil samples were used in an attempt to simulate field conditions. Perforce, reproducibility had a lower priority. Results were much more scattered but not really in conflict with those of the first project.

In the weakly-cohesive soils, pipe sedimentation rates and cumulative discharges were not clearly related to the effective opening sizes (O_{90}) of the envelopes.

The hydraulic conductivities of most observed composite soil/envelope combinations increased during the tests. This is not in accordance with field observations and is caused by a mismatch between the limited size of the permeameters and the volumetric areas of the porous media near a drain in the field. In the laboratory, water is forced to flow through a relatively small volumetric area. In the field this area is much larger, hence at equilibrium a flow pattern will establish such that areas of relatively low hydraulic conductivity are bypassed by flow through areas of higher permeability. In the analogue model tests, very high hydraulic gradients are easily created, forcing water to flow through low-conductivity areas of the soil samples in the permeameters. Recently, Dierickx (1991) imposed hydraulic gradients as high as 20 near drain envelopes in a permeameter flow test, but there is no evidence for the existence of such high gradients in the field.

The structural stability of weakly-cohesive soils near installed drains is difficult to quantify and usually unknown. There is no scientific proof that structural stability is adequately simulated in an analogue laboratory model. Factors like subsoil heterogeneity, soil moisture content while draining, previous soil manipulations (e.g. deep plowing, infilling, levelling) may strongly influence soil/envelope interface interaction because they act upon the structural stability of a soil. Due to the growing awareness of these facts and conflicts with field observations analogue modelling in the laboratory was discontinued. This type of experimental research is not useful for extrapolation to the field. As a more promising alternative it was decided to initiate three new projects, intended to gather more information about the processes in the the immediate vicinity of drains, because persistent lack of such data blocked any further progress (Stuyt, 1986b; Stuyt & Oosten, 1987). In these projects, wrapped laterals, their envelopes and the abutting soils were to be minutely observed. The results of these observations are described in the following chapters. □

REFERENCES

Antheunisse, J. 1979. Observations on the decomposition of coconut fibres. J. Gen. Appl. Microbiol. 25:273-277.

Antheunisse, J. 1980. The breakdown of coconut fibres by Trametes Versicolor and Stereum Rugosum. J. Gen. Appl. Microbiol. 26:167-170.

Antheunisse, J. 1981. Decay of coconut fibres by soil microorganisms. J. Gen. Appl. Microbiol. 27:435-442.

Bakker, D.M. 1988. Doorbraakcurven in onderzoek aan drainage omhullings materialen (Breakthrough curves in drain envelope materials). Nota 1921,

ICW, Wageningen, The Netherlands (in Dutch).
Boumans, J.H. 1963. Over instroming en aanstroming bij draineerbuizen zonder en met afdekking (On entry flow and radial flow towards drain pipes without and with cover material). Cult. Techn. Tijdschr. 2:218-229 (in Dutch).
Cavelaars, J.C. 1965. Hydrological aspects of the application of plastic drain pipes and filter materials. Report, Research Div., Koninklijke Nederlandse Heidemaatschappij, Arnhem, The Netherlands. 65 pp.
Cavelaars, J.C. 1966. Hydrological aspects of the application of plastic drain pipes and filter materials. In: Hydrological and technical problems of the land drainage. Czechoslovak Scientific and technical Soc. Agr. and Forestry Sect., Praha 1, Siroka 5, 17 pp.
Cavelaars, J.C. 1967. Problems of water entry into plastic and other drain tubes. Paper No. 5/E/46, Agr. Eng. Symp., Silsoe, Bedford, England.
Cavelaars, J.C. 1970. Toestromingsweerstanden bij buisdrainage (Flow resistances near drain pipes). Report of research carried out at the Royal Dutch Heidemaatschappij, Arnhem. 38 pp. (in Dutch).
Dierickx, W. and N. Leyman. 1978. Veldonderzoek naar de drainerende werking van verschillende drainagematerialen. Het drainageproefveld te Zomergem. (Field observations of the functioning of various drainage materials. The Zomergem pilot area). Report 71, National Institute for Agricultural engineering, B-9220 Merelbeke, Belgium (in Dutch).
Dierickx, W. 1980. Electrolytic analogue study of the effect of openings and surrounds of various permeabilities on the performance of field drainage pipes. Report 77, National Institute for Agricultural engineering, B-9220 Merelbeke, Belgium, ISBN 90 70142 13 9
Dierickx, W. and Yüncüoglu, H. 1982. Factors affecting the performance of drainage envelope materials in structural unstable soils. Agric. Water Manage. 5:215-225.
Dierickx, W. 1991. Evaluation of Egyptian synthetic envelopes for subsurface drainage. Laboratory Agricultural Water Management, National Institute of Agricultural Engineering, B-9220 Merelbeke, Belgium.
Draper, N.R. and H. Smith. 1981. Applied Regression Aanalysis (2nd edition). Wiley & Sons, New York, N.Y. USA.
Genstat 5 Committee, 1987. Genstat 5 Reference Manual. Clarendon Press, Oxford, England.
Homma, F. 1973. Invloed van de doorlatendheid van de drainsleuf op de werking van een drainagesysteem (Influence of the hydraulic conductivity of the drain trench on the functioning of a drainage system). Cult. Techn. Tijdschr.

12(5):207-218 (in Dutch).
Jager, A.W. de. 1960a. Diameter en perforatie van plastic drainbuizen (Diameter and perforation of plastic drain pipes). De Ingenieur 72: B 167 - B 172 (in Dutch).
Jager, A.W. de. 1960b. Review of plastic drainage in The Netherlands. Neth. Journ. Agric. Sci. 8(4):261-270.
Jonkers, H.J. and G. Miedema. 1975. Resultaten van het onderzoek naar de intreeweerstand van drains op proefvelden (Results of measurements of entrance resistances of laterals in pilot areas). C.D. Mededelingen 114 (in Dutch).
Knops, J.A.C. and F.C. Zuidema. 1977. Aanbevelingen voor de keuze van omhullingsmaterialen voor drainbuizen (Recommendations for selection of envelope materials for drain pipes). Cult. Techn. Tijdschr. 16:274-283.
Knops, J.A.C. 1979. Research on envelope materials for subsurface drains. Proc. Int. Drain. Workshop, ed. J. Wesseling. ILRI, Wageningen, The Netherlands: 368-392.
Knops, J.A.C., F.C. Zuidema, C.L. van Someren and J. Scholten. 1979. Guidelines for the selection of envelope materials for subsurface drains. Proc. Int. Drain. Workshop, ed. J. Wesseling. ILRI, Wageningen, The Netherlands: 439-450.
Meijer, H.J. and R.A. Feddes. 1972. Afdek- en omhullingsmaterialen bij plastic drainbuizen (Cover- and envelope materials for plastic drain pipes). Nota 690, ICW, Wageningen, The Netherlands (in Dutch).
Meijer, H.J. 1973. Enkele bepalingen van de factoren die gebruikt worden bij de kwaliteitseisen voor turfvezel voor drainagedoeleinden (Some determinations of the factors which are used in conjunction with standards for peat fibres which are applied for drainage purposes). Nota 781, ICW, Wageningen, The Netherlands (in Dutch).
Meijer, H.J. 1974. Intreeweerstanden van recent verschenen drainage-, afdek- en omhullingsmaterialen (Entrance resistances of several, recently proposed, cover and envelope materials for drainage). Nota 788, ICW, Wageningen, The Netherlands (in Dutch).
Meijer, H.J. and J.A.C. Knops. 1977. Veldonderzoek naar de bestendigheid van cocosvezels als afdek- en omhullingsmateriaal voor drainbuizen (Field survey into the persistancy of coconut fibres as cover- and wrapping material for drain pipes). Misc. Reprints 201 ICW, Wageningen, The Netherlands (in Dutch).
Nieuwenhuis G.J.A. and J. Wesseling. 1979. Effect of perforation and filter material on entrance resistance and effective diameter of plastic drain pipes.

Agric. Water Manage. 2:1-9.
Scholten, J. 1988. Vijfentwintig jaar drainagematerialenonderzoek bij de rijksdienst voor de IJsselmeerpolders (Twenty-five years of drain envelope research by the Dutch Polder Development Authority). Flevobericht nr. 291, Ministerie van Verkeer en Waterstaat. ISBN 90 369 1040 4 (in Dutch).
Seijger, L.G. 1978. Laboratorium onderzoek van omhullingsmaterialen voor drainbuizen (Laboratory research into envelope materials for pipe drains). Nota 1088, ICW, Wageningen, The Netherlands (in Dutch).
Seijger, L.G. 1980. Ontwikkelingen en het onderzoek op het gebied van drainagematerialen (Developments and the research concerning drainage materials). Polytechnisch Tijdschrift 35: 110-115 (in Dutch).
Someren, C.L. van, and W.H. Naarding. 1965. Enkele in 1963 verkregen resultaten op twee drainage proefvelden in de Provincie Drenthe (Some results, obtained in 1963, from two experimental fields, designed for observations of agricultural drainage systems in the Province of Drenthe). Mededelingen Cultuurtechnische Dienst, Utrecht, The Netherlands (in Dutch).
Stuyt, L.C.P.M. 1981a. A new approach in research into drainage materials. Nota 1276, ICW, Wageningen, The Netherlands.
Stuyt, L.C.P.M. 1981b. Developments in research on drainage filter materials in The Netherlands. Soil and Water 9:12-13.
Stuyt, L.C.P.M. 1982a. Stochastische simulatie van de bepaling van een pF-curve van grofkorrelige materialen (Stochastic simulation of the determination of a suction curve of coarse-textured granular materials). Nota 1336, ICW, Wageningen, The Netherlands (in Dutch).
Stuyt, L.C.P.M. 1982b. A new approach in research into drainage materials. In: Land Drainage. Ed. M.J. Gardiner, Balkema, Rotterdam, The Netherlands.
Stuyt, L.C.P.M. 1983a. Laboratoriumonderzoek aan drainage omhullings materialen: een interim-rapportage (Laboratory research on land drainage envelope materials: intermediate reporting). Nota 1436, ICW, Wageningen, The Netherlands (in Dutch).
Stuyt, L.C.P.M. 1983b. Drainage envelope research in The Netherlands. Proc. Sec. Int. Drain. Workshop, CPTA, Carmel, IN, USA:106-123
Stuyt, L.C.P.M. 1984a. Recherches de laboratoire concernant les sables fins sensibles au colmatage des tuyaux et des materiaux filtrants (Laboratory research concerning fine sandy soils, prone to clog pipes and filter materials). Nota 1528, ICW, Wageningen, The Netherlands (in French).
Stuyt, L.C.P.M. 1984b. Laboratory investigation into soil/envelope material interactions: intermediate results. Nota 1529, ICW, Wageningen, The Netherlands.

Stuyt, L.C.P.M. 1985. Recherches de laboratoire concernant les sables fins sensibles au colmatage des tuyaux et des materiaux filtrants (Laboratory research concerning fine sandy soils, prone to clog pipes and filter materials). Revue du Syndicat National des Entreprises de Drainage, France 28/29:17-21 (in French).

Stuyt, L.C.P.M. 1986a. Land Drainage. In: Geotextiles and Geomembranes in Civil Engineering. Ed. R. Veldhuijzen van Zanten, Balkema, Rotterdam - Boston, 503-526.

Stuyt, L.C.P.M. 1986b. A non-destructive morphological study of mineral clogging of drains. Proc. Int. Sem. on Land Drainage, Helsinki, Finland, 90-111.

Stuyt, L.C.P.M. and T. Cestre. 1986. Common lines in research on drainage envelopes in France and in The Netherlands. Proc. Symp. Agric. Water Managem., Arnhem, The Netherlands. Ed. J. Wesseling and A.L.M. van Wijk, Balkema, Rotterdam, The Netherlands.

Stuyt, L.C.P.M. and A.J. Oosten. 1987. Mineral and Ochre Clogging of Subsurface Land Drainage Systems in The Netherlands. Geotextiles and Geomembranes 5(2): 123-140.

Stuyt, L.C.P.M. 1987. Developments in land drainage envelope materials. Proc. Symp. 25th Int. Course on Land drain., Publication 42, ILRI, Wageningen, The Netherlands.

Wesseling, J. and F. Homma. 1964. Resultaten van het meten van intreeweerstanden van plastiek drainbuizen (Results of measurements of entrance resistances of plastic drain pipes). Nota 251, ICW, Wageningen, The Netherlands (in Dutch).

Wesseling, J. and F. Homma. 1965. Resultaten van het onderzoek naar de invloed op de intreeweerstand van verschillende omhullingsmaterialen voor drainagebuizen (Results of research concerning the influence of various envelope materials on the entrance resistance of drain pipes). Nota ICW, (October 1965), Wageningen, The Netherlands. (in Dutch).

Wesseling, J. and F. Homma. 1967. Entrance resistance of plastic drain tubes. Neth. J. Agric. Sci., 15.3:170-182.

Wesseling, J. and C.L. van Someren. 1972. Drainage Materials. Provisional report of the experience gained in The Netherlands. In: Irr. and Drain. Paper No. 9: "Drainage Materials", FAO Rome: 55-84.

Wesseling, J. 1979. The entrance resistance of drains as a factor in design. Proc. Int. Drain. Workshop, ed. J. Wesseling. ILRI, Wageningen, The Netherlands: 368-392.

Widmoser, P. 1968. Der Einfluss von Zonen geänderter Durchlässigkeit im Bereich von Drän- und Brunnenfilterrohren. (The impact of zones with

modified hydraulic conductivity near drain pipes and wells). Schweiz. Bauzeitg, 86H, 9. (in German).
Willet, J.R. 1962. "Ongerijpte" zandgronden en hun ontwatering ("Unripened" sandy soils and drainage of these soils). Tijdschrift der Koninklijke Nederlandsche Heidemaatschappij, 73(12):403-408 (in Dutch).
Zuidema, F.C. and J. Scholten. 1979. Model tests on drainage materials. Proc. Int. Drain. Workshop, ed. J. Wesseling. ILRI, Wageningen, The Netherlands: 393-401.

UNPUBLISHED REFERENCES

Boers, Th. M. 1975. Some aspects of sand model experiments for testing drainage materials especially with respect to the seepage surface. Unpubl. M. Sc. Thesis, Agricultural University Wageningen, The Netherlands.
Cutuurtechnische Dienst. 1964. Ontwerp keuringseisen voor glasvlies, toe te passen voor omhulling van drainbuizen (Draft testing requirements for glass fibre sheet as envelope material for drain pipes). (in Dutch).
Eskes, B.T.F. 1977. Laboratorium onderzoek naar de poriënverdeling, de filtrerende en hydrologische eigenschappen van synthetische omhullingsmaterialen voor drainbuizen (Laboratory investigation into the pore size distribution, the filtering and hydrologic properties of synthetic envelope material for drain pipes). Intern Rapport ILRI/ICW (Confidential report ILRI/ICW, Wageningen, The Netherlands) (in Dutch).
Feddes, R.A. 1966. Recente ontwikkelingen in plastiek drainage (Recent developments in drainage by plastic materials). Unpubl. M.Sc. thesis, Agricultural University, Wageningen, The Netherlands.
Kumova, Y. 1979. Some aspects of the use of sand models for testing drainage materials in the laboratory. Unpubl. M.Sc. Thesis, M.Sc.-Course on Soil Science and Water Management, Agricultural University, Wageningen, The Netherlands.
Meijer, H.J. 1972. Intreeweerstanden van ribbel-drainbuizen voorzien van machinaal aangebrachte omhullingsmaterialen (Entrance resistances of corrugated prewrapped drain pipes). Interne Nota 689, ICW, Wageningen, The Netherlands (in Dutch).
Oosten, A.J. and L.C.P.M. Stuyt. 1986. Handleiding onderzoek drainage omhullings materialen (Manual drain envelope research). Unpubl. internal Note, ICW, Wageningen, The Netherlands (in Dutch).
Someren, C.L. van, and Th. M. Boers. 1977. Sand model experiments for testing

drainage materials. Unpublished report, Drainage and Reclamation Institute of Pakistan, Hyderabad, Pakistan.
Stuyt, L.C.P.M. en A.J. Oosten. 1986. Het onderzoek aan drainage omhullings materialen; interim-rapport 1 (Research into drainage materials; Intermediate Report 1). Vertrouwelijk rapport, ICW, Wageningen, The Netherlands (Confidential report in Dutch; summary in English).
Stuyt, L.C.P.M. en D.M. Bakker. 1987. Het onderzoek aan drainage omhullingsmaterialen; interim-rapport 2 (Research into drainage materials; Intermediate Report 2). Vertrouwelijk rapport; ICW, Wageningen, The Netherlands (Confidential report in Dutch; summary in English).
Stuyt, L.C.P.M. 1988a. Het onderzoek aan drainageomhullingsmaterialen: Projectvoorstel 1988-1989. / Drainage envelope research: Project Proposal 1988-1989. Intern Rapport, ICW, Wageningen, The Netherlands (bilingual report: English/Dutch).
Stuyt, L.C.P.M. 1988b. Het onderzoek aan drainageomhullingsmaterialen: Eindrapport 1985-1988. Deel 1: tekst (Research into drainage materials: Final Report 1985-1988. Part 1: text) Vertrouwelijk rapport ICW, Wageningen, The Netherlands (in Dutch; summary in English).
Stuyt, L.C.P.M. 1988c. Het onderzoek aan drainageomhullingsmaterialen: Eindrapport 1985-1988. Deel 2: figuren (Research into drainage materials: Final Report 1985-1988. Part 2: figures) Vertrouwelijk rapport ICW, Wageningen, The Netherlands (in Dutch).
Stuyt, L.C.P.M. 1989. Drain envelope research project. Final report 1985-1988. Part 1: text. Confidential Report, ICW, Wageningen, The Netherlands.
Wesseling, J. 1975. Modelonderzoek drainomhulling en afdekking (ICW) (Model tank research on drain envelopes and cover materials (ICW)). Unpublished Note, ICW, Wageningen, The Netherlands (in Dutch).

3 INTERNAL AND GRADE LINE EXAMINATION OF LATERAL DRAINS

3 Internal and grade line examination of lateral drains

ABSTRACT

Using a miniature video camera inspection system, a field survey was made of soil invasion and sedimentation patterns, root penetration and other phenomena in pipe laterals, wrapped with various envelope types and installed in three experimental fields in the Netherlands. These fields are located in areas with very fine-sandy, marine deposits ("Uithuizermeeden" and "Willemstad") and in a raised bog region ("Valthermond"). A total length of 9634.5 m of lateral drain was inspected. All drains were installed in weakly-cohesive, very fine sandy soils where pipe sedimentation is a severe problem. The video images were visually interpreted at 0.5 m intervals. The grade line of the inspected laterals was continuously recorded with special equipment, providing lateral depth at 0.5 m intervals. An attempt was made to correlate the results of this survey to average drain entry and flow resistances of plots, containing various envelope materials. Generally, drainage resistance was not significantly correlated with the experimental field, the envelope category ("thin" or "voluminous") or the envelope material. In the "Valthermond" experimental field however, where drains are also used for subirrigation, plots with voluminous envelopes had significantly lower drainage resistances than plots where thin envelopes had been used. The drains had been installed very accurately, hence neither the grade lines of the drains nor their standard deviations had a significant effect on drainage resistance. The rate of pipe sedimentation differed greatly and significantly between the experimental fields. The soil particle retention capability of envelopes was strongly associated with the effective opening size, O_{90} and also with envelope category. The mechanism of soil invasion into drains observed in the field was different from the processes observed in analogue soil tank models. Generally, sedimentation rates, observed from analogue models are in conflict with field observations.

1 INTRODUCTION

The suitability of drain envelopes to protect subsurface agricultural drains from excessive sedimentation yet promote easy access of water into such drains may be observed in the field or in an analogue soil tank model. Analogue modelling is of limited value if the results cannot be correlated with field observations; see

Chapter 2. In practice, field observations are usually restricted to measurements of drainage resistances. This is insufficient to obtain an unbiased assessment of the functioning of drain envelopes unless accurate sedimentation data are available.

In the Netherlands, few attempts have been made to inspect laterals in situ. Van der Louw (1986) used a modified flexible endoscope system to carry out spot checks. He found that soil was squeezed into drains as saturated slurry. Measurement of pipe sedimentation rates with a video inspection system was considered too costly for general use. An alternative cheaper method is used to check pipe sedimentation rates at local spots. This method is essentially an extension of the technique of drain rodding, which was developed to qualitatively check newly installed drains for grade line precision. A steel pipe, fitted with a torpedo-shaped probe is manually pushed through the drain with the aid of a flexible fibreglass rod, and the force required to do so is qualitatively assessed. Sliding friction is assumed to be proportional to grade line irregularity (Van Zeijts, 1987). While rodding, pipe sedimentation rates are observed as follows. When the friction exceeds a predetermined value, an excavation is made at the location where the probe was trapped and conclusions as to the problem are drawn on the basis of visual inspection. This technique is questionable because the high sliding resistance of the rod may be due to accumulation of sediment during advance, and not to local sedimentation. Hence, this application of the rodding technique is not justified for research purposes. Moreover, rodding does not yield sedimentation data over the entire length of the lateral.

Pipe sedimentation is usually assumed to be related to depth variations of a drain, and to occur preferentially in sags. Grade line irregularity and associated sedimentation may affect the overall hydraulic performance of drains. It is wrong therefore to attribute differences in drainage resistance to differences between envelopes only. For a more accurate interpretation of these resistances grade line data are indispensable.

The survey described in this chapter was not included in the original research programme for the experimental fields. It was added later, motivated by the desire to check the validity of analogue sand tank models, the growing discontent about the persistent lack of sedimentation data and to correct possible misinterpretation of drainage resistance figures. Hence, the data were used for three purposes:

1. *Comparison of pipe sedimentation rates* in the field with results from analogue soil tank models,

2. Investigation of *factors that control pipe sedimentation* rate, such as soil type (i.e. location of experimental field), envelope material (category (i.e.

"thin" or "voluminous")); effective opening size (O_{90}) and grade line parameters,

3. Investigation of *factors that* presumably *affect drainage resistance*, such as soil type, envelope material and grade line parameters.

2 THE EXPERIMENTAL FIELDS

In the early 1980s, three experimental fields were established by research units of more or less autonomous, local offices of the Dutch "Landinrichtingsdienst" (Governmental Service for Land and Water Use) to compare field performances of 12 different envelope materials. All observations, discussed in this Chapter, were made in these fields. The layout of all the drainage systems is singular; they are depicted in Fig. 1. Soil textures are given in Table 1.

Table 1. Textures of soils where the experimental fields are located.

Experimental Field	Soil type	Clay (%)	Silt (%)	Median (μm)
"Uithuizermeeden"	silty sand	8	11	76
"Valthermond"	loamy sand	4	4	120
"Willemstad"	alkaline silt	9	26	69

Each field consists of adjacent blocks: 2 in "Uithuizermeeden" and in "Valthermond" and 3 in "Willemstad". The blocks, in turn, were subdivided into 3 to 8 adjacent plots for testing a specific envelope material. Each plot contained 4 to 6 drains. All lateral drains are approximately 200 m long, except for those in "Valthermond" (70 m). Drain spacings are 10 m ("Uithuizermeeden"), 15 m ("Willemstad") and 10 and 20 m ("Valthermond"). Average drain depth ranges from 1.0 to 1.2 m. Drains in "Uithuizermeeden" and "Willemstad" were intended for groundwater drainage only and were laid with a design slope of 0.15%. Drains in "Valthermond" were to be used for subirrigation too and were laid horizontally. Orthogonality of these field experiments was not pursued; most envelope types were installed in one or two experimental fields only: 9 (3 thin and 6 voluminous) in "Uithuizermeeden", 6 (3 and 3) in "Valthermond" and 6 (4 and 2) in "Willemstad" (Table 2). All drains have 60 mm outside diameters except for pipes wrapped with "Big 'O'", glass fibre membrane, peat-coconut fibre mixture and "Typar" in experimental field "Willemstad" (65 mm). In total, 184 laterals were included in the observations.

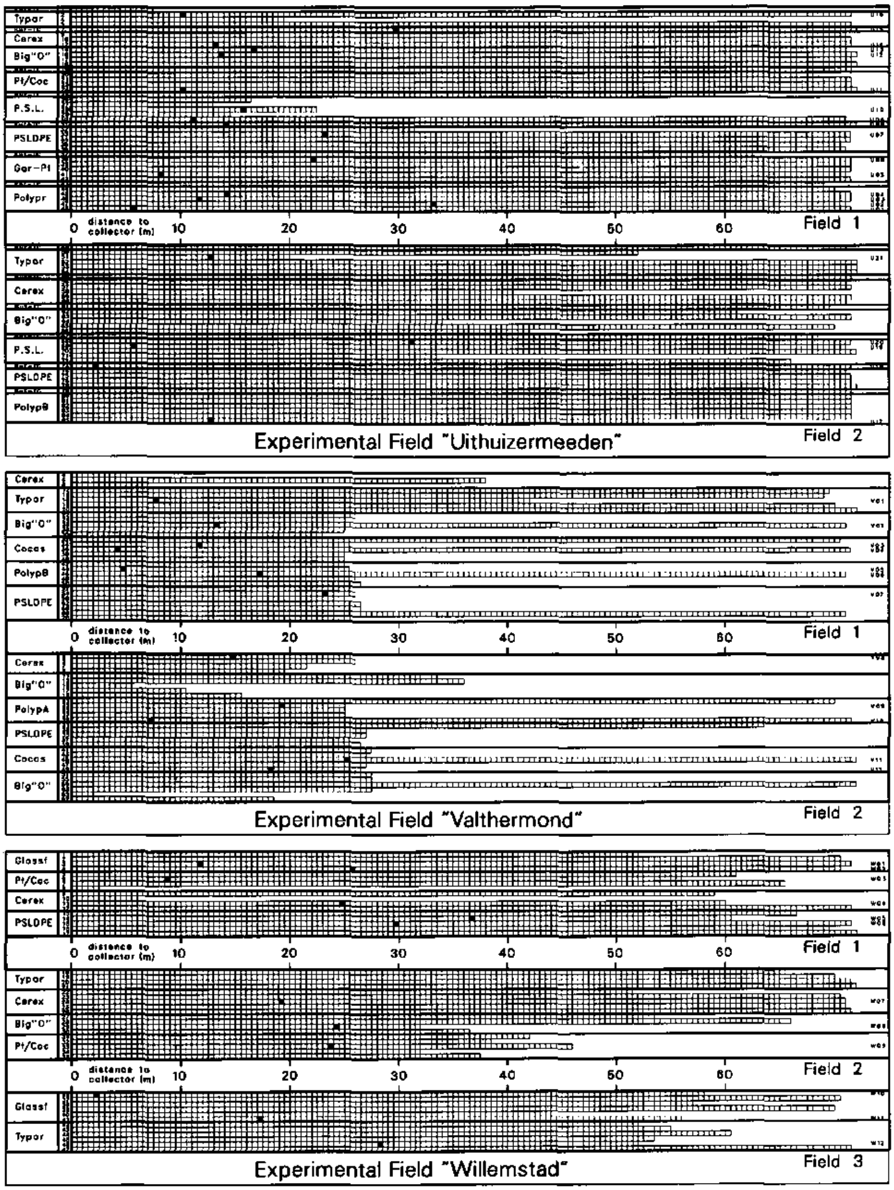

Figure 1. **Layout of the experimental fields. Sample core retrieval locations are indicated as black dots (see Chapter 4).**

Table 2. Total lengths of the investigated laterals, wrapped with 12 different envelopes and located in adjacent blocks of experimental fields located near Uithuizermeeden, Valthermond and Willemstad.

Type of envelope	Uithuizermeeden all laterals length (m)	Valthermond all laterals length (m)	Willemstad all laterals length (m)	Total all laterals length (m)
Thin envelope	1555.0	911.5	1963.5	4430.0
Voluminous env.	3299.5	1184.0	721.0	5204.5
All envelopes	4854.5	2095.5	2684.5	9634.5

	Uithuizermeeden		Valthermond		Willemstad			Total
	block 1	block 2	block 1	block 2	block 1	block 2	block 3	
	length (m)		length (m)		length (m)			length (m)
All envelopes	2528.0	2326.5	1160.0	935.5	986.0	998.5	700.0	9634.5
Thin envelope	663.0	892.0	542.5	369.0	461.0	802.5	700.0	4430.0
Voluminous env.	1865.0	1434.5	617.5	566.5	525.0	196.0	--	5204.5
Big 'O' sock	286.5	278.5	170.0	276.5	--	188.0	--	1199.5
"Cerex"	214.0	325.5	50.0	92.5	196.5	335.5	--	1214.0
Glass fibre mb.	--	--	--	--	264.5	--	355.5	620.0
"Typar"	162.5	288.0	322.5	--	--	279.0	344.5	1396.5
Coconut fibres	--	--	217.5	180.0	--	--	--	397.5
Peat-Coconut f.	283.5	--	--	--	185.0	196.0	--	664.5
Buffer-Peat/Co.	415.5	476.5	--	--	--	--	--	892.0
"Garden" peat f.	357.0	--	--	--	--	--	--	357.0
Polypropyl. A	--	--	174.0	216.5	--	--	--	390.5
Polypropyl. B	355.5	357.5	--	--	--	--	--	713.0
Polystyrene "PSL"	137.5	314.5	--	--	--	--	--	452.0
Polystyrene "PS-LDPE"	316.0	286.0	226.0	170.0	340.0	--	--	1338.0

3 OBSERVATIONAL PROCEDURES

Internal features of laterals were observed with a video inspection system. Grade lines were determined with a specially designed instrument. The video camera was mounted on top of a 70 m long glass fibre rod, hence most drains could be inspected along only part of their length. In total, 9634.5 m of lateral length was examined: 4854.5 m in experimental field "Uithuizermeeden" (28% of the total length of laterals in that experimental field), 2095.5 m in "Valthermond" (43%) and 2684.5 m in "Willemstad" (30 %). 4430.0 m (46%) of the laterals were wrapped with a "thin" envelope (thickness ≤ 1 mm) and 5204.5 m (54%) with a "voluminous" envelope. Features including drain depths were observed at 0.5 m intervals. The total number of observation points was 18901. The singular drain layout meant all laterals were accessible through their outlets in the collector ditches. The outlets were excluded from the analysis.

3.1 Internal inspection of drains

Equipment. Fig. 2 and 3 show the video inspection system. It consists of a remote focus 35 mm diameter b/w camera, 230 mm long, with lights, fitted with a 17 mm vidicon tube and including 100 m of control cable. This is fitted to a console which includes a camera control unit for focus and light intensity, a video monitor, a PAL-VHS video recorder, a video writer, a video monitor and an audio recording facility. Although newer camera types were available, this camera was the only suitable one because of its cable length and small diameter. A 7 mm diameter glass fibre rod was selected after experiment as the pushing agent offering the best compromise between stiffness and flexibility. No automatic meterage count unit was available so the camera control cable was taped onto the glass fibre rod at every 0.5 m, providing distance markers. The camera was not rigidly fixed onto the glass fibre rod but could move independently from the rods' position, allowing it to "climb" over pipe sediment, where possible, instead of pushing it aside. Thus, the risk of sediment collecting on the camera lens was minimized. Power was provided by a 2000 VA petrol generator.

Procedure. The inspection required close cooperation between two operators. The "pushing operator" manually pushed the camera into a drain through its outlet (Fig. 4). The camera was halted for 3 seconds at 0.5 m intervals, producing still, interpretable video images. Simultaneously, the "video operator" coordinated the following: (a) he controlled the video recording system, (b) he prompted the "pushing operator" to slow down the travel speed of the camera in order to accurately record interesting local features, (c) he informed the "pushing operator" about any sudden or gradual deterioration of image quality due to precipitation of dirty water, sediment, mud, roots, spider webs etc. on the camera lens, and (d) he decided on when to pull back the camera to clean the lens.

In theory, each drain could be inspected over a distance of 70 m from its outlet, but in practice the length was occasionally limited due to

1. the *height of the sediment layer*. The camera could pass over pipe sediment layers less than 20 mm thick (60 mm outside diameter drain) or 22 mm thick (65 mm outside diameter drain),

2. the *pushing resistance*. In drains with substantial amounts of mineral deposits the pushing resistance rapidly increased with distance and often prevented further examination,

3. an *excessive grade line irregularity*. Due to grade line irregularities the camera lens was sometimes inevitably pushed into sediment and became dirty,

4. *stagnant water* in the drain. Some low-lying drain sections contained immobile dirty water that blurred the camera lens, and

5. *technical problems*. During the survey, the camera broke down and was temporarily replaced by another unit with only 25 m of control cable. As a consequence, the greater part of the laterals in experimental field "Valthermond" could be inspected over a distance of 25 m only. Later, some laterals were examined again, this time over their entire length of 70 m. In the case of a dirty lens, inspection of a lateral was discontinued after three subsequent, ineffectual attempts.

The survey was made in spring 1988. The preceding winter season had been comparatively dry so few drains were discharging. Additionally, the "Veenmarken" Waterboard had temporarily lowered water levels in the collector ditches of the experimental field "Valthermond" on request. The average pace of inspection was 20.6 $s.m^{-1}$ (all drains), 13.4 $s.m^{-1}$ (experimental field "Uithuizermeeden"), 31.3 $s.m^{-1}$ (experimental field "Valthermond") and 18.7 $s.m^{-1}$ (experimental field "Willemstad"). In total, 55 hours of video images were recorded.

After completion of the field survey, the videotapes were visually examined. This examination was time consuming due to occasional poor image quality, caused by improper camera functioning, water condensation onto the second (internal) lens of the camera and very low-contrast images in dirty pipes. All tapes were examined by one operator, minimizing biased interpretation.

On the video tapes, the following phenomena were clearly visible and could be systematically investigated:

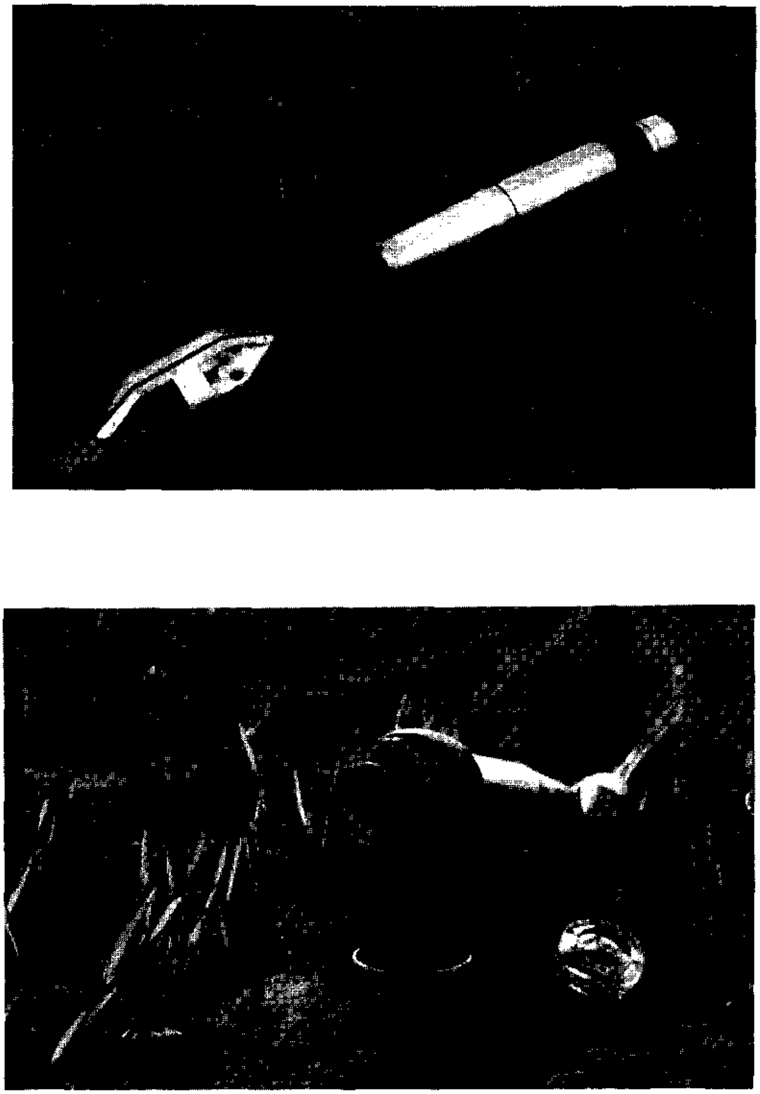

Figure 2. **The video camera: side view (top), frontal view (bottom).**

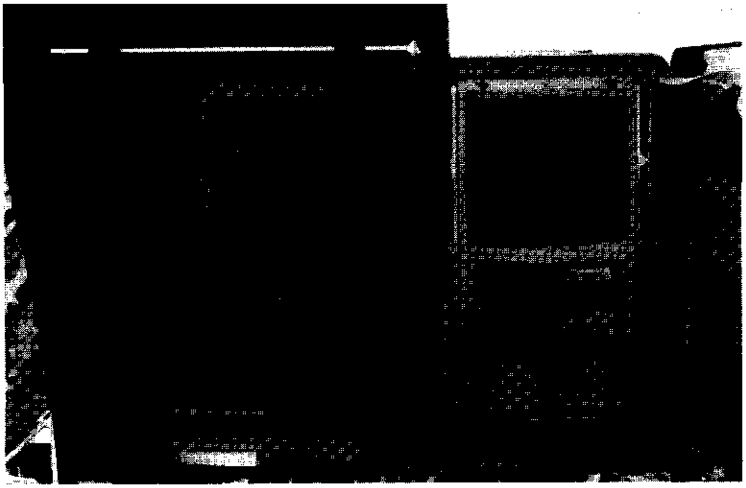

Figure 3. The console with video equipment, containing a remote control unit, a video monitor, a video writer and a PAL-VHS video recorder.

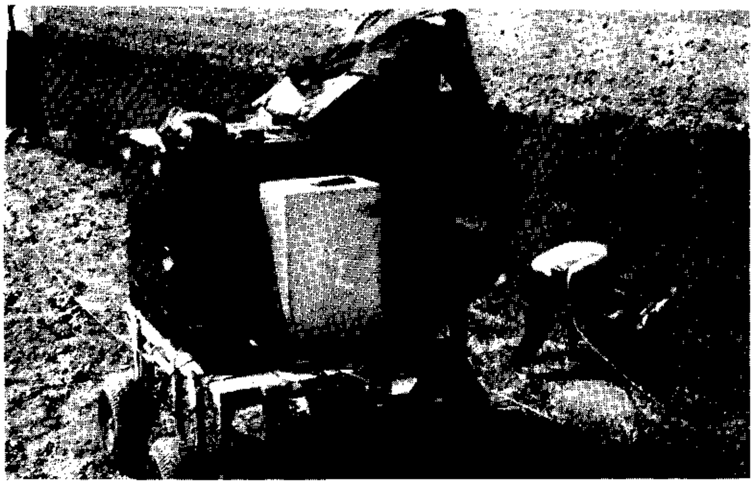

Figure 4. On-site inspection of laterals.

1. Height of the *sediment layer* inside the drain,

2. *Soil invasion* patterns through the *upper* pipe wall section (="downward soil influx"),

3. *Soil invasion* patterns through the *lower* pipe wall section (="upward soil influx"),

4. *Microbiological deposits* (shiny slimes and jelly-like substances),

5. *Stagnant water*, and

6. *Living roots.*

Each of the 18901 drain sections was assigned a qualitative parameter value for every observed phenomenon, as follows:

1. **Sediment layer height**. Parameter: height indicator h = 0.0, 0.5, 1.0, ..., 2.5, 3.0. At h = 3.0, the camera could not pass due to a too high sediment layer; 20 mm in a 60 mm drain and 25 mm in a 65 mm drain. Height indications h [-] were converted into equivalent sediment layer heights H [L] as follows:

$$H = 5.0\ h \qquad (h < 1) \qquad \text{(mm)} \quad (1a)$$

For 60 mm drains:

$$H = 7.5\ h - 2.5 \qquad (h \geq 1) \qquad \text{(mm)} \quad (1b)$$

For 65 mm drains:

$$H = 10.0\ h - 5.0 \qquad (h \geq 1) \qquad \text{(mm)} \quad (1c)$$

where h = qualitative sediment layer height parameter, interpreted from visual inspection of the video image (-), and H = estimated sediment layer height (mm).

2. **Soil invasion** patterns. No soil invasion (0) to excessive soil invasion (5).

3. **Stagnant water** (1) or no stagnant water (0).

4. **Living roots** (1) or no living roots (0).

5. **Microbiological deposits**. No deposits (0) to abundant occurrence of deposits (5).

3.2 Measurement of grade lines

Equipment. The equipment to measure grade lines of drains is schematically depicted in Fig. 5. It consists of a water filled hose connected to a pressure transducer at its lower end, and to an open water tank in which a constant reference level is maintained, at its upper end. The integral pressure transducer monitors the water pressure in a 40 mm diameter brass probe. The water filled hose and the wiring of the transducer are contained in a protective, flexible "HPE" hose. The hose, 200 m long, is coiled on a drum. A 4WD car contains the measuring instrument and a plotter. The measuring system was developed by the "Leichtweiss Institute" of the University of Braunschweig in Germany. It is used by the "Planungsbüro Collins & Schaffer" which has close links with this Institute.

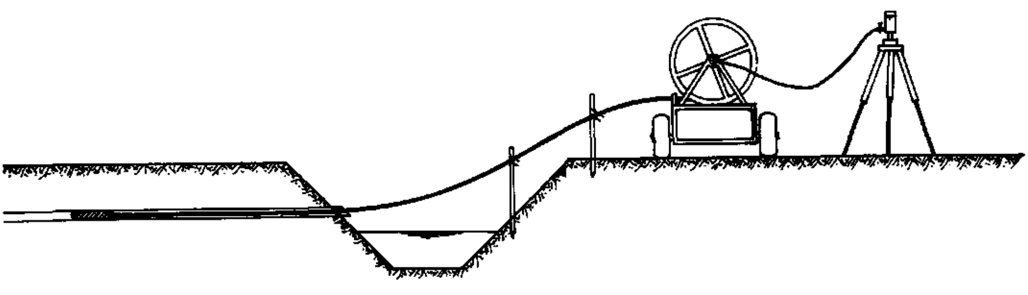

Figure 5. Schematic diagram of the arrangement of the equipment, used for the determination of grade lines of drains. Reprinted with permission from de Boer (1987).

The same equipment had been used in the Netherlands to check the grading accuracy of drains (de Boer, 1987).

Procedure. The equipment was rented including operator service. On site measurement is depicted in Fig. 6. The measuring probe is inserted into the drain by hand. Measurements are made while the probe is pulled out at constant velocity ($0.12\ m.s^{-1}$) by electric power. The water pressure at the transducer is determined from the reference level, basically an open standpipe, and the elevation of the measuring head. Water pressure variations due to vertical travel of the measuring head are detected and converted into electric voltage variations. The vertical elevation of the measuring head relative to reference level is plotted against distance from the drain outlet. The measuring accuracy of the grade line is 2 mm. This part of the survey was made in the autumn of 1989.

After completion of the field survey, the graphical drain depth output data was digitized, yielding depth figures at 0.5 m intervals. Average grade lines and average standard deviations from these lines were calculated for individual drains and for plots containing the same envelope type.

3.3 Drainage Resistance

Drainage resistance data were supplied by the Governmental Service for Land and Water Use ("Landinrichtingsdienst"). During water table recession after wet periods, mid-drain water table elevations H [L] and drain discharges q [$L.T^{-1}$] were observed, yielding drainage resistances γ [T] as

$$\gamma = H.q^{-1} \qquad \text{(d)} \qquad (2)$$

where H = mid-drain water table elevation (m), and q = drain discharge ($m.d^{-1}$).

Drainage resistances are given in Table 3 as averages of 32 plots containing drains which are wrapped with the same envelope. In three cases in the "Uithuizermeeden" experimental field drainage resistances could not be calculated for the following reasons and were excluded from the statistical analysis: (a) Peat-Coconut fibre envelope, due to unreliable data, (b) "Garden" peat envelope, due to unreliable data, and (c) Buffer drains, wrapped with Peat-Coconut fibre envelope and installed between plots with other envelopes.

4 STATISTICAL ANALYSIS

Multiple linear regression was used to investigate, for the 32 observations (i.e.

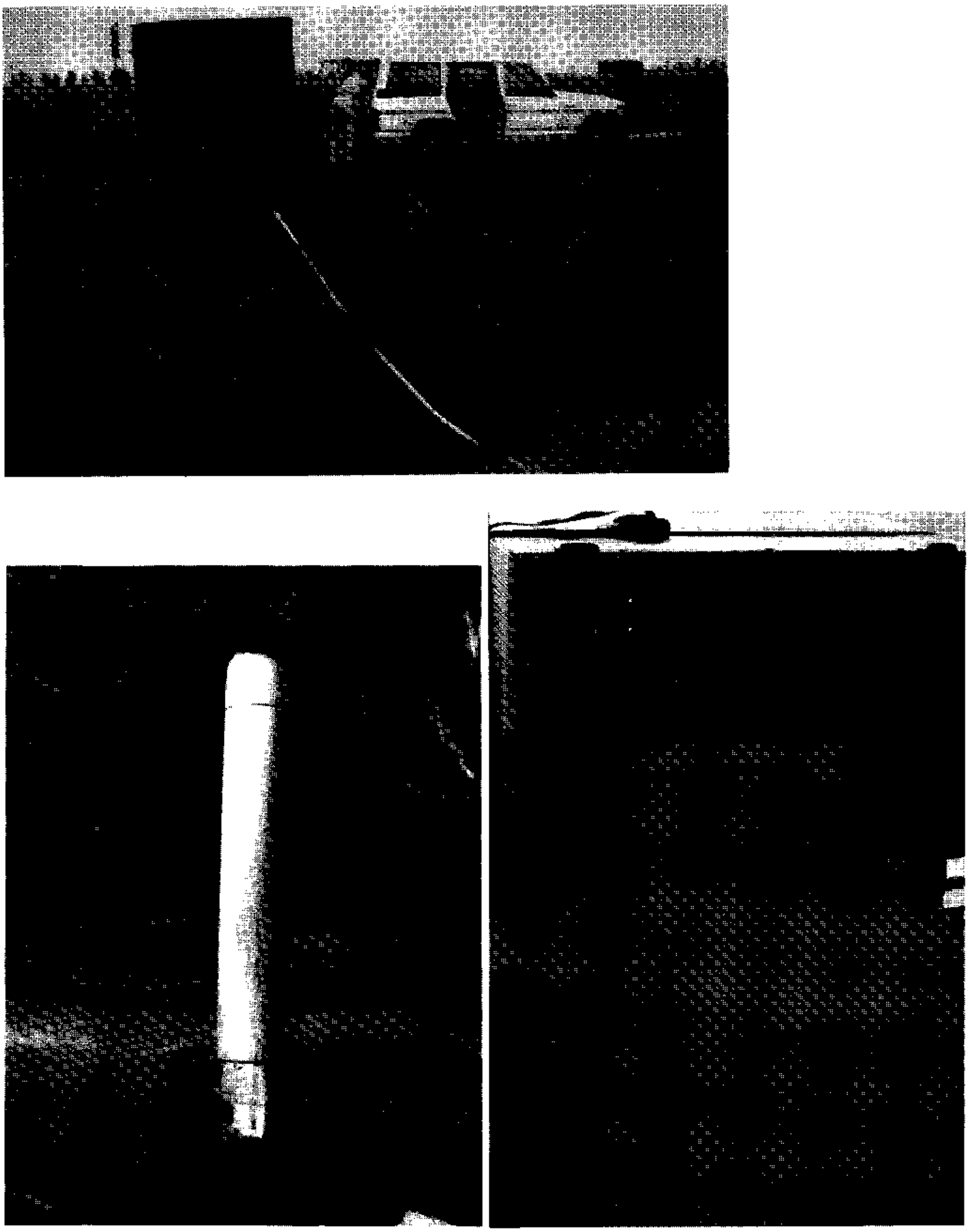

Figure 6. On-site measurement of grade lines of drains: field equipment (top), the 40 mm measuring probe (bottom, left) and continuous graphical output of a grade line (bottom, right).

Table 3. Drainage resistance γ (d), observed at the experimental fields Uithuizermeeden, Valthermond and Willemstad.

	Uithuizermeeden		Valthermond		Willemstad		
	block 1	block 2	block 1	block 2	block 1	block 2	block 3
	resistance γ		resistance γ		resistance γ		
"Big 'O'" sock	113	130	190	106	-	90	-
"Cerex"	197	138	245	275	76	120	-
Glass fibre mb.	-	-	-	-	118	-	98
"Typar"	80	104	524	-	-	95	174
Coconut fibres	-	-	120	92	-	-	-
Peat-Coconut f.	-	-	-	-	84	211	-
Polypropyl. A	-	-	68	118	-	-	-
Polypropyl. B	141	124	-	-	-	-	-
Polystyrene beads "PSL"	140	118	-	-	-	-	-
Polystyrene b. "PS-LDPE"	110	143	-	82	43	-	-

plots) the effect of the following factors and variables on the drainage resistance γ:

1. **soil type,** i.e. location of the experimental field ("Uithuizermeeden", "Valthermond", "Willemstad"),

2. **block within experimental field** (3 blocks in "Willemstad", 2 elsewhere),

3. **envelope material** (12 types; see Table 2),

4. **average grade line** of the drain ($m.km^{-1}$ (‰)),

5. **standard deviation** from the average line (-).

The interaction (location.envelope material) was included in the regression model to see whether differences between envelopes depended on location. A stepwise selection procedure was used to find predictor factors and variables that had a significant effect on γ (Draper & Smith, 1981). The factor "envelope material" was then replaced by envelope category ("thin" or "voluminous") and effective opening size (O_{90}) of an envelope (μm) to find characteristics that explain differences in performance of the envelopes.

A similar regression analysis with 181 observations (i.e.drains) was used to investigate the effect of these factors and variables on pipe sedimentation.

The computations were made with the statistical program "Genstat" (Genstat 5 Committee, 1987).

5 RESULTS

5.1 General

Regularly, a video inspection had to be discontinued: 21 times in experimental field "Uithuizermeeden" (27% of all drains), 13 times in "Valthermond" (22%) and 29 times in "Willemstad" (62%). The reasons for this were:

1. *too high pushing resistance*: "Uithuizermeeden": 9 cases (drains No. 20, 50, 58, 62, 64, 66, 67, 71 and 85); "Valthermond": 2 cases (No. 16 and 65); "Willemstad": 21 cases (No. 1, 6, 7, 11, 13, 14, 16, 28, 29, 30, 31, 32, 33, 35, 36, 41, 42, 43, 44, 45 and 46),

2. *too high sediment layer*: "Uithuizermeeden": 7 cases (drains No. 4, 26, 27, 28, 29, 37 and 43); "Valthermond": 4 cases (No. 6, 7, 31 and 67); "Willemstad": 3 cases (No. 18, 22 and 34), and

3. *dirty camera lens*, due to: iron ochre ("Uithuizermeeden": drains No. 1); roots ("Uithuizermeeden": No. 25 and 65, "Willemstad": No. 38 and 40); sediment ("Uithuizermeeden": No. 32 and 40, "Valthermond": No. 8); wet sediment ("Valthermond": No. 13, and 15, "Willemstad": No. 9); stagnant water ("Valthermond": No. 9, 10 and 17, "Willemstad": No. 8) and weeds ("Valthermond": No. 4).

The results of the field survey are summarized in tables and maps. The values in the tables are averages, weighed with observed lengths of individual drains.

5.2 Grade Lines

In three cases, the grade line of a drain could not be calculated because the measuring probe could not pass through the drain outlet due to subsidence at its connection with the lateral. These cases were excluded from the statistical analysis. Table 4 gives average grade lines. A representative map is presented as Fig. 7. Average standard deviations from grade lines reflect the laying accuracy of laterals. They are given in Table 5, and indicate that, with some minor exceptions,

Table 4. Average grade lines (m.km^{-1}(‰)) of the investigated laterals, wrapped with 12 different envelopes and located in adjacent blocks of experimental fields located near Uithuizermeeden, Valthermond and Willemstad.

Type of envelope	Uithuizermeeden all laterals grade line	Valthermond all laterals grade line	Willemstad all laterals grade line	Total all laterals grade line
Thin envelope	1.15	0.09	0.69	0.63
Voluminous env.	1.40	-0.09	0.73	0.73
All envelopes	1.32	-0.01	0.70	0.68

	Uithuizermeeden		Valthermond		Willemstad			Total
	block 1	block 2	block 1	block 2	block 1	block 2	block 3	
	grade line		grade line			grade line		grade line
All envelopes	1.26	1.38	0.21	-0.23	0.59	0.81	0.82	0.68
"Big 'O'" sock	1.00	1.22	0.16	-0.31	--	0.78	--	0.36
"Cerex"	1.09	1.19	1.96	0.03	0.30	0.72	--	0.84
Glass fibre mb.	--	--	--	--	0.50	--	0.98	0.79
"Typar"	1.10	1.23	-0.17	--	--	0.74	0.66	0.68
Coconut fibres	--	--	0.01	-0.43	--	--	--	-0.21
Peat-Coconut f.	1.46	--	--	--	0.61	0.96	--	0.96
Buffer-Peat/Co.	1.28	1.64	--	--	--	--	--	1.46
"Garden" peat f	1.16	--	--	--	--	--	--	1.16
Polypropyl. A	--	--	-0.03	-0.21	--	--	--	-0.12
Polypropyl. B	0.82	1.30	--	--	--	--	--	1.06
Polystyrene "PSL"	2.02	1.59	--	--	--	--	--	1.80
Polystyrene "PS-LDPE"	1.28	1.38	0.11	-0.04	0.57	--	--	0.59

the laterals were installed with high accuracy. The grade lines of some of these less satisfactory drains and the distribution of pipe sediment are depicted in Fig. 8. Pipe sedimentation rates are given in Table 6 and are depicted in Fig. 9.

5.3 Soil Influx

Soil influx is recognized as "mushroom"-shaped soil patterns near perforations (Fig. 10). Downward influx through the upper pipe wall (most likely trench

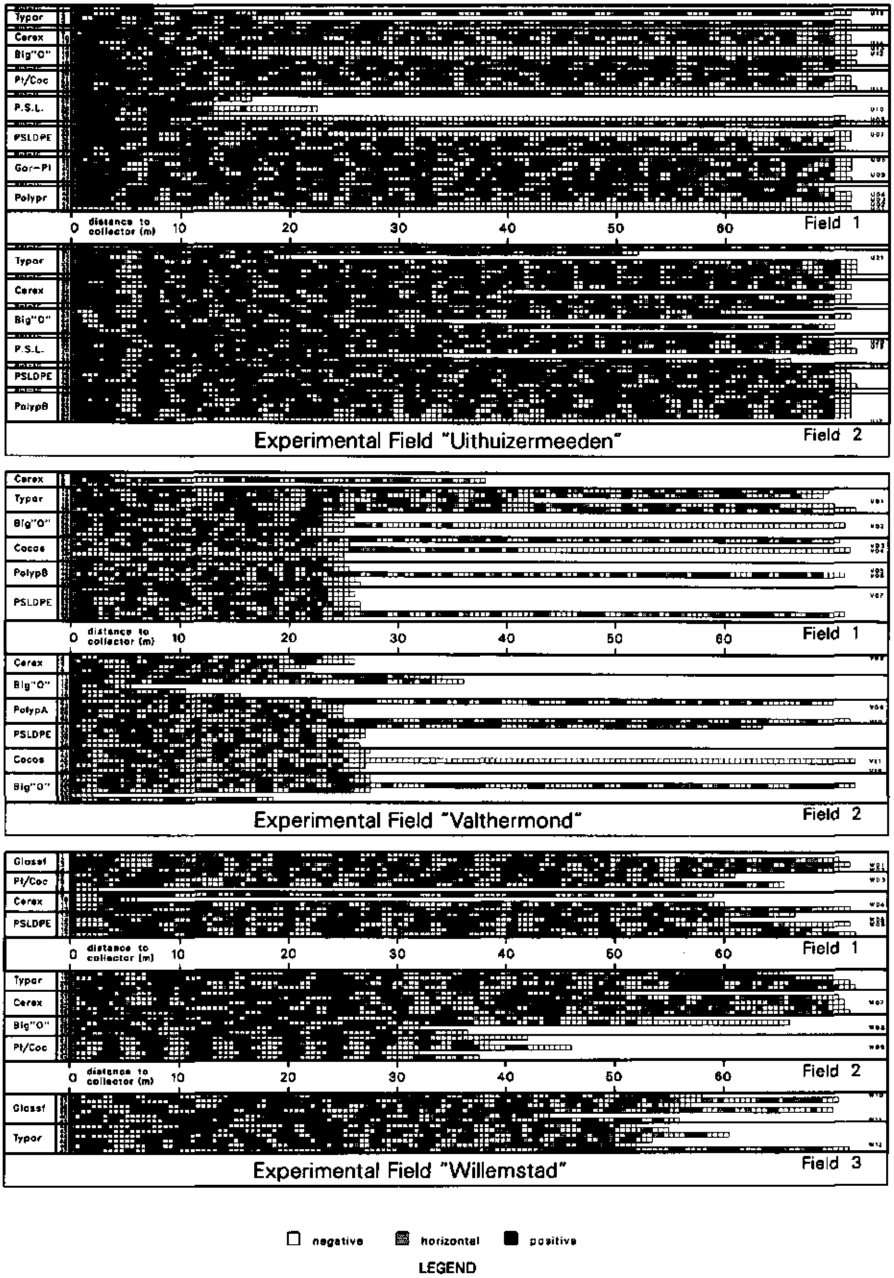

Figure 7. Maps of grade lines of drains.

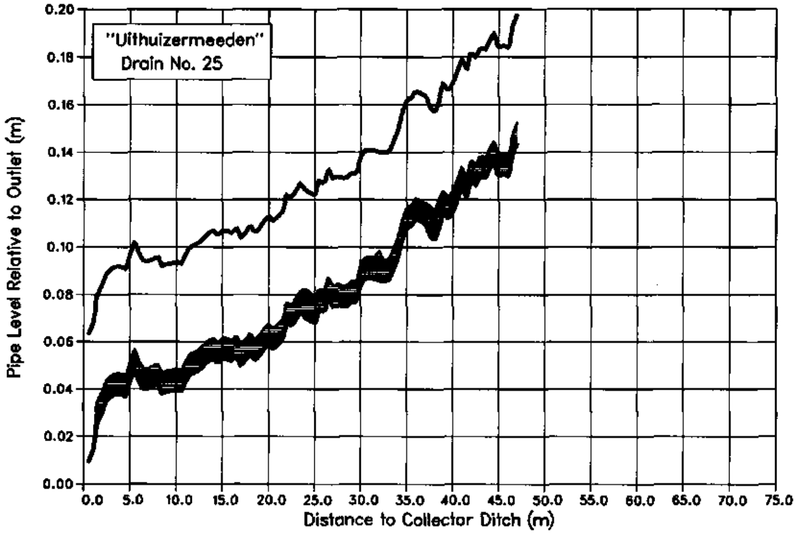

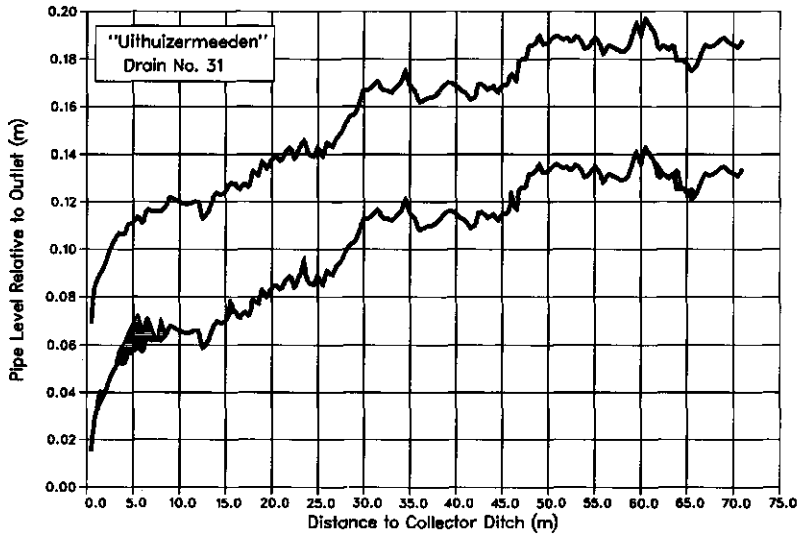

Figure 8. **Examples of comparatively inaccurate grade lines of drains and pipe sedimentation rates. The upper- and lower pipe walls are depicted as solid lines; pipe sediment is mapped as shaded areas.**

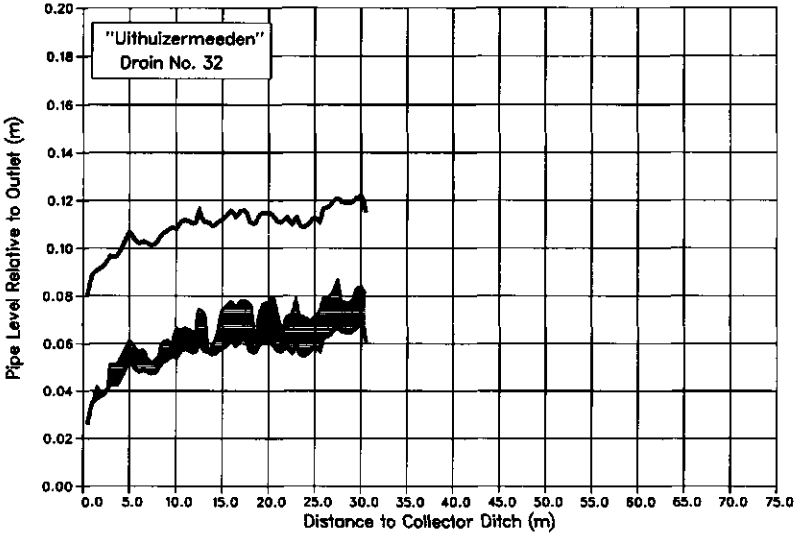

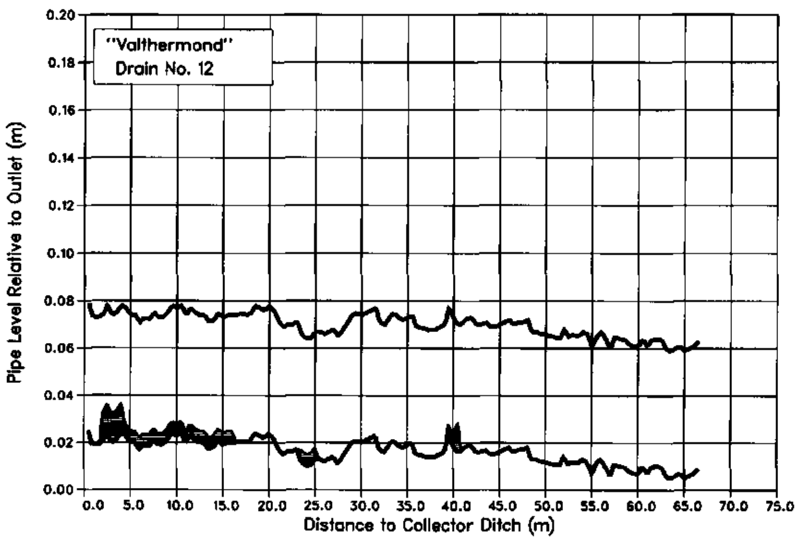

Figure 8 (cont'd). **Examples of comparatively inaccurate grade lines of drains and pipe sedimentation rates.**

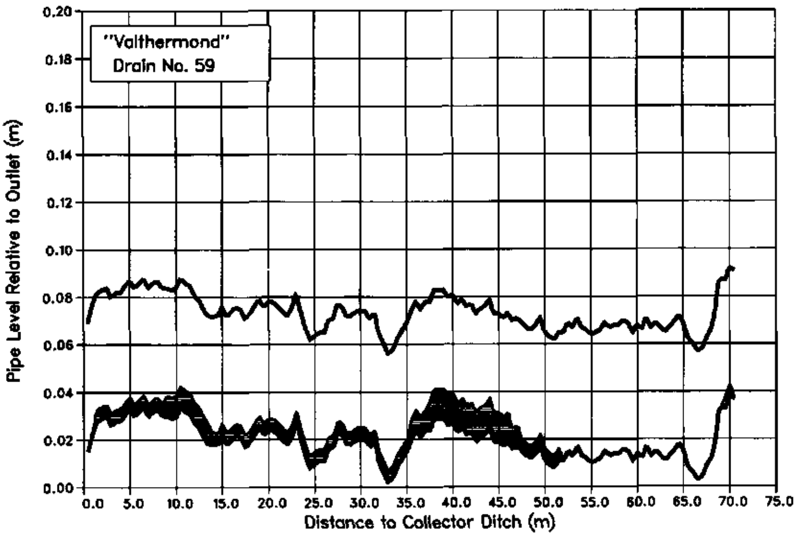

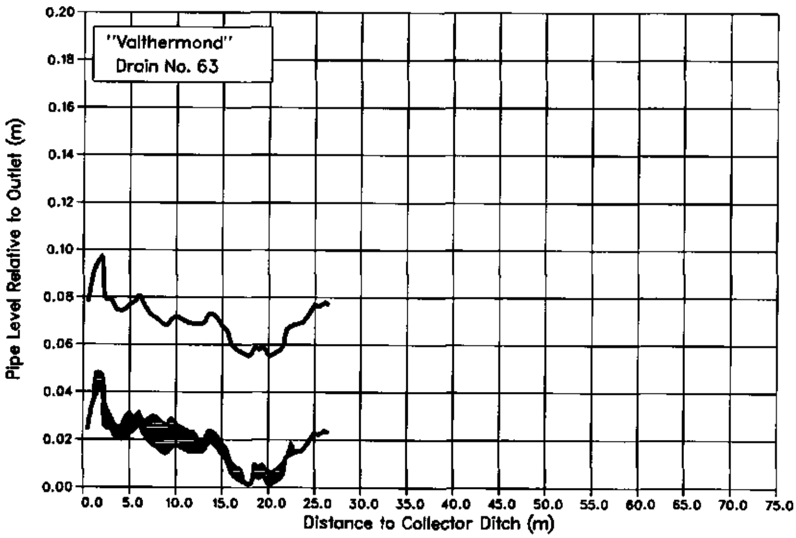

Figure 8 (cont'd). **Examples of comparatively inaccurate grade lines of drains and pipe sedimentation rates**

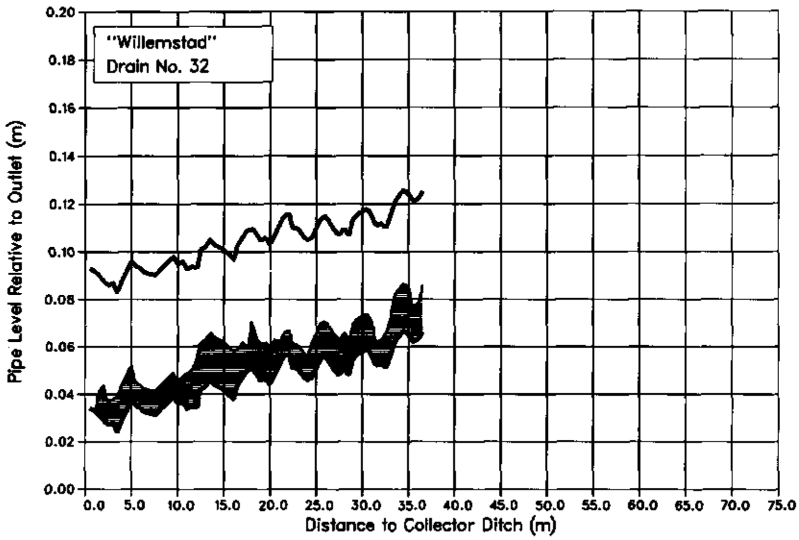

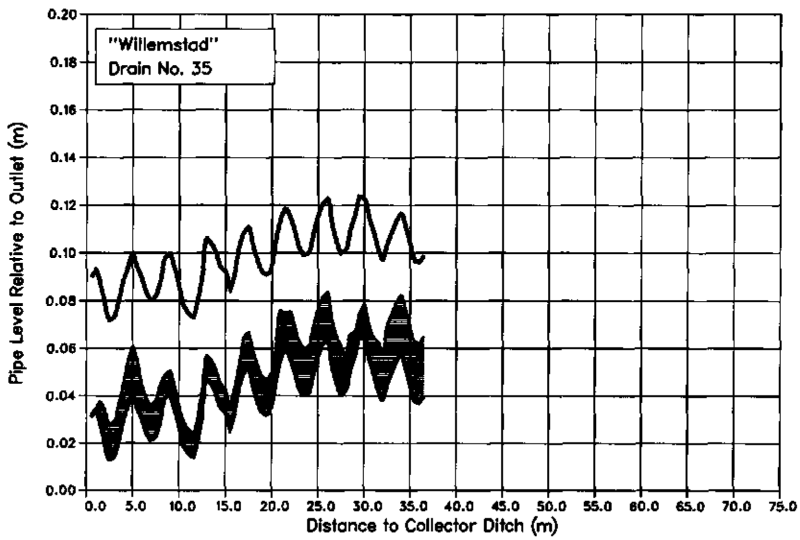

Figure 8 (cont'd). **Examples of comparatively inaccurate grade lines of drains and pipe sedimentation rates**

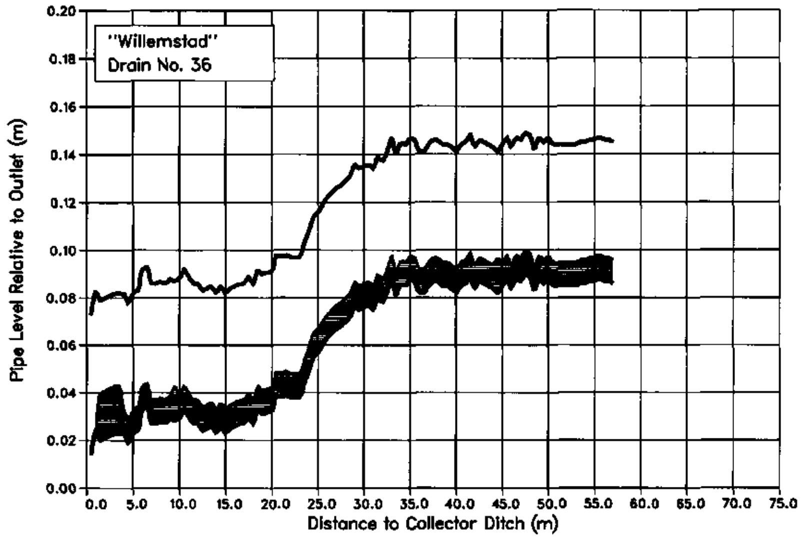

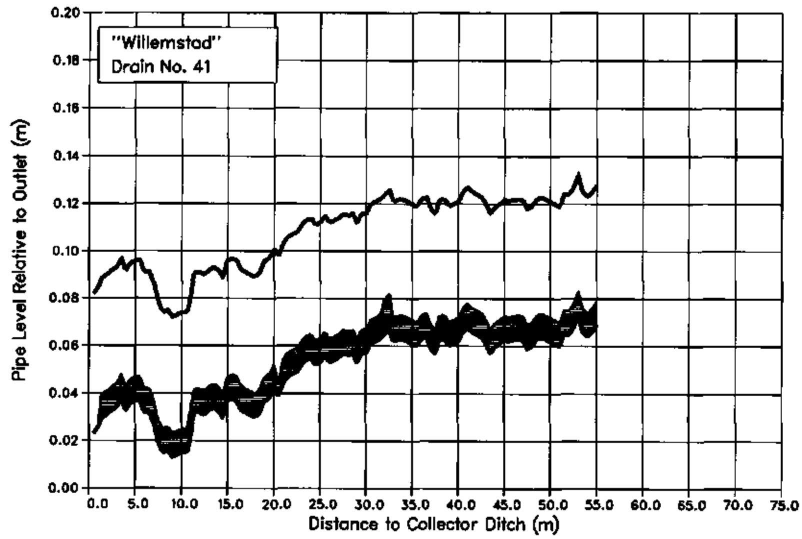

Figure 8 (cont'd). **Examples of comparatively inaccurate grade lines of drains and pipe sedimentation rates**

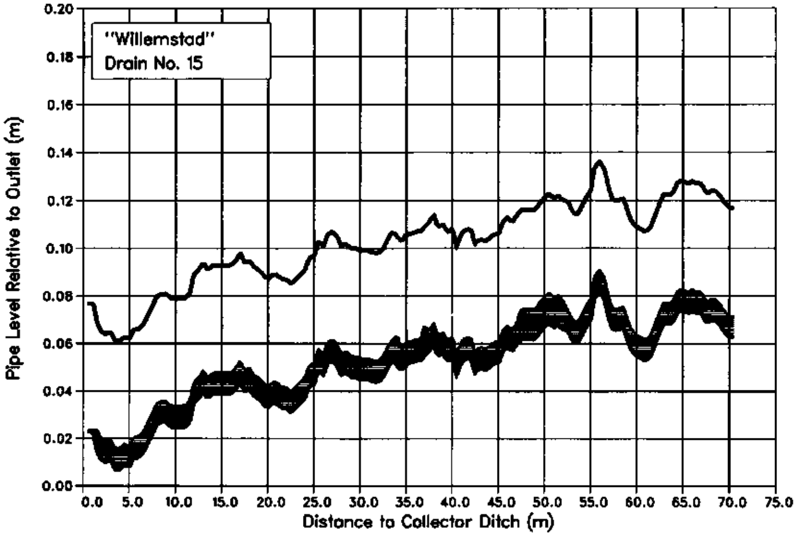

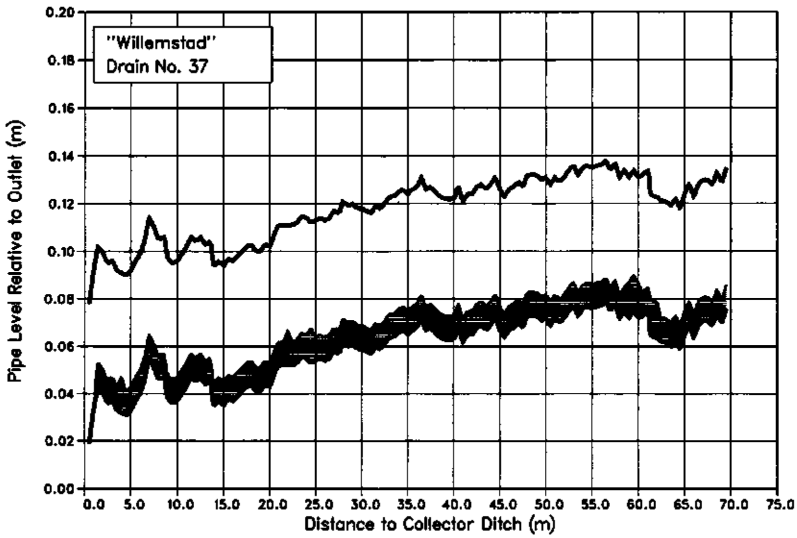

Figure 8 (cont'd). **Examples of comparatively inaccurate grade lines of drains and pipe sedimentation rates**

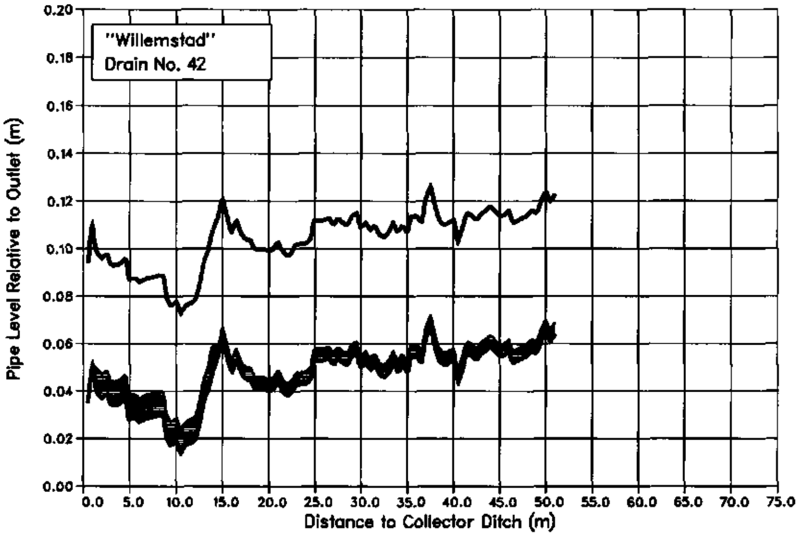

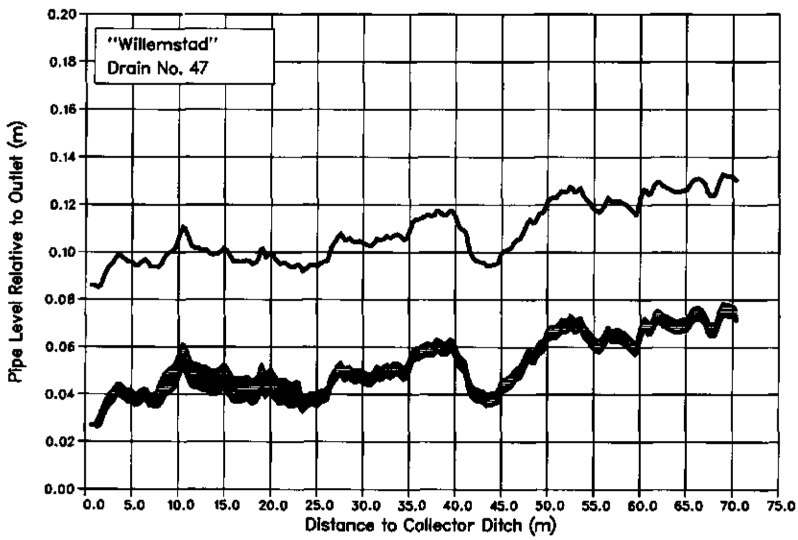

Figure 8 (cont'd). **Examples of comparatively inaccurate grade lines of drains and pipe sedimentation rates**

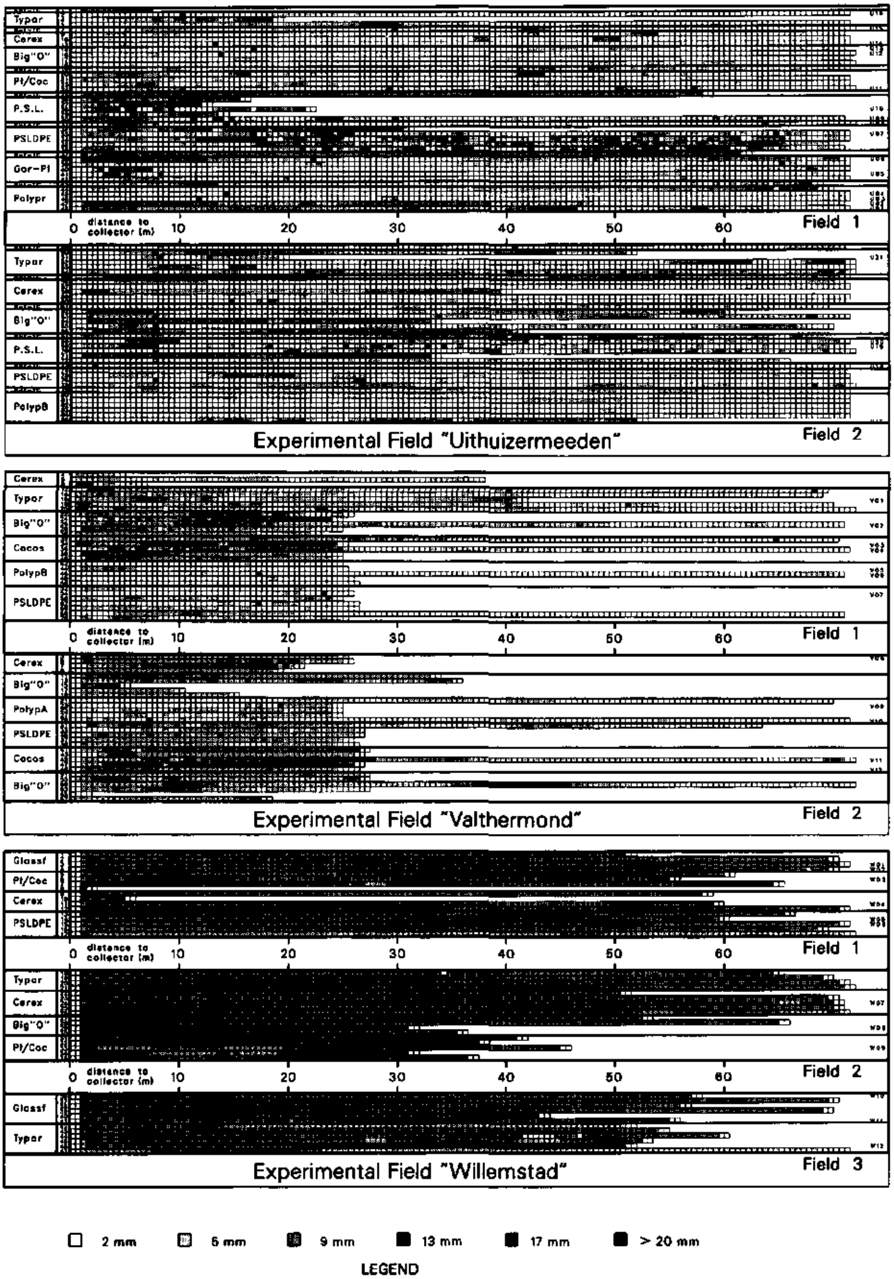

Figure 9. **Maps of sedimentation rates inside lateral drains.**

Table 5. Average standard deviations from grade lines ($m \cdot 10^{-3}$) of the investigated laterals, wrapped with 12 different envelopes and located in adjacent blocks of experimental fields located near Uithuizermeeden, Valthermond and Willemstad.

Type of envelope	Uithuizermeeden all laterals stand. dev	Valthermond all laterals stand. dev	Willemstad all laterals stand. dev	Total all laterals stand. dev
Thin envelope	2.93	2.79	4.28	3.40
Voluminous env.	3.36	3.32	4.19	3.47
All envelopes	3.22	3.08	4.25	3.44

	Uithuizermeeden		Valthermond		Willemstad			Total
	block 1	block 2	block 1	block 2	block 1	block 2	block 3	
	stand. dev		stand. dev		stand. dev			stand. dev
All envelopes	3.23	3.21	3.11	3.06	3.60	4.14	5.33	3.44
"Big 'O'" sock	2.74	3.01	3.44	2.05	--	3.27	--	2.97
"Cerex"	3.54	2.37	2.57	2.58	3.94	4.26	--	3.23
Glass fibre mb.	--	--	--	--	2.88	--	5.75	4.60
"Typar"	3.15	3.07	2.63	--	--	3.89	4.92	3.61
Coconut fibres	--	--	2.37	3.47	--	--	--	2.92
Peat-Coconut f.	3.63	--	--	--	3.01	4.94	--	3.94
Buffer-Peat/Co.	4.10	3.42	--	--	--	--	--	3.76
"Garden" peat f	3.13	--	--	--	--	--	--	3.13
Polypropyl. A	--	--	3.16	3.38	--	--	--	3.27
Polypropyl. B	2.47	4.23	--	--	--	--	--	3.35
Polystyrene "PSL"	2.23	2.65	--	--	--	--	--	2.44
Polystyrene "PS-LDPE"	3.79	3.79	3.93	3.39	4.38	--	--	3.87

backfill) as well as upward influx through the lower wall (subsoil) were observed separately. Average values are given in Tables 7 and 8 and maps are presented in Fig. 11. Soil influx is dominant in "Willemstad" experimental field. Influx through thin envelopes is generally more intense than influx through voluminous envelopes. The main differences in downward influx appear to be caused by soil type (=experimental field), location of drain sections (e.g. near collector ditches in "Uithuizermeeden") and envelope type. Downward influx through thin envelopes in "Valthermond" is comparatively high. Influx through "Typar" in "Willemstad",

Table 6. Layer height of pipe deposit (mm) in the investigated laterals, wrapped with 12 different envelopes and located in adjacent blocks of experimental fields located near Uithuizermeeden, Valthermond and Willemstad.

Type of envelope	Uithuizermeeden all laterals pipe deposit	Valthermond all laterals pipe deposit	Willemstad all laterals pipe deposit	Total all laterals pipe deposit
Thin envelope	2.02	4.40	9.78	4.58
Voluminous env.	2.65	3.20	10.72	3.89
All envelopes	2.45	3.72	10.04	4.84

	Uithuizermeeden		Valthermond		Willemstad			Total
	block 1	block 2	block 1	block 2	block 1	block 2	block 3	
	pipe deposit		pipe deposit		pipe deposit			pipe deposit
All envelopes	2.63	2.26	2.91	4.73	9.81	10.46	9.75	4.84
"Big 'O'" sock	0.43	4.64	5.42	5.72	--	10.96	--	4.97
"Cerex"	0.49	1.10	2.61	6.12	9.30	8.83	--	4.90
Glass fibre mb.	--	--	--	--	10.29	--	10.41	10.36
"Typar"	2.12	3.21	2.54	--	--	10.10	9.05	5.75
Coconut fibres	--	--	4.98	7.15	--	--	--	5.96
Peat-Coconut f.	1.10	--	--	--	12.10	13.31	--	7.74
Buffer-Peat/Co.	3.79	2.55	--	--	--	--	--	3.13
"Garden" peat f	1.65	--	--	--	--	--	--	1.65
Polypropyl. A	--	--	0.45	1.42	--	--	--	0.99
Polypropyl. B	2.65	0.16	--	--	--	--	--	1.40
Polystyrene "PSL"	5.73	3.35	--	--	--	--	--	4.06
Polystyrene "PS-LDPE"	5.91	1.29	1.52	4.05	8.50	--	--	4.61

block 3 is remarkably high. Upward influx is low and is found exclusively when organic envelopes are used, mainly near collector ditches in "Uithuizermeeden". It is found in isolated spots in "Valthermond" but it is a common phenomenon in in "Willemstad".

5.4 Drainage Resistance

In the regression model for drainage resistance, differences between envelopes are significant (at 5% level) in the "Valthermond" experimental field but not at the

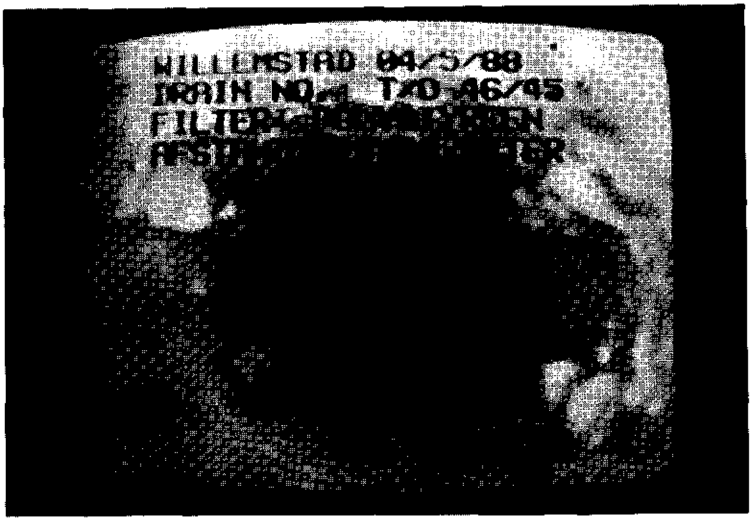

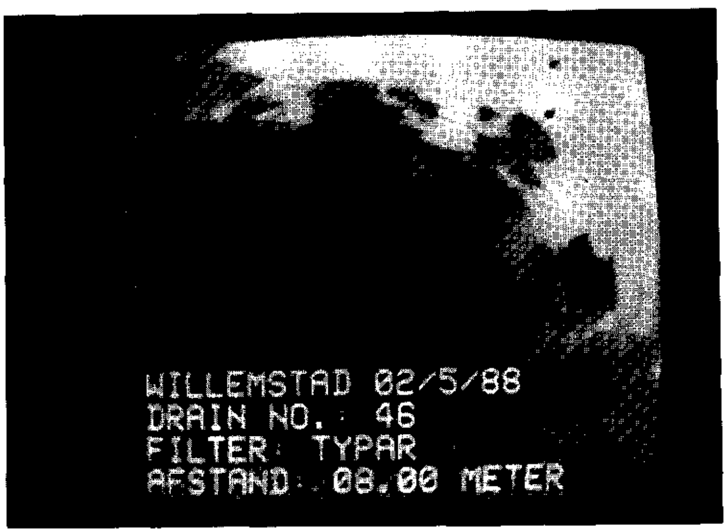

Figure 10. **Examples of common features inside drains: soil invasion through a voluminous envelope (top) and soil invasion through a thin envelope (bottom).**

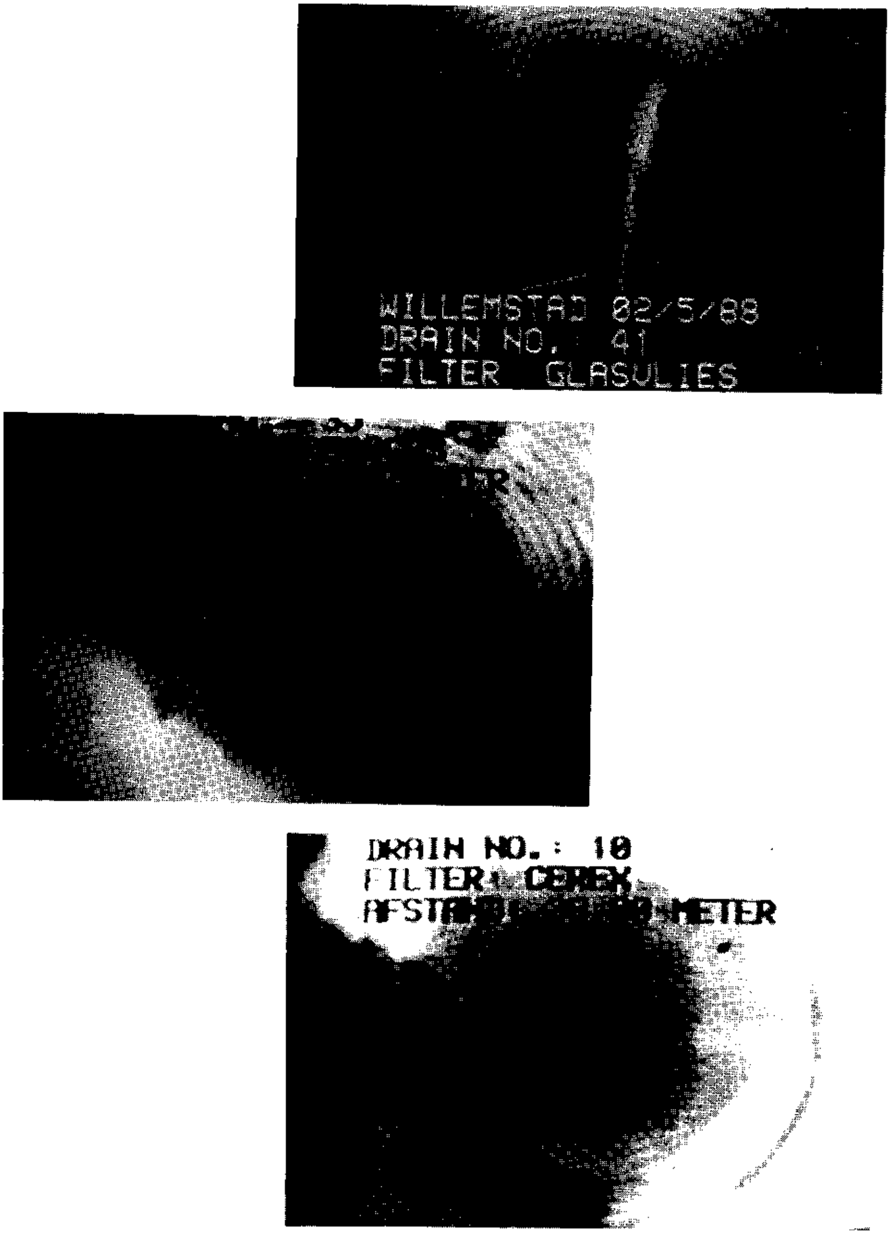

Figure 10 (cont'd). **Examples of common features inside drains: the pipe wall and a root witness transport of suspended soil particles through a drain (top); pipe sediment, prohibiting camera passage (centre) and soil influx at a loose joint (bottom).**

Table 7. Downward soil influx rate index (-) of the investigated laterals, wrapped with 12 different envelopes and located in adjacent blocks of experimental fields located near Uithuizermeeden, Valthermond and Willemstad.

Type of envelope	Uithuizermeeden all laterals downward influx	Valthermond all laterals downward influx	Willemstad all laterals downward influx	Total all laterals downward influx
Thin envelope	0.01	0.25	0.31	0.19
Voluminous env.	0.09	0.07	0.51	0.14
All envelopes	0.06	0.15	0.37	0.17

	Uithuizermeeden block 1	Uithuizermeeden block 2	Valthermond block 1	Valthermond block 2	Willemstad block 1	Willemstad block 2	Willemstad block 3	Total
	downward influx		downward influx		downward influx			downward influx
All envelopes	0.05	0.08	0.08	0.23	0.22	0.34	0.61	0.17
"Big 'O'" sock	0.0	0.0	0.27	0.46	--	0.23	--	0.18
"Cerex"	0.0	0.01	0.04	0.31	0.19	0.12	--	0.09
Glass fibre mb.	--	--	--	--	0.07	--	0.38	0.25
"Typar"	0.01	0.01	0.07	--	--	0.18	0.84	0.26
Coconut fibres	--	--	0.07	0.16	--	--	--	0.11
Peat-Coconut f.	0.10	--	--	--	0.65	1.07	--	0.54
Buffer-Peat/Co.	0.17	0.38	--	--	--	--	--	0.28
"Garden" peat f	0.04	--	--	--	--	--	--	0.04
Polypropyl. A	--	--	0.01	0.04	--	--	--	0.03
Polypropyl. B	0.0	0.0	--	--	--	--	--	0.0
Polystyrene "PSL"	0.0	0.01	--	--	--	--	--	0.01
Polystyrene "PS-LDPE"	0.0	0.0	0.03	0.12	0.11	--	--	0.05

other 2 locations. These differences are largely explained by envelope category ("thin" or "voluminous"). The effective opening size, O_{90}, has no significant effect on drainage resistance. The average grade line and standard deviation of the average grade line have also no significant effect on drainage resistance. For the resulting model, the fitted values are given in Table 9. One observation (a plot containing a "Typar" envelope in the "Valthermond" experimental field) showed an extremely high drainage resistance. After excluding this observation however from the regression model, the conclusions did not change.

Table 8. Upward soil influx rate index (-) of the investigated laterals, wrapped with 12 different envelopes and located in adjacent blocks of experimental fields located near Uithuizermeeden, Valthermond and Willemstad.

Type of envelope	Uithuizermeeden all laterals upward influx	Valthermond all laterals upward influx	Willemstad all laterals upward influx	Total all laterals upward influx
Thin envelope	0.0	0.10	0.36	0.18
Voluminous env.	0.07	0.03	0.51	0.12
All envelopes	0.05	0.06	0.40	0.15

	Uithuizermeeden		Valthermond		Willemstad			Total
	block 1	block 2	block 1	block 2	block 1	block 2	block 3	
	upward influx		upward influx		upward influx			upward influx
All envelopes	0.03	0.06	0.05	0.07	0.39	0.38	0.45	0.15
"Big 'O'" sock	0.0	0.0	0.08	0.15	--	0.20	--	0.08
"Cerex"	0.01	0.0	0.06	0.02	0.65	0.35	--	0.21
Glass fibre mb.	--	--	--	--	0.13	--	0.14	0.13
"Typar"	0.0	0.01	0.11	--	--	0.27	0.77	0.27
Coconut fibres	--	--	0.03	0.05	--	--	--	0.04
Peat-Coconut f.	0.06	--	--	--	0.53	0.77	--	0.40
Buffer-Peat/Co.	0.13	0.28	--	--	--	--	--	0.21
"Garden" peat f	0.03	--	--	--	--	--	--	0.03
Polypropyl. A	--	--	0.02	0.05	--	--	--	0.04
Polypropyl. B	0.0	0.0	--	--	--	--	--	0.0
Polystyrene "PSL"	0.0	0.01	--	--	--	--	--	0.01
Polystyrene "PS-LDPE"	0.0	0.0	0.0	0.02	0.36	--	--	0.09

5.5 Pipe Sedimentation

The rate of pipe sedimentation is largely and significantly determined by location (experimental field). Differences, observed between blocks within experimental fields are not significant. The average grade line and its standard deviation have no significant effect on pipe sedimentation. The type of envelope effects the rate of pipe sedimentation but differences between envelopes depend on location.

The differences between envelopes are strongly associated with the effective

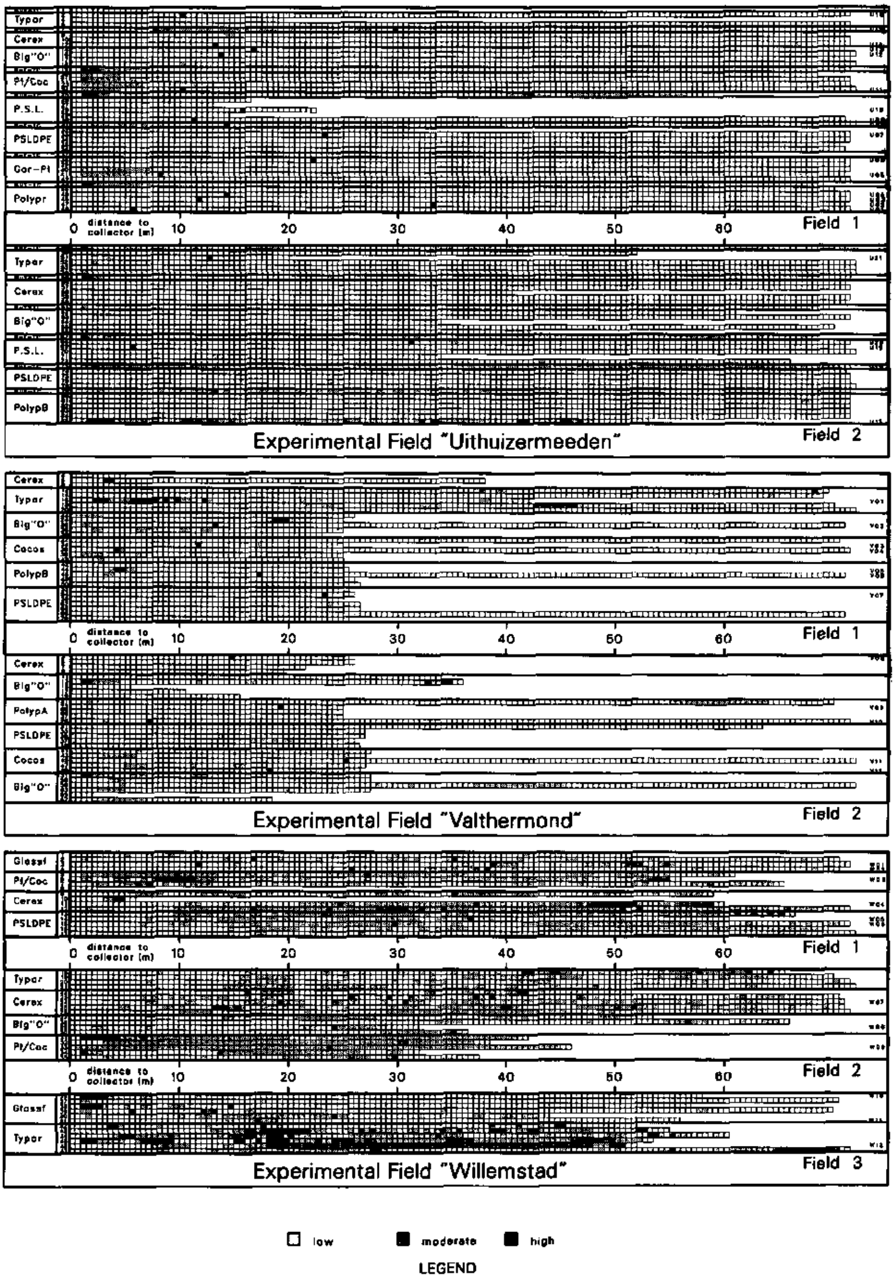

Figure 11. **Maps of the occurrence of upward soil influx, moving from the subsoil into the drain pipes.**

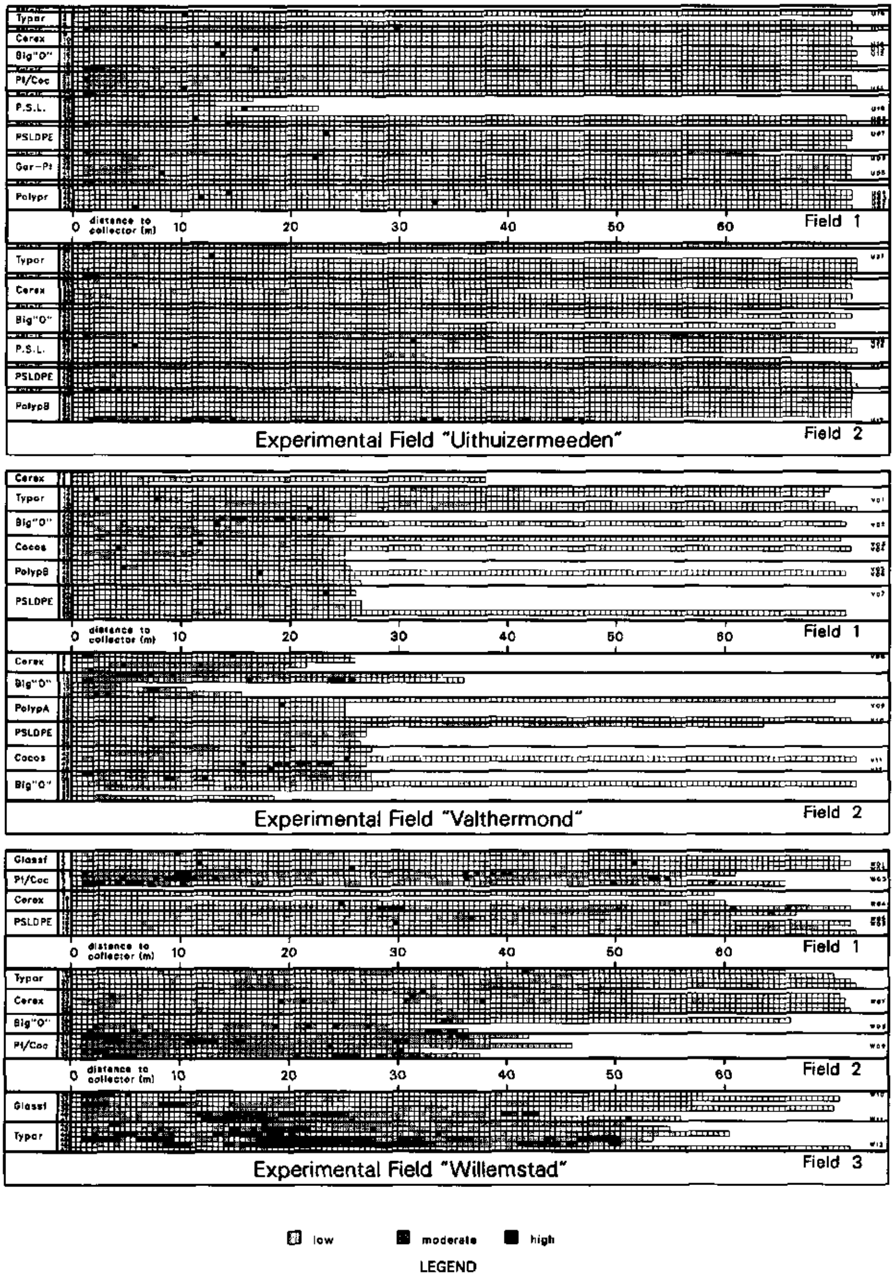

Figure 11 (cont'd). **Maps of the occurrence of downward soil influx, moving from the trench backfill into the drain pipes.**

Table 9. Drainage resistance γ (d) at the experimental fields Uithuizermeeden, Valthermond and Willemstad; fitted values from regression model.

	Uithuizermeeden	Valthermond	Willemstad
	resistance γ	resistance γ	resistance γ
"Thin"	122	235	107
"Voluminous"	129	94	91

opening size, O_{90}. They are also associated with envelope category ("thin" or "voluminous"), particularly in the "Valthermond" experimental field. For constant values of O_{90}, the particle retention capability of "thin" envelopes is consistently worse than that of "voluminous" ones. For the resulting model, predicted sedimentation rates are given for O_{90} = 250, 500 and 1000 μm (Table 10).

Table 10. Pipe Sedimentation (mm); fitted values from regression model, depending on the effective opening size of envelope pores,O_{90} (μm), the envelope category (thin or voluminous) and applied on observations made at the experimental fields Uithuizermeeden, Valthermond and Willemstad.

	Uithuizermeeden		Valthermond		Willemstad	
$O_{90\ (\mu m)}$	thin	voluminous	thin	voluminous	thin	voluminous
	sedimentation rates (thickness of sediment layer (mm))					
250	2.1	0.9	4.5	0.8	9.7	8.5
500	3.9	2.6	6.3	2.5	11.4	10.2
1000	5.6	4.3	8.0	4.3	13.2	11.9

5.6 Microbiological precipitation

Average values of microbiological precipitation (shiny jelly-like substances) are given in Table 11. Microbiological precipitation is most widespread in "Uithuizermeeden", it occurs more frequently in combination with thin envelopes and appears to be linked to local spots in the field.

Table 11. Index, reflection the occurrence of microbiological precipitation (-) in the investigated laterals, wrapped with 12 different envelopes and located in adjacent blocks of experimental fields located near Uithuizermeeden, Valthermond and Willemstad.

Type of envelope	Uithuizermeeden all laterals microb. prec.	Valthermond all laterals microb. prec.	Willemstad all laterals microb. prec.	Total all laterals microb. prec.
Thin envelope	0.17	0.05	0.02	0.08
Voluminous env.	0.05	0.01	0.0	0.04
All envelopes	0.09	0.03	0.01	0.06

	Uithuizermeeden		Valthermond		Willemstad			Total
	block 1	block 2	block 1	block 2	block 1	block 2	block 3	
	microb. prec.		microb. prec.		microb. prec.			microb. prec.
All envelopes	0.11	0.07	0.04	0.02	0.0	0.03	0.0	0.06
"Big 'O'" sock	0.22	0.01	0.0	0.05	--	0.0	--	0.07
"Cerex"	0.38	0.18	0.0	0.0	0.0	0.04	--	0.13
Glass fibre mb.	--	--	--	--	0.0	--	0.0	0.0
"Typar"	0.23	0.06	0.11	--	--	0.06	0.0	0.08
Coconut fibres	--	--	0.05	0.0	--	--	--	0.03
Peat-Coconut f.	0.09	--	--	--	0.0	0.0	--	0.04
Buffer-Peat/Co.	0.13	0.17	--	--	--	--	--	0.15
"Garden" peat f	0.02	--	--	--	--	--	--	0.02
Polypropyl. A	--	--	0.0	0.03	--	--	--	0.02
Polypropyl. B	0.0	0.01	--	--	--	--	--	0.0
Polystyrene "PSL"	0.04	0.0	--	--	--	--	--	0.01
Polystyrene "PS-LDPE"	0.0	0.0	0.0	0.0	0.0	--	--	0.0

5.7 Roots

An index reflecting the occurrence of living roots is given in Table 12 and is mapped in Fig. 12. Living roots are found both in "Uithuizermeeden" and "Willemstad" and are clearly linked to local spots (e.g. "Uithuizermeeden", block 2) and envelope type. Notably "Cerex" and "PS-LDPE" give good protection against it.

Table 12. Index, reflecting the occurrence of living roots (-) in the investigated laterals, wrapped with 12 different envelopes and located in adjacent blocks of experimental fields located near Uithuizermeeden, Valthermond and Willemstad.

Type of envelope	Uithuizermeeden all laterals roots index	Valthermond all laterals roots index	Willemstad all laterals roots index	Total all laterals roots index
Thin envelope	0.29	0.01	0.19	0.19
Voluminous env.	0.34	0.03	0.16	0.24
All envelopes	0.32	0.02	0.18	0.22

	Uithuizermeeden		Valthermond		Willemstad			Total
	block 1	block 2	block 1	block 2	block 1	block 2	block 3	
	roots index		roots index		roots index			roots index
All envelopes	0.12	0.54	0.02	.02	0.15	0.20	0.21	0.22
"Big 'O'" sock	0.21	0.99	0.01	.02	--	0.33	--	0.34
"Cerex"	0.11	0.07	0.0	0.0	0.05	0.07	--	0.07
Glass fibre mb.	--	--	--	--	0.41	--	0.31	0.35
"Typar"	0.03	0.23	0.01	--	--	0.09	0.11	0.10
Coconut fibres	--	--	0.03	0.04	--	--	--	0.03
Peat-Coconut f.	0.18	--	--	--	0.08	0.44	--	0.23
Buffer-Peat/Co.	0.14	0.70	--	--	--	--	--	0.44
"Garden" peat f	0.05	--	--	--	--	--	--	0.05
Polypropyl. A	--	--	0.06	0.01	--	--	--	0.03
Polypropyl. B	0.19	0.42	--	--	--	--	--	0.30
Polystyrene "PSL"	0.08	1.12	--	--	--	--	--	0.81
Polystyrene "PS-LDPE"	0.01	0.22	0.02	0.04	0.04	--	--	0.07

6 DISCUSSION

6.1 Grade Lines

Average grade lines are steepest in "Uithuizermeeden" experimental field and are nearly horizontal in "Valthermond", where the drains are also used for subirrigation (Table 4). In "Valthermond", the average grade line in block 2 is negative. The average grade line in "Willemstad" is comparatively flat, particularly in block 1. Differences between plots, equipped with drains wrapped with different

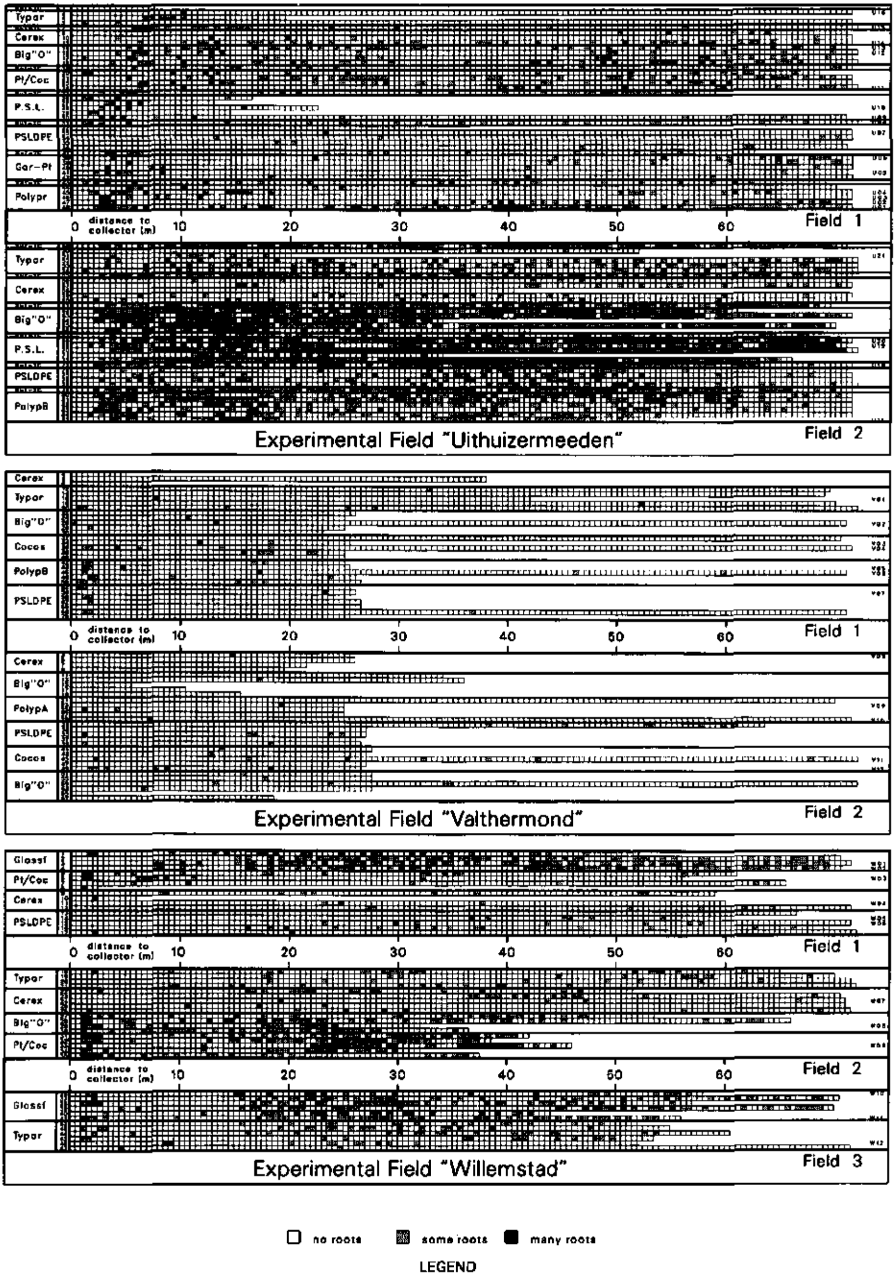

Figure 12. **Maps of root ingrowth into drains.**

envelope materials are small. The grade line of drains, wrapped with a "PSL" envelope in "Uithuizermeeden", block 1, is comparatively high, yet this result is questionable because grade line measurement of these drains was severely restricted due to excessive sedimentation rates (Fig. 7). In "Uithuizermeeden" block 2 and, to a lesser extent, in block 1, all drains have reverse grade lines along a track running parallel to the collector ditch (Fig. 7). This track coincides with a path followed by a trencher prior to drain installation. The trencher purposely cut through existing laterals to prevent them interfering hydrologically with the newly installed laterals.

Average standard deviations from grade lines are small (Table 5). It appears that the deviations are largest in "Willemstad", notably in block 3. Nevertheless, the laying accuracy is quite good, both in terms of average grade lines and standard deviations from grade lines. Hence it is obvious that these variables do not have a significant effect on drainage resistance and pipe sedimentation.

6.2 Soil Influx

Envelopes, made from organic substances appear to be comparatively sensitive to soil influx. Influx patterns in drains, wrapped with "organic" envelopes may however partly consist of decomposed organic substances. The occurrence of soil influx in the form of saturated soil being squeezed through drain envelopes and pipe perforations is so widespread that it is probably the main pipe sedimentation mechanism in this type of weakly-structured, fine-sandy soil. As this phenomenon was never observed in the analogue soil tank models it is doubtful whether analogue models adequately simulate the physical process of soil influx at all. Experimental fields are a much better tool to observe sedimentation rates than analogue models which give scattered and unreliable results (Chapter 2). Unfortunately, measurement of sedimentation rates with a video inspection system, while imperative for accurate analysis, is considered to be too costly.

6.3 Drainage Resistance

Regression analysis of drainage resistance and pipe sedimentation data has produced remarkable results. Generally, neither envelope category ("thin" or "voluminous") nor the type of envelope material has a significant effect on drainage resistance. However, in "Valthermond", drains wrapped with voluminous envelopes have consistantly lower drainage resistances. This may be explained by the fact that "Valthermond" is the only location where drains are used for subirrigation in summer when ditch water is forced to infiltrate into the soil through the drains. This water usually contains many organic substances and bacteria that may cause microbiological clogging of envelopes. Thin envelope materials are considered to be particularly sensitive to this process. In "Willemstad", substantial amounts of iron ochre were found inside drains and envelopes, yet thin envelopes did not perform significantly worse than voluminous envelopes in terms of drainage resistance.

High entrance resistances of (wrapped) drain pipes will induce enhanced drainage resistances, hence they may be a factor of significance in design (Wesseling, 1979). The fact that the observed drainage resistances in "Uithuizermeeden" and "Willemstad" are not significantly related to envelope category is in conflict with conclusions from various mathematical analyses and models in which entrance resistances of wrapped drains are found to be inversely correlated with envelope thickness. Traditional entrance resistance models assume (Widmoser, 1968; Nieuwenhuis & Wesseling, 1979; Dierickx, 1980) (a) that the flow pattern near a drain is radial in a homogeneous and isotropic soil, (b) that envelopes themselves are homogeneous and isotropic, and (c) that clogging of envelopes occurs, homogeneously, at the soil/envelope interface only.

In weakly-cohesive soils, none of these assumptions are supported by field data. On the contrary, during analogue modelling of water and particle flow into drains, backfilled with heterogeneous, weakly-cohesive soil it was observed that the soil around the drains was heterogeneous and anisotropic and that the water flow pattern near drains was not radial but had a complicated, irregular geometry (Chapter 7). This would mean that the classical concept of entrance resistance does not hold for drains which are installed in heterogeneous soil and that envelope thickness is a factor of minor importance. The same conclusion may be drawn from the current observations of drainage resistance. Research efforts should therefore be devoted to the determination of water flow patterns into drains which have been functioning in the field for a few years at least.

The observed indifference of drainage resistance with respect to envelope material used, was unexpected. It was even argued that these experiments had failed. Such reasoning is not particularly scientific and is caused by erroneous expectations.

6.4 Pipe Sedimentation

Pipe sedimentation rates in "Willemstad" are consistently higher than elsewhere. This may be due to a particularly low structural stability of this soil type. While sampling cores for CT examination, however (see Chapter 4) it was found that the subsoil was often saturated and 'reduced' (=the soil appears blue due to a very low oxygen percentage during a prolonged period) below drain level. It is not unlikely therefore that the drains in "Willemstad" have been installed in saturated soil. If so, this may at least partly explain the comparatively high rates of soil invasion into most "Willemstad" drains.

Mapping of sedimentation rates adds a spatial dimension to the data. In both "Uithuizermeeden", and, to a lesser extent, "Valthermond" it can be seen that envelope type as well as local soil properties may be involved. Drains running

Table 13. Average sedimentation rates in drains (mm), observed with 12 different envelope materials in experimental fields near Uithuizermeeden, Valthermond and Willemstad. References are made to observations, made during tests with analogue soil tank models. "Lab 1" = model tests with cohesionless "Almere sand, "Lab 2" = model tests with weakly-cohesive soil samples (see Chapter 2). "-" = no observations made.

Envelope material	Field	Lab 2	Field	Lab 2	Field	Lab 2	Lab 1
	sedimentation rates (thickness of sediment layer (mm))						
"Cerex"	0.9	-	4.9	-	9.0	0.1	12.0
Glass fibre membr.	-	-	-	-	10.4	0.1	2.0
Polypropyl. A	-	-	1.0	-	-	-	>60.0
Polypropyl. B	1.4	-	-	-	-	-	12.0
"Typar"	2.8	-	2.5	7.8	9.5	-	10.0
"Big 'O'" sock	2.5	2.3	5.6	12.3	11.0	-	4.0
"Garden" peat f	1.7	16.0	-	-	-	-	-
Peat-Coconut f.	1.1	10.0	-	-	12.7	-	-
Buffer-Peat/Co.	3.1	-	-	-	-	-	-
Polystyrene "PS-LDPE"	3.7	22.5	2.6	24.1	8.5	-	22.0
Polystyrene "PSL"	4.1	-	-	13.3	-	21.3	-
Coconut fibres	-	-	6.0	9.0	-	-	54.0

near borders of fields may contain more sediment due to past soil manipulation. "Uithuizermeeden" drains 47 and 48 in block 1 run near and partly through an area where a ditch was relocated in 1961. These drains contain more sediment than adjacent drains. "Uithuizermeeden" drain 58 in block 2 runs parallel and near a former ditch. Obviously, local soil stability is low and more soil is found inside this drain. Comparatively high sedimentation rates are found in the central area of block 1. This appears to be due to local soil instability as well as to envelope properties. Similar tendencies are observed in blocks 1 and 2 of experimental field "Willemstad". In "Uithuizermeeden", block 2, a track, running parallel to the collector ditch and disclosed earlier in Fig. 7, contains comparatively much deposit. The soil particle retention capability of Polypropylene Fibres "A" envelope in experimental field "Valthermond" is remarkable. The observed sedimentation rates are well within Dutch criteria (maximum allowed sediment layer height = 15 mm).

Average observed pipe sedimentation rates of drains are given in Table 13. Where available, these figures may be compared with sedimentation rates, observed in analogue soil tank models, i.e. "Lab 1" (tests with cohesionless "Almere sand") and "Lab 2" (tests with weakly-cohesive samples), see Chapter 2.

Contrary to results of observations made on analogue laboratory models, field observations indicate that the effective opening size, O_{90}, appears to be a useful particle retention capability parameter. Laboratory models give quite scattered results.

A sediment layer in a drain section results from local clogging, supply of sediment from upstream and removal of sediment in a downstream direction. Moreover, pipe sedimentation is usually related to local grade line variations (Fig. 8). A local sediment layer height is therefore not a reliable indicator of local pipe sedimentation rate. A better indicator is soil influx through pipe wall perforations, but it is difficult and quite laborious to observe soil influx at regular intervals.

7 CONCLUSIONS

The water acceptance of subsurface pipe drains (hence the drainage resistance) and pipe sedimentation rates are determined by the structural stability of the soil, installation practice and properties of envelopes. The effects of these contributing factors can only be assessed in situ. Results of tests made with analogue soil tank models, equipped with weakly-cohesive soils cannot be extrapolated to field conditions with confidence. Researchers have to accept that the suitability of drain envelopes must be assessed in the field; a process which is time-consuming and tedious. The effective opening size of envelopes, O_{90}, is significantly correlated with their soil retention capability or 'sand tightness'. □

REFERENCES

Boer, K.S. de. 1987. Grading precision of subsurface drains. Meded. Landinrichtingsdienst 185a.

Dierickx, W. 1980. Electrolytic analogue study of the effect of openings and surrounds of various permeabilities on the performance of field drainage pipes. Report 77, National Institute for Agricultural engineering, B-9220 Merelbeke (Belgium), ISBN 90 70142 13 9

Draper, N.R. and H. Smith. 1981. Applied Regression Aanalysis (2nd edition). Wiley & Sons, New York.

Genstat 5 Committee, 1987. Genstat 5 Reference Manual. Clarendon Press, Oxford, England.

Van der Louw, C. 1986. Drainoscopie, een optische inspectiemethode voor drainagesystemen (Drainoscopy, an optical inspection method for subsurface drains). Cult. Techn. Tijdschrift 25(5):357-367 (in Dutch).

Nieuwenhuis G.J.A. and J. Wesseling. 1979. Effect of perforation and filter material on entrance resistance and effective diameter of plastic drain pipes. Agric. Water Manage. 2:1-9.

Wesseling, J. 1979. The entrance resistance of drains as a factor in design. Proc. Int. Drain. Workshop, ed. J. Wesseling. ILRI, Wageningen, The Netherlands: 368-392.

Widmoser, P. 1968. Der Einfluss von Zonen geänderter Durchlässigkeit im Bereich von Drän- und Brunnenfilterrohren (The impact of zones with modified hydraulic conductivity near drain pipes and wells). Schweiz. Bauzeitg, 86H, 9 (in German).

Zeijts, T.E.J. van. 1987. Quality control of subsurface drainage works in the Netherlands. Proc. Third Int. Workshop on Land Drainage, The Ohio State University, Columbus, Ohio U.S.A.

4 FIELD SAMPLING OF SECTIONS OF LATERAL DRAINS

4 Field sampling of sections of lateral drains

ABSTRACT

In three experimental fields in the Netherlands, 45 lateral drain sections were selected for core sample retrieval and subsequent scanning by x-ray computerised tomography (CT). Selection was based on the occurrence of mineral pipe clogging, as observed with a video inspection system. Sampling sites were located in the field by a miniature radio transmitter. Physical limitations of CT impose restrictions on sample geometry and size, which were determined through a trial and error procedure. An "undisturbed" sample core, 200 mm diameter by 300 mm long, was non-destructively taken at each site. Each core contained a wrapped drain section with surrounding soil. Most envelopes were sampled four times with specially developed tools. The cores were transported to a scanning laboratory in a passenger car equipped with a shock-absorbing unit, within hours after core retrieval.

1 INTRODUCTION

Engineering systems involving soils are difficult to investigate. Among such systems, subsurface wrapped drains pose special problems as a result of the interaction between the drain, its envelope and the surrounding soil. Investigation of processes involved in envelope functioning and water acceptance of such drains, therefore, requires spatial quantification of processes like water flow and movement of sediment. The flow of water and soil particles in weakly-structured soils and envelopes near drains is not well understood due to the inability to monitor these phenomena without disturbing the system.

Analogue simulation of this flow in laboratories with various types of soil samples has not been very successful because this type of simulation could not be calibrated with field data. Many of the results therefore are questionable and ambiguous. In addition, phenomena like soil failure and subsequent mineral clogging near subsurface drains, in which soil structural stability is involved, cannot be accurately simulated in a physical laboratory setup, simply for lack of field data with which to calibrate the results. It is therefore impossible to establish whether or not such a simulation is in accordance with field conditions. Due to the geometrically heterogeneous flow pattern, available techniques are inadequate for monitoring water movement in the immediate vicinity of lateral field drains. Yet information on this water movement is indispensable for an assessment of the functioning of drain envelopes. In the present study, the water movement has therefore been recorded indirectly by detection and quantification of contact erosion patterns near soil/envelope interfaces. A non-destructive and non-invasive technique called x-ray computerised tomography (CT) scanning was used; it involves the computation of a digital two-dimensional image of a thin internal section ("slice") through an object, from a large number of measurements of the attenuation rate of narrow, collimated x-ray beams which are transmitted through this slice. If consecutive, parallel sections through an object are scanned, internal features of the object may be imaged and quantified in three dimensions. X-ray CT was applied to evaluate soil structure and envelope clogging rates in samples taken at selected sites. After site selection, but prior to CT analysis, the sample cores must first be retrieved, preserved and transported to the scanning laboratory with a minimum of disturbance. The following stages can be distinguished in the core sampling procedure: (a) selection of sampling locations, (b) determination of the required sample geometry and -size, (c) development of sampling tools, (d) sample core retrieval, and (e) transport of cores to the scanning laboratory. In the next sections, these stages will be discussed.

2 SELECTION OF SAMPLING LOCATIONS

The sampling locations were selected on the basis of data collected with a miniature video inspection system (Chapter 3). Three phenomena have been considered: (a) sediment layer height in the drain pipe (mm), (b) upward soil influx rate into the pipe and (c) downward soil influx rate. Averages of these phenomena have been assessed for each 0.5 m pipe section of each lateral drain. These averages were summed as a qualitative indicator for the relative occurrence of pipe sedimentation, PSI (= "Pipe Sedimentation Index"). Each group of laterals wrapped with one of 12 envelope types was considered with respect to PSI, regardless of experimental field. Laterals with maximum and minimum PSI values were selected for core sampling without further consideration. Two additional laterals having intermediate values of PSI were also selected. In total, 45 sample retrieval sites were identified at representative locations along the laterals. Two envelope types which are not widely used, namely "Garden" peat fibres and a Peat/Coconut fibre mixture, were also included, two and three samples of these being taken.

This selection procedure did not take into account the fact that the grade line of drains may have a significant effect on the height of sediment layers. This was because at the time when the sample core retrieval locations were selected, grade lines had not been measured. Fortunately, in a later stage it was established that grade lines did not have a significant effect as the drains had been laid very accurately.

The core retrieval sites were located with the aid of a survey and locating system, "Tracka Mina"[1], manufactured by Woodbridge Electronic Services, U.K.. It consists of a 38 mm diameter probe, housing a miniature radio transmitter emitting elctromagnetic pulses which penetrate through a wide range of soils, up to 4¼ metres distance. The position of the transmitter underground is located from above ground by means of a hand held receiver containing micro electronic circuits tuned to convert the magnetic pulses from the transmitter into an audio signal. The accuracy of location can be improved by decreasing the receiver sensitivity. The transmitter probe was mounted on top of a glass fibre rod. After marking this rod at the desired distance, the transmitter was pushed into the lateral from the collector ditch. Location of the transmitter and the corresponding core retrieval site is very rapid.

3 DETERMINATION OF THE REQUIRED SAMPLE GEOMETRY- AND SIZE

Limitations, associated with the CT process, impose restrictions on sample geometry and size. The process of x-ray computerised tomography will be described in Chapter 7. Some aspects of CT must however be dealt with here. For a fuller description of the terminology used, the reader is referred to Annex 5.

Computerised tomography is subject to physical limitations, leading to errors in the CT measurements. In turn this leads to deviations in the images, obtained from these measurements. It is important to understand both the nature of these limitations and the way in which the images are influenced by such errors. The effect of the limitations can be reduced in several ways.

In this study, a Philips Tomoscan 350 medical CT scanner was used designed to accurately scan human tissue. Scanning of soils may produce artifacts in the output, consisting of two-dimensional digital representations of the density distribution in cross-sectional "slices" through these soils. There are inherent limitations due to the statistical nature of the process of x-ray photon production, to photon interaction with matter and to subsequent photon detection but these are not considered since they are beyond our control. Two limitations which are

[1]This equipment was placed at our disposal by Horman Drainagefilter BV, 's-Gravendeel, the Netherlands.

however linked to drain sample geometry and size, *beam hardening* and *photon scatter*, are briefly discussed, because they may be minimized by proper sampling methods.

1. **Beam hardening**. An x-ray beam used in CT consists of photons of different energies (polychromatic x-rays). "Soft" x-rays or photons with low energy are absorbed more intensely than those with higher energy. As a result, the relative energy distribution spectrum of the x-ray beam shifts ("hardens") on its way through the object. Beam hardening results in edge-brightening artifacts, often referred to as "cupping": an image of a uniform object demonstrates increased apparent density (brightness) near its perimeter. In small, high density samples, beam hardening can be so severe that the cupping effect, usually limited to sample edges, can extend throughout the entire sample, completely obliterating any structure present. Contemporary CT-scanners, designed for scanning human tissue incorporate corrections for beam hardening but these are unreliable when scanning soils. A scanner may be recalibrated for scanning soil samples in order to minimize beam hardening artifacts. After such recalibration, CT has been successfully applied to reveal anatomical structures inside hominid skulls which are partly covered or filled with calcite or rock matrix (Zonneveld et al, 1989). In this study, recalibration was not possible and beam hardening effects were minimized by limiting the travel lengths of x-ray beams through the soils. This fact imposed limitations to the maximum diameter of future samples.

2. **Photon scatter**. A CT scanner uses an array of detectors counting photons which have travelled through the scanned object. Any photon scattered out of its path towards the detector array may very well reach another detector and be counted by it. The ratio of scattered photons to unscattered photons which reach a detector is, in a complicated way, dependent on the object to be reconstructed. Image artifacts due to photon scatter may also be reduced by restricting sample dimensions.

Even if beam hardening and scatter are minimized, the reconstructed (=computed) digital images of cross-sections of the sample cores may not be perfect mappings of the scanned objects. This is because a computed cross-section cannot be unambiguously determined from a finite number of CT measurements. The best that CT can do is to *estimate* the cross-section from the CT data measured (Herman, 1980). The latter statement implies that various geometric shapes of objects give rise to image artifacts. Contrary to diagnostic radiology where object shape is largely invariable and predetermined, the shape of our field samples may be more or less optimized in an effort to minimize artifacts.

The use of x-ray CT in drain envelope research is unprecedented and its applicability potential was unknown. An empirical reconaissance survey was made rather than a theoretical feasibility study because this was considered to be more pragmatic and faster. The survey was made on the basis of "real" soil and envelope samples. In cooperation with a physisist (H. Venema, personal communication[2]) and a CT specialist (B. Verbeeten jr, personal communication[2]), a trial and error procedure was followed to establish the optimum limits for sample geometry and -size. To determine the optimum limit the following samples were examined:

1. a small diameter cylindrical core with undisturbed soil (Fig. 1),
2. a similar sample containing a pipe section surrounded by soil (Fig. 2),
3. an envelope sample disc in a laboratory flow permeameter,
4. a 400 x 400 x 400 mm soil cube,
5. a large diameter cylindrical core containing part of an artificial drain trench and a section of a wrapped drain, and
6. a large diameter cylindrical core containing a drain section and surrounding soil, sampled from an existing drainage system.

The techniques used and findings were as follows:

1. *Two small diameter cylindrical cores*

Low x-ray attenuation, 150 mm inside diameter, acrylic (plexiglass) cylinders enclosed (a) an undisturbed soil sample and (b) a section of 60 mm outside diameter corrugated drain, wrapped with a fabric envelope and backfilled with soil (Fig. 1 and 2). Pencils were used to create artificial "macropores" in the undisturbed soil sample. The sections were examined by a Philips Tomoscan 310 scanner at 120 kV and 1.5 mm slice thickness, at the Medical School of the AMC

[2]Medical School, AMC Hospital, University of Amsterdam, The Netherlands.

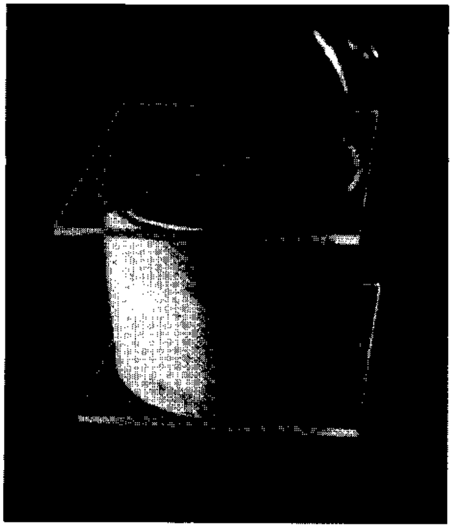

Figure 1. A ø 150 mm plexiglass pipe section, filled with soil, used to empirically determine the maximum possible sample diameter.

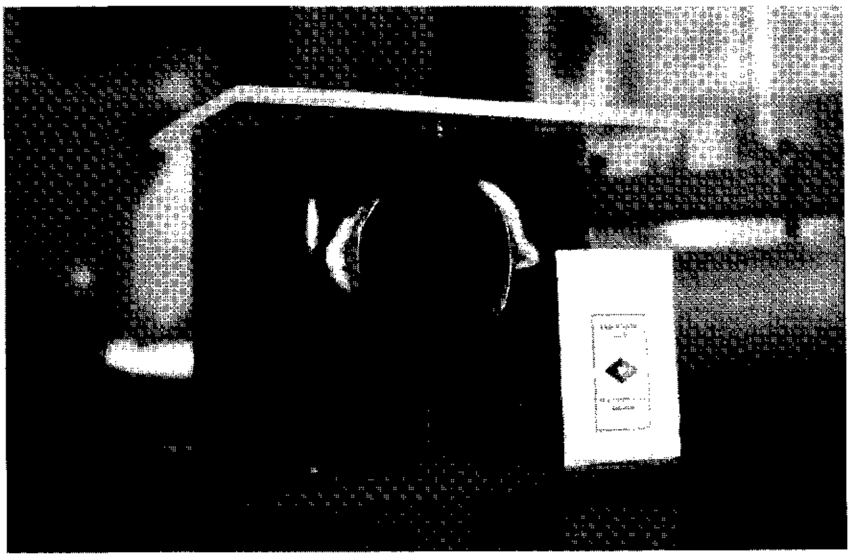

Figure 2. A ø 150 mm plexiglass pipe section, filled with soil and a piece of wrapped, corrugated PVC drain pipe, used to empirically assess the spatial resolution of computerised tomography (CT).

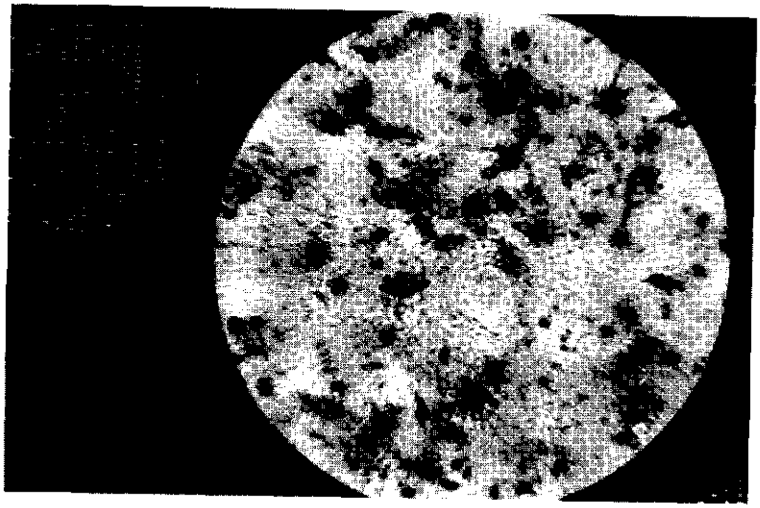

Figure 3. A 1½ mm thick CT scan image through the sample depicted in Fig. 1. Macropores are black and comparatively dense soil areas have a bright appearance.

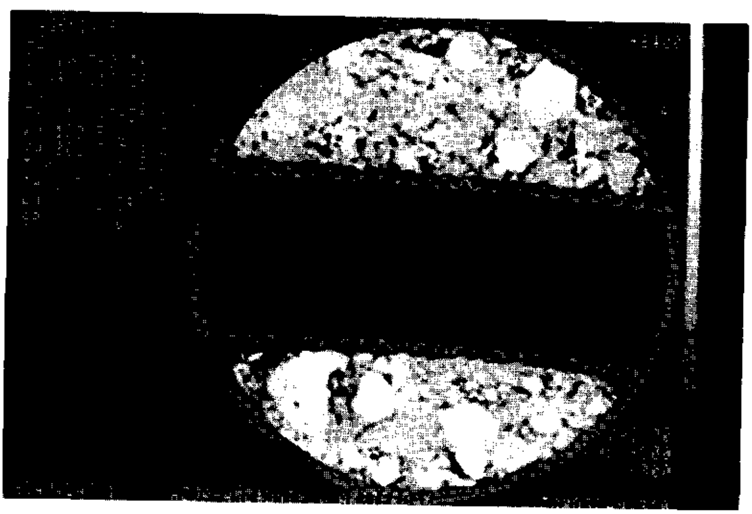

Figure 4. A 1½ mm thick CT scan image through the sample depicted in Fig. 2. Soil density is proportional to grey level. Pipe perforations are clearly visible in the lower pipe wall.

Hospital of the University of Amsterdam. Results are presented in Fig. 3 and 4. They show that the spatial resolution is sufficient to accurately examine macroscopic soil structural features. Beam hardening and photon scatter artifacts were virtually absent. It was concluded that 150 mm diameter soil cores could be satisfactorily examined with a medical CT scanning system.

2. *An envelope sample disc in a laboratory flow permeameter*

A voluminous envelope sample disc mounted in a laboratory flow permeameter was examined next using a different scanner. Scans were made by a Deltascan 100 scanner at 6 mm slice thickness at the Juliana Hospital in Apeldoorn, The Netherlands. The steel bolts, holding the sample together, produced large image artifacts (Fig. 5 and 6). As this instrument had a comparatively poor spatial resolution, all subsequent scans were made on a Philips Tomoscan 350 scanner, installed in the "AMC" Academic Hospital in Amsterdam, replacing the Tomoscan 310.

3. *A 400 x 400 x 400 mm soil cube*

The first field sample was a 400 x 400 x 400 mm soil cube, contained in a 20 mm thick gypsum casing without drain section. This cube was sampled in a fine-sandy soil at "Sinderhoeve" experimental farm, Renkum, The Netherlands. CT images contained noticeable streak artifacts, connecting opposite sample edges (Fig. 7). Scanning of a corner area of the sample however produced images without streak artifacts (Fig. 8). Based on the visual inspection of these artifacts it was concluded that a sample should have cylindrical rather than rectangular outside boundaries and that it must be of limited size.

In addition, this cube was too heavy to handle in the field and required much preparation time. When sampling drain sections, the available time is often restricted due to problems caused by groundwater seepage and drain discharge into the sampling pit, prompting the need for a fast sampling technique.

4. *A large diameter cylindrical core containing an artificial sample*

Following these results it was decided to scan a 200 mm outside diameter cylindrical core, filled with soil with a 60 mm pipe section running axially through its centre. The drain section was wrapped with "PS-LDPE" envelope, consisting of polystyrene beads, wrapped in a perforated low density polyethylene sheet. The sample was artificially prepared in topsoil in the field to also test the sampling

Figure 5. Image of a CT scan image made through an envelope sample disc which was mounted in a flow permeameter. Steel bolts cause large image artifacts.

Figure 6. The same object as in Fig. 5, but depicting the spatial "density variation" through the sample disc, caused by object-dependent image artifacts.

Figure 7. Image of a CT scan image through a 400 x 400 x 400 mm sample cube, contained in gypsum. Note the "streak" artifacts connecting the edges of the cube.

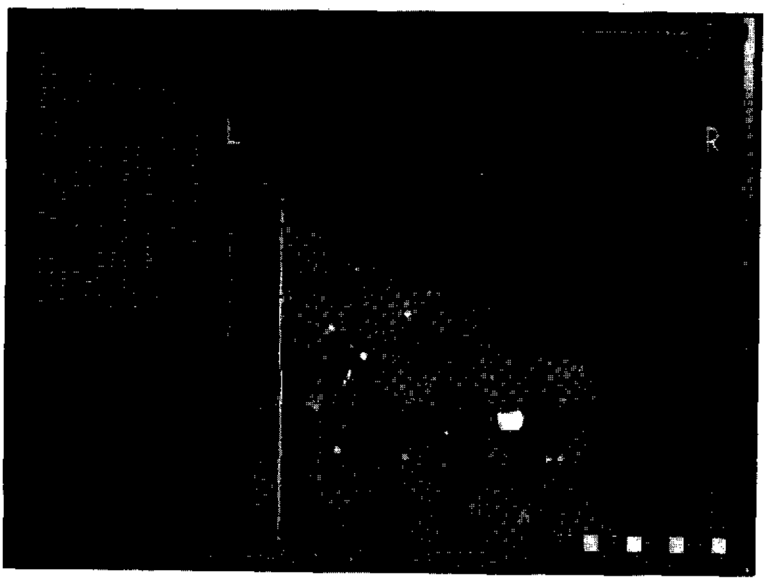

Figure 8. Image of a CT scan image through a corner area of the sample depicted in Fig. 10.

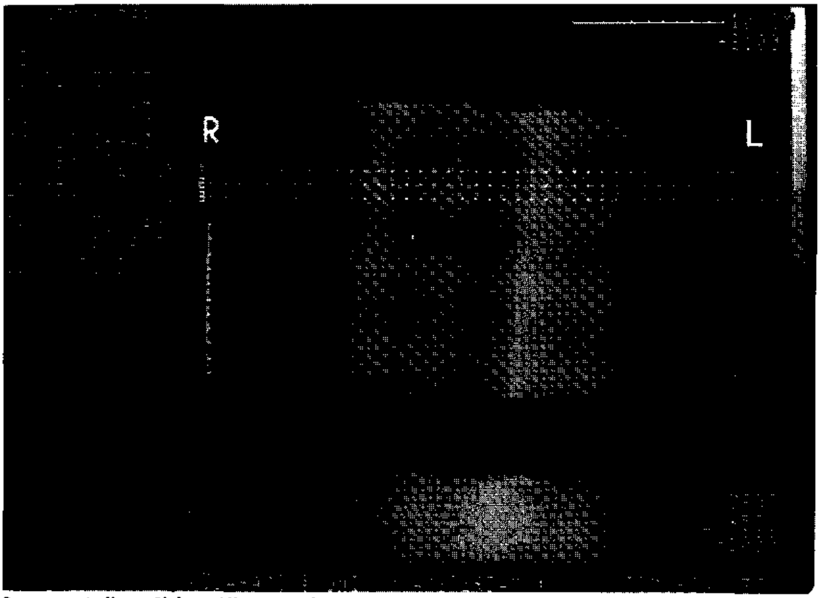

Figure 9. A "traditional" x-ray image or scanogram through a sampled drain section with surrounding soil. Dashed lines indicate subsequent CT scan locations through the section.

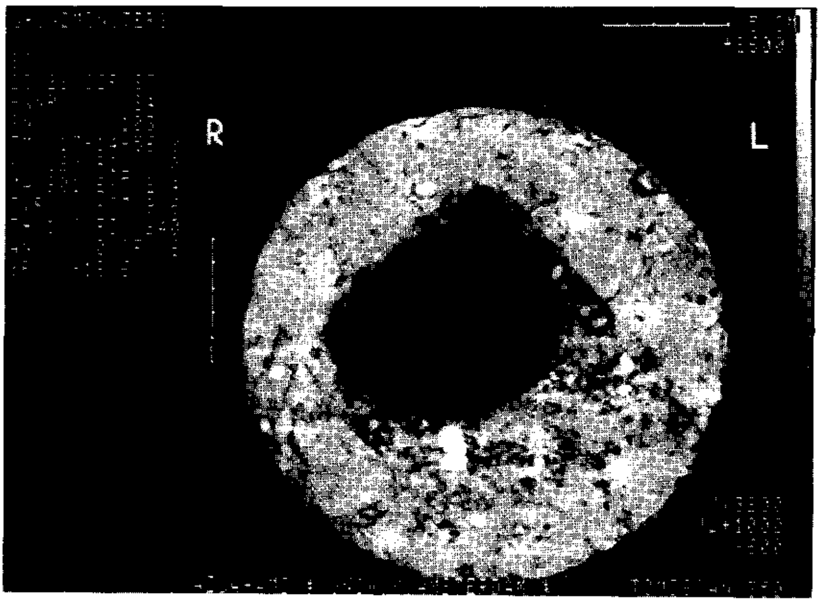

Figure 10. Image of a CT scan through the sampled section, depicted in Fig. 9. The image is largely free of artifacts. The drain pipe appears as a faint white circle. The envelope material - of low density - is black.

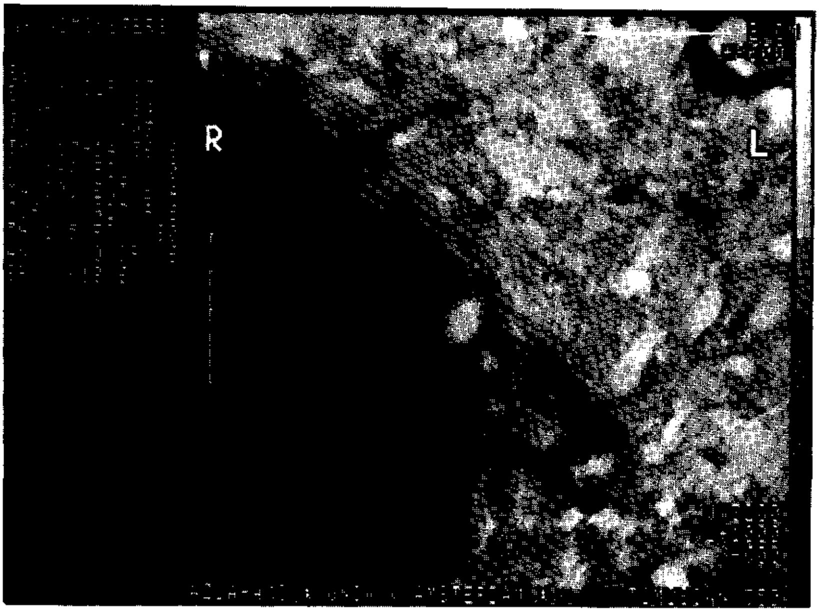

Figure 11. Enlarged area of Fig. 10. In the mid-lower section, soil which has invaded the envelope is seen as white areas near polystyrene beads which are mapped as black

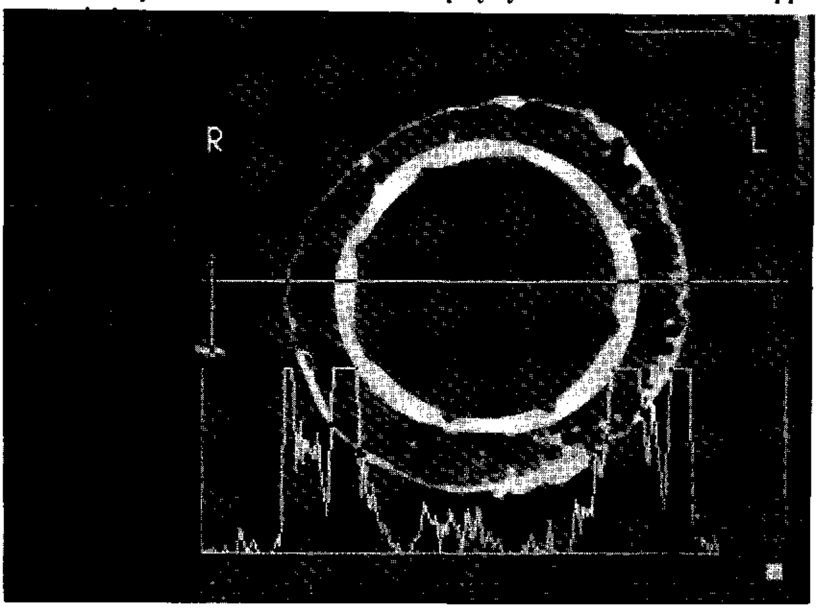

Figure 12. Mapping of a cross-section of the envelope of the sampled section, depicted in Fig. 9. White areas coincide with invaded soil material.

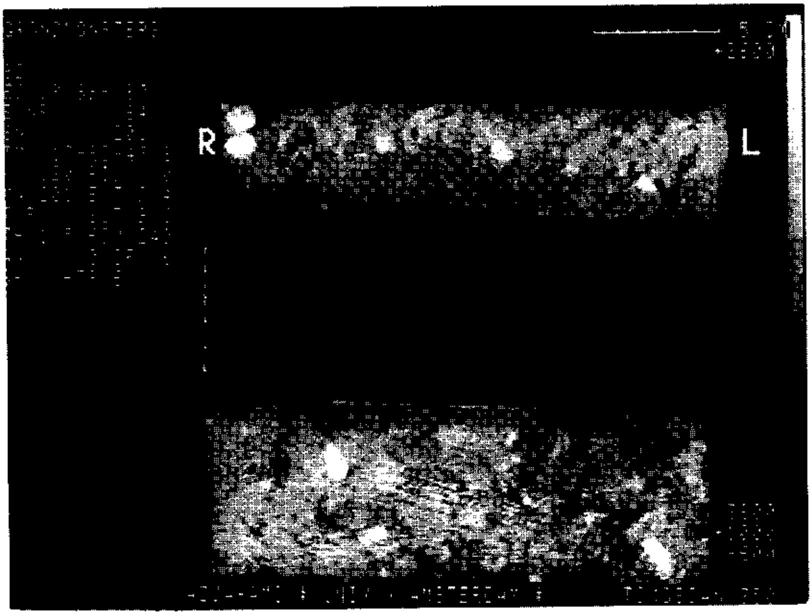

Figure 13. Image of a CT scan, made lengthwise through the sampled section, depicted in Fig. 9. The corrugated drain is clearly visible. Note weak streak artifacts under the drain.

technique. It was scanned at 120 kV with a slice thickness of 1.5 mm. A "traditional" x-ray view or scanogram is depicted in Fig. 9. A slice through the core and an enlarged area near the drain show good spatial resolution; artifacts are virtually non-existent (Fig. 10 and 11). The envelope itself was qualitatively examined. White spots as seen in Fig. 11 and 12 are mappings of invaded soil. A lengthwise scan contains weak streak artifacts (Fig. 13).

5. *A wide diameter cylindrical core containing a real sample*

Following the encouraging results with the artificially prepared sample a cylindrical core containing a section of drain pipe, its envelope and abutting soil, 200 mm in diameter and 300 mm long, was sampled at "Valthermond" experimental field as a prototype. A 1.5 mm CT slice through this core is depicted in Fig. 14. Some streak artifacts are visible in the subsoil. Nevertheless the slice image contained much information so far unknown. It was decided to proceed with the CT analysis standardising on the physical dimensions of this prototype.

4 DEVELOPMENT OF SAMPLING TOOLS

Prior to core sampling a sampling technique was developed. Most of the equipment required was available or could be bought in hardware shops. The remainder had to be developed specially. The items which were readily available

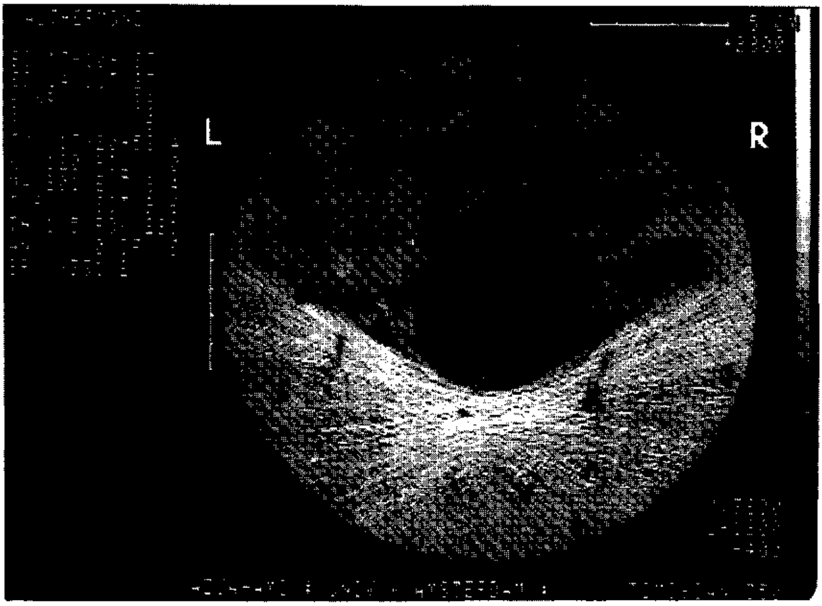

Figure 14. **CT image of a scan through the first sample, taken from an existing drain. Note the relatively dense subsoil and the heterogeneous trench backfill. Some streak artifacts are seen underneath the drain.**

are listed in Annex 3. The following special purpose items were manufactured:

1. **Core sampling tools**: (a) a heavy duty jacking device with detachable centering rod (Fig. 15); (b) a heavy duty pressure reaction plate with adjustable ram mount (Fig. 16); (c) a 1.2 m long, ø 15 mm steel pipe (fixed distance marker) and (d) a pointer stick with purposely made fittings (Fig. 17).

2. **Core sampling and sealing hardware**: (a) 45 plexiglass pipe sections, 200 mm diameter by 300 mm long, (b) 90 pvc end caps for the pipe sections with 100 mm holes drilled at their centres, (c) 2 pvc end caps with flexible rubber bands and attachments, (d) 90 rubber foam rings, 200 mm diameter with 80 mm holes drilled at their centres. Auxiliary: a toolbox and a shock-absorbing device designed for simultaneous transport of two sample cores by car (Fig. 18).

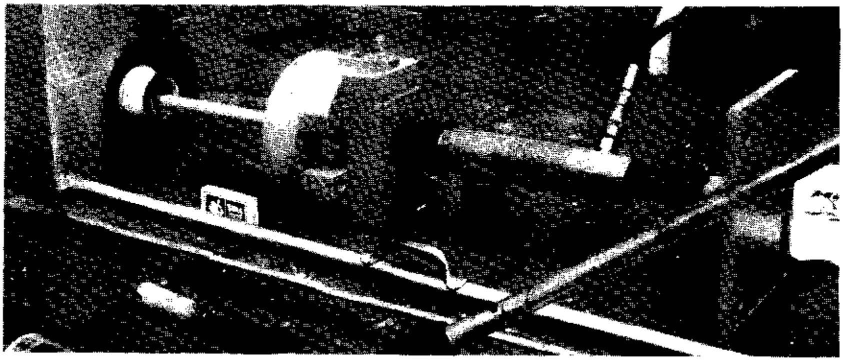

Figure 15. **Heavy duty jacking device with detachable centering rod.**

5 SAMPLING AND CORE RETRIEVAL PROCEDURE

The process of sampling and core retrieval consisted of seven steps: (1) machine-assisted digging, (2) manual digging, (3) preparation of soil profile prior to sampling, (4) installation and adjustment of sampling tools, (5) sampling, (6) sample core removal, preservation and sealing, and (7) repair of damaged lateral and backfilling of pit. These steps are discussed below. They are illustrated in two diagrams: Fig. 19 and 20. The retrieval sites are depicted in maps on page 72.

1. Machine-assisted digging

At each location, a backhoe was used to prepare the pits. At marked locations, soil was very carefully removed to within 0.25 m of the top of the pipe lateral. Utmost care was needed so that the hoe did not touch the drain nor compress its surrounding soil layer. A person continually monitored the depth of the hoe relative to drain depth. The pit dimensions were 2 m (perpendicular to the drain) by 1.2 m lengthwise.

2. Manual digging

Just upstream of the sample to be taken, soil was removed to a depth of approximately 0.4 m below drain level. Some additional soil was removed around the upstream end of the drain to accomodate a rubber stopper at a later stage.

The length of the undisturbed drain section left in the pit must match the 1.2 m long distance marker. The pipe was then carefully cut at the upstream end, as closely as possible to the wall of the pit. In the case of a thick synthetic fibre envelope a hacksaw was used. The pipe in the wall was closed with a rubber stopper, the end being flush with the cut edge. While doing this it was very important not to move the now partly cut off drain section more than necessary. In

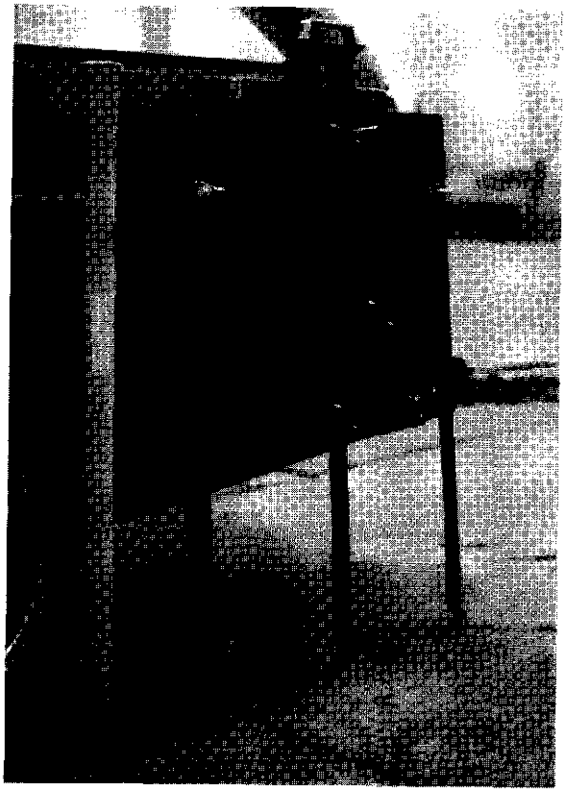

Figure 16. **Heavy duty pressure reaction plate with adjustable ram mount.**

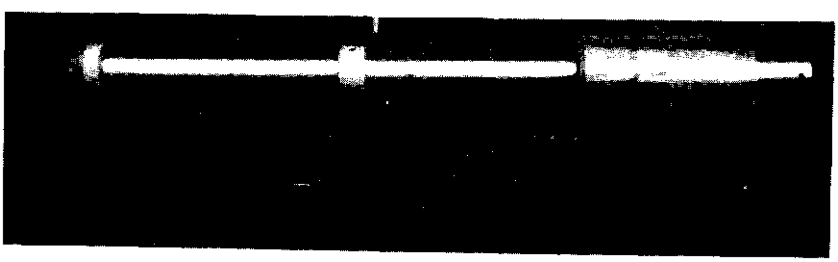

Figure 17. **Pointer stick with purposely made fittings.**

case of discharge water leaking alongside the stopper, some soil was used to try to seal off the upstream pipe section. With substantial water pressure at the stopper, approximately 20 minutes were usually available for sampling before the walls of the pit started to fail. Finally, the downstream end of the drain was cut off very carefully, remembering that the soil core was to be removed here.

3. **Preparation of soil prior to sampling**

The upstream wall of the pit was carefully scraped off until vertical over the entire depth. In case of groundwater seepage and/or discharge from the upstream drain section, a soil barrier had to be made on the floor of the pit to prevent the water reaching the zone to be sampled. The downstream end of the pit was trimmed with a spatula, removing as little soil as possible, until vertical. This face was carefully checked with a level.

4. **Installation and adjustment of sampling tools**

A hammer was used to pound the heavy duty reaction plate vertically into the soil at the upstream end of the pit. The plate should not touch the rubber stopper that plugs the upstream drain section and its legs must fully penetrate the soil. The pointer stick with its fittings was carefully inserted into the drain section to be sampled, such that the perforated pvc probe at the top of the pointer was fully inserted and the perforated ring-shaped fitting coincided with the downstream end of the pit. This stick now indicated the desired orientation of the ram while sampling, thus allowing the sample to be taken centrally and parallel to the drain. The ram mount was fixed onto the reaction plate. Using the butterfly nuts and the pointer stick, the ram was aligned with the centre line of the drain (Fig. 21). This adjustment was critical; the slightest deviation from the exact axial orientation of the ram would cause very high friction losses, failure of the hydraulic jacking devices, severe sample disturbance or cracking of the plexiglass cylinder sections.

5. **Sampling**

The pointer stick was carefully removed from the drain. The centering rod with perforated pvc probe was attached to the heavy duty jacking device. A plexiglass pipe section was placed onto the rim of the jacking device. The pvc probe was now inserted into the drain, the plexiglass cylinder was centered around it and was then held firmly against the soil. While holding the jacking device and the plexiglass cylinder in this position, oil was slowly pumped to the ram, moving it outward until the head of the ram fitted firmly into the drilled chamber in the jacking device (Fig. 22). With everything carefully positioned, the sample was then taken by pumping oil into the hydraulic ram, moving the plexiglass cylinder into the soil around the drain. The two extension sections were fitted to the ram during sampling to achieve the desired movement. It took approximately ten minutes to push the plexiglass cylinder fully into the soil. Reaction forces were high, causing the 5 mm thick, welded and reinforced reaction plate to be pushed backward with some slight deformation. Occasionally, the orientation of the ram had to be readjusted during sampling. This was mainly due to the fact that the the undisturbed subsoil is usually firmer than the trench backfill, resulting in a tendency for the plexiglass cylinder to tilt

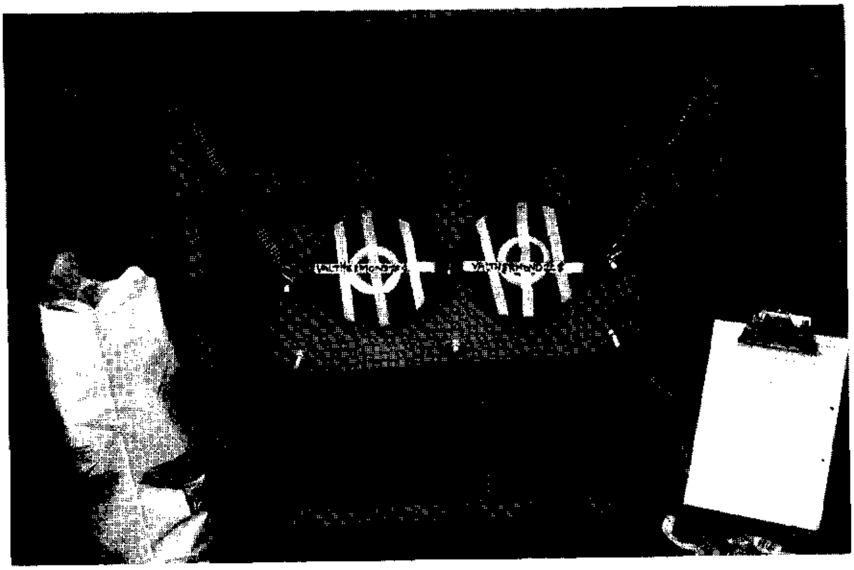

Figure 18. **Shock-absorbing device for simultaneous transport of two sample cores by car.**

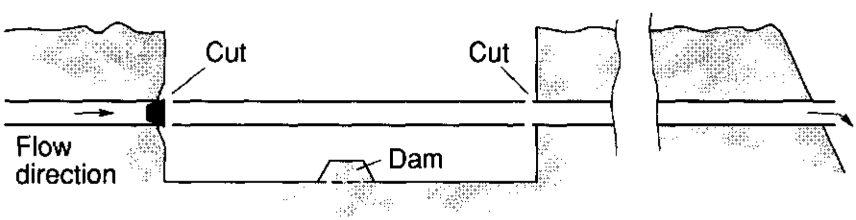

Figure 19. **First stage of the sampling procedure.**

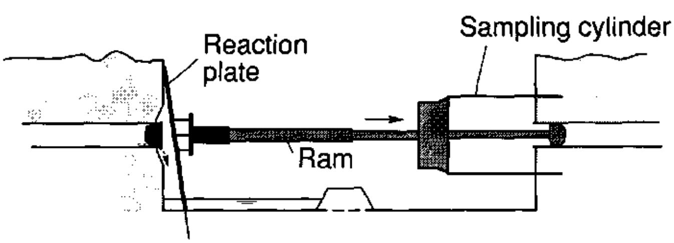

Figure 20. **Second stage of the sampling procedure.**

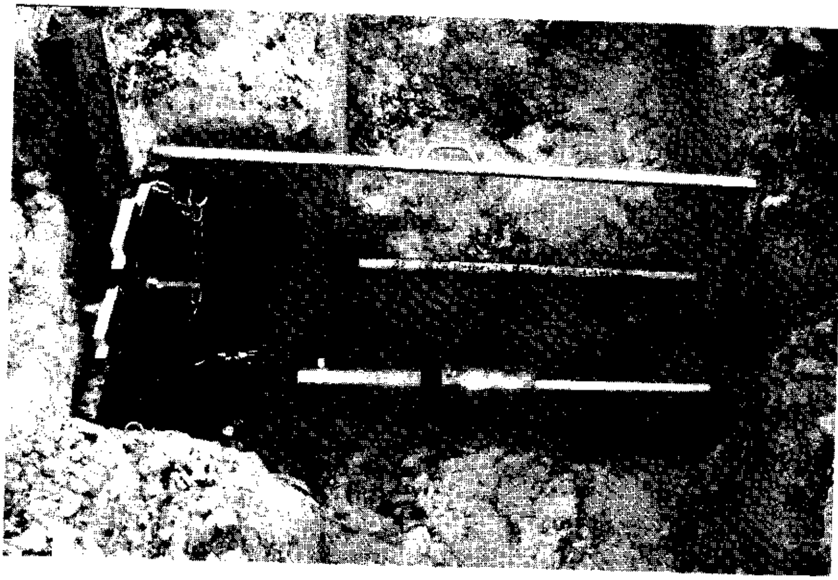

Figure 21. The hydraulic ram pointing in line with the drain.

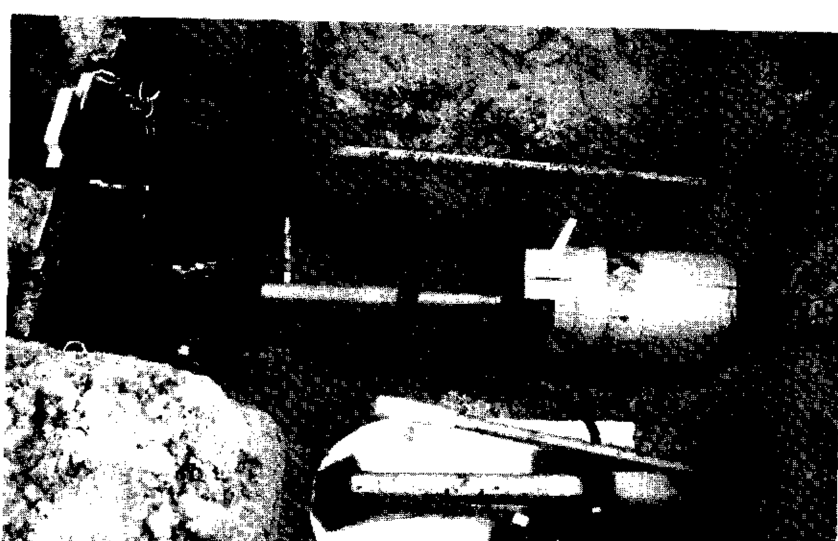

Figure 22. The hydraulic ram fits into the drilled chamber of the jacking device. Note the oblique orientation of the ram (mount) relative to the pressure reaction plate.

downward while sampling.

6. **Sample core removal, preservation and sealing**

After completion of pushing, the core was removed. All sampling hardware was removed from the pit and when necessary, excess water was baled out. Soil was removed from above the sampling cylinder and from beyond the core. The drain beyond the core was cut. The core was removed, maintaining the same alignment as in situ. It was laid down near the edge of the pit.

The stability of a freshly retrieved core is strongly influenced by its water content; water saturated cores may be very difficult to handle without disruption. A tray, resembling a wine bottle bin, was used to keep the core at the required orientation prior to transport. Protruding pipe ends were burnt off. Caps containing foam rubber rings were fixed at either end and were held in place with clamps. Finally, the samples were sealed with water resistant tape.

7. **Repair of damaged lateral and backfilling of pit**

A piece of unperforated corrugated pipe replaced the removed drain section at the sampling site. Normal pipe fittings were used for connections. The envelope material at both cut off drain sections was fixed. The area underneath the freshly installed pipe section was backfilled with comparatively dry soil from the excavations. In the case of very wet conditions, bricks or large clods, chunks etc. were used. Finally, the pit was backfilled.

6 TRANSPORT OF CORES TO THE SCANNING LABORATORY

Two cores were sampled daily. They were scanned as soon as possible. Two cores at a time were shipped to the CT laboratory in a shock-absorbing device, containing springs (Fig. 18). Shaking, especially at high frequencies, may disrupt soil structure in the cores, rendering them useless for further analysis.

Drain sample core retrieval requires personnel who are experienced and are familiar with the subtleties of this technique. High ground water levels can make retrieval very difficult if not impossible. Old drains, running through the sample location as well as pebbles or wood chunks may severely obstruct or prevent sampling. □

REFERENCES

Herman, G.T. 1980. Image Reconstruction from Projections, the Fundamentals of Computerized Tomography. Computer Science and Applied Mathematics, A series of Monographs and Textbooks. Academic Press, New York, N.Y.

Zonneveld, F.W., C.F. Spoor and J. Wind. 1989. The use of CT in the study of the internal morphology of hominid fossils. Medicamundi 34(3):117-128.

5 PARTICLE SIZE ANALYSIS OF SOIL NEAR DRAINS

5 Particle size analysis of soil near drains

ABSTRACT

The influence of envelope specifications and the particle size distribution of a soil on the movement of soil particles near pipe drains was investigated by microgranulometric analysis. Micro soil samples were taken from 45 soil cores, containing drain sections and surrounding soils. These cores were sampled at three locations in The Netherlands. All drain sections had been functioning in weakly-cohesive, fine-sandy soils for at least 5 years. The micro soil samples were removed at increasing distances from the soil/envelope interface, above and below the drain. Soil fractions, retained within the envelopes themselves were also analysed. In total, 720 analyses were made. In most cases, the finest soil particles were found to be concentrated near the soil/envelope interface. This tendency can be largely accounted for by the textural composition of the soil. Formation of a "natural soil filter", i.e. washing out of fine particles near the drain, rarely occurred. Only occasionally did the effective opening size, O_{90}, of envelopes or their composition have a significant effect on particle movement, hence the envelopes provided mechanical support to soils rather than acting as filters.

1 INTRODUCTION

The flow of water towards drain pipes exerts a drag force on soil particles and aggregates. This force is induced by the hydraulic gradient of the flowing water (Luthin et al., 1968). Soils differ in their ability to resist such forces without structural disintegration. In the case of cohesionless or weakly-cohesive soils, particles and aggregates may be suspended in the flowing water and be washed into the drain. This is often observed in newly installed singular drainage systems where lateral drains have free outlets into collector ditches. During a restricted period, drain water will be turbid due to particles that originate from backfilled soil. In some cases, however, sediment entry into drains may continue.

Much has been written about particle movement near agricultural drains. Many statements are of speculative nature, particularly in the case of weakly-cohesive, heterogeneous soils. Some drain envelopes are supposed to promote the development of an area with enhanced hydraulic conductivity around the drain due to the washing out of fines. Others have such fine pores that filter cakes could develop at their interface with the soil. Envelope thickness is often assumed to be of paramount importance for these so-called "selective filtration" properties of envelopes.

This study seeks to detect soil- and envelope features that have a significant effect on particle movement inside the soil around drains. At the contact interface with openings in envelopes or drains, the soil particles hinder each other from being washed out due to the so-called arch effect (Peschl, 1969; Gourc, 1982). The arch effect is characteristic for the static load condition near soil/envelope interfaces (Ogink, 1975).

A very thorough treatment of mechanisms of particle and aggregate movement in soils is given by Ziems (1969). He describes two mechanisms of soil movement at the interface of two media: *contact erosion* and *"natural filter build-up"*.

With *contact erosion*, particles of all sizes are washed out locally due to soil failure or disintegration, resulting in modification of the soil skeleton which transmits the effective stresses (Fig. 1). Samani and Willardson (1981) developed the concept of an empirical parameter called the "hydraulic failure gradient" (HFG) which is the hydraulic gradient at which instability commences. Contact erosion is not discussed here; it will be treated in more detail in Chapter 7.

In the case of *"natural filter build-up"*, only the fine particles are washed out, leaving the larger particles behind (Fig. 2). It may eventually weaken the skeleton of the soil, leading to contact erosion. Willardson and Walker (1979) showed that confinement or physical support of soils greatly influences their structural stability.

Various analogue laboratory tests have been developed to study particle movement near drains (Stuyt (1981), Dierickx (1982), Stuyt (1982), Stuyt & Cestre (1985), Bentarzi (1985), Lennoz-Gratin & Zaïdi (1987)). Results of these tests are reproducible only if performed with cohesionless soil samples or with sieved soil aggregates. Large inconsistencies occur with more realistic heterogeneous, weakly cohesive soil samples. Lennoz-Gratin (1989, 1991) acknowledges that current analogue laboratory models are not very useful when equipped with heterogeneous, weakly-cohesive soils which are representative of field conditions (Stuyt, 1990). This fact gave rise to the present study which was carried out to investigate soil particle movement near drains under field conditions. Unlike the laboratory simulations, the investigated soils have been subjected to water flow under natural conditions for at least five years. The study comprised the following steps:

1. *Taking samples* at selected micro-locations along assumed flow lines near the drain;

2. Determination of the *particle size distribution* of these samples;

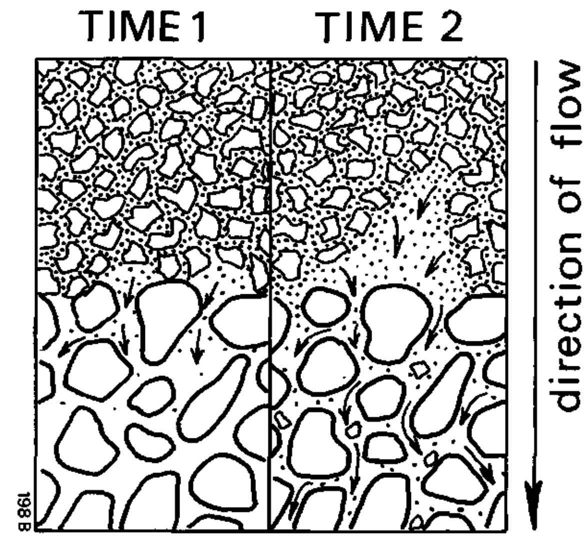

Figure 1. Contact erosion at the interface between the soil (top) and a granular envelope (bottom).

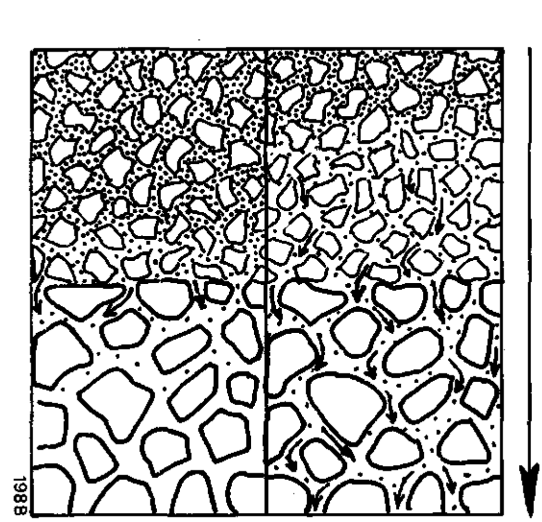

Figure 2. "Natural filter buildup" in the soil (top) near the interface with a granular envelope (bottom).

3. *Statistical analysis* of the data, namely:

   a. *Modelling and estimation* of the peripheral effect, induced by soil/envelope interaction. A curve fitting technique is used to describe the change of the particle size distribution of the soil as a function of the distance from the drain;

   b. *Significance testing* to determine whether this peripheral effect differs from zero;

   c. *Regression analysis* to determine whether the peripheral effect depends on soil properties (origin, particle size distribution, influence of tillage on structural stability) and/or envelope properties (effective opening size (O_{90}), thickness, composition).

Separate analyses were made for seven, 10 μm wide, particle size weight fractions ranging from 10-20 μm to 70-80 μm.

2 SAMPLING LOCATIONS

Migration of soil particles near pipe drains due to flowing water is reflected in the spatial distribution of the particle size distribution of the soil. Particles of a given size may be retained inside the soil, at the soil/envelope interface or in the envelope itself. Selection of the sampling locations must be adapted to the expected spatial distribution. It was based on two considerations.

1. Particle migration proceeds in the direction of the water flow. In the soil therefore must be sampled along an assumed flow line.

2. The rate of migration is likely to be proportional to the hydraulic gradient. The sampling interval must, therefore, be inversly proportional to this gradient. In theory, the hydraulic gradient is maximum at the soil/envelope interface near a drain and is inversely proportional to distance (see Annex 4). The sampling interval should, therefore, be closest at the soil/envelope interface and increase with distance.

The investigated soils were initially sampled as 200 mm diameter by 300 mm long cores for other observations (see Chapters 4, 6 and 7). They contained drain sections complete with the surrounding soils. A total of 45 cores were sampled.

Tentative granulometric analyses were made to determine sampling intervals along assumed flow lines, i.e. perpendicular to the soil/envelope interface. It was concluded that sampling at distances of ½, 1½, 2½, 3½, 4½, 8½ and 14½ mm from the interface was likely to produce the most useful information. With 45 soil cores and 7 granulometric analyses both above and below the drain, 630 analyses were to be made. In addition, the soil retained inside the envelopes was sampled twice at each core (top and bottom), bringing the total number of samples to 720. Due to the narrow sampling interval, only small samples were taken.

3 INSTRUMENTATION

The large number of samples necessitated a rapid though accurate size analysis technique. The method used in this study, appropriate to small sample size, was based on the "Coulter" principle of counting and sizing particles (Coulter, 1956). The instrument used was a Particle Data ElectroZone/Celloscope[1], Model 112, connected to a PDP 11/23 minicomputer (Fig. 3). Elsewhere, this 'particle counter' was used successfully to measure the concentration and size distribution of suspended particles in sea water in coastal regions of the Netherlands (Baretta et al., 1980). This instrument applies a direct current across a narrow aperture and records the voltage pulses which are developed when (dielectric) soil particles, suspended in an electrolyte, are sucked through it. The size of the pulses is related to particle volume. Both the number and magnitude of the pulses are recorded and assigned to one of 256 calibrated size channels. The size of the aperture was 300 μm, providing a measurable size span of 9 to 180 μm (Karuhn and Berg, 1982). The Particle Data counter was selected because of its logarithmic amplifier which greatly expands the dynamic range of analysis and because of the high resolution of its 256 channel analogue-to-digital size converter. Only a small amount of soil (50 mg) is required for an analysis. Detailed treatments of the electro-resistance sizing theory are given by Berg (1958) and Walker & Hutka (1971). Electro resistance sizing results are in close agreement with sieving results (McCave and Jarvis, 1973) as well as with pipette techniques (Shideler, 1976; Behrens, 1978). Experience with the ElectroZone system has shown however that the operator must have considerable practice before the results become reliable and repeatable (Schiebe et al., 1983).

---

[1]'ElectroZone' is a registered tradename of Particle Data, Inc., Elmhurst, IL, USA

Figure 3. The Particle Data ElectroZone/Celloscope electronic particle size analysis instrument.

4 SAMPLING AND PARTICLE SIZE ANALYSIS

Samples for the particle size analysis were taken from each of the 45 large plexiglass sample cores using a stainless steel sampling tube.

Procedure. Two 11 mm wide holes were drilled in the wall of the plexiglass cylinder, one above the drain (i.e. in the backfilled trench) and the other at the bottom. A piston inside the 8 mm inside diameter stainless steel sampling tube, depicted in Fig. 4, was screwed fully inwards. The piston was lubricated slightly and surplus oil removed with a tissue. The tube was carefully inserted a few mm's into the soil core through the hole in the plexiglass cylinder, perpendicular to the centre line of the drain (Fig. 5). The tube was slowly pushed into the soil until it touched the envelope (Fig. 6), then withdrawn with the sampled soil. The sampling tube was wiped clean and adhesive tape wound stiffly around it to cover its entire length. With the tube mounted in a holder, open end pointing upward, the piston was slowly screwed outward until a 1 mm thick layer of soil material was extruded from the open end. If dry, the soil was wetted by a small drop of water applied through a syringe. The soil layer was removed with a

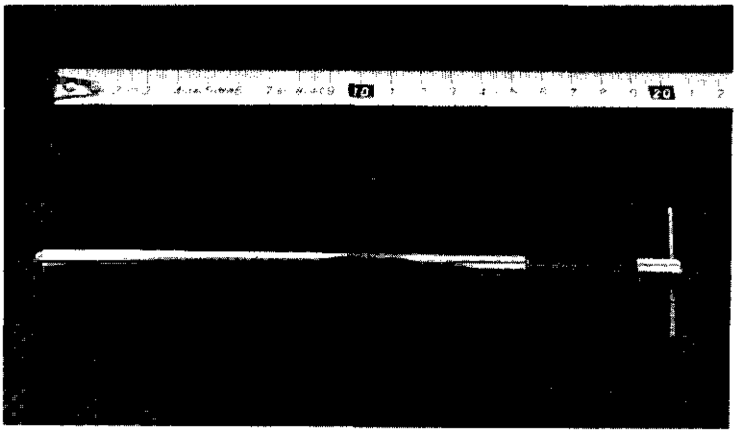

Figure 4. The stainless steel sampling tube with brass piston.

razor blade and transfered into a sample beaker through a 30 mm wide sieve with 150 µm mesh aperture. A small brush was used to force as many particles as possible through the sieve into the beaker (Fig. 7). Sieving at 150 µm was necessary because the upper size limit of the measuring instrument was approximately 165 µm; larger particles or organic substances like fibres would easily obstruct its sensing aperture. The sieved sediment was analysed and the next, 1 mm of sample extruded, by making one full rotation of the spindle of the sampling tube.

Soil material, ***retained inside the envelopes***, was sampled in a slightly different manner. A piece of hard wood was shaped into a solid cylindical section to fit exactly inside a drain (Fig. 8). This plunger was pushed into the drain to coincide with the envelope sampling location and an 8 mm diameter portion of envelope material together with a disc out of the pipe wall was cut using a strong steel sampling tube with sharpened rim (Fig. 9). Loose, voluminous envelopes were immersed in water and retained soil particles washed out through the sieve into the sample beaker. Thin envelopes were immersed and rinsed until clean. Some sample discs are depicted in Fig. 10.

After analysis, the population of measured particles was available as a frequency distribution in 256 size channels. This was transformed to a volume or weight distribution, assuming spherical particles. The following statistical parameters and soil characteristics were estimated or calculated: mode [L], median particle size (D_{50}) [L], uniformity coefficient U (D_{60}/D_{10}) [-] and weight percentiles at 10, 20, ..., 90, 100 and 125 µm [-].

5 STATISTICAL ANALYSIS

An analysis was made to see if and how the particle size distribution changed

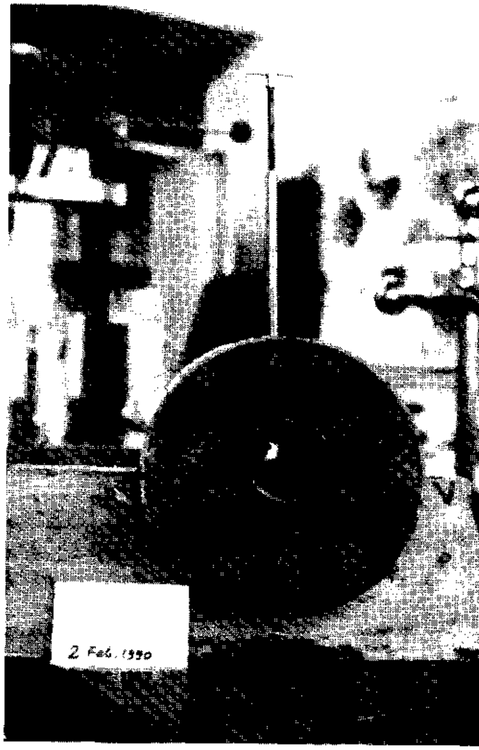

Figure 5. The sampling tube should point exactly towards the drain.

along assumed flow lines near a drain. Separate analyses were made for seven, 10 µm wide, particle size fractions s, ranging from 10-20, 20-30, ..., 70-80 µm. Sometimes no clear relation was observed between the relative weight of a particle size fraction s and the distance d from the soil/envelope interface. In other cases, however, relations were found as depicted in Fig. 12. This corresponds to expectations: the relative weight of a size fraction is constant further away from the drain and changes in its vicinity. Mostly, the effect levels off within 3 to 5 mm from the drain.

The *peripheral effect*, along a streamline, on an observed weight fraction fr_s (**d**), could be defined simply as

$$\Delta fr = fr_s\ (0.5) - fr_s\ (14.5) \qquad (-) \qquad (1)$$

Figure 6. **A micro soil sample is taken by pushing the tube carefully downward until it touches the envelope.**

Δfrs being the difference between the observed weight fractions at d = 0.5 mm and d = 14.5 mm. Nevertheless, a more useful estimate, using all observations could be made as follows:

1. The observed weight percentages of the size fractions s were fitted to distance from the interface, d [L] as F_s (d) [-] using a non-linear equation

   $$F_s(d) = a + b.r^d \qquad (-) \qquad (2)$$

   This accomodates an increasing peripheral effect on $F_s(d)$ with decreasing

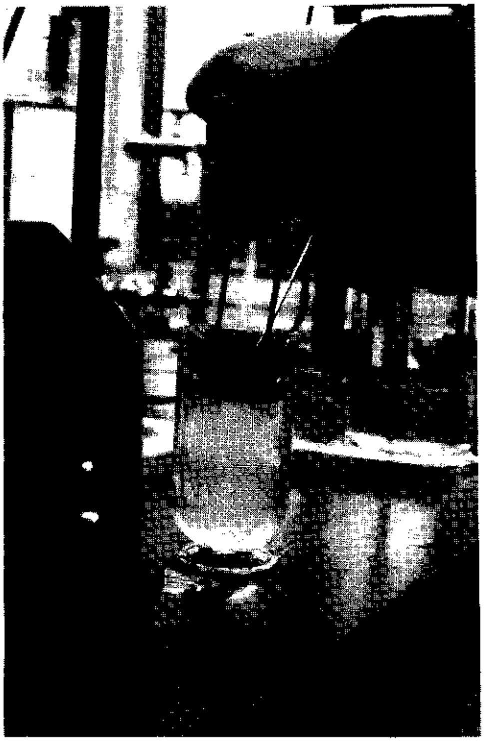

Figure 7. Wet sieving of particles into the sample beaker.

distance d from the drain/envelope interface. In Eq. (1), a [-] is the weight percentage of a soil fraction as d tends to infinity; b [-] and r [-] are regression parameters.

2. If this equation gave a reasonable fit, the peripheral effect was estimated as

$$\Delta F_s = F_s\,(0.5) - F_s\,(14.5) \qquad (-) \qquad (3)$$

being the difference between the fitted weight fractions at d = 0.5 mm and d = 14.5 mm.

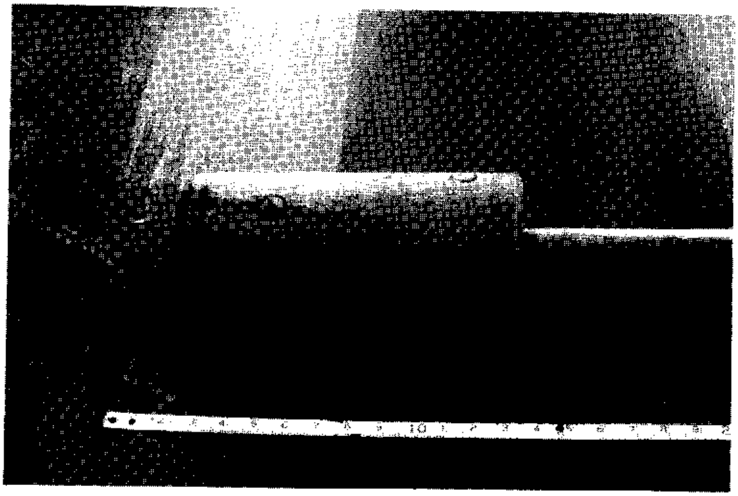

Figure 8. **Wooden plunger, fitting exactly inside a drain (see text).**

The peripheral effect ΔF_s was set to zero if

1. the residual variance exceeded the variance accounted for by regression (poor fit of the curve),

2. parameter r in Eq. (1) was larger than 1 which implies that there is no asymptotical value of F_s for large d, or

3. the effect is limited to the area within 1.5 mm from the soil/envelope interface. This excludes cases where the effect is determined by one

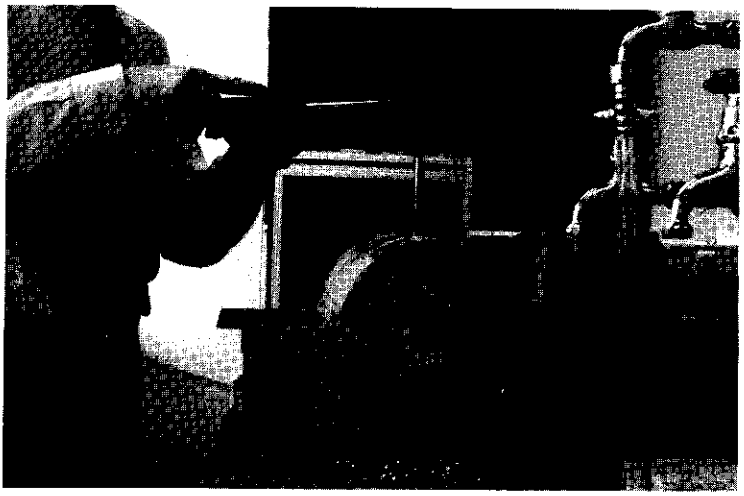

Figure 9. **Taking an envelope sample disc including retained soil.**

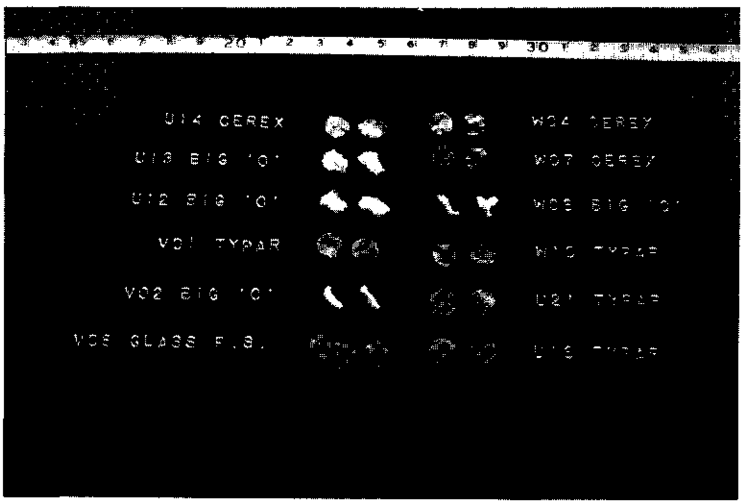

Figure 10. **Some sample discs of thin or sheet envelopes.**

observation only (at d = 0.5 mm).

The remaining curves were visually checked for adequate geometric fit. A small number of curves were considered to be inadequate descriptions of fr_s (d) due to poor geometric fit and were rejected. Corresponding values of ΔF_s were set to zero. Having determined the peripheral effect ΔF_s for the 90 locations (top and bottom of each core), multiple linear regression was used to see whether this effect

1. equalled some constant value (either positive or negative),
2. was (partly) accounted for by soil particle size distribution and/or structure, and
3. was (partly) accounted for by design parameters of the envelopes.

In the regression model, seven predictor variables x_1, x_2, ..., x_7 were included, as follows:

$$\Delta F_s = a_0 + a_1 x_1 \quad a_2 x_2 + a_3 x_3 + a_4 x_4 + a_5 x_5 + a_6 x_6 + a_7 x_7 + e \qquad (4)$$

Variables or factors related to the **soils** are:

1. *origin* (experimental field) [x_1],
2. *particle size distribution* (D_{50}) [x_2],
3. *uniformity coefficient* (D_{60}/D_{10}) [x_3],
4. *structure* (undisturbed or backfilled) [x_4].

Variables or factors related to the **envelopes** are:

1. *thickness* ("thin" (< 1 mm) or "voluminous") [x_5],
2. *effective opening size* of pores (O_{90}) [x_6],
3. *raw material* (12 different kinds) [x_7].

The coefficients a_0, a_1, ..., a_7 were estimated from the 90 observations; e is the residual term of the model (unexplained variation). A stepwise selection procedure was used to find predictor variables which have a significant effect on ΔF_s (Draper & Smith, 1981). Regression and selection of variables was carried out for seven, 10 µm wide, particle size fractions s, ranging from 10-20, 20-30, ..., 70-80 µm.

The same regression model was used to examine selective filtering of soil particles by envelopes which is reflected in the size distribution of particles that are retained inside these, EFr_s. The same particle size ranges have been considered and the same predictor variables have been used (x_1, x_2, ..., x_7). The computations were made with the statistical program "Genstat" (Genstat 5 Committee, 1987).

6 RESULTS

The average number of analyzed particles in the soil samples was 42474 ("Uithuizermeeden" experimental field), 24552 ("Valthermond"), 54388 ("Willemstad"), 40872 (all samples). The number of particles, retained inside envelopes was 38912, 31252, 34715, and 35750, respectively. Average particle size distributions at 14½ mm from the soil/envelope interface are depicted in Fig. 11. Median particle sizes (D_{50}) and uniformity coefficients U (D_{60}/D_{10}) are given in Table 1. These particle size parameters are generally used as indicators for soil structural stability. A soil with a median particle size (D_{50}) between 50 and 200 µm may disintegrate due to its low structural stability if exposed to pressure of flowing water (Stuyt, 1983). All examined soils satisfied this criterion. The uniformity coefficient (D_{60}/D_{10}) gives an indication of the particle size range of a soil. The risk of mineral clogging of envelopes and drain pipes is assumed to be inversely proportional to the value of the uniformity coefficient, which was therefore included in the regression analyses.

Examples of curves, fitted to observed weight percentages of soil fractions $fr_s(d)$ are depicted in Fig. 12. The occurrence of successfully fitted peripheral effects ΔF_s on weight percentages of soil fractions $fr_s(d)$ near drains was inversely proportional to particle size (Table 2). For smaller soil particles more often a peripheral effect was observed than for larger ones.

Nevertheless, the effect on weight percentages of small (10-30 µm) particles near drains was ill-defined, cf. Table 3 where values of coefficients a_0, a_1, ..., a_7 of the regression analysis dealing with the peripheral effect on the particle size distribution of the soil near drains, ΔF_s, are given. Only significant terms (at 5% level) have been included in the regression model. Both positive and negative effects were found. In case of a negative coefficient the involved variable or factor induced a decrease of the peripheral effect relative to previous variables or factors,

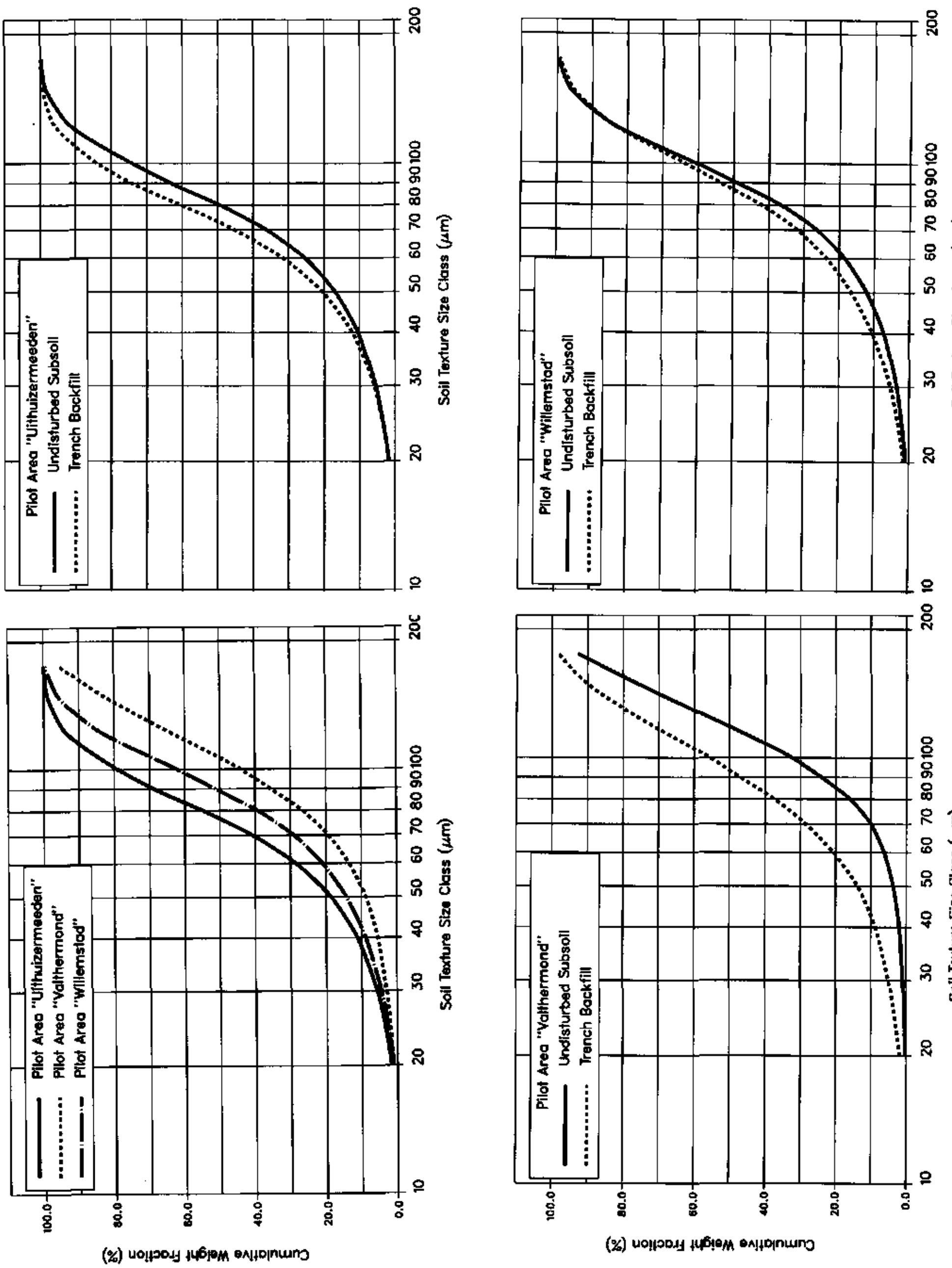

Figure 11. **Average particle size distributions at 14½ mm from the soil/envelope interface: averages, observed at the experimental fields, and trench backfill and subsoil depicted for each experimental field separately.**

Table 1. Particle size classification parameters of soils (median particle size D_{50} (μm) and uniformity coefficient D_{60}/D_{10} (-)), located at experimental field near Uithuizermeeden, Valthermond and Willemstad.

Experimental field	Soil Configuration	D_{50}	D_{60}/D_{10}
Uithuizermeeden	Trench	72.9	2.09
	Subsoil	79.5	1.85
	Trench + Subsoil	76.2	1.97
Valthermond	Trench	93.5	2.28
	Subsoil	119.2	1.89
	Trench + Subsoil	106.4	2.08
Willemstad	Trench	87.4	2.47
	Subsoil	91.8	2.11
	Trench + Subsoil	89.6	2.29
All fields	Trench	82.2	2.24
	Subsoil	93.4	1.93
	Trench + Subsoil	87.8	2.09

e.g. the soils in "Willemstad" and "Valthermond" experimental fields, compared to "Uithuizermeeden" (coefficient a_1). Similarly, positive coefficients reflect an increase of the peripheral effect, e.g. the median particle size (coefficient a_2). The

Table 2. Successfully fitted peripheral effects ΔF_s, '✓', expressed as fractions of all observations (-) (n = 90) for particle size fractions ranging from 10 to 80 μm.

Size fraction (μm)	
10 - 20	0.80
20 - 30	0.62
30 - 40	0.64
40 - 50	0.63
50 - 60	0.59
60 - 70	0.56
70 - 80	0.54

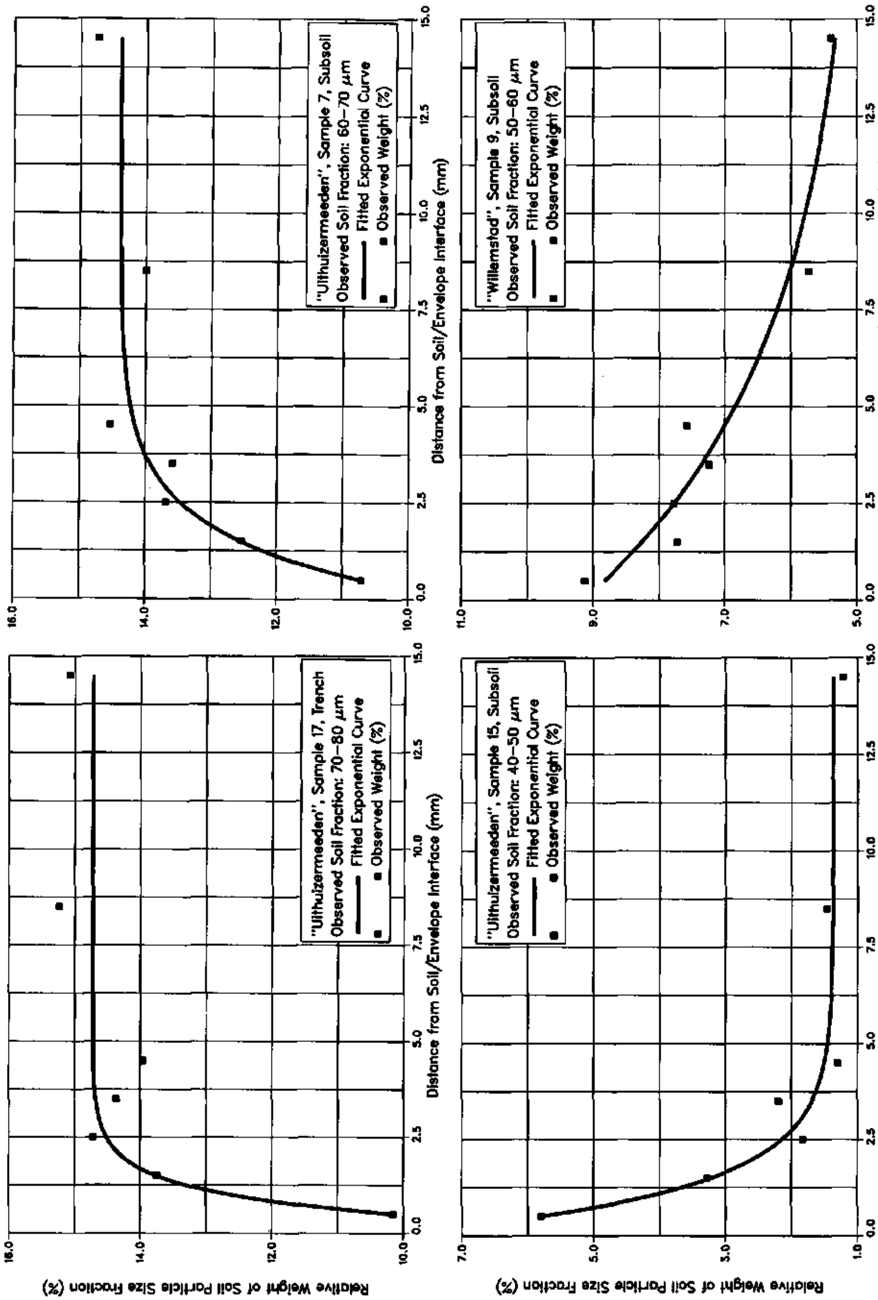

Figure 12. **Relative weight variation of particle size fractions of soils near drains. The variation is maximum near the soil/envelope interface and tends to a constant value with distance.**

Table 3. Coefficients of multiple linear regression. Analysis of the peripheral effect, ΔF_g, with distance from the drain.

Coefficient		Particle Size Fraction (μm)						
		10-20	20-30	30-40	40-50	50-60	60-70	70-80
a_0		0.75	-	-4.72	-6.23	-7.72	-8.68	-6.32
a_1	**Experimental field**							
☞	Uithuizermeeden	-	-	-	-	-	-	-
☞	Valthermond	-	-	-	-2.52	-3.52	-3.37	-2.53
☞	Willemstad	-	-	-	-	-	-2.17	-2.48
a_2	**Median particle size (D_{50})**	-	-	0.06	0.08	0.11	0.12	0.10
a_3	**Uniformity coefficient (D_{60}/D_{10})**	-	-	-	-	-	-	-
a_4	**Soil structure**							
☞	undisturbed (subsoil)	-	-	-	-	-	-	-
☞	disturbed (trench)	-	-	-	-	-	-	-
a_5	**Envelope thickness**							
☞	"thin" (≤ 1 mm)	-	-	-	-	-	-	-
☞	"voluminous" (> 1 mm)	-	-	-	1.49	-	-	-
a_6	**Effective opening size of envelope (O_{90})**	-	-	-	-	-	-	0.002
a_7	**Type of envelope**							
☞	Big "O" fabric	-	-	-	-	-2.34	-	-
☞	Cerex nonwoven	-	-	-	-	-	-	-
☞	Coconut Fibres	-	-	-	-	-	-	-
☞	"Garden" Peat Fibres	-	-	-	-	-	-	-
☞	Glass Fibre Membrane	-	-	-	-	-	-	-
☞	Peat-Cocos fibre mix	-	-	-	-	-	-	-
☞	Peat-Cocos fibre mix (buffer)	-	-	-	-	-	-	-
☞	Polypropylene Fibres "A"	-	-	-	-	-	-	-
☞	Polypropylene Fibres "B"	-	-	-	-	-	-	-
☞	Polystyrene beads "PS-LDPE"	-	-	-	-	-	-	-
☞	Polystyrene beads "PSL"	-	2.49	-	-	-	-	-
☞	Typar	-	-	-	-	-	-	-

value of coefficient a_0 is meaningless unless all other coefficients are zero. In the latter case, a_0 reflects the average peripheral effect.

The peripheral effect on weight percentages of larger particles depended largely on the median particle size of the soil and on the experimental field. It did not depend on the uniformity coefficient, soil structure, envelope thickness, the effective opening size of an envelope or the type of envelope. Moderately fine sands (D_{50} > 80 μm) tended to retain comparatively small soil particles near the drain. No effect was observed on soils with 70 μm ≤ D_{50} ≤ 80 μm. Soils with many fine particles (D_{50} < 70 μm) tended to lose fine particles, leading to "natural filter build-up" near the drain. An example from "Valthermond" experimental field is given in Fig. 13. This phenomenon was observed rather frequently in the backfill of "Uithuizermeeden" experimental field. Considering all observations, however, "natural filter build-up" was found in only a minority of cases. Most sampled soils had larger median particle sizes. These soils (D_{50} > 65 μm) tended to clog internally near the soil/envelope interface (Fig. 14).

In brief, internal soil clogging was the dominant process and is likely to occur with fine-sandy soils; the reverse process ("natural filter build-up") was observed occasionally and only with soils which contain many fine particles. Generally, the influence of envelope characteristics on the movement of soil particles in unstable soil near a drain was not significant.

Regression parameters concerning the size distribution of soil particles inside envelopes, EFr_s, are given in Table 4. Only significant terms (at 5% level) have been included in the regression model. Obviously, the composition of the soil largely determined the size distribution of retained soil. Some envelopes ("Big 'O'", Polystyrene beads and "Typar") had relatively poor retaining capacities for small particles. Most of these envelopes had a preference to retain large particles. Envelopes made from peat litter retained larger amounts of particles of intermediate sizes.

7 DISCUSSION

In this research, the particle size distribution of soil which has stabilized near the interface with the envelope, was analysed. The assumption that envelope properties largely determine the movement of soil particles near drains is widespread. Nevertheless, this assumption is not supported by the results of this analysis; no significant values were found for coefficient a_7 of the regression model which accomodates the type of envelope (Table 3). In weakly-cohesive Dutch soils, soil properties rather than envelope properties appear to determine the movement of soil particles near drains (coefficients a_1 and a_2 in Table 3).

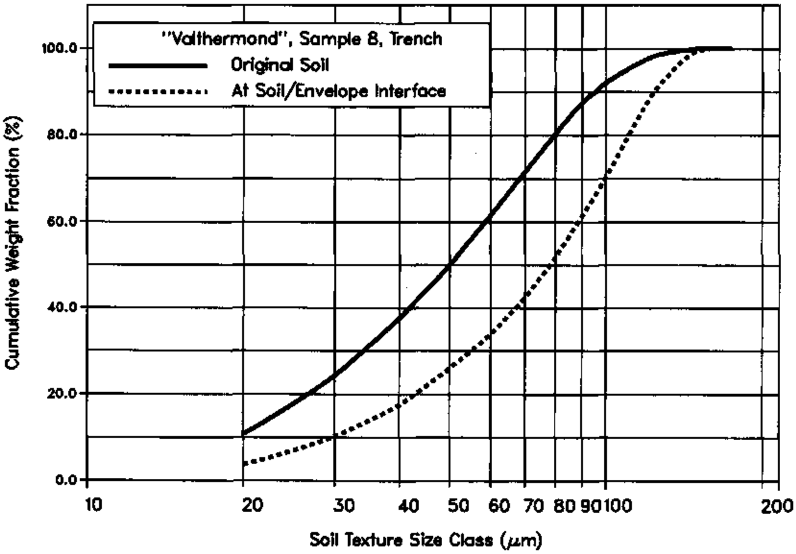

Figure 13. Example of "natural filter buildup" in a soil near a drain. The soil at the interface with the envelope is coarser than the soil at greater distance.

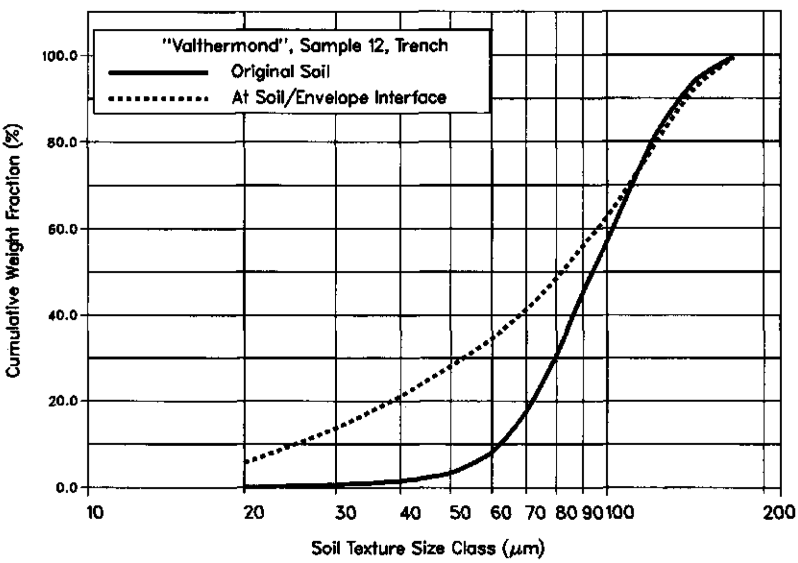

Figure 14. Example of "internal soil clogging" in a soil near a drain. The soil at the interface with the envelope is finer than the soil at greater distance.

Table 4. Coefficients of multiple linear regression. Analysis of the size distribution of soil particles inside envelopes, EFr_s.

Coefficient		Particle Size Fraction (µm) 10-20	20-30	30-40	40-50	50-60	60-70	70-80
a_0		6.09	8.89	12.92	12.74	13.60	14.17	13.32
a_1	**Experimental field**							
☛	Uithuizermeeden	-	-	-	-	-	-	-
☛	Valthermond	-	-3.05	-	-	-2.45	-3.99	-4.66
☛	Willemstad	-	-	-	-	-3.01	-4.39	-4.71
a_2	**Median particle size (D_{50})**	-	-	-0.06	-0.06	-0.06	-0.05	-0.05
a_3	**Uniformity coefficient (D_{60}/D_{10})**	-	-	-	-	-	-	-
a_4	**Soil structure**							
☛	undisturbed (subsoil)	-	-	-	-	-	-	-
☛	disturbed (trench)	-	-	-	-	-	-	-
a_5	**Envelope thickness**							
☛	"thin" (≤ 1 mm)	-	-	-	-	-	-	-
☛	"voluminous" (> 1 mm)	-	-	-	-	-	-	-
a_6	**Effective opening size of envelope (O_{90})**	-	-	-	-	-	-	-
a_7	**Type of envelope**							
☛	Big "O" fabric	-4.65	-4.27	-2.88	-	-	3.37	3.70
☛	Cerex nonwoven	-	-	-	-	-	2.29	-
☛	Coconut Fibres	-	-	-	3.47	3.23	-	-
☛	"Garden" Peat Fibres	-	-	-	-	-	-	-
☛	Glass Fibre Membrane	-	-	-	-	-	-	-
☛	Peat-Cocos fibre mix	-	-	-	2.36	-	2.64	-
☛	Peat-Cocos fibre mix (buffer)	-	-	-	2.47	2.20	-	-
☛	Polypropylene Fibres "A"	-	-	-	-	-	-	-
☛	Polypropylene Fibres "B"	-	-	-	-	-	-	-
☛	Polystyrene beads "PS-LDPE"	-3.80	-	-	-	-	-	-
☛	Polystyrene beads "PSL"	-4.16	-3.16	-	-	-	-	2.14
☛	Typar	-3.35	-	-	-	2.67	3.15	2.83

Comparatively small soil particles ($\leq$ 30 µm) are more easily mobilized by flowing water than larger ones (Table 2). The average peripheral effect however was zero (coefficient a_0 in Table 3), so small particles, once suspended, may equally well be evacuated from the soil as be trapped in it. Larger particles are less easily mobilized but the average peripheral effect is well defined. Generally, such particles are retained in the soil near the drain which itself is a very fine filter.

When a soil clogs internally, its textural composition is modified by a local influx of fine particles which block its pores. Fahmy (1961) established that small amounts of suspended clay particles may lead to a substantial decrease of saturated hydraulic conductivities of sandy soils due to filling up of pores. Eventually, virtually impermeable so-called filter cakes, i.e. soil areas with very low porosity, may develop. Equations describing cumulative size distributions of soils with minimum porosity are given by Ziems (1969) and are generally of the form

$$p_i = (d_i . d_{max}^{-1})^{\alpha} \cdot 100\% \qquad (-) \qquad (6)$$

where p_i = weight percentage of soil fraction with $d \leq d_i$ (-)

d_{max} = maximum particle diameter in soil (m)

α = dimensionless exponent $0.3 \leq \alpha \leq 0.5$ (-)

To allow a comparison of the particle size distributions found in these tests with those of possible "filter cakes" that could develop in these soils, curves of soils with minimum porosity were calculated for α = 0.4 and included in Fig. 15 and 16. In the case of internal soil clogging (Fig. 16) the particle size distribution of the soil at the soil/envelope interface appears to have developed toward that of a soil with minimum porosity.

Once soil particles are evacuated from the soil, drain envelopes clearly act as selective filters. Some envelopes retain comparatively small numbers of very fine particles (< 30 µm) as is reflected in negative values of coefficient a_7 in table 4 (Big "O", "PS-LDPE", "PSL" and "Typar". Others have better than average retaining properties for particles > 40 µm, e.g. envelopes which contain peat litter. Nevertheless, the size distribution of particles, retained inside envelopes is not necessarily indicative for their filtering properties. A soil could stabilise over the greater part of the area of the soil/envelope interface but the stable arches may break down locally (the soil "fails") and subsequent contact erosion at the soil/envelope interfaces could lead to envelope clogging and/or pipe sedimentation.

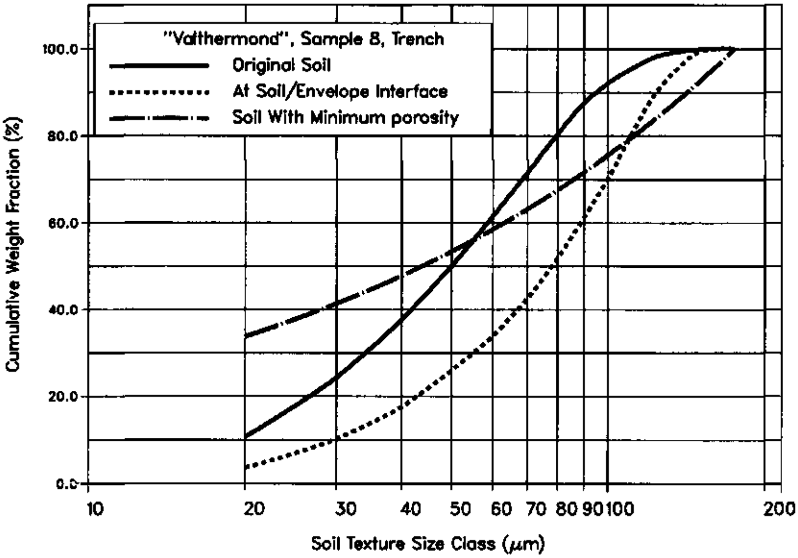

Figure 15. Example of "natural filter buildup" in a soil near a drain. With time, the size distribution of the soil at the soil/envelope interface has not developed towards that of a soil with minimum porosity.

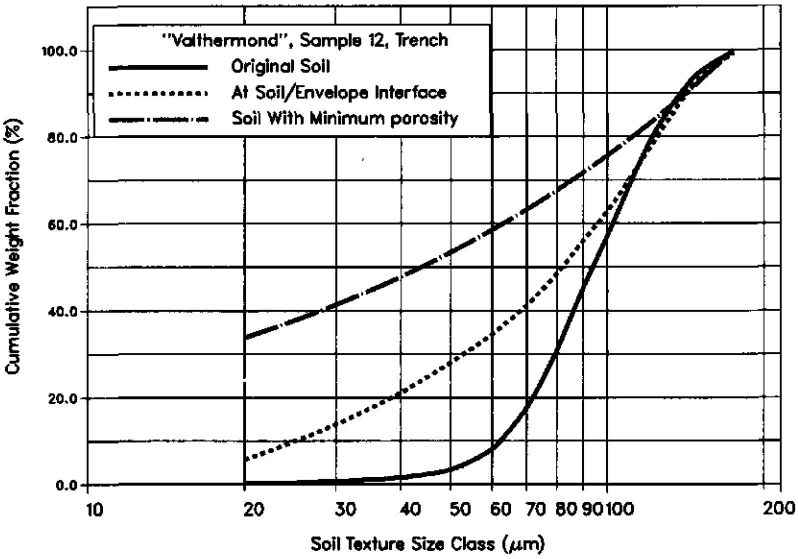

Figure 14. Example of "internal soil clogging" in a soil near a drain. With time, the size distribution of the soil at the soil/envelope interface has developed towards that of a soil with minimum porosity.

This is another important phenomenon which must be examined before the functioning of envelopes can be accurately assessed. The process of contact erosion is discussed in Chapter 7 and pipe sedimentation is covered in Chapter 3. □

REFERENCES

Baretta, J.W., J.G. Baretta-Bekker, V.N. de Jonge, L.A. Villerius and P. de Wolf. 1980. Slibspecielozingen in het Eems estuarium nabij Delfzijl, zoals gemeten volgens verschillende meetmethoden (Analyses of sediment, released in the Eems estuary near Delfzijl, made with various methods). Publicaties en verslagen No. 4, Biologisch Onderzoek Eems-Dollard Estuarium (BOEDE). NIOZ, Texel, The Netherlands.

Behrens, E.W. 1978. Further comparisons of grain size distributions determined by electronic particle counting and pipette techniques. Journ. Sedim. Petrol. 48(4):1213-1218.

Bentarzi, A. 1985. Test de stabilité de quelques sols avec un drain nu. Experiences en perméamètres (Soil stability tests with a plain drain. Experiences with permeameters). Memoire de DEA, CEMAGREF, ENITRTS, 1-73 (in French).

Berg, R.H. 1958. Electronic size analysis of subsieve particles by flowing through a small liquid resistor. A.S.T.M. Spec. Tech. Publ. No. 234:245-255.

Coulter, W.H. 1956. High speed automatic blood-cell counter and cell size analyser. Proc. Nat. Elec. Conf. 12:1034-1042.

Dierickx, W. 1982. Hydraulic gradients near subsurface drains and soil erosion. A.S.A.E. Paper No. 82-2568: 1-8.

Draper, N.R. and H. Smith. 1981. Applied Regression Analysis (2nd edition). Wiley & Sons, New York, N.Y. USA.

Fahmy, M.I. 1961. The influence of clay particles on the hydraulic conductivity of sandy soils. Doctoral thesis, Agricultural University, Wageningen, The Netherlands.

Genstat 5 Committee, 1987. Genstat 5 Reference Manual. Clarendon Press, Oxford, England.

Gourc, J.P. 1982. Quelques aspects du comportement des Geotextiles en Mécanique des sols (Some aspects of the behaviour of geotextiles with respect to soil mechanics). Thèse, Université scientifique et medicale / Institut National Polytechnique, Grenoble, France (in French).

Karuhn, R.F. and R.H. Berg. 1982. Practical aspects of electrozone size analysis. Particle Data Laboratories, Ltd., Elmhurst, IL 60126 USA.

Lennoz-Gratin, Ch. and K. Zaïdi. 1987. Hydraulique au voisinage du drain (Hydraulics near the drain). Etudes du CEMAGREF, 2:1-139 (in French).

Lennoz-Gratin, Ch. 1989. Effect of Envelopes on Flow Pattern Near Drain Pipe. Journ. Irr. Drain. Eng. 115(4):626-641.

Lennoz-Gratin, Ch. 1991. Hydraulique à l'interface sol-drain. Application à la prévision du risque de colmatage minéral des drains agricoles (Hydraulics near the drain. Application with emphasis on the risk of mineral clogging of agricultural drains). Thèse, études du CEMAGREF, série Hydraulique Agricole, No. 9, CEMAGREF-DIVOCA, PB 22, 92162 ANTONY CEDEX, France (in French).

Luthin, J.N., G.S. Taylor and C. Pietro. 1968. Exit gradients into subsurface drains. Hilgardia 39(15):419-428.

McCave, I.N. and J. Jarvis. 1973. Use of the Model T Coulter Counter in size analysis of fine to course sand. Sedimentology 20:305-315.

Ogink, H.J.M. 1975. Investigations on the hydraulic characteristics of synthetic fibres. Publ. 146, Delft Hydraulics Laboratory, Delft, The Netherlands.

Peschl, I.A.S.Z. 1969. Gewelfvorming in bunkers (Formation of stable arches in bins). Doctoral thesis, Technical University Eindhoven, The Netherlands (in Dutch).

Samani, Z.A. and L.S. Willardson. 1981. Soil Hydraulic Stability in a Subsurface Drainage System. Trans. Amer. Soc. Agr. Eng., Vol. 24, No. 3, pp. 666-669.

Schiebe, F.R., H.H. Welch and L.R. Cooper. 1983. Measurement of Fine Silt and Clay Size Distributions. Transact. ASAE 1983: 491-496.

Shideler, G.L. 1976. A comparison of electronic particle counting and pipette techniques in routine mud analysis. Journ. Sedim. Petrol. 46(4):1017-1025.

Stuyt, L.C.P.M. 1981. Developments in research on drainage filter materials in the Netherlands. Soil and Water 9(2).

Stuyt, L.C.P.M. 1983. Drainage envelope research in the Netherlands. Proc. 2nd Int. Drain. Workshop, Washington DC. Ed. CPTA, Carmel, Indiana USA:106-123.

Stuyt, L.C.P.M. and T. Cestre. 1985. Common lines in research on drainage envelopes in France and in the Netherlands. Proc. Symp. on Agr. Water Managem., Arnhem, the Netherlands, pp. 163-173.

Stuyt, L.C.P.M., 1990. Computed tomography for envelope clogging determination and visualisation. Proceedings of the Symposium on land drainage for salinity control in arid and semi-arid regions, 25 February-2

March 1990, Cairo, Egypt, Vol. 3:105-116.

Walker, P.H. and J. Hutka. 1971. Use of the Coulter Counter (Model B) for Particle-Size Analysis of soils. Tech. Pap. Div. Soils, C.S.I.R.O. Aust. 1, 39 pp.

Ziems, J. 1969. Beitrag zur Kontakterosion nichtbindiger Erdstoffe (Contribution to contact erosion of cohesionless soils). Ph.D. thesis, Techn. Univ. Dresden, DDR. 209 pp. (in German).

6 FINITE ELEMENT SIMULATION OF FLOW INTO DRAINS

Effect of radial soil heterogeneity around a subsurface drain on the water table height computed using a finite element model. (T. Zissis and L.C.P.M. Stuyt).

Published in *Agricultural Water Management*, 20 (1991) 47-62

Effect of radial soil heterogeneity around a subsurface drain on the water table height computed using a finite element model

T. Zissis[a] and L.C.P.M. Stuyt[b]

[a]*Dept. of Hydraulics, Soil Science and Agricultural Engineering, School of Agriculture, Aristotle University of Thessaloniki, 54006 Thessaloniki, Greece*

[b]*The Winand Staring Centre for Integrated Land, Soil and Water Research, P.O. Box 125, 6700 AC Wageningen, The Netherlands*

(Accepted 24 January 1991)

ABSTRACT

Zissis, T. and Stuyt, L.C.P.M., 1991. Effect of radial soil heterogeneity around a subsurface drain on the water table height computed using a finite element model. *Agric. Water Manage.*, 20: 47–62.

The problem of two-dimensional saturated flow towards a subsurface drain wrapped with a voluminous envelope, was solved by a finite element approach. Special attention was given to water flow in the vicinity of the pipe and to the permeability pattern of the envelope and the surrounding soil. Therefore nonlinear elements were used for a better representation of the geometry around the drain, and for more accurate predictions of hydraulic heads due to nonlinear interpolation. Soil heterogeneity around the drain detected and quantified using data from X-ray computed tomography (CT) images and textures analyses, was expressed as gradually varying hydraulic conductivity in the radial direction. Results showed the influence of the heterogeneous soil zone as well as clogging of the envelopes on the water table height at the midpoint between the drains. The hydraulic conductivity of the envelope was found to be the most significant factor with respect to the functioning of the drain.

INTRODUCTION

In recent years, flow in the immediate vicinity of drains has been extensively studied. Soil disturbance during installation, the dimensions and the hydraulic properties of the envelope materials, soil texture and structure and the movement of soil particles towards the envelope and the drain perforations have a severe impact on the flow pattern, on the functioning of the drain and consequently on the water table height.

Analogue (Dierickx, 1980) and mathematical models (Van Deemter, 1950; Widmoser, 1968; Gureghian and Youngs, 1975; Zaradny and Feddes, 1979; Niewenhuis and Wesseling, 1979; Fipps et al., 1986) have been used in the past for the simulation of flow towards subsurface drains. The simplifying

0378-3774/91/$03.50

assumption of a homogeneous and isotropic soil surrounding a drain pipe wrapped with homogeneous envelope is commonly used.

The two-dimensional saturated flow problem in the vertical (x,z) plane is depicted in Fig. 1, where a recharge rate, q (LT^{-1}), vertically reaches the water table between parallel drain pipes installed at a spacing, L (L), and at height d (L) above the impermeable layer. The water table heights, with respect to drain level, midway and immediately above the drain are h_m (L) and h_0 (L), respectively. Many theoretical studies have been devoted to this fundamental land drainage problem (Lovell and Youngs, 1984). As a result, numerous analytical solutions as well as approximations, based upon simplifying assumptions, are available as drain spacing equations.

Finite element models are well-suited for the simulation of this flow problem. Two-dimensional finite element solutions where attempts are made to accurately represent the drain as a hole in the finite element mesh have been proposed by Gureghian and Youngs (1975) for the case of saturated flow, and by Zaradny and Feddes (1979) and Fipps et al. (1986) for saturated–unsaturated flow. In all these models, linear elements have been used. Moreover it is acknowledged that accurate computation of flow rates into the drain calls for a large number of very small elements in its immediate vicinity because flow is almost radial and the hydraulic head varies logarithmically with radial distance from the drain wall. All studies cited assumed a homogeneous, isotropic soil. Additionally, Gureghian and Youngs (1975) have examined a case of multilayered soils.

Contrary to those assumptions, X-ray examination of undisturbed field sample cores, containing wrapped drains and the surrounding soil and taken

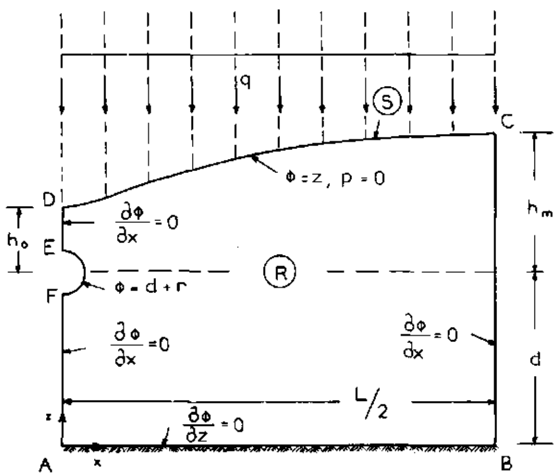

Fig. 1. Flow region and boundary conditions for the drainage problem under consideration.

after a mean service life of five years, often show the development of a heterogeneous zone in the immediate vicinity of a drain.

In this paper, the influence of the heterogeneous zone around the drain as well as envelope clogging at the water table height was studied using a two-dimensional finite element model developed specifically for this purpose. The finite element mesh consisted of nonlinear eight-node rectangular isoparametric elements covering the entire region of flow, R, shown in Fig. 1. At this point it should be apparent that the only, 'real' drains which can be represented by such a two-dimensional model are smooth drain tubes with continuous longitudinal slits. The variable extent of clogging, the blocking of the envelopes and the development of a 'natural, inverse' filter in the soil abutting the envelope, as detected and quantified through the use of digital X-ray computed tomography images as well as texture analyses of micro soil samples around the drain pipe, were incorporated in the model. More specifically, the heterogeneous zone was treated as a region with the hydraulic conductivity gradually varying with the radial distance from the drain pipe wall. The analysis was restricted to steady-state flow which is considered adequate for subsurface drainage (i.e. envelope) design.

FINITE ELEMENT SOLUTION

The two-dimensional drainage problem shown in Fig. 1, was solved by a finite element method. Within the region R, the groundwater flow is governed by the equation

$$\nabla \cdot (K \nabla \phi) = 0 \qquad (1)$$

which is obtained by combining the continuity equation with the Darcy equation. In eqn. (1), K is the hydraulic conductivity tensor (LT^{-1}) and ϕ is the hydraulic head (L), given by:

$$\phi = p/\rho g + z \qquad (2)$$

where p is the groundwater pressure ($ML^{-1}T^{-2}$), ρ is the density of the water (ML^{-3}), g is the gravitational acceleration (LT^{-2}) and z is the elevation from the impermeable layer (L) taken as datum level.

The boundary conditions for the considered case (Fig. 1) are as follows:

$$K_z \frac{\partial \phi}{\partial z} = 0 \text{ on AB} \qquad (3a)$$

$$K_x \frac{\partial \phi}{\partial x} = 0 \text{ on BC, DE and AF} \qquad (3b)$$

$$K_x \frac{\partial \phi}{\partial x} \cos(n,x) + K_z \frac{\delta \phi}{\delta z} \cos(n,z) = \mathrm{q} \cdot \cos(n,z) \text{ on CD} \qquad (3c)$$

where n is the normal direction to the boundary CD and (n,x), (n,z) are the angles which n makes with the axes x and z, respectively. Also on CD we have:

$$\phi = z \text{ and } p = 0 \tag{3d}$$

The boundary EF is a boundary of prescribed head for the case of an 'ideal drain' running full without back pressure. The hydraulic head is given by:

$$\phi = d + r \tag{3e}$$

where d is the distance of the impermeable layer relative to the drain level (L) and r is the radius of the drain (L).

For those cases where the boundary EF represents real drains, only the area of the perforations is treated as a boundary of prescribed head [eqn. (3e)], while the other parts of the drain wall constitute impermeable boundaries.

In the above expressions for the boundary conditions it is assumed that the medium is anisotropic, with x and z directions, as the principal axes of anisotropy and that the recharge rate, q (LT^{-1}), reaches the water table, CD, vertically.

For the numerical solution the flow region R is discretized using a network of eight-node quadrilateral isoparametric elements. In each element the unknown function ϕ is expressed as a function of its nodal values using the appropriate quadratic interpolation functions in a local coordinate system (ξ, η). The origin of a local coordinate system is located on the element which becomes square and the integrals required in finite element solution are most easily evaluated. The simple geometrical shape of the element in the local coordinate system may transform into a curved-sided quadrilateral element in the global coordinate system (x,z) (Segerlind, 1984). This element is more suited for the representation of the drain pipe, the envelope, the heterogeneous zone around the drain and the water table.

According to the Galerkin formulation of the finite element method we may write for each element in the flow region R

$$\int\int_{R^{(e)}} N_i(\nabla \cdot K \nabla \phi) \mathrm{d}x\mathrm{d}z = 0 \tag{4}$$

where N_i, $i = 1,...,8$ are the shape functions (Segerlind, 1984), which are the same as the interpolation functions.

After integration by parts, eqn. (4) may be written as follows:

$$\int\int_{R^{(e)}} [B]^T[K][B]\{\phi\}|J_D|\mathrm{d}\xi\mathrm{d}\eta = \int_{S^{(e)}} [N_n]^T[N_m^1]q\{X_n\}\mathrm{d}\xi \tag{5}$$

where

$$[B]=[J]^{-1}\begin{bmatrix}\partial N_1/\partial\xi & \partial N_2/\partial\xi & \dots & \partial N_8/\partial\xi\\ \partial N_1/\partial\eta & \partial N_2/\partial\eta & \dots & \partial N_8/\partial\eta\end{bmatrix} \tag{6a}$$

$$[J]=\begin{bmatrix}\partial x/\partial\xi & \partial z/\partial\xi\\ \partial x/\partial\eta & \partial z/\partial\eta\end{bmatrix} \tag{6b}$$

$[K]$ is the matrix of the hydraulic conductivity coefficients, J_D is the determinant of the Jacobian matrix $[J]$, which represents the relationship between the two coordinate systems, $[N_n]$ and $[N_m^1]$ are the matrices of the interpolation functions and their derivatives with respect to ξ, respectively, on the side of the element which is part of the boundary S of the water free surface where the recharge rate, q, is prescribed, and $\{X_n\}$ is the matrix of the x coordinates of the element nodes.

The integration over each element is performed numerically using Gaussian quadrature and the system of the linear algebraic equations which is obtained after the assemblage of all the elements in the entire flow region, is solved using Gaussian elimination.

In the considered problem the position of the free surface of the groundwater is not known a priori and an iterative procedure must be followed for the finite element solution. The finite element mesh is designed to give an initial estimate of the position of the free surface. During the first iteration eqn. (1) is solved using eqn. (3c) as the boundary condition on the free surface. Then the finite element mesh is modified by shifting the nodes above the drain level to a new position to satisfy the condition given by eqn. (3d). Then, to find the new finite element mesh corresponding to the latest estimate of the free surface elevation the coefficient matrices are computed again and a new solution is obtained. This iterative procedure stops when the computed heads for the free surface are close enough to the free surface elevations to satisfy a preset convergence criterion.

DATA FROM COMPUTED TOMOGRAPHY IMAGES

In recent years computed tomography (CT) has been proposed as a research tool in detecting and quantifying structural characteristics in soils (Stuyt and Oosten, 1987; Anderson et al., 1990). This technique produces images of the internal structure of cross-sectional slices or scans through an object via the reconstruction of a matrix of X-ray attenuation coefficients.

Petrovic et al. (1982) and Anderson et al. (1988) used CT as a tool to determine soil bulk density. They established that absorption of X-rays, expressed in Hounsfield units (H.U.) is linearly related to soil bulk density. Petrovic et al. (1982) found that the slope of linear regression lines varied only slightly between samples composed of glass beads and soils. We therefore

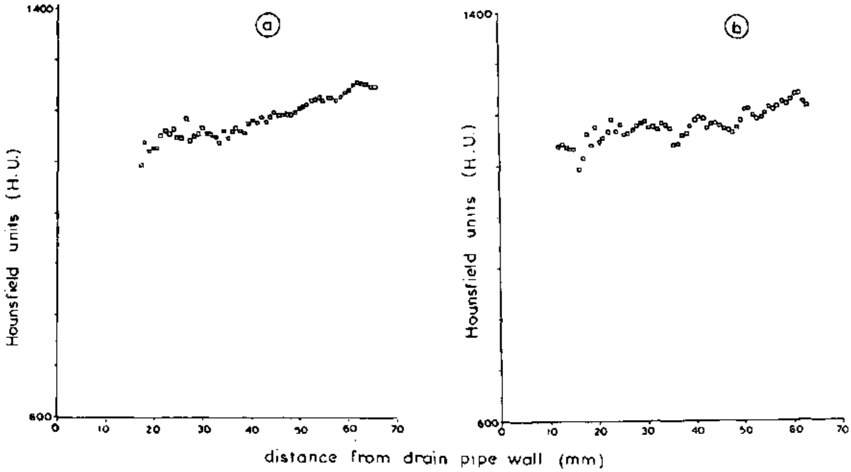

Fig. 2. Relationships between average X-ray attenuation rate for the soil underneath the drain in H.U. and radial distance from drain pipe wall, for the two characteristic cases (a) and (b).

assumed that regression lines for different soils will vary only slightly, provided that these soils contain negligible amounts of organic matter.

The CT images obtained by scanning cylindrical undisturbed soil–drain sample cores (Stuyt, 1990) were processed by us in order to derive conclusions about the development of the hydraulic conductivity pattern in the immediate vicinity of subsurface drains, wrapped with various envelope types.

In most of our CT images a linear relationship was found between the average X-ray attenuation rate in H.U. and the radial distance from the soil–envelope interface (Fig. 2). This implies that the average bulk density of the soil around the drain increases with distance from this interface. In some other CT images, however, the average bulk density slightly decreased linearly with distance from the soil–envelope interface.

Accepting Petrovic's regression coefficient to be valid for the soils in our samples, allows bulk density differences to be evaluated. Using the measured mean values of bulk density and the specific density of soil particles, 2.65 gcm^{-3}, the values of soil porosities at the soil–envelope interface and at 6 cm from this interface can be obtained.

Soil texture above and below the drains was determined at two locations: at average distances of 8.5 and 14.5 mm from the soil–envelope interface. In nearly all cases, soil texture did not vary significantly with radial distance. The Kozeny–Carman equation (Reeve and Luthin, 1957; Fahmy, 1961) indicates that for the same soil texture the saturated hydraulic conductivity is determined by soil porosity only. Therefore the ratio between the saturated hydraulic conductivities at the soil–envelope interface and at 6 cm from this interface, using the Kozeny–Carman equation is given by:

$$\frac{K_1}{K_2}=\frac{n_1^3/(1-n_1)^2}{n_2^3/(1-n_2)^2} \qquad (7)$$

where K_1, K_2 are the saturated hydraulic conductivities (LT^{-1}) at the soil–envelope interface and at 6 cm from this interface, respectively, and n_1, n_2 are soil porosities (–). Using eqn. (7) the obtained values of K_1/K_2 were found to be 1.56 and 1.9 for the two examples shown in Fig. 2, respectively. Furthermore, using values of porosities in the above-mentioned ranges, from eqn. (7) it follows that for linearly varying porosity the assumption of linearly varying saturated hydraulic conductivity is reasonable. In some cases, soil texture analyses at very small average distances from the soil–envelope interface show internal soil blocking at this interface and therefore this situation was also considered in the numerical simulations.

Visual inspection of CT images shows that the occurrence of envelope clogging is not necessarily linked to the locations of the pipe perforations. No systematic differences in envelope degree of clogging are observed with radial distance form the pipe wall. Although the degree of envelope clogging on top of the pipe sometimes appeared to be different from clogging at the pipe bottom, it is considered adequate to represent envelopes in the finite element grid by equivalent homogeneous and isotropic media.

NUMERICAL SIMULATIONS

The finite element mesh used for the land drainage problem presented in Fig. 1 consisted of 692 elements and 2223 nodes. A drain pipe of 60 mm diameter was assumed and the 7 cm thick zone around the pipe was divided into 140 elements as is shown in Fig. 3. A network with this density was required in order to take into account the radial flow pattern and to accurately discretize the envelope and the heterogeneous soil. Using this mesh, the computed discharge into the drain was underestimated by 3.35%. The differences in computed hydraulic heads in the vicinity of the drain when using a coarser mesh of 168 elements and 577 nodes remained negligible, whereas the underestimate of the discharge rose to 4.75%. This error was due to slightly inaccurate values for the computed hydraulic heads in the vicinity of the drain which are transformed into significant differences in computed hydraulic gradients at the drain wall and consequently in computed discharges.

The accuracy achieved with the 692 element model was due to the use of nonlinear elements, nonlinear interpolation for approximating hydraulic heads and a logarithmic head distribution in the immediate vicinity of the drain, and was considered satisfactory for the problem where the drain wall is considered as a boundary of prescribed head.

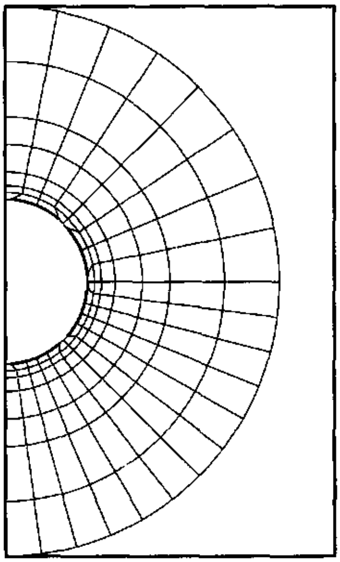

Fig. 3. Finite element mesh in the immediate vicinity of a drain.

Ideal drain

The first set of numerical applications was conducted in order to examine the functioning of an 'ideal drain' surrounded by a thick, highly permeable, homogeneous isotropic envelope. Envelopes 5 and 10 mm thick were assumed. As expected, increasing the envelope thickness was found to lower the water table height mid-way between the drains (Fig. 4a), although the differences are small. The influence of various values of hydraulic conductivity of the envelopes as well as various envelope degree of clogging on the water table heights was examined and the results are presented in Fig. 5.

In Fig. 6a, hydraulic head losses underneath the drain are presented. The results are almost the same for large values of the ratio of envelope hydraulic conductivity, K_e, and soil hydraulic conductivity, K_s, (K_e/K_s) and it is obvious that the hydraulic gradients within the 10 mm thick envelope are very small. These hydraulic gradients increase as the envelope becomes less permeable. It is also obvious that the hydraulic gradients at the soil–envelope interface, for all values of the ratio K_e/K_s, vary only slightly. The results for a 5 mm thick envelope are similar to the above-mentioned ones.

Since these results correspond to the functioning of an 'ideal drain', they were used only as a reference for the simulated cases with real drains.

Real drains

Two kinds of real drains were considered next; smooth drain tubes, one with four and the other with eight continuous longitudinal slits. Only this

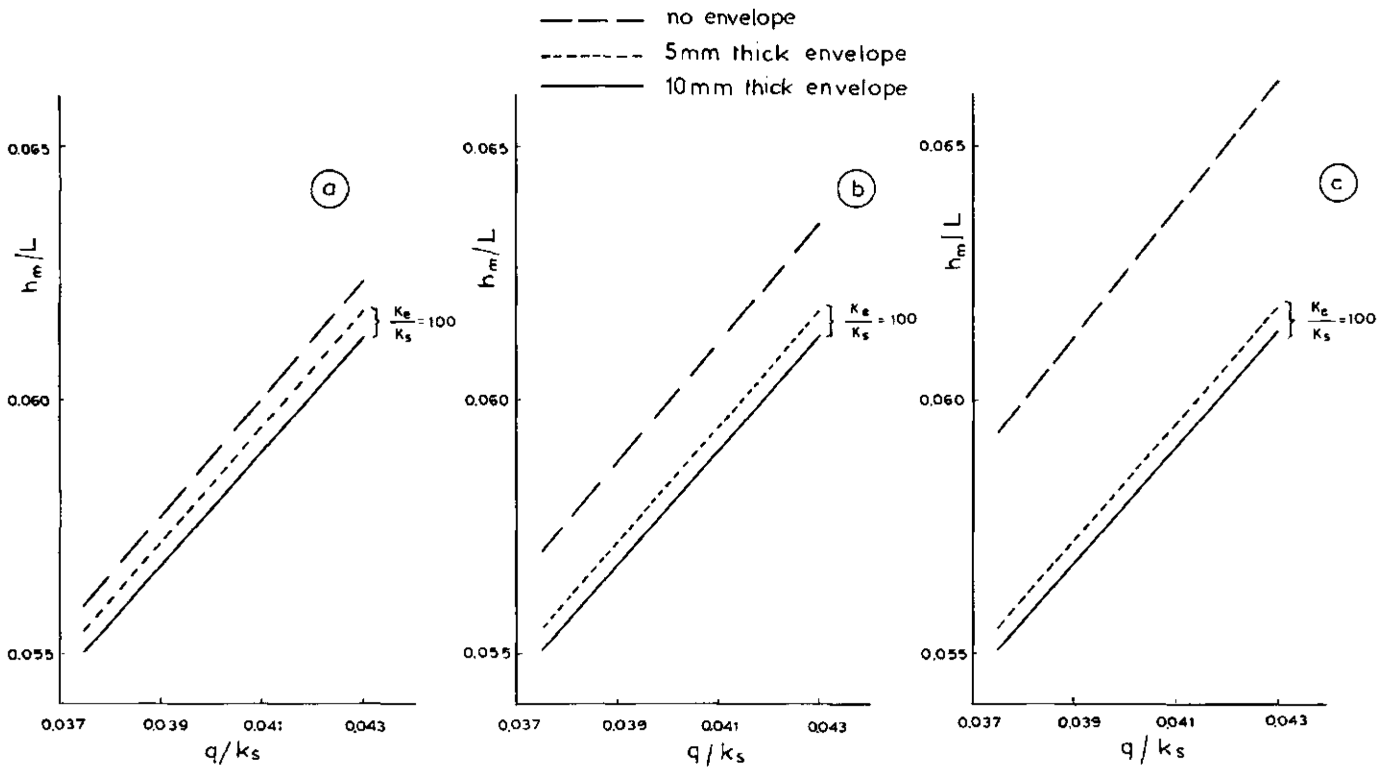

Fig. 4. Relationships between water table heights at the midpoint between the drains, expressed as the ratio h_m/L and q/K_s for the cases of (a) 'ideal drain', (b) real drain with eight-slits and (c) real drain with four-slits. ($d/L=0.1$, $r/L=0.0015$).

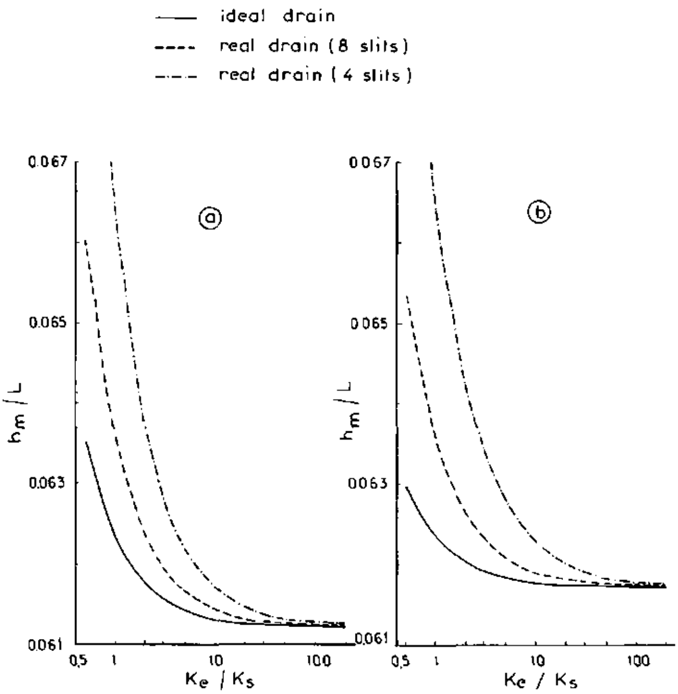

Fig. 5. Variation of water table height expressed as the ratio h_m/L with the envelope hydraulic conductivity expressed as the ratio K_e/K_s for the case of (a) 10 mm thick envelope and (b) 5 mm thick envelope. ($q/K_s=0.043$, $d/L=0.1$, $r/L=0.0015$).

kind of 'real' drain, which is hypothetical and does not exist in reality, can be represented in a two-dimensional finite element mesh. The width of the slits was assumed to be 4 mm. The envelope and the surrounding soil were assumed to be homogeneous and isotropic, though each with different hydraulic conductivities.

In Fig. 4 the water table height midway between the drains is presented for the different values of recharge, q. These results show that a 5 mm thick highly permeable envelope makes both real drain types behave as 'ideal drains'.

In Fig. 5 the water table height midway between the drains is presented for different values of the ratio K_e/K_s. From these results it is seen that, depending on the envelope thickness, for values of the the ratio K_e/K_s greater than 5–10 for the four-slit drain pipe and 2–3 for the eight-slit drain pipe, the drain functions better than the case of an 'ideal drain' without envelope (as is usually assumed in designing land drainage systems). It is also seen that for $K_e/K_s < 1$ the water table rises rapidly, especially for the case of the four-slit drain pipe.

In Fig. 6 b,c the losses of the hydraulic head underneath the examined real

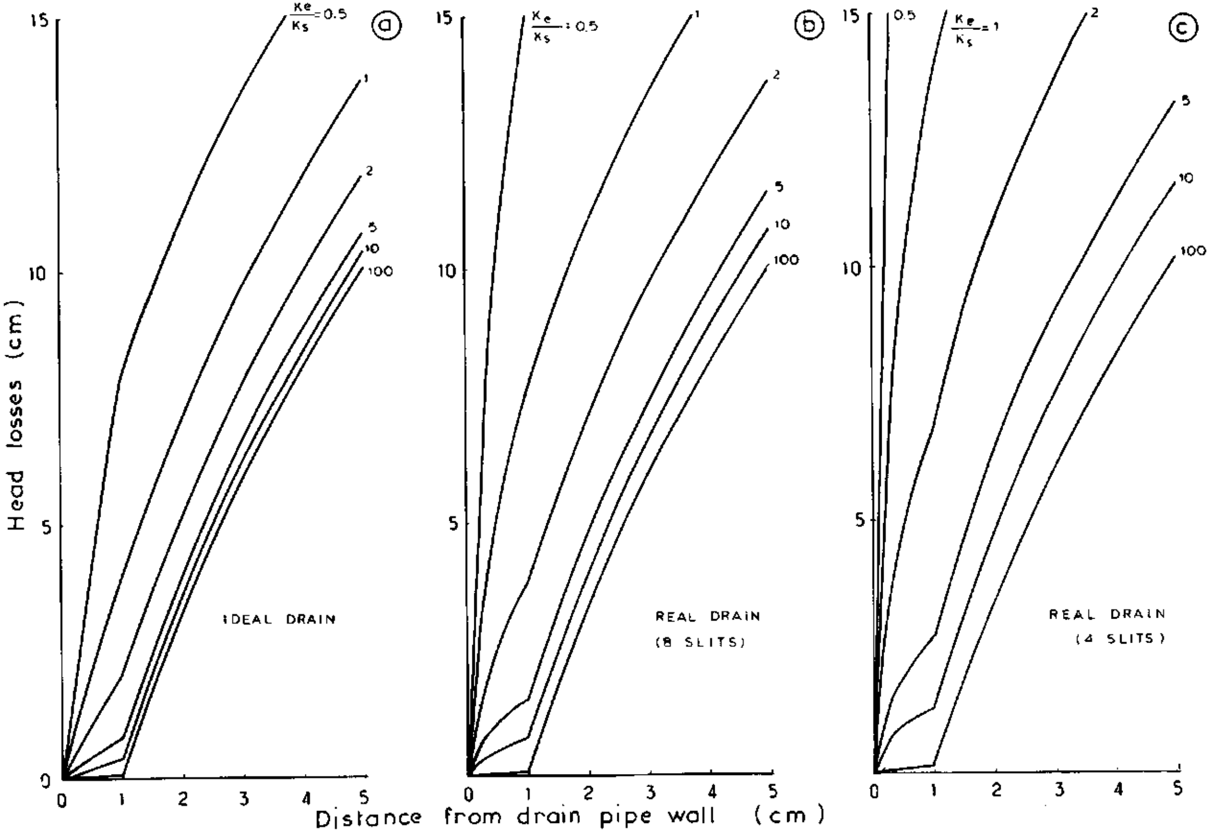

Fig. 6. Head loss underneath the drain as a function of distance from drain pipe wall, for the cases of 'ideal' and real drains, for various envelope hydraulic conductivities. ($q/K_s=0.043$, $d/L=0.1$, $r/L=0.0015$).

drains wrapped with 10 mm thick envelope are presented. It is shown that for large values of K_e/K_s there is no significant difference as compared with the 'ideal drain' (Fig. 6a). However the hydraulic gradients become larger within the envelope as K_e/K_s becomes smaller, especially for the four-slit real drain. It is also shown that at the soil–envelope interface the increase in hydraulic gradients is small, with the eight-slit pipe being closer to the case of the 'ideal

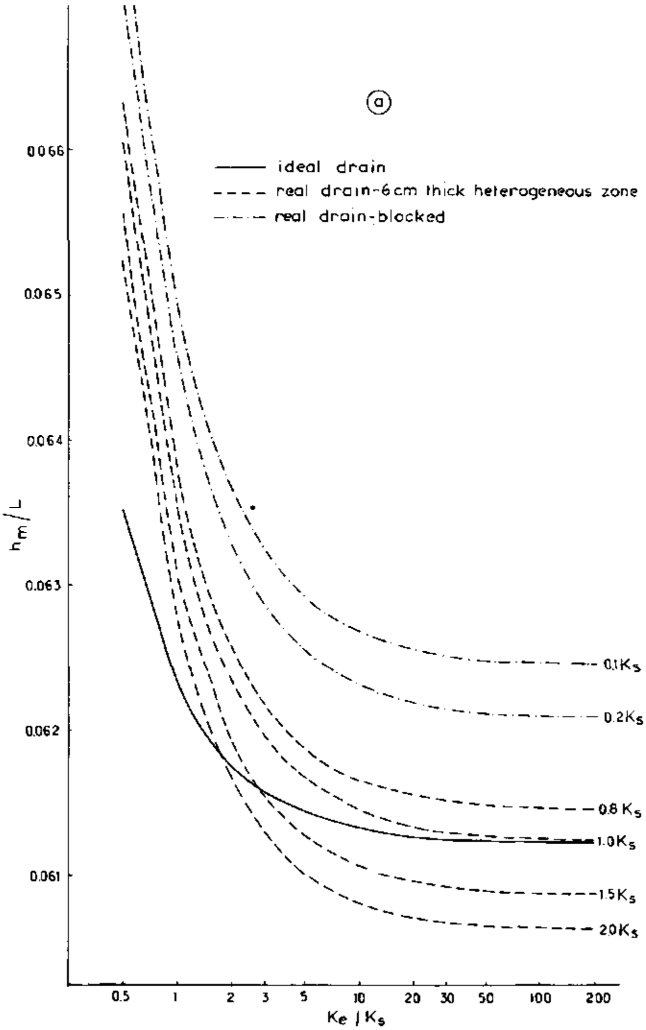

Fig. 7a. Variation of h_m/L with K_e/K_s for the cases of blocked envelopes and the 6 cm thick heterogeneous zone. Real drains with eight continuous longitudinal slits. ($q/K_s=0.043$, $d/L=0.1$, $r/L=0.0015$, 10 mm thick envelope).

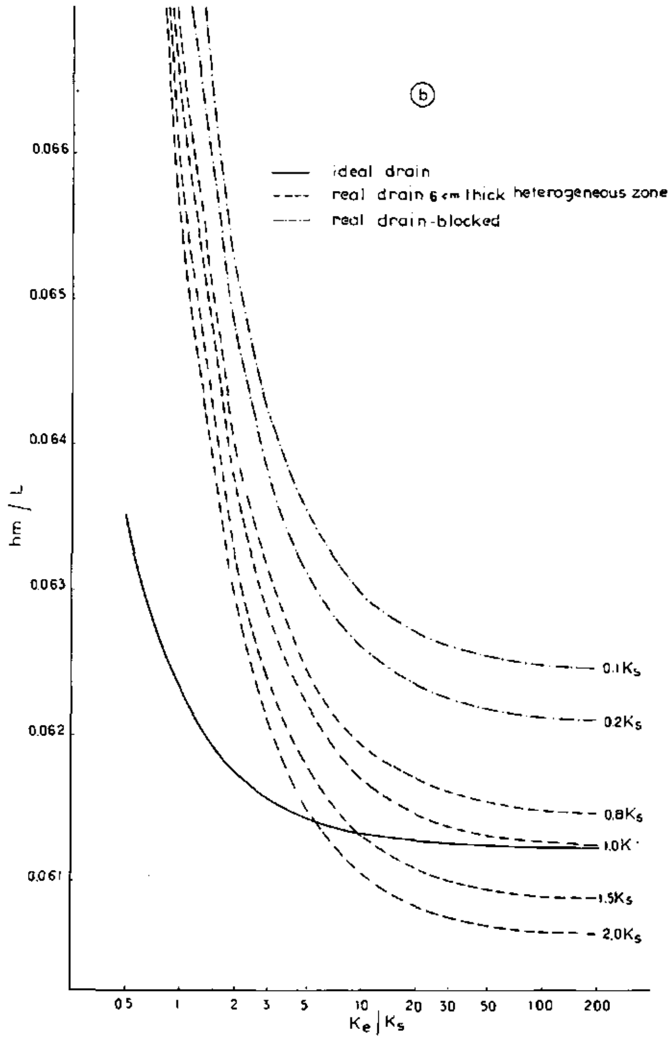

Fig. 7b. Variation of h_m/L with K_e/K_s for the cases of blocked envelopes and the 6 cm thick heterogeneous zone. Real drains with four continuous longitudinal slits. ($q/K_s=0.043$, $d/L=0.1$, $r/L=0.0015$, 10 mm thick envelope).

drain'. The results obtained for the case of 5 mm thick envelope show larger hydraulic gradients on the soil–envelope interface.

Influence of the heterogeneous zone

Numerical simulations were made in order to establish the influence of the heterogeneous zone around the drains on the water table height. The hydraulic conductivity in this zone was assumed to vary linearly with radial distance and in the radial direction only. In finite element analysis, a value for the component in the radial direction, K_r, was assigned to each node of the mesh in this zone. This was done according to certain patterns of linear variations in density, as observed in the CT images. Next, within each element, K_r was approximated using a set of interpolation functions N_i, $i=1,...,8$ and is given by:

$$K_r = [K_r] \cdot \{N_n\} \tag{8}$$

where $[K_r]$ is the matrix of nodal values of hydraulic conductivity, in the radial direction, in each element of the heterogeneous zone.

In Fig. 7a the results are shown for the cases of increasing or decreasing soil hydraulic conductivity towards the real drain with eight continuous longitudinal slits wrapped with 10 mm thick envelope. The hydraulic conductivity component in the radial direction was assumed to be 2, 1.5, 1 and 0.8 times its original value at the soil–envelope interface, and it was assumed to vary linearly and reach its original value at 6 cm outside the envelope. It is seen that the results for each case are shifted almost parallel to each other, for various values of K_e/K_s. Differences in water table elevation due to the development of this heterogeneous zone are small.

Also in Fig. 7a, results are presented for the case of blocked envelopes. In that case, the saturated hydraulic conductivity of the soil near the soil–envelope interface is drastically reduced. In these simulations, two cases were assumed in which the saturated hydraulic conductivity of the soil decreases linearly in a 1 cm thick soil area near the envelope. The value of the hydraulic conductivity of the soil at the soil–envelope interface was 0.1 and 0.2 times its original value.

In these cases, too, a parallel shift of the results is observed. The same numerical applications were conducted for the case of a real drain with four continuous longitudinal slits. The results, which are similar to the ones discussed previously, are presented in Fig. 7b.

CONCLUSIONS

A finite element model was developed and successfully applied for the simulation of two-dimensional flow towards a subsurface drain. Nonlinear elements were used for better approximation of heads in the immediate vicinity of the drain. Also a relatively large number of small elements were used to discretize for the drain wall, the envelope and the heterogeneous zone around the drain.

Examination of CT images as well as texture analyses of micro soil samples, taken at the immediate vicinity of the drain showed that the saturated hydraulic conductivity of the soil around the drain increases, in radial direction, towards the drain in a majority of cases. In some instances the hydraulic conductivity decreases slightly while in a few cases blocking of the envelope was detected.

The results of the numerical applications showed that envelopes which have or retain a high hydraulic conductivity make real drains behave as 'ideal drains'. On the other hand, a clogged envelope makes the water table rise drastically and inside the clogged envelope the increase in hydraulic gradients is large.

The increase in hydraulic gradient at the soil–envelope interface as the envelope becomes less permeable, was found to be small. This increase was found to be larger in case of a real drain with four slits showing the significance of the perforation pattern on the functioning of a drain. In the case of an 'ideal drain' there was a negligible increase in hydraulic gradients at the soil–envelope interface.

The development of the heterogeneous zone around the drain with increasing or decreasing hydraulic conductivity had a minor influence on the water table heights. The hydraulic conductivity of the envelope itself was found to be the most significant factor with respect to the functioning of the drain, as reflected in the computed maximum water table elevation.

REFERENCES

Anderson, S.H., Gantzer, C.J., Boone, J.M. and Tully, R.J., 1988. Rapid nondestructive bulk density and soil-water content determination by computed tomography. Soil Sci. Soc. Am. J., 52: 35–40.

Anderson, S.H., Peyton, R.L. and Gantzer, C.J., 1990. Evaluation of constructed and natural soil macropores using X-ray computed tomography. Geoderma, 46: 13–29.

Dierickx, W., 1980. Electrolytic analogue study of the effect of openings and surrounds of various permeabilities on the performance of field drainage pipes. Comm. Nat. Inst. of Agr. Eng. 77; 238 pp, Merelbeke, Belgium.

Fahmy, M.I., 1961. The influence of clay particles on the hydraulic conductivity of sandy soils. Ph.D. Thesis Agricultural University Wageningen.

Fipps, G., Skaggs, R.W. and Nieber, J.L., 1986. Drains as a boundary condition in finite elements. Water Resour. Res., 22(11), 1613–1621.

Gureghian, A.B. and Youngs, E.G., 1975. The calculation of steady-state water-table heights in drained soils by means of the finite-element method. J. Hydrol., 27: 15–32.

Lovell, C.J. and Youngs, E.G., 1984. A comparison of steady-state land drainage equations. Agric. Water Manage., 9: 1–21.

Nieuwenhuis, G.J.A. and Wesseling, J., 1979. Effect of perforation and filter material on entrance resistance and effective diameter of plastic drain pipes. Agric. Water Manage., 2: 1–9.

Petrovic, A.M., Siebert, J.E. and Rieke, P.E., 1982. Soil bulk density analysis in three dimensions by computed tomographic scanning. Soil Sci. Soc. Am. J., 46(3): 445–450.

Reeve, R.C. and Luthin, J.N., 1957. Methods of measuring soil permeability. In: J.N. Luthin (Editor), Drainage of agricultural lands, Agronomy 7, Am. Soc. Agron., Madison, WS, pp. 395–445.

Segerlind, L.J., 1984. Applied finite element analysis. Wiley, New York, 411 pp.

Stuyt, L.C.P.M. and Oosten, A.J., 1987. Mineral and ochre clogging of subsurface land drainage systems in The Netherlands. Geotext. Geomembr., 5(2): 123–140.

Stuyt, L.C.P.M., 1990. Computed tomography for envelope clogging determination and visualisation. Proc. Symp. land drainage for salinity control in arid and semi-arid regions, 25 February–2 March 1990, Cairo, Egypt, Vol., 3: 105–116.

Van Deemter, J.J., 1950. Theoretische en numerieke behandeling van ontwaterings- en infiltratie stromingsproblemen. Versl. Landb. Onderz., 56(7): 1–67.

Widmoser, P., 1968. Der Einfluss von Zonen geänderter Durchlässigkeit im Bereich von Drain und Brunnenfilterrohren. Schweiz. Bauztg., 86(9): 135–144 (in German).

Zaradny, H. and Feddes, R.A., 1979. Calculation of non-steady flow towards a drain in saturated-unsaturated soil by finite elements. Agric. Water Manage., 2: 37–53.

7 THE PHYSICAL INTERACTION BETWEEN ENVELOPES AND SOILS

7 The physical interaction between envelopes and soils

ABSTRACT

A method is proposed for the detection, display and evaluation of the most permeable areas inside drain envelopes and surrounding soils which are physically connected to agricultural drains and are responsible for conveying most of the water to such drains. The observed drains were installed with trenchers and had an "in situ" service life of at least 5 years. Sections of these drains have been sampled, including the surrounding soil. Important features of the method are the absence of further sample preparation, its non-invasive and non-destructive nature and the three-dimensional data structure. The data are available as CT-image sequences, recorded with a medical x-ray CT scanner. The method has allowed the recognition of the spatial distribution of structural features around wrapped subsurface drains. The results suggest that soil structure and its stability largely determine the service life of wrapped drains. Water flow patterns into most drains and clogging patterns in voluminous envelopes are quite heterogeneous. The effect of envelope materials on the physical interactions between an envelope and the surrounding soil appears less important than is generally assumed. On the contrary, soil properties are decisive.

1 INTRODUCTION

In drainage engineering, installation techniques and -machinery as well as pipe materials have been continuously improved during the past decades. In contrast the design of drain filters has not progressed to the same degree. This must be attributed to the limited understanding of the complex and dynamic interactions occurring within soil/envelope systems, notably in weakly-cohesive soils. This, in turn, is caused by the inability to observe these systems in their natural state at an appropriate scale. In recent papers addressing this problem, Lennoz-Gratin (1989, 1991) acknowledged that neither mineral clogging of drain filters in weakly-structured soils, nor the water flow near and through these filters can be described by deterministic models.

If a method for quantitative, "in situ" examination of wrapped drains could be developed, a sound basis would be created for future efforts to improve the design criteria for envelope materials under various circumstances. In the method proposed here, a medical x-ray CT scanner is used to generate CT-sequences of soil cores, including wrapped drain sections, building up images in three-dimensional ("3D") space as geometrically precise mappings of these cores. The method was applied to 45 core samples, retrieved from three experimental fields in The Netherlands. All drains had been installed in very fine sandy soils having low structural stabilities; they were sampled after a service life of at least 5 years. The drains were checked internally for pipe sedimentation rate and other features with a video inspection system (Chapter 3). Based on the findings of this survey, 45 locations were selected for sample core retrieval. Cores were sampled with purposely designed tools and transported to a CT scanning laboratory (Chapter 4). The resulting CT image sequences were used to detect and quantify meaningful soil and envelope features like areas of mineral clogging and patterns of erosion channels which are connected to the drain.

General methodological aspects of data acquisition and -processing will be discussed in the next section. Subsequently, the specific procedures used to obtain meaningful features from image data will be described. The method used locates and quantifies the three-dimensional ("3D") geometry of density distributions in drain filters and the surrounding soils. The results have been used to assess the water flow pattern into, and to describe the the water acceptance of the involved drain sections in a qualitative way.

2 DATA ACQUISITION TOOLS AND PROCEDURES

In this section the procedures for data acquisition and image data handling will be reviewed. In the first paragraph the technique of x-ray computerised tomography ("CT") including the image reconstruction procedure are briefly discussed. Subsequently, application of CT in the soil and water related sciences is reviewed. CT has been used to image and quantify natural and man-made soil structural features with considerable success in two dimensions ("2D"). Applications involving 3D-imaging are extremely rare. CT scanning of the core samples, and preparatory image processing steps will be described in the next paragraph. The vast amount of data, compatibility problems and the different data formats called for the development of "tailor-made" image processing software.

2.1 The process of x-ray computerised tomography

X-ray computerised tomography ("CT") is a non-destructive and non-invasive imaging technique. Transmission measurements of a narrow beam of x-rays, made at several different angles or projections around a given object, are used to resynthesize slices of interest within the object with the aid of an appropriate computer program. The first clinically useful CT system was pioneered by Godfrey Hounsfield of EMI Ltd. in England, and installed in 1971 in a hospital near London (Hounsfield, 1972, 1980). In less than 20 years, CT has become an important medical diagnostic tool. It is used to obtain cross-sectional images of patients, both for diagnosis and treatment. As a result of extensive research and development efforts, CT is now able to resolve small differences in density and water content over distances of a few millimeters. This makes it an appropriate though expensive tool for observation of distributions of density and water content in soils. For a brief description of the CT process the reader is referred to Annex 5. A thorough discussion is found in Herman (1980).

2.2 The use of CT in soil and water related sciences

Conventional x-ray technology has been used to study soil systems (Chancellor & Schmidt, 1962) and the pore structure in soils in particular (Rogaar, 1976). Bouma (1969) and Krinitzsky (1970) have reviewed the application potential of x-ray radiography in earth science studies. Using this conventional technique, laborious sample preparation is required involving impregnation with polyester resin, slicing etc. (Rogaar & Thiadens, 1975).

Several years later, x-ray CT technology has become available in the soil and water related sciences. CT is non-destructive and non-invasive and requires much less sample preparation than conventional radiography. It is used to image cross-sections of soil samples yielding information on the nature of features inside such samples. These cross-sections are available as digital descriptive images of density variations which are computed as a map of linear attenuation coefficients for x-rays. These provide quantitative information about internal features of an object like mineral densities and their distribution in the soil. Being costly, the use of CT in soil science has been limited although the results appear promising. Petrovic et al. (1982) established a linear relationship between mean soil bulk density and mean x-ray attenuation rate. Hainsworth & Aylmore (1983) used CT to examine spatial soil water content changes near living roots. Bergosh et al. (1985) established that all open and partially open macropores greater than 0.5 mm in width can be detected with CT. Crestana et al. (1985, 1986) developed a dedicated CT miniscanner for research on soils and studied wetting fronts. Macropores in soils have been characterized with CT by Anderson et al., (1988, 1990) and Grevers et al. (1989). Phogat et al. (1989, 1991) have investigated the sensitivity, linearity, spatial resolution and suitability of CT as a method for assessing the structural status and the water content of a soil. Anderson & Gantzer (1989) compared the potential of magnetic resonance imaging (MRI) methods with CT for determining water content in soil. Stuyt (1987) and Stuyt & Oosten (1987) investigated the suitability of CT in envelope research.

2.3 CT scanning of core samples

The set of CT-images used in the present study consists of 45 sequences of 256 x 256 x 16 bit cross sections (=CT scans). Each sequence contains 50 scans. The total number of scans is 2250, recorded on samples from three experimental fields (see Chapter 3): 21 samples from "Uithuizermeeden", 12 samples from "Valthermond" and 12 from "Willemstad". They were recorded on a Philips Tomoscan 350 scanner as 3 mm thick slices (Fig. 1 and 2). All cross sections were taken at 3 mm pitch, effectively scanning the entire volume of a 150 mm wide central section of the cores lengthwise. The cores were inserted in a purposely made plexiglass holder which could be slid into a phantom holder which was mounted on the headrest of the patient table of the scanner (Fig. 3). During a scan session, this holder is moved through the CT gantry under computer control by a precision translational table (Fig. 4). Reference CT numbers were obtained for air, water, plexiglass and "trovidur" (=polypropylene) by scanning a reference disc before and after completion of a series of 50 sequential cross-sectional images. Fig. 5 depicts a scan through this disc. The reference CT numbers were used to correct all pixel values, taking account of possible measurement accuracy variations of the scanner, either during scanning of a single core or between individual cores. All images were computed by the system computer and were recorded on magnetic tape. Sampling and scanning was done during the 1989-1990 winter season. Average scan time was 47 minutes for an entire core (50 core scans plus 2 scans of the reference disc).

The method proposed here utilizes various type of equipment, computers with different operating systems and image data formats. The amount of data involved is very large. In order to manage the data and to solve the compability problems a "tailor made" data handling and -processing procedure has been developed. Its major features are described in Annex 6.

3 IMAGE ANALYSIS CONCEPTS AND PROCEDURES

In this section, general methodology aspects of analyses of CT scans and of the 3D image space will be discussed, namely

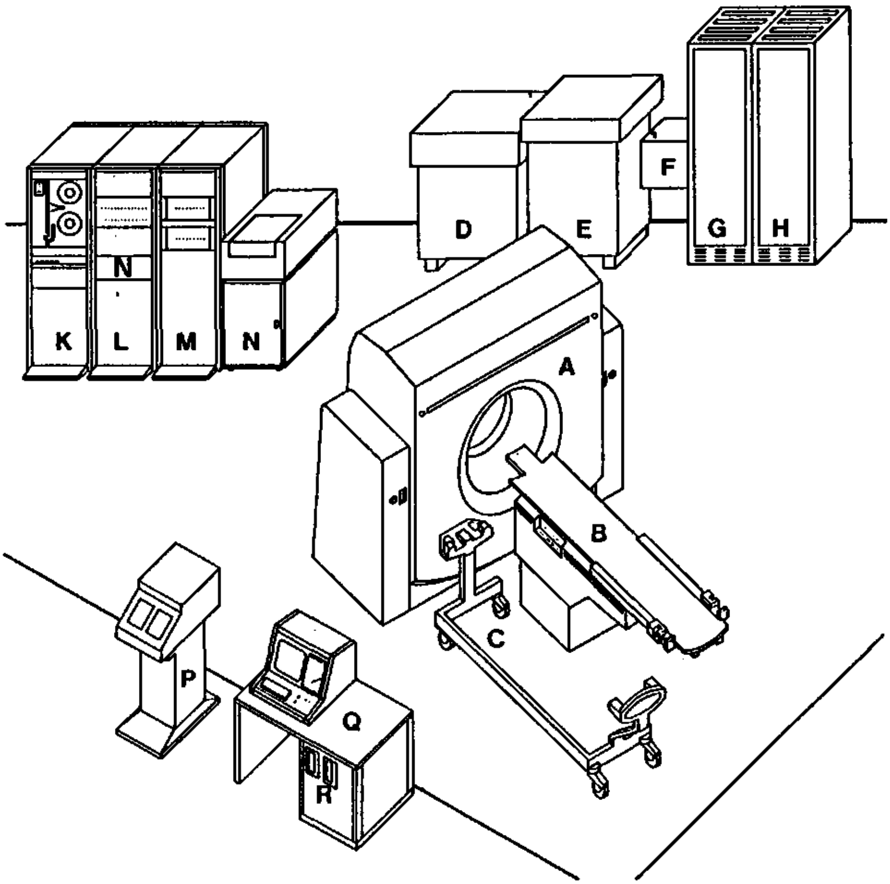

Figure 1. The Philips Tomoscan 350 basic system. A = gantry, B = patient support, C = patient trolley, D = tetrode tank, E = high-tension transformer, F = cooling control unit, G = power cabinet, H = control cabinet, K = computer cabinet with magnetic tape unit, L = computer cabinet, M = computer cabinet, N = data disk unit, P = multiformat camera, Q = operator's console, R = floppy disk unit.

1. Removal of image artifacts, caused by "Compton scattering",
2. Recognition and quantification of pipe and envelope parameters,
3. Determination of regions of interest,
4. Sampling of macroporosity statistics near the drain,

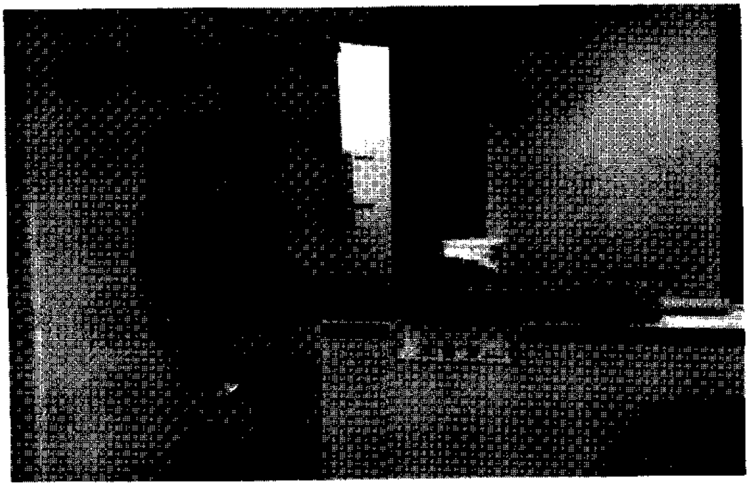

Figure 2. **Scanning of a drain/soil core in the Tomoscan 350 scanner in a CT laboratory of the "Academisch Medisch Centrum" (AMC), Amsterdam, The Netherlands.**

5. Assessment of the water acceptance of the drain sections,

6. Assessment of soil heterogeneity near the drain.

3.1 Removal of image artifacts caused by Compton scattering

Ray-paths of x-ray photons are assumed to be straight lines. In practice, a path of a photon may be altered while it traverses an object due to interactions with matter (i.e. electrons) in such objects. This "Compton scattering" leads to measuring distortions that, in turn, cause errors in CT images that are generally referred to as "reconstruction artifacts". The artifact in our type of sample cores consists of a lowering of density values in the central area of the images, producing a "cupping" effect. This artifact was found in all images and an a posteriori correction was made. The procedure is described in Annex 6.

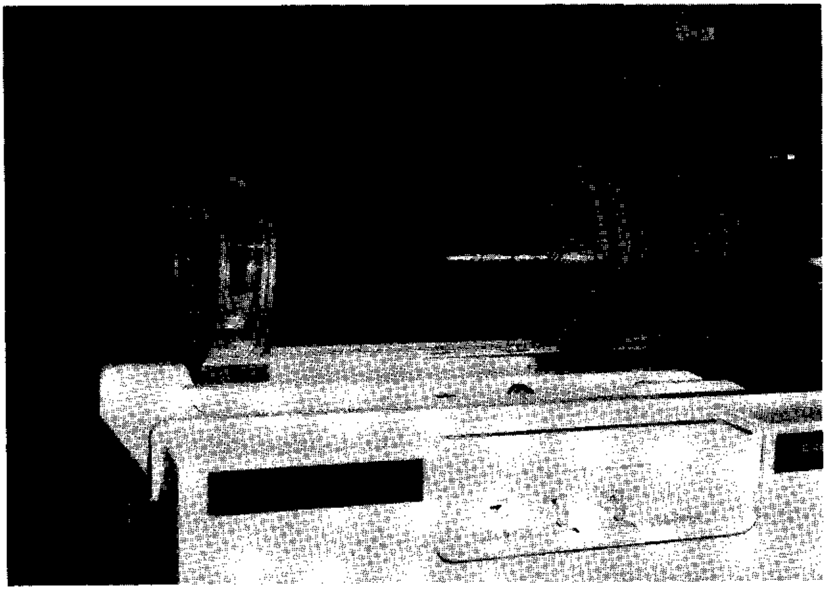

Figure 3. A purposely made plexiglass holder, designed to fit into the phantom holder of the scanner at the headrest of the patient table.

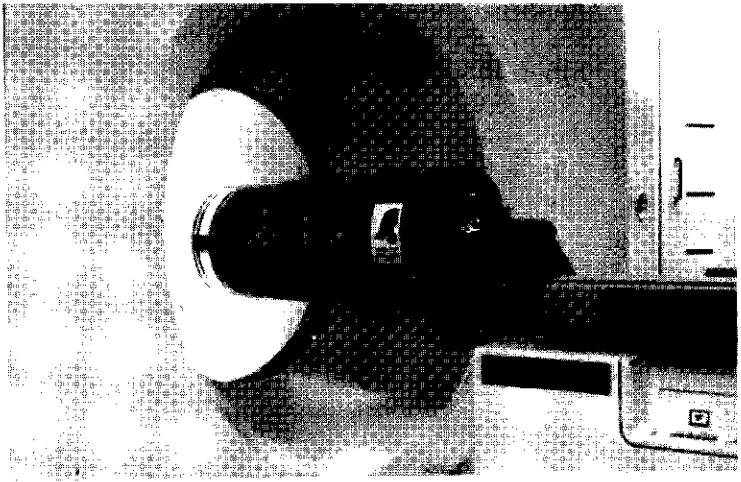

Figure 4. A drain/soil core in the scanning gantry of the Tomoscan 350.

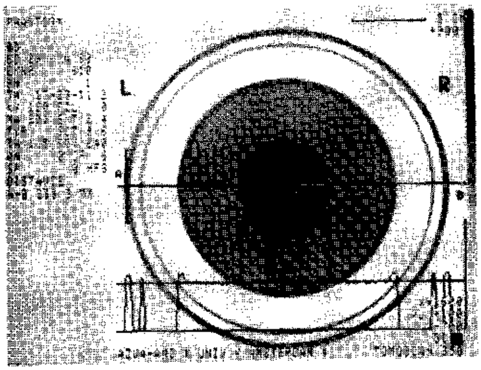

Figure 5. A scan image of the reference disc.

3.2 Recognition and quantification of pipe and envelope parameters

A 3D image is digitized into rectangular parallelopipeds, usually referred to as volume elements or "voxels" p(i,j,k) and containing k=50 slices, each of dimension i=256 by j=256. It is described in terms of a Cartesian coordinate system with p(1,1,1) located at the origin, hence p(1,1,1) is located in the nearby lower left hand corner of the image space and p(256,256,50) in the distant upper right hand corner. All image processing is done in this rectangular voxel coordinate system. Distances, volumes and surface areas are expressed as numbers of voxels.

Image processing results are converted from voxels into "real world" length units (i.e. mm) in an equivalent rectangular coordinate system of real-valued sample dimensions (x,y,z). Such simple conversions are justified because the nature of the analyses is qualitative. The dimensions of the image space are: width (x) 218 mm, height (y) 218 mm and depth (z) 150 mm, hence voxel dimensions are x=y=0.85 mm by z=3 mm. At the lower, left-hand corner or origin x=y=z=0 mm and at the upper, right hand remote corner, x=y=218 mm and z=150 mm.

All image processing steps which are discussed in this section are made on a 2D image by image basis rather than in the 3D image space. They are explained on the basis of the (x,y) coordinate system in which they were conceived. The 3D data are available as volume elements or voxels, calibrated in Hounsfield units (H.U.) [-] in which x-ray attenuation rates in CT are expressed. Voxels containing air are mapped with -1000 H.U., the "CT number" of water is 0 H.U., envelopes range from -500 to +500 H.U. and soils from 500 to approximately 2200 H.U. (see Annex 5).

3.2.1 The drain pipe

Accurate determination of the locus of the centre line of a drain pipe in the 3D image space is essential because subsequent image processing steps are related to this line. The locus of the centre line is determined by field sampling accuracy (see chapter 5) and is influenced by sample tilt while scanning. In the image data, the line was sampled as a point set: in each CT scan image, the centre of the drain (x_0,y_0) was found by a heuristic procedure (see below).

The pipe wall is mapped in the 3D image space as an elliptical cylinder with some pipe deflection in the horizontal direction. In each CT scan image, an ellipse $ep_0(x,y)$ with centre (x_0,y_0) and axes a_0 and b_0 was fitted to its cross section. An automated search for (x_0,y_0) was made from a starting coordinate (x_s,y_s) with average pixel value $s_{min}(x_s,y_s)$. This initial centre was found as the lowest of 9 averages $s(x,y)$ of 16 pixel values $h(x,y)$ which are contained in 9 square image subsets, equally distributed around the central area of that CT image. From (x_s,y_s), an interactive search determines both the centre (x_0,y_0) of ep_0, and the lengths of both axes a_0 and b_0 [L]. The following equation gave the closest fit to the ellipse:

$$(x-x_0)^2/a_0^2 + (y-y_0)^2/b_0^2 = 1 \qquad (1)$$

where a_0 = semi-major axis = horizontal inside pipe radius (mm)

b_0 = semi-minor axis = vertical inside pipe radius (mm)

For all 50 CT images, averages of a_0 (a) and b_0 (b) and the average eccentricity ε which is a measure of pipe deflection

$$\varepsilon = (a^2-b^2)^{½}/a \qquad (-) \qquad (2)$$

were calculated. If there was no pipe deflection the pipe wall was circular and eq. (1) reduced to a circle with radius $r = a_0 = b_0$.

3.2.2 Estimation of the volumetric area of voluminous envelopes

Regions of CT slices en(x,y) with low attenuation rates (-500 to +500 H.U.) and lying around the drain were assumed to be mappings of cross sections of voluminous envelopes. This means that the voxels in these regions obey the following conditions:

$$(x-x_0)^2/a^2 + (y-y_0)^2/b^2 = 1 \quad (3)$$

with semi-major axes $a = a_0 + n \cdot 0.85$ (mm) (4)

semi-minor axes $b = b_0 + n \cdot 0.85$ (mm) (5)

for $n = 0,1, ...,16$ (pixels)

and $-500 \leq en(x,y) \leq 500$ (H.U.) (6)

All voxels in 3D images, containing voluminous envelopes, which satisfy these conditions were segmented by an automated procedure. Their total number was multiplied by their volume yielding total envelope volume. The segmentation boundaries (eq. (6)) were deduced from all image data sets which contain voluminous envelopes.

Volumes of envelopes, composed of polystyrene beads could not be measured by this procedure because their x-ray attenuation rate was below -500 H.U.. Decreasing this lower segmentation boundary however, would lead to erroneous volumetric assessments of the other envelopes. Instead, the volumetric areas of "polystyrene" envelopes were estimated from three CT scan images of each data set (No. 1, 25 and 50) by a manual procedure.

3.3 Determination of regions of interest

Macroporosity statistics were sampled in so-called regions of interest around the drain. These regions were to be defined relative to the locus of the pipe wall of the drain and not relative to the boundaries of the sample core because the pipe wall has an elliptic cylindrical shape which is not centred inside the core. Hence, 2D regions $ep_n(x,y)$ were selected as elliptical sectors outside, and at 4 locations relative to the drain: above it ("T"), below it ("B"), at its "right" side ("R") and at its "left" side ("L") (Fig. 6). The loci of these sectors are centered around the mapped elliptical cross-section of the drain $ep_0(x_0,y_0)$, and they have semi-major axes $a_n > a_0$ and semi-minor axes $b_n > b_0$.

Coordinates of ep_0 and ep_n were point sampled at regular intervals in the x- and y-direction, as follows. Along their upper and lower sections, i.e. $|x-x_0| \leq |y-y_0|$, y was calculated for regularly increasing values of x. Along their "left" and "right" hand sections, i.e. $|y-y_0| < |x-x_0|$, a similar procedure was followed for y. At the sampled coordinates, pixel values $ep_0(x,y)$ and $ep_n(x,y)$ were obtained by interpolation.

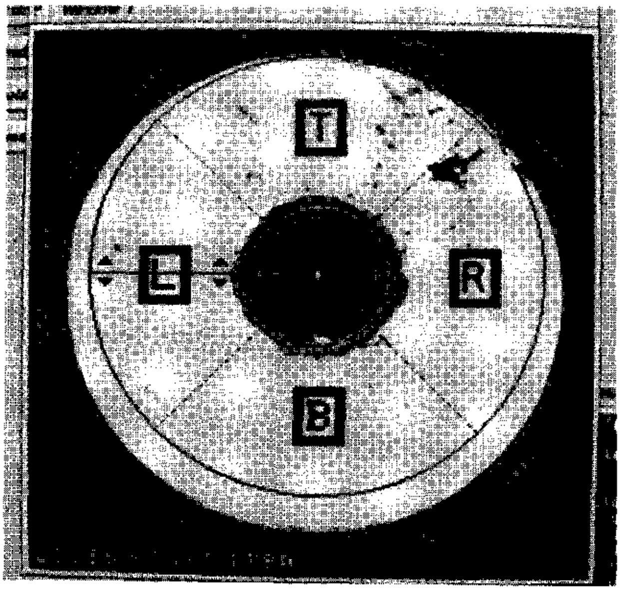

Figure 6. **Example of regions of interest in a CT scan image. The region is bordered by an elliptical curve and segmented into four equally large regions around the drain: "T" = top, "R" = right, "B" = bottom and "L" = left.**

The 2D area of interest around the pipe wall, ep(x,y), contains n_{max} adjacent elliptical regions of interest $ep_n(x,y)$ with centre (x_0,y_0) and

$$\text{semi-major axes} \quad a_0 + n \cdot 0.85 \qquad \text{(mm) (7)}$$

$$\text{semi-minor axes} \quad b_0 + n \cdot 0.85 \qquad \text{(mm) (8)}$$

for n = 0,1, ...,n_{max} (pixels), where n_{max} is inversely proportional to the distance d between (x_0,y_0) and the centre of the circular cross-section of the plexiglass sample container, (x_p,y_p). The distance d can be defined as

$$d = ((x_0-x_p)^2+(y_0-y_p)^2)^{1/2} \qquad \text{(mm) (9)}$$

In the investigated samples, n_{max} ranged from 50 (minimum) to 79 (maximum) pixels (42.5 to 67.2 mm, respectively).

In each CT scan image, ep(x,y) was segmented into four equally large parts: top $ep_t(x,y)$, bottom $ep_b(x,y)$, "right" $ep_r(x,y)$ and "left" $ep_l(x,y)$, separated by line sections $y-y_0=x-x_0$ and $y-y_0=-(x-x_0)$ and labelled as "T", "B", "R", and "L" respectively (Fig. 6).

The inclination of the centre line of the drain relative to the sample core axis causes n_{max} to be slice-dependent yet the smallest n_{max} was used in all 50 slices creating an elliptic cylindrical 3D area of interest instead of a conical one. Thus, in a sequence of 50 scans, the 3D area of interest EP(x,y,z) was defined as the set of 50, stacked 2D regions ep(x,y) with smallest n_{max}. In turn, EP(x,y,z) is segmented into subsets $EP_T(x,y,z)$, $EP_B(x,y,z)$, $EP_R(x,y,z)$ and $EP_L(x,y,z)$.

3.4 Sampling of macroporosity statistics near the drain

The data are precise mappings of the spatial distribution of heterogeneities inside envelopes and of the macroporosity of the soil around drains. Within a well structured soil matrix, two major types of soil pores may be distinguished: *textural pores* inside soil aggregates, and *macropores* (voids, cracks) which separate these aggregates. Macropores have a strong effect on important soil properties like infiltration capacity, aeration, root development and saturated hydraulic conductivity. The hydraulic conductivity of soils is associated with the macropore volume rather than with the total pore volume. In this study, the saturated hydraulic conductivity of the soil near drains is important. Hence, our interest is mainly centred on the macropore volume and its spatial distribution around drains. In CT scanning of weakly-cohesive, fine-sandy soils, macroporosity is classified as follows (Phogat & Aylmore, 1989).

1. The macroporosity of soil regions with minimum CT density, i.e. voids, is 100% (minimum x-ray attenuation rate; -1000 H.U.).

2. The macroporosity of soil regions with maximum CT density, i.e. inside aggregates (having a textural porosity of e.g. 50%), is 0% (maximum x-ray attenuation rate, i.e. 2188 H.U.).

3. Intermediate macroporosities are calculated from x-ray attenuation measurements. The regression line of x-ray attenuation rate and macroporosity is linear:

$$\text{macroporosity MP} = (2188\text{-H.U.})/31.88 \cdot 100\% \tag{10}$$

Basic statistics of the frequency distributions of macroporosity were gathered in the four regions of interest around the drain: $EP_T(x,y,z)$, $EP_B(x,y,z)$, $EP_R(x,y,z)$ and $EP_L(x,y,z)$.

3.5 Assessment of the water acceptance of the drain sections

3D macroporosity data may, in principle, be converted into estimates of saturated hydraulic conductivities $K_{sat}(x,y,z)$, creating a database for numerical simulation of saturated water flow toward drain sections. This type of computer experiment could not however be conducted because the relationship between macroporosity and saturated hydraulic conductivity is ill-defined. Although high macroporosity often coincides with high conductivity, this is not always the case. Similarly, there is no direct correlation between hydraulic conductivity and the Hounsfield Unit (Hunt & Engler, 1987). In addition, a modelling tool (i.e. a three-dimensional numerical model) was not available, hence a two-dimensional model was developed to predict the effect of soil heterogeneity around drains on the water table height (Chapter 6; Zissis & Stuyt, 1991). In this model, only the heterogeneity in a radial direction was considered.

For the future, a 3D numerical model would be an excellent tool to detect and recognise the patterns and features of internal soil erosion and of mineral clogging of envelopes which have developed due to the flow of water and soil particles toward the drain. Such information is indispensable for a better understanding of the functioning of envelopes in weakly-cohesive soils. In the absence of such a model, a procedure was developed to analyse (i.e. visualise and quantify) the spatial distribution of macroporosity in drain envelopes and surrounding soils. This procedure, described in the following paragraphs, will provide estimates of the water acceptance of wrapped drains in weakly-cohesive soils where the traditional concept of entrance resistance does not hold due to soil heterogeneity.

3.5.1 Limiting macroporosity ("LMP") concept and water acceptance

The analysis into limiting macroporosity and water acceptance may be summarized as follows.

1. The basic idea is the rather drastic assumption that water flow from any soil- or envelope unit (i.e. image voxel) towards the drain proceeds along the path or trajectory with the highest overall hydraulic conductivity

between this unit and the drain. This means that bypass flow through other, less favourable channels is neglected.

2. Along this trajectory, the flow is governed by the soil or envelope unit with the lowest (=limiting) hydraulic conductivity which acts as a throttle.

3. As yet, hydraulic conductivities cannot be quantified from x-ray data. As a first approximation however, hydraulic conductivity is considered to be proportional to macroporosity which, in turn, is inversely proportional to x-ray attenuation (eq. (10)).

4. Water flow from any soil or envelope unit towards the drain is assumed to be governed by the unit with the lowest (=limiting) macroporosity ("LMP") along its trajectory.

5. The LMP, associated with each soil- or envelope unit in the digitized 3D image must be located downstream of this unit.

6. A search procedure is used to find all soil- and envelope units which are associated with a given LMP. This procedure is described in more detail in section 3.5.3.

7. At the end of this procedure, an LMP will be assigned to each unit in the digitized 3D scene.

8. By approximation, the water acceptance of a drain will be calculated from the weighed average of all LMP's of all units.

An example may illustrate the LMP concept. If the hydraulic conductivity of an envelope is drastically reduced due to widespread mineral clogging of its pores, most LMP's will be located inside the envelope. Their values will be low and water flow from the soil toward the drain will be severely restricted. If however the envelope would be fully clogged except for a local spot where an erosion channel has developed, all elementary soil and envelope units which are physically connected with this channel will have comparatively high LMP's and, for these units, discharge through this channel will be easy. Hence, the water acceptance of the involved drain section may be reasonably good.

The frequency distribution of macroporosity contains 110 classes, ranging from -1000 Hounsfield Units ("H.U.") (100% macroporosity) to 2188 H.U. (0%

macroporosity). For computational reasons, however, the number of classes of the LMP had to be reduced. In the final analysis, 29 classes have been distinguished, from 100% to 0% LMP. Separate searches are made in both the trench backfill and the undisturbed subsoil.

Visual perception and interpretation of features of soil structure near drains and patterns of mineral clogging of envelopes is achieved by a stereoscopic display of descriptive 3D images which emerge from the computations. These images consist of segmented regions which contain voxels, assigned to particular LMP's.

3.5.2 Preparatory image editing

Prior to the analysis, the images were edited to facilitate and control the search process. The air inside the drain is the sink for the groundwater and, as such, the physical basis of the calculation of the water acceptance of the drain. In each CT image, air (-1000 H.U.; 100% macroporosity) is edited into an elliptical region near the inside pipe wall with the following set of coordinates:

$$(x-x_0)^2/(a_0-r_a)^2+(y-y_0)^2/(b_0-r_a)^2=1 \qquad (11)$$

where $2.98 \leq r_a \leq 4.25$ (mm)

removing pipe sediment.

Searches in the 3D space are subject to limitations. Trench backfill and subsoil must be analyzed separately because their structures are often different. Hence, the upper and the lower section of each 3D image were "physically" separated by editing, into each CT slice, artificial, impermeable (2200 H.U.), horizontal lines through the centre (x_0,y_0) of the drain. This creates a plane which runs through the drain axis in 3D space delineating two search areas; an upper and a lower one.

Preferably, the volumes of both search areas should be equal. This was achieved by introducing an artificial, impermeable, elliptic cylindrical barrier around the drain near the sample core container. This barrier was edited into each CT slice separately. It coincides with the largest possible elliptical regions of interest $ep_{n,max}(x,y)$, cf. eq. (1), (7) and (8). Hence, shape and size of both search areas are determined by spatial characteristics of the imaged objects such as the location and orientation of the drain in the sample core and by individual object attributes like drain diameter and pipe deflection.

Finally, an impermeable zone was edited into the central area inside the drain:

$$(x-x_0)^2/(a_0-2.98)^2+(y-y_0)^2/(b_0-2.98)^2 \leq 1 \qquad (12)$$

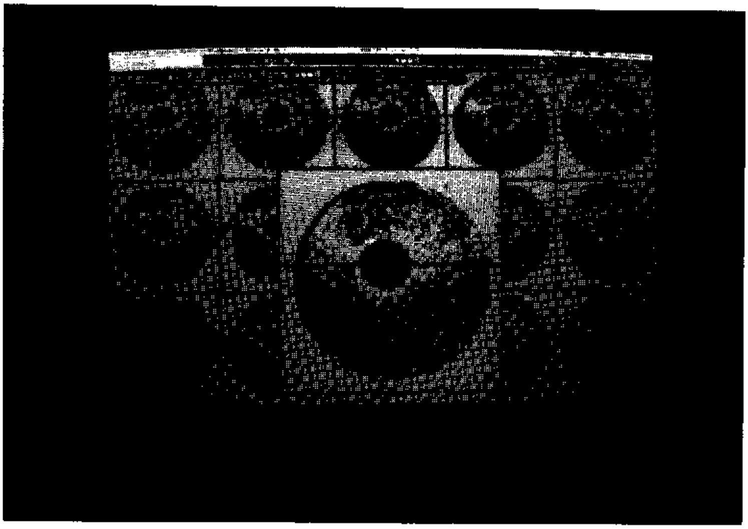

Figure 7. **Example of a result of preparatory image editing, depicted in a CT slice image. The region of interest around the drain is separated in an upper and a lower search area.**

where (x_0,y_0) = the centre of the ellipse which coincides with the pipe wall,

a_0 = horizontal inside pipe radius (mm)

b_0 = vertical inside pipe radius (mm)

This impermeable zone was introduced merely for cosmetic reasons. As a result, drain sections which are displayed in computed 3D images will have a realistic appearance. An example of the result of image editing in a CT slice is depicted in Fig. 7.

3.5.3 Selection procedure for LMP's

The water acceptance of the upper and lower drain sections was estimated by calculating the weighed averages of the selected LMP's above and under the drain. The weighing factors are the numbers of soil- and envelope units which are associated with these LMP's. The following procedure was used.

1. The cumulative frequency distribution of all Hounsfield units in both search areas, F(B), was determined in the range -1000 H.U. to 2188 H.U. (3188 classes).

2. Cumulative frequency distributions of Hounsfield units in both the upper and the lower search area, F(U) and F(L), were determined also.

3. All frequency distributions were converted to cumulative macroporosity distributions F'(B), F'(U) and F'(L), following eq. (10).

4. Macroporosity values were calculated at 29 percentiles, (p(i),i=1, ..., 29) of F'(B): 0.75, 1.0, 2.0, 3.0, 4.0, 5.0, 10.0, ..., 90.0, 95.0, 97.5, 99.0, 99.5, 99.9, and 100%. These macroporosities were selected as "Limiting Macroporosities" for water flow into the drain:

$$LMP_{(p(i),\ i=1,\ \ldots,\ 29)} \quad (\%) \quad (13)$$

5. For computational reasons, the grey scale resolution was reduced from 3188 classes to 110 classes.

6. For each

$$LMP_{(p(i),\ i=2,\ \ldots,\ 29)} \quad (\%) \quad (14)$$

   the 3D macroporosity (=grey value) image was binarized such that all voxels in both search areas with macroporosity MP $\geq LMP_{p(i)}$ were set to 1; all other voxels were set to 0.

7. In the binary image, *three dimensional region growing* was performed in both the upper and the lower halves of the image. Three dimensional region growing is the process of finding all voxels of value 1 which are connected to the inside of the drain. Each connected voxel is in turn used as a seed to find other connected voxels with the required macroporosity until all of them are found. A result of the process of three dimensional region growing is illustrated in Fig. 8 and Fig. 9.

8. For each $LMP_{(p(i),\ i=2,\ \ldots,\ 29)}$ (%) (14)

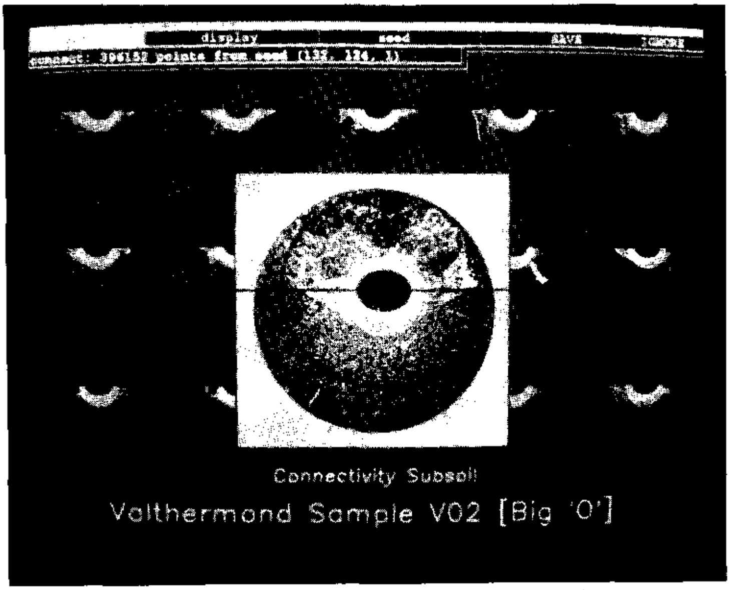

Figure 8. Example of a result of three dimensional region growing. A 2D cross-section through a set of voxels which belong to the 3D set of voxels with macroporosity values ***above*** a particular LMP are depicted in the central binary image. A series of consecutive cross-sections with ***subsets*** of these voxels ***which are connected to the lower sink inside the drain*** are displayed in the remainder of the image.

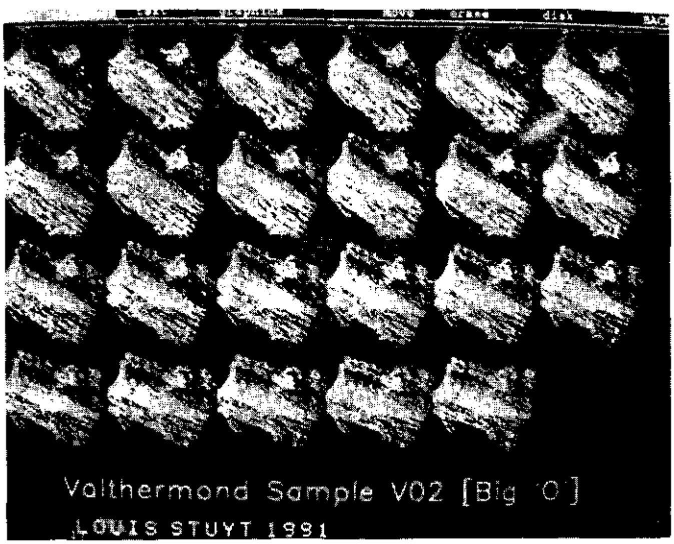

Figure 9. The bordering region in 3D space, associated with a particular LMP below the drain is displayed as seen from various positions of the eye.

the number of connected voxels $n_{(p(i),\ i=2,\ \ldots,\ 29)}$ (15)

with macroporosity values MP

$$LMP_{p(i)} < MP \leq LMP_{p(i-1)} \qquad (\%) \quad (16)$$

in both the upper and the lower connected regions was counted.

9. The water acceptance of both the upper and the lower drain sections was calculated as follows as a weighed average of all LMP's, where the numbers of connected voxels in the matching regions are used as weights:

$$\overline{LMP} = \sum_{i=2}^{29} (LMP_{p(i)} \cdot n_{p(i)}) / \sum_{i=2}^{29} n_{p(i)} \qquad (\%) \quad (17)$$

10. For each $LMP_{(p(i),\ i=2,\ \ldots,\ 29)}$ (%) (14)

a rough estimation of the surface area of both the upper and the lower connected regions was made by counting the number of bordering voxels of each connected region on a 2D image by image basis.

3.6 Assessment of soil heterogeneity near the drain

Simultaneous with the calculation of average LMP's, average ratios of

$$\frac{\text{numbers of voxels in a connected region (=volume)}}{\text{numbers of voxels bordering the region (=surface area)}} \qquad (-) \quad (18)$$

for each LMP, were calculated as qualitative, rough estimates of the heterogeneity, "HI" of the connected regions at the soil/drain interface. This very simple estimate is based on the idea that, depending on its geometry, a three dimensional region with a specified volume may have numerous shapes. If its volume is contained in a sphere, HI will be maximum (maximum possible heterogeneity). In any other shape, the zone will occupy a more distributed area in 3D space, that is, its appearance will be more homogeneous. Obviously, HI is not a perfect heterogeneity indicator, but is the best of the alternatives currently available. HI varies from 1.5 for low heterogeneity to approx. 4.5 for macropores.

The areas of interest in this analysis were those with relatively high macroporosity at the soil/envelope interface, such as contact erosion patterns and macropores. Hence, the evaluation of LMP's was limited to LMP ≥ 45%.

4 RESULTS

In this section the results of the analyses will be given without comment; discussion will be postponed to section 5.

Average geometric parameters of pipes and regions of interest around the pipes as well as average macroporosities are presented in Table 1. The extent of pipe deflection could not be calculated in Valthermond sample No. 2 due to a data-dependent problem with the applied automated image processing procedure which caused inaccurate fitting of an ellipse to the pipe wall. Most drains are slightly compressed in the vertical direction, and in most samples the drain is not located exactly in the centre of the core. In 18 cases out of 45, the average macroporosity of the trench was lower than that of the subsoil. This occurred most frequently in the "Willemstad" experimental field (8 samples or 66% of all cases) but was uncommon in the two other fields (33% in "Uithuizermeeden" and 25% in "Valthermond").

Two types of soil structural features were commonly found in the subsoil:

1. *Horizontal layering*; often found in "Willemstad" and occasionally in "Uithuizermeeden".

2. *Vertically oriented macropores*; found exclusively in "Valthermond".

In the remaining cases, no obvious structural features were observed. Examples of horizontal layering and of a vertical pore system are illustrated in Fig. 10 and 11, and in Plates 1 and 2. These plates are printed as anaglyphs and allow for stereoscopic depth perception if observed through a pair of red/green spectacles, included at the back cover of this thesis. Frequency distributions of macroporosity around drains are plotted for 4 representative cases in Fig. 12 to 15. Example plots of the distribution of macroporosity inside a voluminous envelope are given in Fig. 16. The heterogeneity of mineral clogging of voluminous envelopes is illustrated in Fig. 17 in the form of transformed images in which envelopes are displayed as flat surfaces. Volumetric areas of voluminous envelopes are given in Table 2. The envelopes, composed of polystyrene beads presented problems because the automated image processing procedure was unable to distinguish the interior of the drain from the envelopes because their x-ray attenuation rates were identical.

Table 1. Average inside horizontal and vertical pipe diameters, average pipe eccentricity, volume of region of interest around the pipe and average macroporosities in the trench and in the subsoil. Experimental fields: "Uit"="Uithuizermeeden", "Val"="Valthermond" and "Wil"="Willemstad".

		average pipe horizontal	inside diameter vertical	eccen-tri-city	volume of region of interest	average macroporosity trench	subsoil
		2a $m\cdot10^{-3}$	2b $m\cdot10^{-3}$	ε (-)	v $m^3\cdot10^{-3}$	MP_{tr} (%)	MP_{ss} (%)
"Big 'O' fabric	Val 2	†	†	†	2524.6	34.93	31.44
	Wil 8	60.24	56.24	0.36	3316.5	35.31	36.00
	Uit 13	54.80	52.99	0.26	2940.9	35.20	34.89
	Uit 12	55.42	53.23	0.28	3078.0	37.09	34.81
"Buffer" Peat/ Cocos mixture	Uit 17	55.35	54.73	0.15	2376.7	37.04	37.57
	Uit 8	55.83	55.01	0.17	2616.4	37.60	38.52
	Uit 18	55.38	53.54	0.26	2534.2	36.66	39.22
	Uit 15	55.15	54.53	0.15	2842.6	37.86	35.25
"Cerex" nonwoven	Wil 7	54.80	52.38	0.29	3316.5	35.53	35.50
	Wil 4	54.70	52.14	0.30	3377.5	34.92	35.35
	Uit 14	55.21	52.58	0.31	2405.6	39.07	36.97
	Val 8	55.76	53.71	0.27	2368.6	49.41	34.45
Coconut Fibres	Val 4	55.25	53.95	0.22	2092.0	40.99	37.65
	Val 11	55.69	54.87	0.17	2160.9	39.39	29.05
	Val 12	56.27	56.10	0.08	2878.0	46.79	34.40
	Val 3	55.38	53.74	0.24	2479.1	36.43	37.31
Glass Fibre membrane	Wil 12	59.21	56.31	0.31	2381.7	38.27	33.98
	Wil 11	59.28	56.10	0.32	2437.7	33.79	37.93
	Wil 2	59.69	55.32	0.38	2045.7	39.06	37.04
	Wil 1	60.24	58.87	0.21	2718.7	35.89	37.75
Polypropylene Fibres	Val 5	55.83	54.87	0.18	1287.1	44.00	48.45
	Val 10	56.24	54.46	0.25	2108.7	54.03	40.65
	Val 9	55.42	55.01	0.12	3040.0	40.15	35.32
	Val 6	55.49	54.32	0.20	1789.7	41.69	43.58
Polypropylene Fibres "PPB"	Uit 2	55.49	54.80	0.16	2551.3	35.75	37.11
	Uit 1	54.87	53.50	0.22	2469.9	35.42	36.62
	Uit 4	56.17	54.05	0.27	3036.7	35.87	33.89
	Uit 3	54.84	54.73	0.06	3028.2	37.84	35.50
Polystyrene Beads "P.S.L."	Uit 19	55.52	53.33	0.28	2892.8	40.52	40.03
	Uit 20	56.00	52.38	0.35	2411.2	42.15	45.82
	Uit 10	54.12	53.88	0.09	2523.0	44.37	42.27
	Uit 9	55.86	52.72	0.33	3076.3	40.86	42.07
Polystyrene Beads "PS-LDPE"	Wil 5	55.76	54.02	0.25	2429.7	40.34	42.99
	Wil 6	55.32	52.92	0.29	3398.1	38.92	38.16
	Uit 7	55.32	54.60	0.16	3224.8	40.55	39.55
	Val 7	56.07	54.22	0.25	3164.9	41.84	35.13
"Garden" Peat Fibres	Uit 6	55.73	54.09	0.24	2844.1	39.23	37.29
	Uit 5	55.56	55.76	‡	2223.3	38.55	38.35
Peat/Coconut Fibre mix	Wil 3	59.42	59.21	0.08	2361.7	37.10	38.81
	Wil 9	59.90	58.12	0.24	3014.8	36.55	37.77
	Uit 11	55.08	53.85	0.21	3276.1	36.58	35.90
"Typar" nonwoven	Val 1	55.59	53.20	0.29	2474.2	39.25	35.44
	Wil 10	59.73	56.92	0.30	2996.2	35.76	37.05
	Uit 21	55.42	52.96	0.29	2704.1	37.33	34.71
	Uit 16	54.56	53.13	0.23	2815.9	36.56	35.49

†) could not be computed (see text). ‡) not defined.

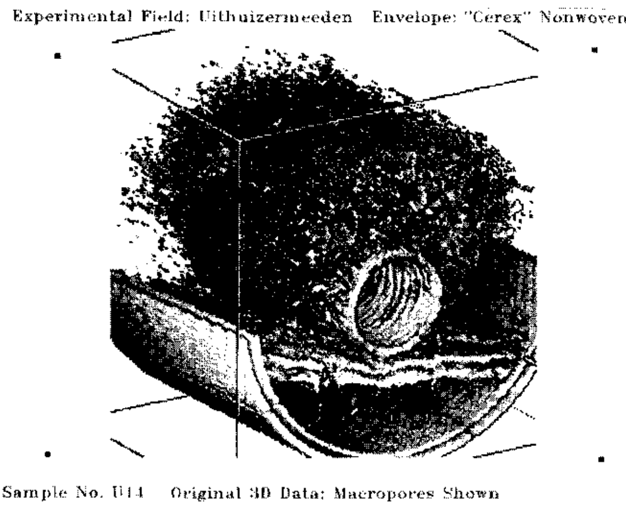

Figure 10. **Example of a layered subsoil. Parts of the plexiglass rims of both the sample container and the sample holder of the scanner were cut away by image processing techniques. Experimental field: Uithuizermeeden, envelope material: "Cerex" nonwoven, sample No. U14. See also Plate 1.**

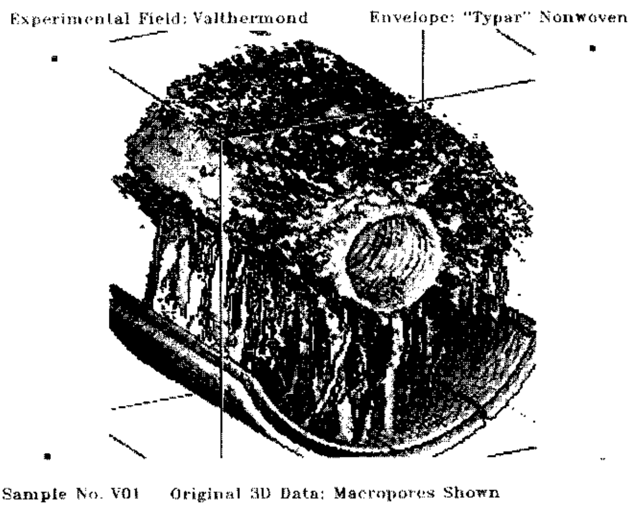

Figure 11. **Example of a subsoil with vertically oriented macropores, assumingly developed as a result of plant roots. Experimental field: Valthermond, envelope material: "Typar" nonwoven, sample No. V01. See also Plate 2.**

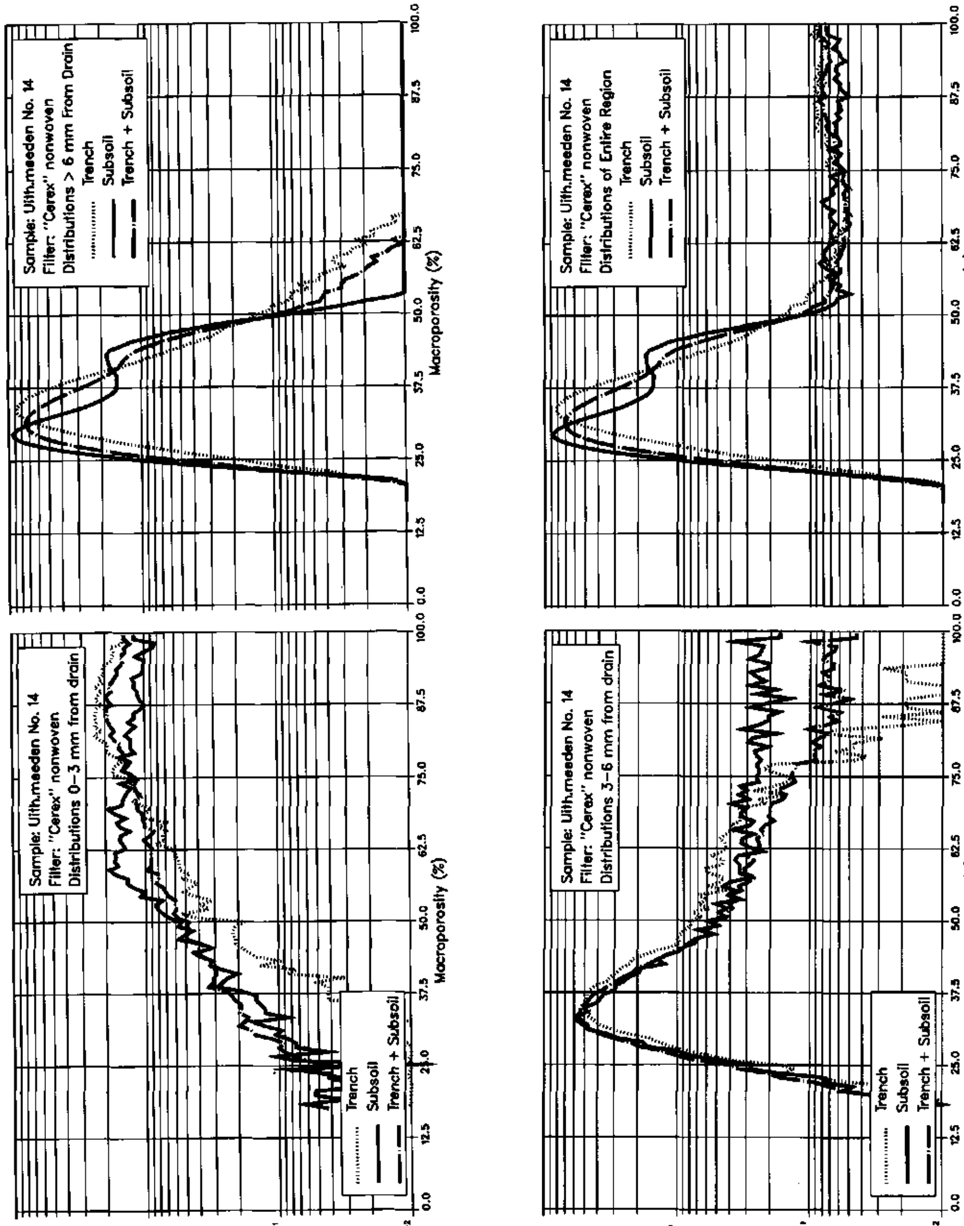

Figure 12. **Frequency distributions of the macroporosity (MP) of the soil around the drain in sample No. U14 of experimental field "Uithuizermeeden" in four regions of interest. The macroporosity decreases rapidly with distance from the drain and is larger in the trench backfill than in the subsoil.**

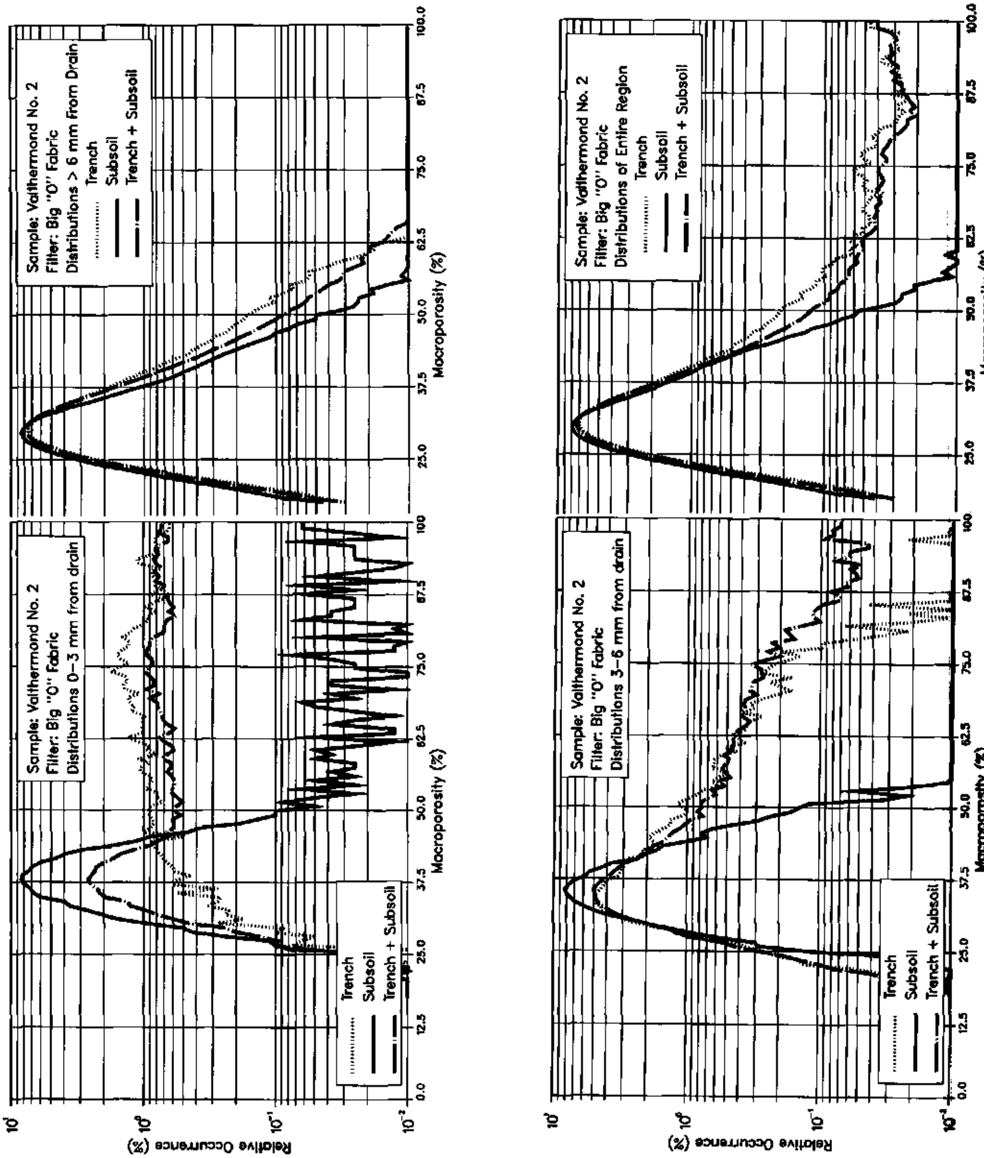

Figure 13. **Frequency distributions of the macroporosity (MP) of the soil around the drain in sample No. V02 of experimental field "Valthermond" in four regions of interest. The soil in this sample was among the most densely packed of all samples. The trench backfill contained various dense areas, except for the area near the drain which is partly occupied by the envelope. Data noise is obvious in the subsoil near the drain. It is caused by a data-dependant problem with the automated image processing procedure, i.e. inaccurate fitting of an ellipse to the pipe wall. The error is without further consequence at larger distance from the drain.**

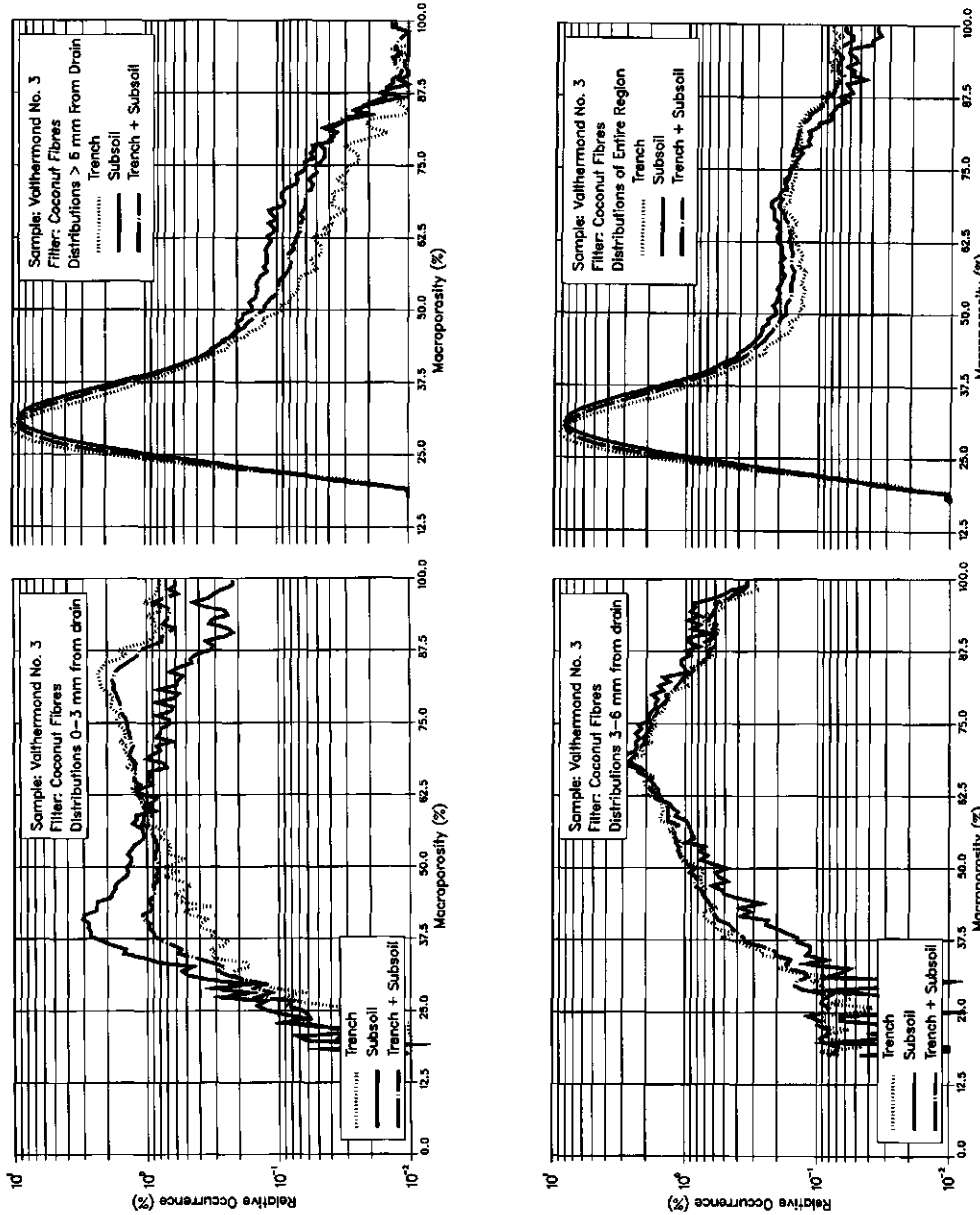

Figure 14. Frequency distributions of the macroporosity (MP) of the envelope and the soil around the drain in sample No. V03 of experimental field "Valthermond" in four regions of interest. Further away from the drain the trench backfill has a higher density than the subsoil. The inside area of the envelope under the drain appears to be clogged with soil particles; the outside area is "clean", cf. Figure 16.

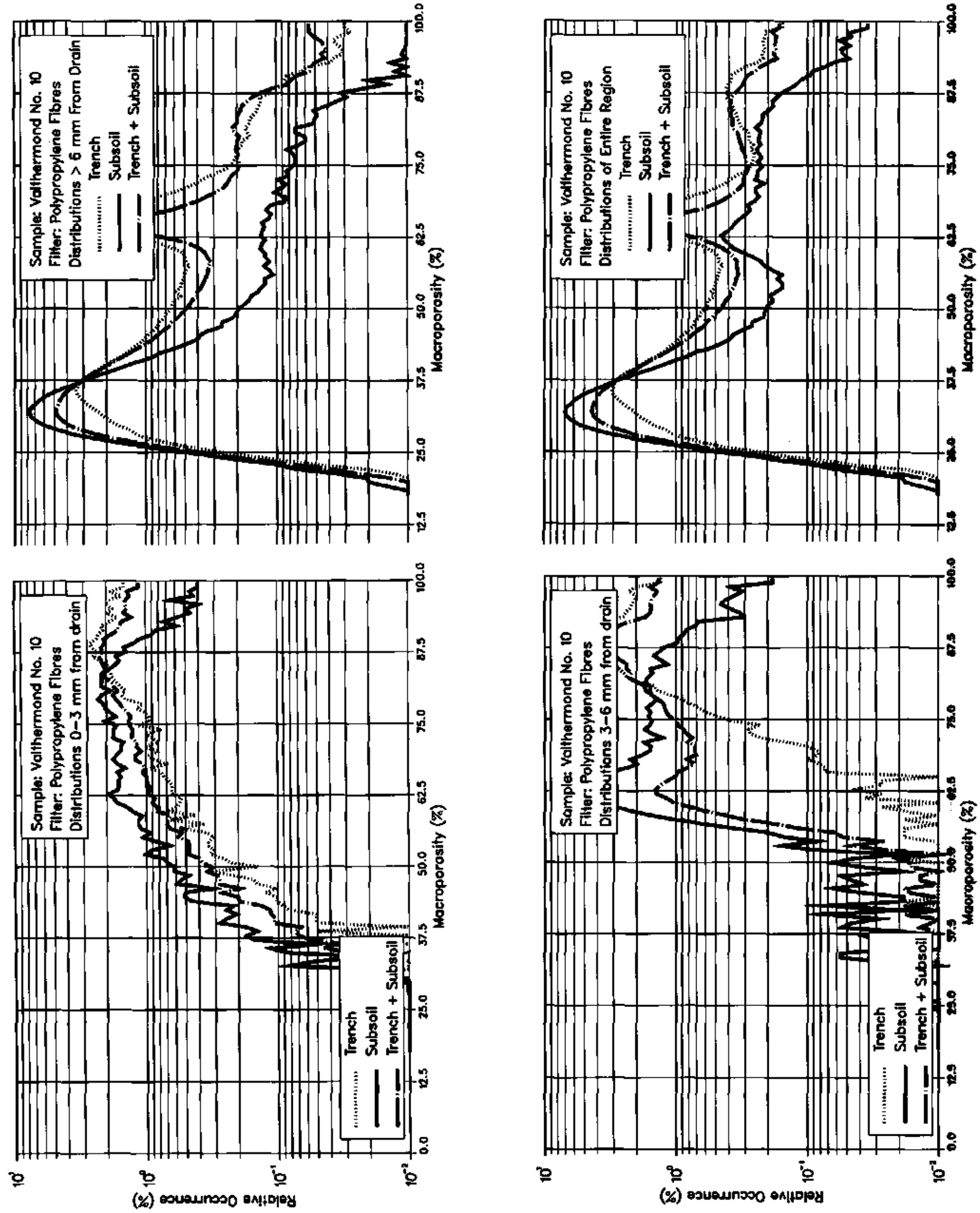

Figure 15. **Frequency distributions of the macroporosity (MP) of the envelope and the soil around the drain in sample No. V10 of experimental field "Valthermond" in four regions of interest. At the interface with the drain the envelope is globally yet only slightly clogged. Further away, the top side of the envelope is "clean" while the bottom side is clogged.**

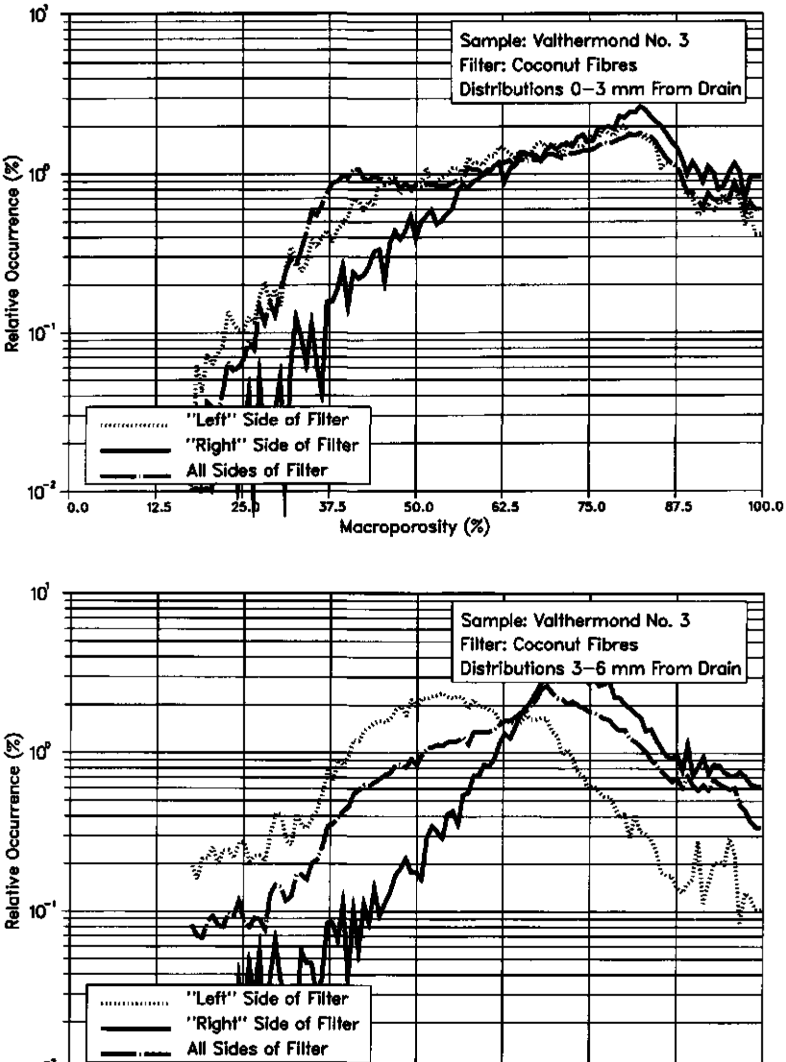

Figure 16. Local mineral clogging inside the Coconut fibre envelope of sample No. V03 of experimental field "Valthermond" is reflected in the distribution of macroporosity. At the interface with the drain, the "left" side of the envelope is slightly more clogged than the "right" side. Further away, the difference is more pronounced. Water entered this drain largely through the "left" bottom area of the trench.

Manual, interactive determination, taking the volume between the drain and the soil slice by slice, proved to be too time demanding. Instead, the volumetric areas of such envelopes were estimated from three CT slice images of each data set (No. 1, 25 and 50) by a manual procedure.

Table 2. Volumetric areas of voluminous envelopes ($m^3 \cdot 10^{-6}$).

"Buffer" Peat/	Uit 17	172.65	Polypropylene	Uit 2	99.51
Cocos mixture	Uit 8	211.16	Fibres "PPB"	Uit 1	119.59
	Uit 18	152.12		Uit 4	108.65
	Uit 15	155.54		Uit 3	122.28
Coconut Fibres	Val 4	135.23	"Garden" Peat	Uit 6	248.11
	Val 11	170.91	Fibres	Uit 5	46.61
	Val 12	174.08			
	Val 3	154.67			
Polypropylene	Val 5	220.14	Peat/Coconut	Wil 3	149.70
Fibres	Val 10	173.43	Fibre mix	Wil 9	215.55
	Val 9	165.54		Uit 11	158.79
	Val 6	171.58			
Polystyrene	Uit 19	280.98†	Polystyrene	Wil 5	312.91†
Beads "P.S.L."	Uit 20	294.52†	Beads "PS-LDPE"	Wil 6	393.92†
	Uit 10	293.94†		Uit 7	285.30†
	Uit 9	287.70†		Val 7	338.49†

†) Values, estimated from 3 CT scans.

Average macroporosities (MP), average limiting macroporosities (LMP) and differences ((LMP-MP)/MP) · 100%, are given in Table 3. LMP is plotted against MP in Fig. 18.

Regions of volume elements (voxels) in the 3D image space which were assigned particular LMP's have complicated geometric shapes. Such regions are important because they represent heterogeneous flow patterns of water towards drains and show the effect of the soil structure and the envelope material on such patterns. Hence, some of these regions are depicted as stereoscopic plates (Fig. 19-23 and Plates 3-7). The geometry of patterns of mineral clogging of voluminous envelopes which is depicted in transformed, flat surfaces (cf. Fig. 17) is also illustrated in Fig. 24 and in Plate 8, revealing the complexity of such patterns in 3D space.

Values of the heterogeneity indicator, HI, are given in Table 4 and are depicted in Fig. 25. HI could not be calculated accurately for drain sections which were

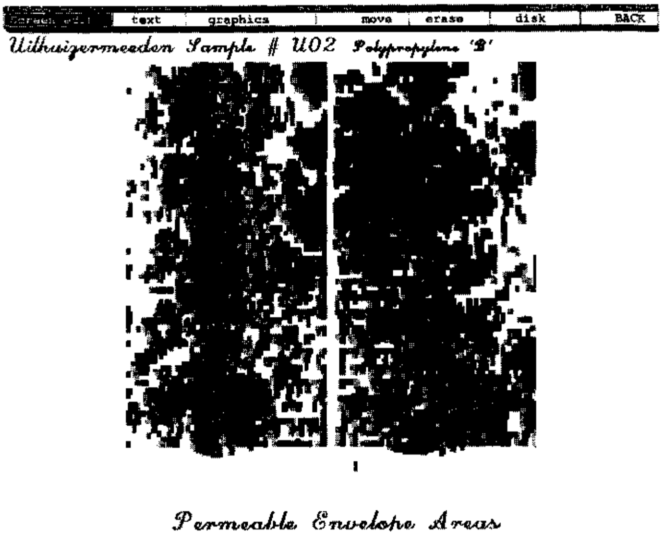

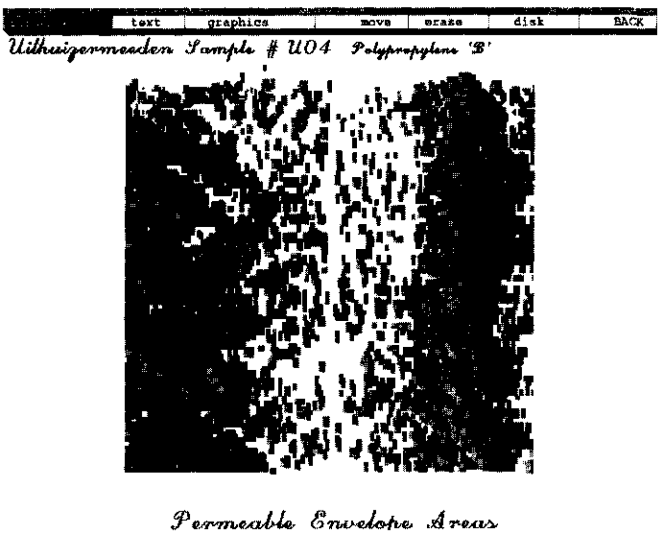

Figure 17. **Two examples of the heterogeneity of patterns of mineral clogging inside voluminous envelopes as depicted in transformed images in which these envelopes are displayed as flat surfaces. Envelope regions with average macroporosity lower than the median macroporosity are mapped as solid, shaded dark areas and are considered the most permeable. Other regions which are (partly) clogged are not depicted.**

Table 3. Average macroporosity (MP), average limiting macroporosity (LMP) in the trench and in the subsoil. Experimental fields: "Uit"="Uithuizermeeden", "Val"="Valthermond" and "Wil"="Willemstad".

		trench			subsoil		
		MP %	LMP %	(LMP-MP)/MP ·100%	MP %	LPM %	(LMP-MP)/MP ·100%
"Big 'O' fabric	Val 2	34.93	31.07	-11.05	31.44	29.18	-7.19
	Wil 8	35.31	30.75	-12.91	36.00	31.96	-11.22
	Uit 13	35.20	31.01	-11.90	34.89	30.32	-13.10
	Uit 12	37.09	32.20	-13.10	34.81	30.77	-11.61
"Buffer" Peat/ Cocos mixture	Uit 17	37.04	32.63	-11.91	37.57	33.60	-10.57
	Uit 8	37.60	32.25	-14.23	38.52	34.33	-10.88
	Uit 18	36.66	32.89	-10.28	39.22	35.52	-9.43
	Uit 15	37.86	33.06	-12.86	35.25	31.46	-10.75
"Cerex" nonwoven	Wil 7	35.53	31.27	-11.99	35.50	31.89	-10.17
	Wil 4	34.92	31.28	-10.42	35.35	31.75	-10.18
	Uit 14	39.07	32.77	-16.12	36.97	32.20	-12.90
	Val 8	49.41	38.72	-21.64	34.45	30.49	-11.49
Coconut Fibres	Val 4	40.99	35.41	-13.61	37.65	34.21	-9.14
	Val 11	39.39	34.08	-13.48	29.05	28.53	-1.79
	Val 12	46.79	41.65	-10.99	34.40	31.97	-7.06
	Val 3	36.43	32.27	-11.42	37.31	32.97	-11.63
Glass Fibre membrane	Wil 12	38.27	32.90	-14.03	33.98	31.24	-8.06
	Wil 11	33.79	29.50	-12.70	37.93	32.60	-14.05
	Wil 2	39.06	32.03	-18.00	37.04	30.89	-16.60
	Wil 1	35.89	31.18	-13.12	37.75	32.89	-12.87
Polypropylene Fibres	Val 5	44.00	37.82	-14.05	48.45	41.50	-14.34
	Val 10	54.03	44.22	-18.16	40.65	37.35	-8.12
	Val 9	40.15	34.18	-14.87	35.32	31.21	-11.64
	Val 6	41.69	34.69	-16.79	43.58	35.29	-19.02
Polypropylene Fibres "PPB"	Uit 2	35.75	30.90	-13.57	37.11	32.50	-12.42
	Uit 1	35.42	32.92	-7.06	36.62	34.34	-6.23
	Uit 4	35.87	30.73	-14.33	33.89	29.68	-12.42
	Uit 3	37.84	33.02	-12.74	35.50	32.09	-9.61
Polystyrene Beads "P.S.L."	Uit 19	40.52	32.26	-20.38	40.03	32.54	-18.71
	Uit 20	42.15	32.97	-21.78	45.82	35.75	-21.98
	Uit 10	44.37	33.93	-23.53	42.27	33.09	-21.72
	Uit 9	40.86	32.14	-21.34	42.07	33.23	-21.01
Polystyrene Beads "PS-LDPE"	Wil 5	40.34	33.54	-16.86	42.99	36.73	-14.56
	Wil 6	38.92	32.65	-16.11	38.16	34.09	-10.67
	Uit 7	40.55	32.51	-19.83	39.55	31.73	-19.77
	Val 7	41.84	33.55	-19.81	35.13	30.35	-13.61
"Garden" Peat Fibres	Uit 6	39.23	33.96	-13.43	37.29	33.15	-11.10
	Uit 5	38.55	33.37	-13.44	38.35	33.97	-12.99
Peat/Coconut Fibre mix	Wil 3	37.10	33.55	-9.57	38.81	33.60	-13.42
	Wil 9	36.55	32.67	-10.62	37.77	34.30	-9.19
	Uit 11	36.58	32.82	-10.28	35.90	31.31	-12.79
"Typar" nonwoven	Val 1	39.25	36.13	-7.95	35.44	31.61	-10.81
	Wil 10	35.76	31.33	-12.93	37.05	32.78	-11.52
	Uit 21	37.33	32.07	-14.09	34.71	30.32	-12.65
	Uit 16	36.56	31.63	-13.48	35.49	30.67	-13.58

wrapped with polystyrene beads due to the heterogeneity inside these voluminous envelopes with their very low x-ray attenuation rates. The automated image

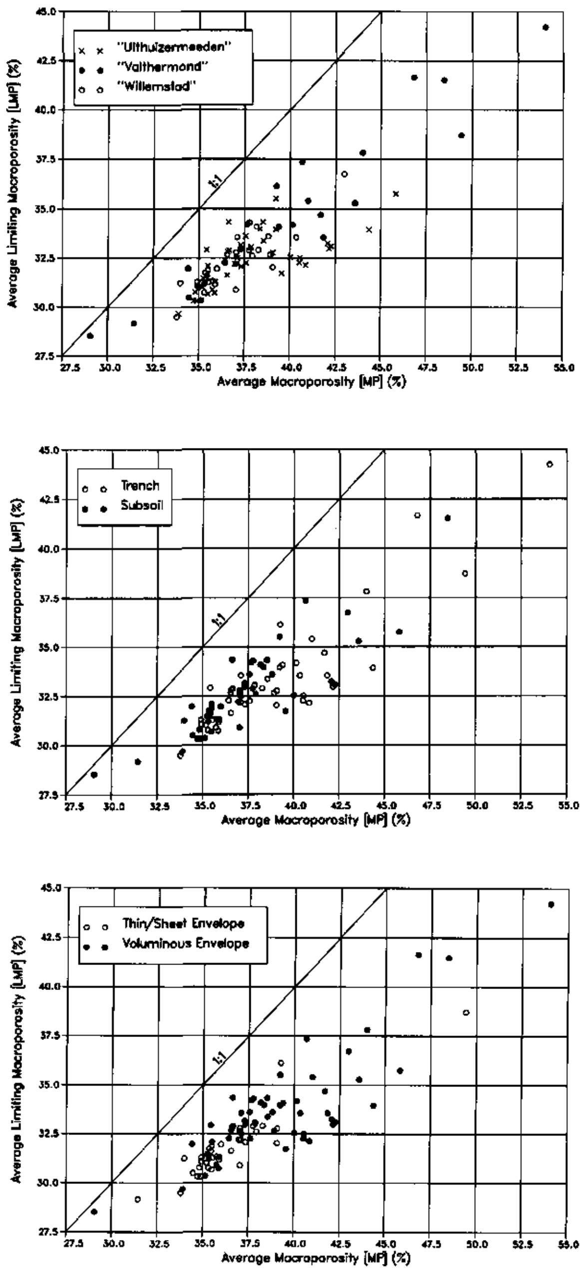

Figure 18. **Average macroporosity (MP) around drains, plotted against average limiting macroporosity (LMP), for three categories: experimental field, trench vs. subsoil and type of envelope.**

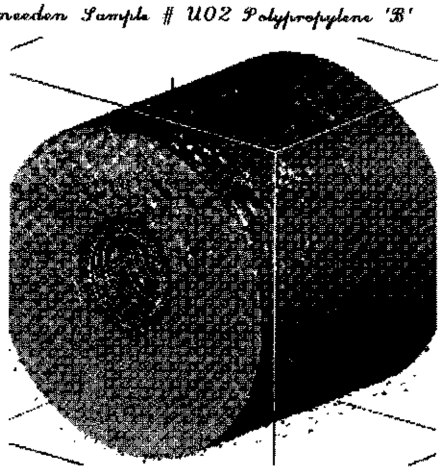

Figure 19. **CT scan image depicting all voxels that border the soil in a sample core. Experimental field: Uithuizermeeden, envelope material: Polypropylene 'B', sample No. U02.**

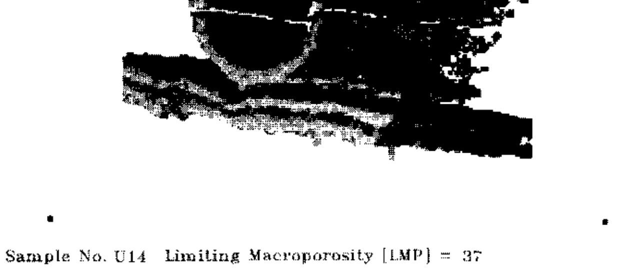

Figure 20. **Image areas containing all voxels with Limiting Macroporosity LMP ≥ 37%. Subtle banding is evident under the drain. The trench contains some geometrically complex areas. Experimental field: Uithuizermeeden, envelope material: "Cerex" nonwoven, sample No. U14. See also Plate 4.**

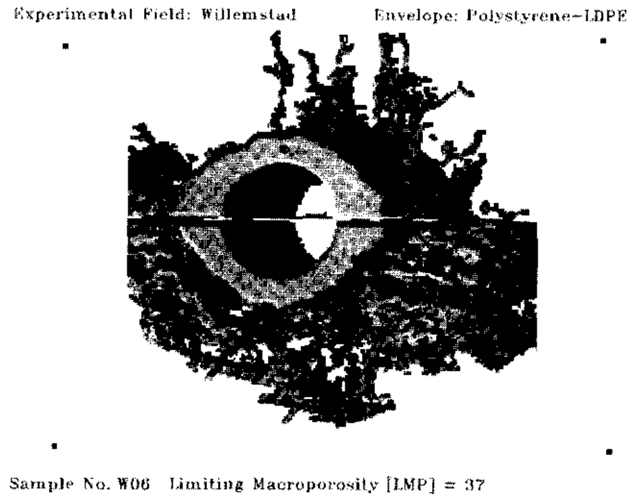

Figure 21. Image areas containing all voxels with Limiting Macroporosity LMP ≥ 37%. This drain was installed in a soil layer with a relatively high conductivity. Water flow through the trench is restricted at this LMP, possibly due to structural deterioration of the backfill material. Experimental field: Willemstad, envelope material: Polystyrene beads "PS-LDPE", sample No. W06. See also Plate 5.

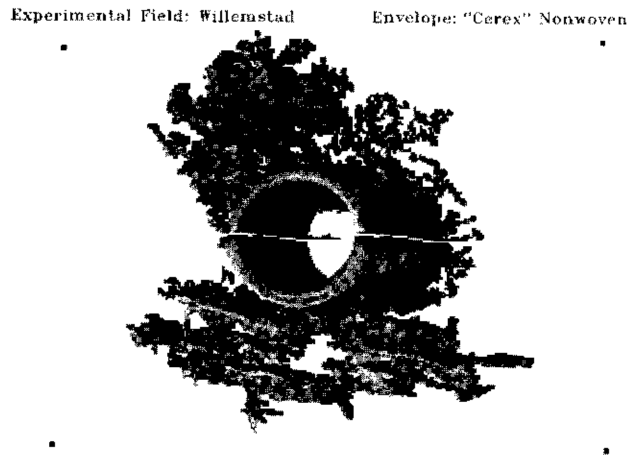

Figure 22. Image areas containing all voxels with Limiting Macroporosity LMP ≥ 35%. Water enters this drain through a complicated system of soil layers underneath and through one side of the trench. Experimental field: Willemstad, envelope material: "Cerex" nonwoven, sample No. W07. See also Plate 6.

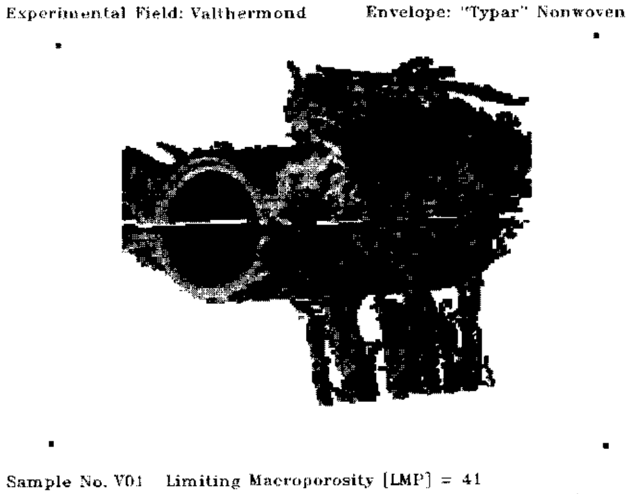

Figure 23. Image areas containing all voxels with Limiting Macroporosity LMP $\geq$ 41%. Water access to this drain proceeds through a series of parallell vertically oriented macropores. Not all macropores are involved at this LMP, however, see Figure 11 and Plate 2. Experimental field: Valthermond, envelope material: "Typar" nonwoven, sample No. V01. See also Plate 7.

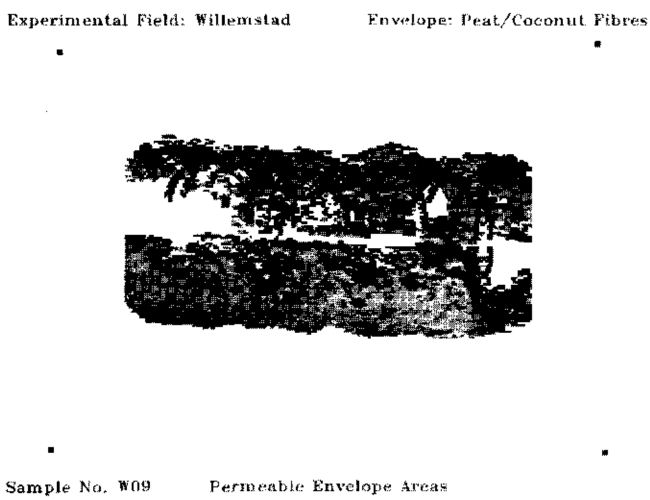

Figure 24. Image areas containing all voxels where the most permeable envelope areas are mapped. The envelope is mainly clogged at the interface area with the trench. Experimental field: Willemstad, envelope material: Peat/Coconut fibre mixture, sample No. W09. See also Plate 8.

processing procedure failed to discriminate soil heterogeneity at the soil/envelope interface from envelope heterogeneity. Again, manual interactive editing on a 2D slice by slice basis could have been used to calculate HI for these cases but this procedure proved too time consuming.

Table 4. Values of the heterogeneity indicator, HI, in the trench and in the subsoil. Experimental fields: "Uit"="Uithuizermeeden", "Val"="Valthermond" and "Wil"="Willemstad".

	sample	trench HI (-)	subsoil HI (-)		sample	trench HI (-)	subsoil HI (-)
"Big 'O' fabric	Val 2	2.04	1.55	Glass Fibre	Wil 12	1.58	1.41
	Wil 8	2.48	2.12	membrane	Wil 11	2.28	1.54
	Uit 13	2.31	4.60		Wil 2	2.43	3.14
	Uit 12	3.48	3.53		Wil 1	4.59	2.12
"Buffer" Peat/	Uit 17	2.62	3.42	Polypropylene	Val 5	2.35	4.28
Cocos mixture	Uit 8	7.02	4.33	Fibres	Val 10	3.80	4.32
	Uit 18	2.17	1.77		Val 9	2.58	5.03
	Uit 15	6.58	4.09		Val 6	3.55	2.93
"Cerex"	Wil 7	4.72	2.41	Polypropylene	Uit 2	2.51	2.82
nonwoven	Wil 4	3.21	1.94	Fibres "PPB"	Uit 1	2.86	2.43
	Uit 14	3.51	3.22		Uit 4	4.84	2.68
	Val 8	2.11	2.29		Uit 3	3.81	4.93
Coconut Fibres	Val 4	1.61	1.99	"Garden" Peat	Uit 6	2.98	3.87
	Val 11	2.52	2.22	Fibres	Uit 5	3.98	3.86
	Val 12	2.06	2.56				
	Val 3	2.79	2.28				
"Typar"	Val 1	2.02	1.82	Peat/Coconut	Wil 3	2.10	1.72
nonwoven	Wil 10	3.69	2.55	Fibre mix	Wil 9	1.94	2.16
	Uit 21	4.01	2.53		Uit 11	3.80	4.49
	Uit 16	3.45	2.77				

5 DISCUSSION

The drains are slightly compressed in the vertical direction by the pressure of the overburden. Their eccentricity can be accurately measured with CT. Pipes, wrapped with voluminous envelopes are slightly less compressed than pipes, wrapped with thin envelopes. Obviously, the soil overburden pressure is partly absorbed by the compression of voluminous envelopes.

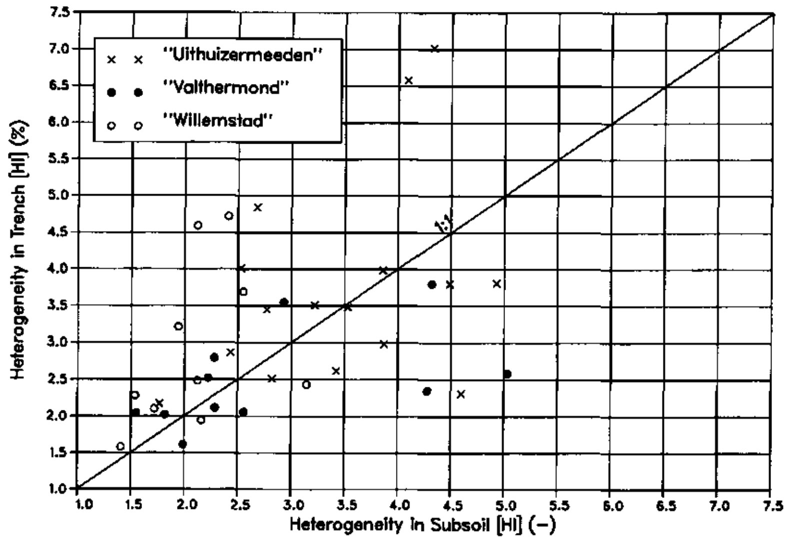

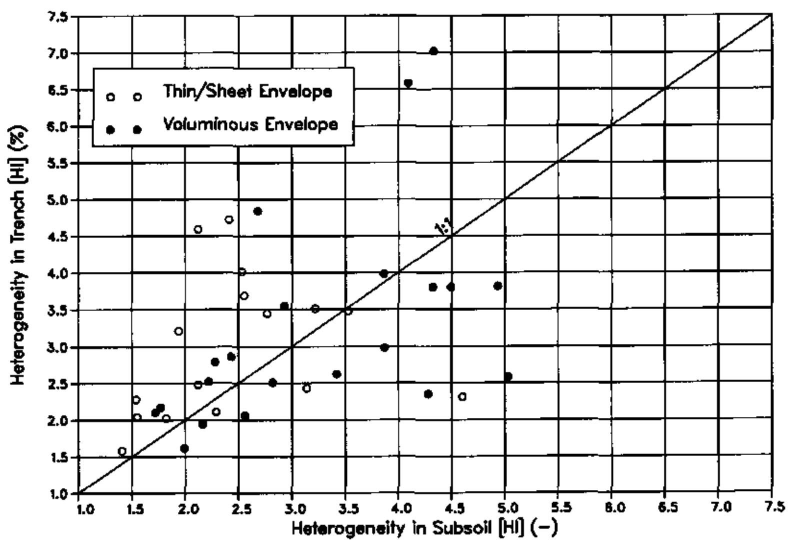

Figure 25. **Soil macropore heterogeneity indicator (HI) in the trench and in the subsoil, for two categories: experimental field (top) and envelope category (bottom).**

The volume of the region of interest around the drain is quite sensitive to the location and orientation of the drain in a sample core. Inaccurate sampling of drain sections is likely to occur when the penetration resistance of the trench is much lower than that of the subsoil. This was often the case in the "Valthermond" experimental field where peat remnants are found in the trench. In such cases, the plexiglass sampling cylinder tended to tilt downward and the drain pipe was not well centred in the sampled core. Hence, the smallest regions of interest were found in cores sampled at "Valthermond". Generally, the volumes of regions of interest vary from $1287 \cdot 10^{-6}$ m^3 to $3398 \cdot 10^{-6}$ m^3, so the largest area is 2.6 times as big as the smallest one.

On average, the volumetric areas of the voluminous envelopes occupy 7.5% of the regions of interest. The variability of this figure is somewhat smaller for synthetic envelopes than for envelopes manufactured from natural substances. Envelopes, manufactured from polystyrene beads have the largest volumetric areas in the areas of interest with the smallest variability. The most expensive envelope, needlefelt "Polypropylene Fibres" has a comparatively large average thickness; its cheap variety, "PPB" the smallest.

Averages of macroporosity MP and of limiting macroporosity LMP are widely scattered (Fig. 18). The scatter is mainly caused by differences between the soils, i.e. in trench backfill and in the undisturbed subsoil. The effect of voluminous envelopes on the average macroporosity is slight because they occupy only a small part of the area of interest (7.5% on average).

If drains are installed at appropriate soil moisture content, soil macropores in the backfilled trench are usually most abundant just after construction. Their continued existence depends on the stability of the soil aggregates. In unstable soils like the fine-sandy "problem" soils in The Netherlands, the macropores become smaller both in size and total volume because the soil slakes and disperses on wetting. The average macroporosity in "Valthermond" trenches remains high with time, because the backfill often contains peaty substances, although the soil inbetween is often very dense.

Trench macroporosity is sometimes lower than the macroporosity in the subsoil. The number of such cases is too low to draw significant conclusions, yet attention is drawn to the fact that trench macroporosity was inferior to subsoil macroporosity in 3 out of 4 samples which contain the "Buffer" Peat/Cocos mixture envelope. Generally, however, there is no proof that the type of envelope has a substantial effect on the development of the soil structure in the trench backfill with time. The bandwidth of "Willemstad" macroporosities is the smallest (Fig. 18). Differences between MP and LMP (Table 3) appear slightly larger for the trench backfill than for the undisturbed subsoil. This may be explained by occasional structural deterioration of trench backfill with time. As the soil settles, smaller particles may fill up existing pores (internal soil clogging; see Chapter 5). As a result, its macroporosity and its hydraulic conductivity decrease accordingly.

Differences between MP and LMP are more varied for voluminous envelopes than for thin ones, particularly in soils with high macroporosity, such as in the trench area, where the differences reach maximum values. Voluminous envelopes give support to drain pipes, resulting in lower pipe deflections, yet such beneficial effects are apparently realized at the expense of severe compression of such envelopes, leading to a substantial decrease of envelope pore size. This enhances the risk of blocking by soil particles, which is most likely to occur in the trench area. Thin envelopes are barely compressible, hence the risk of pore size reduction is accordingly lower. The largest differences between MP and LMP were found for the following combination of factors: (a) in the trench backfill, (b) with voluminous envelopes and (c) in "Uithuizermeeden".

Generally, the slightly enhanced macroporosities, found around voluminous envelopes do not necessarily guarantee more favourable hydraulic conditions near the drain because comparatively low average LMP's were also occasionally found with such envelopes.

Visual interpretation of the volumetric regions which are associated with various LMP's (Fig. 19-24; Plates 3-8) shows that these regions may be geometrically complex and that they are dependent on soil structure rather than on envelope type. Obviously, the effect of an envelope on the water flow pattern towards a drain is limited as is its effect on radial and entrance resistance. Hence, difference in these flow resistances must be ascribed to soil structural features, i.e. macroporosity and its distribution near the drain; not to envelope characteristics.

The variability of the average LMP between all envelopes was relatively small. Hence, it is unjustified to conclude that the water acceptance of drains, wrapped with voluminous surrounds is larger than that of drains, wrapped with thin envelopes. This observation is confirmed by the fact that drainage resistances of laterals in pilot areas "Uithuizermeeden" and "Willemstad" were independent of envelope thickness (Chapter 3). Given the systematic difference between MP and LMP (10-15% on average) drainage resistance is more likely to be determined by soil macroporosity than by hydraulic properties of the envelopes. The soil around the drain is the major throttle to water flow into the drain.

Thin envelopes, installed in "Valthermond", give rise to higher drainage resistances than voluminous ones (Chapter 3). "Valthermond" drains are used for subsurface irrigation in summer and, as such, they may be clogged with organic substances. The CT scanner is not very suitable to detect such substances. This may explain the comparatively favourable LMP's, calculated for those thin envelopes in this field. Probably these substances may be detected by a technique called MRI or "Magnetic Resonance Imaging". The value of the heterogeneity indicator, HI, is quite variable and appears independent of envelope category, experimental field or soil structure (i.e. trench backfill or subsoil). The number of cases analysed is too small however, and the variety of soil/envelope combinations is too big to draw significant conclusions. Nevertheless, the effect of envelope specifications on the development of (a) a filter cake or (b) areas with enhanced macroporosity in the abutting soil appears to be negligible. Possibly, a better heterogeneity indicator is needed in the framework of a more thorough analysis of soil heterogeneity near envelopes to provide more conclusive results.

The successful use of the LMP as a qualitative indicator to analyse the water acceptance of drains in a heterogeneous medium demonstrates that a "traditional" analysis in 2D cross-sections through such drains is inadequate and must be replaced by an analysis in 3D space. In heterogeneous media, the mere use of macroporosity as such or the use of (bulk) density data to estimate hydraulic conductivities (Chapter 6) is likely to yield erroneous modelling results because it neglects the complex 3D geometry of density differences in the soil matrix and the resulting flow patterns.

6 CONCLUSIONS

Computerised tomography, combined with 3D image analysis is a powerful technique to investigate and quantify the physical interaction between drain filters and surrounding fine-sandy, weakly-cohesive soils. A visualisation study revealed that water flow patterns near drains are often heterogeneous. They depend on soil structure rather than on envelope type. Patterns of mineral clogging of envelopes were also found to be heterogeneous. Envelopes act as permeable constraints which support the soil near the drain. Good installation practice is the decisive factor to secure a long service life of wrapped drains. Good envelopes will not cancel out adverse effects of poor installation; the main envelope is the soil and the contractor determines its quality and long-term properties at the time of installation. Installation under wet conditions must be avoided, if possible, in all situations. □

REFERENCES

Anderson, S.H. and C.J. Gantzer. 1987. Determination of soil water content by X-ray computed tomography and NMR imaging. Proc. Int. Conf. on

Measurement of Soil and Plant Water Status: Vol. 1, Utah State University, Logan, UT USA: pp. 239-245.

Anderson, S.H., C.J. Gantzer, J.M. Boone and R.J. Tully. 1988. Rapid nondestructive bulk density and soil-water content determination by computed tomography. Soil Sci. Soc. Am. J. 52:35-40.

Anderson, S.H. and C.J. Gantzer. 1989. Determination of soil water content by X-ray computed tomography and magnetic resonance imaging. Irrig. Sci 10:63-71.

Anderson, S.H., R.L. Peyton and C.J. Gantzer. 1990. Evaluation of constructed and natural soil mocropores using x-ray computed tomography. Geoderma 46:13-29.

Bergosh, J.L., T.R. Marks and A.F. Mitkus. 1985. New core analysis techniques for naturally fractured reservoirs. Soc. Petrol. Engin. SPE 13653. Bakersfield, CA USA March 27-29, 8 pp.

Bouma, A.H. 1969. Methods for the study of sedimentary structures. John Wiley & Sons, New York, USA.

Chancellor, W.J. and R.H. Schmidt. 1962. Soil deformation between surface loads. Transact. ASAE 5(2):235-239.

Crestana, S., S. Mascarenhas and R.S. Pozzi-Mucelli. 1985. Static and dynamic three-dimensional studies of water in soil using computed tomography scanning. Soil sci. 140(5): 326-332.

Crestana, S., R. Cesareo and S. Mascarenhas. 1986. Using a Computed Tomography Miniscanner in Soil Science. Soil Sci. 142 1:56-61.

Glover, G.H. 1982. Compton scatter effects in CT reconstructions. Med. Phys. 9(6):860-867.

Grevers, M.C.J., E. De Jong and R.J.St. Arnaud. 1989. The characterization of soil macroporosity with CT scanning. Can. J. Soil Sci. 69:629-637.

Hainsworth, J.M. and L.A.G. Aylmore. 1983. The use of computer-assisted tomography to determine spatial distribution of soil water content. Austral. Journ. of soil Res. 21(4): 435-443.

Herman, G.T. 1980. Image Reconstruction from Projections, the Fundamentals of Computerized Tomography. Computer Science and Applied Mathematics, A series of Monographs and Textbooks. Academic Press, New York, USA

Hunt, P.K. and P. Engler. 1987. Computed Tomography as a Core Analysis Tool: applications and Artifact Reduction Techniques. Soc. Petrol. Engin. SPE 16952. Dallas, TX USA, Sept. 27-30, 8 pp.

Hounsfield, G.N. 1972. A method of and apparatus for examination of a body by radiation such as x-ray or gamma-radiation. British Patent No. 128,3915, London.

Hounsfield, G.N. 1980. Computed medical imaging. Med. Phys. 7(4)283-290, Jul./Aug. 1980.

Krinitzsky, E.L. 1970. Radiography in the earth science and soil mechanics. Plenum Press, New York, USA.

Lennoz-Gratin, Ch. 1989. Effect of Envelopes on Flow Pattern Near Drain Pipe. Journ. Irr. Drain. Eng. 115(4):626-641.

Lennoz-Gratin, Ch. 1991. Hydraulique à l'interface sol-drain. Application à la prévision du risque de colmatage minéral des drains agricoles (Hydraulics at the soil-drain interface. Application to the prediction of the risk of mineral clogging of drains). Etudes Hydraulique Agricole No. 9, CEMAGREF/USTL, France

Petrovic, A.M., J.E. Siebert and P.E. Rieke. 1982. Soil bulk density analysis in three dimensions by computed tomography scanning. Soil Sci. Soc. Amer. Journ. 46(3): 445-450.

Phogat, V.K. and L.A.G. Aylmore. 1989. Evaluation of Soil Structure by using Computer Assisted Tomography. Aust. J. Soil. Res. 27:313-323.

Phogat, V.K., L.A.G. Aylmore and R.D. Schuller. 1991. Simultaneous measurement of the spatial distribution of soil water content and bulk density. Soil Sci. Soc. Am. J. 55:908-915.

Rogaar, H. and R.A.H. Thiadens. 1975. X-rays applied to the study of the pore structure in soils. Neth. J. Agric. Sci. 23 (1975): 321-333.

Rogaar, H. 1976. Radiografie van het grondbewerkingsproefveld "Westmaas" (Radiography of soil tillage experimental field "Westmaas"). Internal Report, Laboratory for Soil Science and Geology, Agricultural University, Wageningen, The Netherlands (in Dutch).

Stuyt, L.C.P.M. and A.J. Oosten. 1987. Mineral and Ochre Clogging of Subsurface Land Drainage Systems in The Netherlands. Geotextiles and Geomembranes 5(2): 123-140.

Stuyt, L.C.P.M. 1987. Developments in land drainage envelope materials. Proc. Symp. 25th Int. Course on Land drain., Publication 42, ILRI, Wageningen, The Netherlands, pp. 82-98.

Zissis, T. and L.C.P.M. Stuyt. 1991. Effect of radial soil heterogeneity around a subsurface drain on the water table height computed using a finite element model. Agric. Water Manage., 20:47-62.

8 SUMMARY AND CONCLUSIONS

8 Summary and Conclusions

1 PURPOSE OF THE STUDY

The water acceptance of lateral drain pipes in agricultural drainage systems is largely determined by the hydraulic conductivity of the zone immediately surrounding these laterals. The investigations in this thesis deal with the design of this zone in soils with poor structural stability. In such soils, laterals must be wrapped with a suitable envelope material to avoid clogging of the pipes and to safeguard the hydraulic conductivity, which tends to decrease with time due to the pressure of the overburden and the drag force of the water discharged. Suitable envelopes control the rate of pipe sedimentation yet remain highly conductive for water flow. Envelopes are also thought to have an effect on the movement of nearby soil particles and -aggregates, although there is no clear evidence in support of this concept. Nevertheless, the functioning of lateral drains depends on envelope specifications in an intricate manner. These studies were made to unravel the effect of such specifications on water flow towards pipe drains. The systems studied were used for groundwater drainage in a humid climate.

Since the mid-1950s, two developments in drainage engineering caused an unintentional threat to the establishment of a stable, permeable zone around laterals. These were:

1. The mechanisation of pipe installation.

2. The gradual replacement of tile drains, backfilled with traditional filters by corrugated pipes pre-wrapped with various materials.

The introduction of mechanisation allowed drain installation under adverse conditions (shallow groundwater tables, general wetness) and made the control of the quality of the work more difficult. Concurrently, traditional drain filters, composed of natural materials like peat litter became scarce, prompting a search for alternatives. In contrast to these earlier filters/envelopes, the physical dimensions of the new envelopes are "approaching the limit" as a result of attempts to bring down construction costs. The difficulties, encountered with mechanised installation were thought to be unavoidable and were accepted.

Attention was focused instead on the envelopes that, if properly designed and installed, were supposed to have a beneficial effect on the hydraulic conductivity of the surrounding soil. It was (and is) even suggested that envelopes could compensate for adverse effects induced by poor installation practice. There is, however, no field evidence in support of such speculations. The effects of an envelope on the service life of drains are still unclear, particularly in relation to the effect of other crucial factors such as the soil and weather conditions at installation and the tillage practices of the farmer. The first study reported in this thesis deals with experiments using two versions of a "traditional" analogue simulation model, designed to rapidly examine the suitability of envelopes for different soils. After reviewing the results of these experiments and of similar trials made elsewhere, it was concluded that contact erosion and mineral clogging at soil/envelope interfaces were indeed observed, but there was little understanding of the processes involved. As a consequence, recognition and quantification of the inherent mechanisms was not possible, a drawback which inhibited further progress in improving envelope design. More quantative data were needed to advance beyond the current position of almost complete stagnation. The greater part of this thesis therefore deals with the collection and interpretation of such data.

The investigations were centred in the following six areas:

1. *Examination of envelope properties in analogue simulation models and assessment of the utility of such models*

   Samples of envelopes and adjacent soils were subjected to water flow analysis using two versions of an analogue laboratory model. Both cohesionless and weakly-cohesive soil samples were used, originating from areas with very fine-sandy, marine deposits ("Almere" sand, "Lelystad", "Uithuizermeeden" and "Willemstad") and from a raised bog region ("Valthermond"). "Almere" sand and "Lelystad" are found in the IJssellake Polders in the Netherlands. In the other three areas, located elsewhere in the Netherlands, experimental fields had been established to observe the functioning of drains, wrapped with various envelope materials. The suitability of envelopes to convey water and to retain soil was quantified and analysed statistically. In addition, pore size distributions of envelopes were determined from moisture retention curves. The practical value of analogue modelling depends on whether or not the results may be extrapolated to the field **(Chapter 2)**.

2. *Internal and grade line examination of lateral drains*

Using a miniature video camera inspection system, a field survey was made of soil invasion and sedimentation patterns, root penetration and other phenomena in laterals, wrapped with various envelope types and installed in three experimental fields: "Uithuizermeeden", "Willemstad" and "Valthermond". Over 9600 m of lateral drains were inspected. All drains had been functioning for at least five years. They were installed in weakly-cohesive, very fine sandy soils where pipe sedimentation is a severe problem. The video images were visually interpreted at ½ m intervals. The grade line of the inspected laterals was continuously recorded with specialist equipment, indicating their depth at ½ m intervals. Statistics were used to test the effect of soil origin, envelope specifications and grade line parameters on the rate of pipe sedimentation and on drainage resistance. The results were used to select 45 locations for subsequent sampling of drain sections, together with the surrounding soil **(Chapter 3)**.

3. *Field sampling of drain sections*

A technique was developed to sample cores containing drain sections and surrounding soils. Although this type of sampling is generally considered to be difficult, 45 cores were sampled successfully. The drains from which the samples were taken had been installed at least five years earlier in the "Uithuizermeeden", "Willemstad" and "Valthermond" experimental fields. The dimensions of the cores were suitable for examination by x-ray computerised tomography (CT) **(Chapter 4)**.

4. *Analysis of particle size distributions of soil near drains*

In this project, microgranulometric analysis was used to study the effect of (a) the particle size distribution of a soil and (b) envelope specifications, on the movement of soil particles near wrapped drains. Above and under such drains, micro soil samples were taken from 45 sample cores that had been retrieved earlier for CT analysis. In total, 720 analyses were made. Statistics were used to investigate the effect of envelope specifications and the particle size distribution of the soils on the migration of soil particles **(Chapter 5)**.

5. *Finite element simulation of flow into drains*

Two-dimensional (2D) saturated flow towards a subsurface drain wrapped with a voluminous envelope was solved by a finite element approach. Special attention was given to water flow in the vicinity of the pipe and to the pattern of hydraulic conductivity in the envelope and the surrounding soil. Nonlinear elements were used for a better representation of the geometry around the drain, and non-linear interpolation for more accurate predictions of hydraulic heads. Soil heterogeneity around the drain, detected and quantified using data from x-ray computerised tomography (CT) images and texture analyses from the 45 sample cores, was averaged over the circumference and expressed as a gradually varying hydraulic conductivity in a radial direction **(Chapter 6).**

6. *The physical interaction between envelopes and soils*

A method was developed to detect, display and evaluate highly permeable areas inside drain envelopes and the surrounding soils which are physically connected to agricultural drains and are responsible for conveying most of the water to such drains. The data were gathered with a computerised tomography (CT) scanner as geometrically precise mappings of three-dimensional (3D) density distributions near the 45 drains sections. Macroporosity distributions around the drains were evaluated. A "Limiting Macroporosity (LMP)" concept was introduced to assess the water acceptance of drains and the effect of the envelope material and of the soil on the water acceptance was investigated. Visual perception of the complicated 3D water conveying network near drains was facilitated by stereoscopic images, produced by a computer **(Chapter 7).**

2 MAJOR FINDINGS

The major findings of the investigations are presented for each area separately.

Chapter 2 deals with the results of analogue simulation of mineral clogging of envelopes in laboratory models. In the cohesionless "Almere" soil, particle retention was much better with "thin" envelopes (thickness < 1 mm) than with "voluminous" materials. All "thin" envelopes satisfied the Dutch criterion ($\leq$ 15 mm sediment in a 60 mm drain) whereas most voluminous envelopes did not. Sedimentation rates were neither related to average pore sizes (D_{50}) of envelopes nor to uniformity coefficients (D_{60}/D_{10}) of their pore size distributions. Most entrance resistances were quite low and would not markedly influence the design of field drainage systems. Nevertheless, the significance of the findings for the functioning of real drains in weakly-cohesive soils is doubtful. Unless confirmed by field observations, such laboratory tests should be considered inappropriate to solve problems of this kind.

In the weakly-cohesive soils ("Lelystad", "Uithuizermeeden", "Willemstad" and "Valthermond"), both the hydraulic performance and the soil particle retention capability of envelopes were highly erratic. Evaluation of the findings showed: a) a better particle retention capability of "thin" envelopes as compared to "voluminous" ones; b) generally, the development of a zone with higher hydraulic conductivity near the drains, especially if wrapped with "voluminous" envelopes, and c) no clear relationship between the particle retention capability of envelopes and their effective opening size (O_{90}). A certain degree of pipe sedimentation enhanced the hydraulic conductivity near the drain. The effect of both the envelope category ("thin" or "voluminous") and the origin of the soil sample on the "Envelope Suitability Index" (ESI), in which hydraulic performance and soil particle retention capability were integrated was often significant. With "Lelystad" and "Valthermond" soils, both "voluminous" and "thin" envelopes were better than no envelope. With "Uithuizermeeden" soil, "thin" envelopes were significantly better than "voluminous" ones which in turn were better than no envelope. With "Willemstad" soil, no significant differences were found, though it appears that drainage without an envelope may be possible, and that "voluminous" envelopes performed slightly worse than "thin" ones.

Chapter 3 shows the results of observations, made in the "Uithuizermeeden", "Willemstad" and "Valthermond" experimental fields, of the effect of envelopes and the grade line (accuracy) of laterals on drainage resistance, pipe sedimentation rate, influx of soil and root growth. It was established that: a) the laying accuracy was quite good, both in terms of average grade and of standard deviations from the average grade; b) neither the envelope category ("thin" or "voluminous") nor the type of envelope had a significant effect on the total resistance encountered by the flow of water from points midway between the laterals to the outlets; c) if drains were to be used for both subirrigation and drainage, "voluminous" envelopes would offer considerable advantages, having consistently lower drainage resistances than "thin" ones; d) pipe sedimentation rates were significantly correlated with the effective opening size (O_{90}) of envelopes and soil sample origin; e) soil influx into drains appears to occur most frequently with envelopes made from natural organic substances, and f) soil is commonly squeezed into the drains while saturated; this mechanism is obviously different from the sedimentation mechanism which is simulated in laboratory tests where transport of separate particles is the dominant process.

Chapter 4 reports on the development of a technique and procedure for the retrieval of "undisturbed" sample cores, 200 mm diameter and 300 mm long, containing drain sections and the surrounding soil zones. These cores were to be examined by x-ray computerised tomography ("CT"). Physical limitations of CT impose restrictions on sample geometry and size, which were determined by trial and error. In the "Uithuizermeeden", "Willemstad" and "Valthermond" experimental fields 45 samples were taken, containing 12 different envelope materials. Most envelopes were sampled four times. Undisturbed sampling of drain sections was difficult, particularly with shallow groundwater tables.

Chapter 5 describes the results of observations of particle size distributions of soils near drains and inside envelopes, sampled in the "Uithuizermeeden", "Willemstad" and "Valthermond" experimental fields. It is often speculated that envelopes have a significant effect on the movement of soil particles near drains. The findings do not support this concept. In weakly-cohesive Dutch soils the particle size distribution of the soil has a significant effect; not the envelope. Small soil particles (≤ 30 μm) are more easily mobilized by flowing water than larger ones. Once suspended, such particles may either be leached from the soil or be trapped in it. Larger particles are less easily mobilized and are commonly retained in the soil near the drain. In some cases, the particle size distribution of the soil near the drain appeared to have developed towards that of a soil with minimum porosity. The washing out of fine particles near the drain, a process often referred to as the formation of a "natural soil filter" and generally assumed to occur frequently, was observed in only a few cases. Instead, internal soil clogging appeared to be the common process. Drain envelopes clearly act as selective filters for particles which are leached from the soil. Nevertheless, the soil in the zone around the drain is a much finer and more important filter than the envelope, which is essentially a permeable support, helping to stabilise the soil.

Chapter 6 deals with a study to quantify the effect of a heterogeneous zone around a wrapped drain and envelope clogging, on the mid-drain water table height. The study was made with a two-dimensional (2D) finite element model. In these simulations, the hydraulic conductivity of the envelope was found to be the most significant factor with respect to the performance of the drain. Soon after completion of this study, however, it was established that flow in the zone around drains is conveyed through, geometrically complex, three-dimensional (3D) structures like horizontal layering and macropores. Hence, a "traditional" analysis based on 2D cross-sections is inadequate and must be replaced by an analysis in 3D space.

In **Chapter 7** the results are reported of a quantitative three dimensional (3D) analysis of density distributions in the zone around 45 wrapped drain sections, sampled in the "Uithuizermeeden", "Willemstad" and "Valthermond" experimental fields. The data were available as CT-image sequences. The method has allowed the recognition of the spatial distribution of structural features around these sections. The results showed: a) soil structure and its stability largely determine the service life of wrapped drains; b) water flow patterns into most drains and clogging patterns in voluminous envelopes are quite heterogeneous: the main water conveying features are inter-aggregate voids, macropores, made by worms and plant roots, and thin, relatively permeable horizontal soil layers, and c) the effect of soil properties on the water acceptance of drains surpasses that of the envelopes.

3 CONCLUSIONS

Since the 1960s, experiments have been carried out to develop criteria for the design and the application of low-cost envelopes for agricultural drains. Many field experiments, laboratory experiments and mathematical analyses have been reported in the literature. With time, however, it has become obvious that the major obstacle to further progress is the persistent lack of field data about the inherent physical processes. Only if such data would become available, could assumptions be replaced by facts.

There has never been a full awareness of the complexity of the physical processes that take place near drain envelopes. Hence, the gathering of adequate field data has not been given the high priority it deserved. For example, pipe sedimentation rates have rarely been monitored, and results of occasional excavations were considered to be representative of great lengths. In the mid-1980s, the monitoring of head losses near drains was discontinued because accurate observation of such losses was considered too laborious and expensive. The few observations that were made were absolutely inadequate, due to the heterogeneous flow pattern near drains. Many analogue model simulations have been made, yet the results have never been seriously compared with results from field experiments. Such a comparison was made for the first time in this study, revealing that analogue models are unreliable prediction tools when used for weakly-cohesive soils. The reasons for this are: a) the mechanism of soil influx into the drain in the field is different from the processes, observed in such model tests; b) the physical dimensions of the analogue models are too small relative to the scale of heterogeneities in the zone around drains that convey most of the water towards these drains, and c) the highly complex physical interaction between weakly-cohesive soils and envelopes, both in space and time, cannot be accurately observed in such models. Hence, in such soils, results of analogue model tests cannot be extrapolated to the field. The value of analogue modelling is therefore in serious doubt and the continued use of such models needs to be reconsidered.

Another complicating factor is the attitude toward field and laboratory experiments. There is a tendency to "use" experiments to have one's assumptions confirmed. If results are in accordance with such assumptions they are accepted; results that are not are rejected or ignored. Inconclusive field experiments where quite different envelopes have a similar effect on drainage resistance are rejected without further consideration, not only by manufacturers but also by researchers, whereas those which show differences are retained. On the other hand; the effect of installation conditions on the service life of drains, while generally acknowledged, are usually ignored.

The observed particle size distributions at the interface of the envelope and the soil and the existence of three-dimensional (3D) structural features in the zone near drains, suggest that the pattern of water flow into drains is strongly heterogeneous. The flow is concentrated in the most permeable areas, like inter-aggregate voids in the trench backfill and tiny permeable soil layers and root channels in the undisturbed subsoil. The bottom section of the trench backfill was found to convey much water toward the side-walls of the drain; the backfill just above the drain was often slaked and of low permeability. Due to the the drag force of the water, soil particles and aggregates are eroded, suspended and carried into the drain, enhancing the hydraulic conductivity of the conveying channels even further. Concurrent with this, the lower hydraulic conductivity of the remaining areas is still further reduced as a result of soil slaking and dispersion on wetting, whilst the flow rate is comparatively small. As a result, it is probable that the range of initial conductivities of the zone around the drain increases with time, resulting in a few higly conductive zones and many areas with negligible flow. Water enters the envelope at a few locations only (the conveying areas) whereas the major part of the contact zone between envelopes and soils is hydraulically inert (the supporting areas). The effect of the envelope type on this process is small.

The results of studies, made with two-dimensional (2D) mathematical models in which hydraulic properties of envelopes are linked to envelope thickness were not confirmed by field observations. Most of these models assume the soil and the envelope to be homogeneous and isotropic. Heterogeneity is sometimes incorporated, but only in the radial direction. Such models neglect the complicated three dimensional (3D) structural features near drains which convey most of the water. Such features were found to be largely determined by the soil. Hence the soil and not the envelope material is the crucial factor in the physical interaction between both media. The only envelope parameter of significance was the effective opening size (O_{90}). Otherwise, envelopes have no effect on the development of water flow patterns in the zone around drains.

From these results, the conclusion emerges that, at least for groundwater drainage systems in weakly-cohesive soils, research into envelopes has been based on erroneous concepts, concentrating on envelope specifications while neglecting soil properties. More attention should be directed to the soil, whose crucial properties cannot be simulated in a laboratory test but should be observed in the field.

In any drainage system, the zone near the pipe is of paramount importance. The success of drainage is not merely dependent on the type of pipe wrapped with a certain envelope. Rather, "drainage" is a product in which the installation determines the physical properties of this zone. The installer may easily destroy the important properties of this zone if installation is carried under adverse conditions. This fact is well known, yet in the case of problems it is usual to blame the envelopes, rather than poor installation practice.

4 MAJOR PRACTICAL CONSEQUENCES

From this research, the following practical consequences emerge:

1. If the effective opening size, O_{90}, of envelopes is within the suitable range (approximately 300 to 1000 μm), most envelope materials are acceptable.

2. If drains are also used for subirrigation, the use of "thin" envelopes (thickness < 1 mm) is not recommended. This is also true if there is a severe risk of clogging by iron ochre or microbiological products.

3. Drains must be carefully installed, and only if moisture conditions permit. After installation, careful maintenance (i.e. "jetting" with moderate water pressure) is often recommended but not self-evident. In case of a risk of biochemical and/or iron ochre clogging of prewrapped drain pipes, regular

maintenance may have a beneficial effect on the service life of a subsurface drainage system.

4. The use of analogue model tests for the assessment of the suitability of envelopes for use in weakly-cohesive soils must be discontinued.

5. Only accurate monitoring of potentially suitable envelopes in experimental fields yields valid information. It must be accepted that this procedure is expensive and time consuming.

6. Field experiments should always include unwrapped pipes and their design should allow for a sound statistical analysis of the observations.

5 GUIDELINES FOR FUTURE APPROACHES

After many years of research from the 1960s onwards, much has been revealed about the functioning of drain envelopes in weakly-cohesive Dutch soils. The research however has been limited to groundwater drainage systems without microbiological or ochre clogging. The extension of this research into such clogging areas is not recommended, since the formation of iron ochre and microbiological clogging will continue, regardless of the envelope. Its effects can only be controlled through the installation of "voluminous" synthetic envelopes (thickness $\geq$ 1 mm) and regular maintenance.

The functioning of envelopes is regionally dependent. While the results in other regions may well be similar, it is not justified to merely extrapolate them to such regions. The same is true for drainage systems designed to prevent salinization in irrigated areas. In such systems, pilot area research is recommended, and researchers have to accept the fact that the search for suitable envelopes may be time-consuming and tedious.

9 SAMENVATTING EN CONCLUSIES

9 Samenvatting en conclusies

1 DOEL VAN HET ONDERZOEK

Het vermogen van zuigdrains om water uit de omringende grond op te nemen wordt grotendeels bepaald door de hydraulische doorlatendheid van de zône die deze drains omringt. Het in dit proefschrift beschreven onderzoek is gericht op de eigenschappen (aard, gesteldheid) van deze zône in gronden met een lage struktuurstabiliteit. In zulke gronden moeten zuigdrains worden voorzien van een geschikt omhullingsmateriaal om verstopping van de buizen met gronddeeltjes tegen te gaan en om verzekerd te zijn van een goede hydraulische doorlatendheid. De doorlatendheid neemt gewoonlijk met de tijd af ten gevolge van de gronddruk en de stromingsdruk van het door de drains afgevoerde water. Geschikte omhullingsmaterialen verminderen de mate van inzanding van draineerbuizen maar blijven toch goed doorlatend voor water. Van omhullingsmaterialen wordt tevens aangenomen dat zij de verplaatsing van nabijgelegen gronddeeltjes en -aggregaten gedeeltelijk beheersen, maar dit is nooit overtuigend aangetoond. Niettemin hangt de werking van draineerbuizen op een ingewikkelde manier samen met specificaties van omhullingsmaterialen. Het onderzoek was erop gericht meer inzicht te krijgen in de invloed van deze specificaties op de waterstroming naar draineerbuizen. De bestudeerde drainagesystemen waren ontworpen voor ontwatering van landbouw-percelen in gematigde, humide klimaatszônes.

Twee ontwikkelingen in de drainagetechnologie in de landbouw vormen sinds het midden van de vijftiger jaren een ongewilde bedreiging voor de vorming van een stabiele, goed-doorlatende zône rond draineerbuizen. Dit zijn:

1. De mechanisatie van het installeren van draineerbuizen.

2. Het geleidelijk vervangen van kleibuizen, met traditionele filtermaterialen, door plastic ribbelbuis, voorzien van omhullingsmaterialen.

Ten gevolge van mechanisatie werd het mogelijk draineerbuizen te installeren onder ongunstige omstandigheden (ondiepe grondwaterstanden, natte omstandigheden), terwijl de kwaliteit van de installatie moeilijker kon worden gecontroleerd. Bovendien werden de traditionele filtermaterialen, bestaande uit natuurlijke grondstoffen als turfstrooisel, schaars waardoor naar andere materialen moest worden gezocht. De dikte van moderne omhullingsmaterialen is, in tegenstelling tot die van traditionele filters, zo gering mogelijk zodat aanzienlijk op kosten kan worden bespaard. De moeilijkheden die de gemechaniseerde installatie met zich meebrachten werden onvermijdelijk geacht en aanvaard. De aandacht concentreerde zich op de omhullingsmaterialen die, mits goed ontworpen en geïnstalleerd, werden verondersteld een gunstige invloed te hebben op de hydraulische doorlatendheid van de omringende grond. Er werd (en wordt) zelfs gesuggereerd dat de door slechte installatiepraktijken veroorzaakte ongunstige effecten door omhullingsmaterialen zouden kunnen worden gecompenseerd. Dergelijke suggesties kunnen echter niet worden onderbouwd met veldervaringen. Het effect van een omhullingsmateriaal op de levensduur van draineerbuizen is nog steeds onduidelijk, met name met betrekking tot effecten van andere beslissende faktoren zoals de grond, de weersomstandigheden tijdens het leggen van de buizen en de op het betreffende bedrijf uitgevoerde grondbewerkingen.

De eerste onderzoekingen waarvan in dit proefschrift verslag wordt gedaan betreffen experimenten, uitgevoerd met twee versies van een "traditioneel" analoog simulatiemodel dat werd ontworpen om snel de geschiktheid van omhullingsmaterialen in verschillende bodemtypen te kunnen vaststellen. Na evaluatie van de resultaten van deze experimenten en die van vergelijkbare, elders uitgevoerde proefnemingen, werd vastgesteld dat er op de grens van grondmonsters en omhullingsmaterialen weliswaar sprake was van kontakterosie en minerale verstoppingsprocessen, maar dat deze processen niet goed werden begrepen. Daarom was het onmogelijk om de onderhavige mechanismen te herkennen en te kwantificeren, waardoor vooruitgang bij het ontwikkelen van verbeterde ontwerpcriteria voor omhullingsmaterialen werd geblokkeerd. Er waren meer kwantitatieve gegevens nodig om de ontstane patstelling te doorbreken. De in dit proefschrift gerapporteerde aktiviteiten betreffen dan ook grotendeels het verzamelen en interpreteren van zulke gegevens.

De onderzoekingen werden verricht op de volgende zes terreinen:

1. *Onderzoek naar de eigenschappen van omhullingsmaterialen in analoge simulatiemodellen en evaluatie van de bruikbaarheid van dergelijke modellen.*

   In twee versies van een analoog doorstromingsmodel, opgesteld in een laboratorium, werden monsters van omhullingsmaterialen en aangrenzende grondmonsters aan waterstroming blootgesteld. Er werd gebruik gemaakt van struktuurloze en zwak-cohesieve grondmonsters, afkomstig uit gebieden met zeer fijnzandige, mariene afzettingen ("Almere" zand, "Lelystad", "Uithuizermeeden" en "Willemstad") en uit de veenkolonieën ("Valthermond"). De grondmonsters "Almere" zand en "Lelystad" zijn afkomstig uit Flevoland. In de andere drie gebieden werden proefvelden ingericht om de werking van draineerbuizen, voorzien van verschillende omhullingsmaterialen, te observeren. De geschiktheid van omhullingsmaterialen om water door te laten en gronddeeltjes tegen te houden werd statistisch geanalyseerd. Daarnaast werden poriegrootteverdelingen van sommige omhullingsmaterialen bepaald uit zuigspanningscurves. De praktische waarde van analoge modelproeven is afhankelijk van de mate waarin de nagebootste processen representatief zijn voor die welke zich onder veldomstandigheden afspelen **(Hoofdstuk 2)**.

2. *Inwendige inspectie van draineerbuizen en bepaling van de helling van deze buizen in het veld.*

Met behulp van een videocamera met geringe afmetingen werd op de proefvelden "Uithuizermeeden", "Willemstad" en "Valthermond" veldonderzoek uitgevoerd waarbij de indringing van grond, de hoogte van afzettingen van sediment, de indringing van wortels en andere fenomenen werden geregistreerd in draineerbuizen, voorzien van verschillende typen omhullingsmaterialen. In totaal werd meer dan 9600 m draineerbuis onderzocht. Alle buizen hadden minstens vijf jaar in het veld gefunctioneerd. Zij waren geïnstalleerd in zwak-cohesieve, zeer fijnzandige gronden waar draineerbuizen geregeld verstopt raken met gronddeeltjes. De videobeelden werden intervalsgewijs, i.c. op iedere ½ m geïnterpreteerd. De helling van de drains werd met speciale apparatuur vastgelegd en op hetzelfde interval gekwantificeerd. Met behulp van statistische technieken werden de effecten van bodemtype, omhullingsmateriaal en hellingparameters op de mate van buisverstopping en de drainageweerstand onderzocht. De resultaten werden tevens gebruikt om 45 locaties te selecteren voor bemonstering van drainsecties, inclusief de omringende grond **(Hoofdstuk 3)**.

3. *Bemonstering van drainsecties*

Voor het steken van cylindrische monsters met drainsecties en omringende grond werd een nieuwe techniek ontwikkeld. Hoewel dergelijke bemonsteringen moeilijk zijn werden 45 monsters met succes gestoken. De draineerbuizen waaruit secties werden bemonsterd waren tenminste vijf jaar eerder geïnstalleerd in de proefvelden "Uithuizermeeden", "Valthermond" en

"Willemstad". De afmetingen van de monsters werden zodanig gekozen dat onderzoek met behulp van een CT-scanner mogelijk was (**Hoofdstuk 4**).

4. *Analyse van de korrelgrootteverdeling van grond nabij draineerbuizen*

In deze studie werden granulometrische analyses uitgevoerd om het effect van (a) de korrelgrootteverdeling van grond, en (b) specificaties van omhullingsmaterialen op het transport van gronddeeltjes nabij vooromhulde draineerbuizen vast te stellen. Aan de boven- en onderzijde van de 45 drainsecties, eerder bemonsterd ten behoeve van het CT-onderzoek, werden zeer kleine grondmonsters genomen. In totaal werden 720 granulometrische analyses uitgevoerd. Met behulp van statistische technieken werd het effect van specificaties van omhullingsmaterialen en de korrelgrootteverdeling van gronden op de beweging van gronddeeltjes onderzocht (**Hoofdstuk 5**).

5. *Eindige elementen analyse van waterstroming naar draineerbuizen*

Met behulp van een voor dit doel ontwikkeld eindige elementen model werden numerieke oplossingen verkregen van tweedimensionale, verzadigde waterstroming naar vooromhulde draineerbuizen. Bijzondere aandacht werd geschonken aan waterstroming vlakbij de buis en aan de variabiliteit van de hydraulische doorlatendheid in het omhullingsmateriaal en de omringende grond. Om de geometrie van de stroming vlakbij de buis nauwkeurig na te bootsen werden niet-lineaire elementen gebruikt. De hydraulische drukhoogteverschillen konden nauwkeurig worden gemodelleerd door gebruik te maken van niet-lineaire interpolatietechnieken. De heterogeniteit van de grond rond de draineerbuis, geregistreerd en gekwantificeerd met behulp van CT-beelden, en analyse van de textuur van deze grond in 45 grondmonsters, werd gemiddeld en in radiale richting beschreven als een geleidelijk veranderende hydraulische doorlatendheid (**Hoofdstuk 6**).

6. *De wisselwerking tussen omhullingsmaterialen en gronden*

Er werd een methode ontwikkeld voor de detectie, afbeelding en evaluatie van relatief goed-doorlatende zônes van omhullingsmaterialen en omringende gronden, die met draineerbuizen in verbinding staan, en via welke het door deze buizen af te voeren water grotendeels toestroomt. Met behulp van een computertomograaf ("CT-scanner") werden de gegevens verzameld in de vorm van geometrisch exacte, gedigitaliseerde afbeeldingen van driedimensionale

(3D) dichtheidsverdelingen nabij de 45 bemonsterde secties van de draineerbuizen. De macroporositeit van de grond rond draineerbuizen werd geanalyseerd. Het "Limiting Macroporosity (LMP)" (=beperkende macroporositeit) concept werd geïntroduceerd om het vermogen van draineerbuizen om water uit de omringende grond op te nemen kwalitatief te kunnen vaststellen. Het effect van het omhullingsmateriaal en van de omringende grond op genoemd vermogen werd onderzocht. Visuele perceptie en interpretatie van het, geometrisch complexe, water-geleidende netwerk nabij draineerbuizen werd mogelijk gemaakt door gebruik te maken van, door een computer berekende en getekende, stereoscopische afbeeldingen van dit netwerk **(Hoofdstuk 7)**.

2 BELANGRIJKSTE BEVINDINGEN

De belangrijkste bevindingen worden, voor elk deelonderzoek afzonderlijk, gepresenteerd.

Hoofdstuk 2 beschrijft de resultaten van analoge simulatie van minerale verstopping van omhullingsmaterialen in laboratoriumopstellingen. In cohesieloos "Almere" zand waren "dunne" omhullingsmaterialen (dikte < 1 mm) veel beter in staat om gronddeeltjes tegen te houden dan "volumineuze" materialen. Alle "dunne" materialen voldeden aan het Nederlandse criterium (ten hoogste 15 mm sediment in een 60 mm drain); de meeste "volumineuze" materialen voldeden daarentegen niet. De mate van inzanding in draineerbuizen was niet gerelateerd aan de gemiddelde poriegrootte van omhullingsmaterialen (D_{50}) noch aan de uniformiteitscoefficient van hun poriegrootteverdeling (D_{60}/D_{10}). De intreeweerstanden voor waterstroming waren meestal zo laag dat het ontwerp van drainagesystemen er niet door wordt beïnvloed. Niettemin is de betekenis van de resultaten voor het functioneren van zuigdrains in zwak-cohesieve gronden twijfelachtig. Deze analoge simulaties zijn weinig zinvol indien de resultaten niet worden bevestigd door veldwaarnemingen.

In de zwak-cohesieve gronden ("Lelystad", "Uithuizermeeden", "Willemstad" en "Valthermond") liepen de hydraulische eigenschappen en het vermogen van de omhullingsmaterialen om gronddeeltjes tegen te houden sterk uiteen. Het onderzoek toonde het volgende aan: a) "dunne" omhullingsmaterialen zijn beter in staat om gronddeeltjes tegen te houden dan "volumineuze" materialen; b) in het algemeen ontwikkelt zich in de rond de drains een zône met verhoogde hydraulische doorlatendheid, in het bijzonder wanneer "volumineuze" omhullingsmaterialen zijn toegepast, en c) er bestaat geen duidelijk verband tussen het vermogen van omhullingsmaterialen om gronddeeltjes tegen te houden en de karakteristieke poriegrootte (O_{90}) van deze materialen. Een zekere mate van inslibbing in de draineerbuis ging gepaard met een toename van de hydraulische doorlatendheid nabij de drain. Het effect van het soort omhullingsmateriaal ("dun" of "volumineus") en het grondmonster op de "Envelope Suitability Index" (ESI), een kwalitatieve geschiktheidsindicator voor omhullingsmaterialen waarin de hydraulische en de grondkerende eigenschappen van deze materialen werden ondergebracht, was veelal significant. Bij de grondmonsters "Lelystad" en "Valthermond" gaf toepassing van zowel "volumineuze" als "dunne" materialen betere resultaten dan drainage zonder omhullingsmateriaal. Bij grondmonsters "Uithuizermeeden" voldeden "dunne" omhullingsmaterialen significant beter dan "volumineuze" die op hun beurt significant beter voldeden dan drainage zonder omhullingsmateriaal. Bij proefnemingen, uitgevoerd met "Willemstad" bodemmateriaal werden geen significante verschillen gevonden, al waren er aanwijzingen dat drainage zonder omhullingsmateriaal wellicht mogelijk is en dat "volumineuze" materialen iets minder goed voldoen dan "dunne".

Hoofdstuk 3 toont de resultaten van waarnemingen, gedaan in de proefvelden "Uithuizermeeden", "Willemstad" en "Valthermond", naar het effect van omhullingsmaterialen en de (variabiliteit van de) helling van zuigdrains op de drainageweerstand, de hoogte van sliblagen in draineerbuizen, instroming van bodemmateriaal en wortelgroei in deze buizen. Vastgesteld is: a) de nauwkeurigheid van de helling van de zuigdrains was zeer groot en de variabiliteit van de helling in veruit de meeste gevallen zeer laag; b) noch het type omhullingsmateriaal ("dun" of "volumineus"), noch het soort omhullingsmateriaal had een significant effect op de totale drainageweerstand, zijnde de stromingsweerstand die het water ondervindt tussen punten waar het freatisch vlak het dichtst onder het maaiveld komt, en het inwendige van zuigdrains; c) indien drains gebruikt werden voor zowel ondergrondse irrigatie als drainage, verdienen "volumineuze" omhullingsmaterialen de voorkeur boven "dunne" omdat met zulke materialen beduidend lagere drainageweerstanden worden gerealiseerd; d) de slibhoogtes in draineerbuizen waren significant gecorreleerd met de karakteristieke poriegrootte (O_{90}) van omhullingsmaterialen en met het soort bodemmateriaal; e) het instromen van grond in draineerbuizen lijkt met meest voor te komen bij toepassing van omhullingsmaterialen, bestaande uit natuurlijke, organische grondstoffen, en f) grond wordt gewoonlijk in verzadigde toestand de draineerbuizen ingeperst; een mechanisme dat wezenlijk verschilt van het in analoge laboratoriumexperimenten waargenomen mechanisme waarbij het transport van afzonderlijke gronddeeltjes overheerst.

In **Hoofdstuk 4** wordt verslag gedaan van de ontwikkeling van een techniek en een procedure voor het steken van "ongestoorde" cylindervormige veldmonsters met een diameter van 200 mm en een lengte van 300 mm, bevattende secties van draineerbuizen met omringende grond. Deze monsters moesten onderzocht worden met behulp van een computertomograaf ("CT-scanner"). CT-analyse legt beperkingen op aan de geometrie en afmetingen van de monsters; deze werden proefondervindelijk vastgesteld. In de proefvelden "Uithuizermeeden", "Willemstad" en "Valthermond" werden 45 monsters gestoken, met 12 verschillende omhullingsmaterialen. De meeste omhullingsmaterialen werden vier maal bemonsterd. Ongestoorde bemonstering van drainsecties was niet eenvoudig, in het bijzonder bij hoge grondwaterstanden.

Hoofdstuk 5 beschrijft de resultaten van bepalingen van de korrelgrootteverdeling van grond vlakbij en in omhullingsmaterialen, afkomstig van de proefvelden "Uithuizermeeden", "Willemstad" en "Valthermond". Vaak wordt gesteld dat omhullingsmaterialen een significant effect hebben op de beweging van gronddeeltjes nabij draineerbuizen. De bevindingen zijn hiermee niet in overeenstemming. In zwak-cohesieve Nederlandse gronden heeft de korrelgrootteverdeling van de grond een significant effect; het omhullingsmateriaal niet. Kleine gronddeeltjes (≤ 30 μm) worden gemakkelijker door stromend water in beweging gebracht dan grotere. Eenmaal in suspensie worden zij hetzij elders in de grond tegengehouden dan wel in de draineerbuis gespoeld. Grotere deeltjes geraken moeilijker in suspensie en worden gewoonlijk in de grond nabij de draineerbuis tegengehouden. In sommige gevallen heeft de samenstelling van de grond nabij de draineerbuis zich ontwikkeld tot die van een grond met minimale porositeit. Het uitspoelen van fijne gronddeeltjes nabij een draineerbuis, een proces dat vaak wordt omschreven als de vorming van een "natuurlijk filter in de grond" en waarvan wordt aangenomen dat het regelmatig voorkomt, werd slechts incidenteel waargenomen; gewoonlijk verstopt de grond door het tegenhouden van elders in suspensie geraakte gronddeeltjes. Omhullingsmaterialen hebben een selectief filtrerende werking op uitspoelende gronddeeltjes. Niettemin is de grond in de zône rond de drain een veel fijner en belangrijker filter dan het omhullingsmateriaal, dat voornamelijk fungeert als een ondersteunende laag waarop de grond zich stabiliseert.

In **Hoofdstuk 6** worden onderzoekingen beschreven die werden uitgevoerd om het effect van een heterogene zône rond een vooromhulde draineerbuis en dat van verstopping van een omhullingsmateriaal op de werking van het drainagesysteem kwantitatief vast te stellen. De studie werd uitgevoerd met een tweedimensionaal (2D) eindige elementen model. De hydraulische doorlatendheid van het omhullingsmateriaal bleek het meest significante effect te hebben op de ontwaterende werking van een draineerbuis. Spoedig na de voltooiïng van dit onderzoek werd echter vastgesteld dat water, dat in de richting van draineerbuizen stroomt, in de onmiddelijke nabijheid van dergelijke buizen voornamelijk wordt aangevoerd via geometrisch ingewikkelde, driedimensionale (3D) structuren als horizontale bodemlaagjes en macroporiën. Daarom is een "traditionele" analyse van een dergelijke stroming, gebaseerd op 2D doorsneden niet toereikend; zij moet worden vervangen door een analyse in het driedimensionale (3D) en zeer heterogene domein rond de draineerbuis.

In **Hoofdstuk 7** wordt verslag gedaan van de resultaten van een kwantitatieve, driedimensionale (3D) analyse van de dichtheidsverdeling in de zône rond 45 secties van draineerbuizen, bemonsterd in proefvelden te "Uithuizermeeden", "Valthermond" en "Willemstad". De gegevens werden verzameld als reeksen van CT-beelden. Met deze methode kon de ruimtelijke verdeling van structuurkenmerken van de grond rond draineerbuizen worden vastgelegd en gekwantificeerd. De resultaten toonden: a) de levensduur van vooromhulde draineerbuizen wordt grotendeels bepaald door de structuur en de stabiliteit van de grond; b) de patronen van het vlakbij draineerbuizen stromende water en de patronen van verstopping van omhullingsmaterialen zijn in hoge mate heterogeen: de voornaamste watergeleidende structuren zijn de open ruimtes tussen bodemaggregaten, macroporiën, veroorzaakt door wormen en wortels, en dunne, relatief goed-doorlatende bodemlaagjes, en c) het effect van de eigenschappen van de grond op de wateropnamecapaciteit van draineerbuizen is aanzienlijk groter dan dat van de omhullingsmaterialen.

3 CONCLUSIES

Sedert de zestiger jaren zijn experimenten uitgevoerd, gericht op het ontwikkelen van criteria voor het ontwerp en de toepassing van goedkope omhullingsmaterialen voor draineerbuizen, bestemd voor landbouwkundige toepassingen. In de literatuur is uitgebreid gerapporteerd over een groot aantal veldexperimenten, laboratoriumexperimenten en wiskundige analyses. Langzamerhand werd echter steeds duidelijker dat vooruitgang goeddeels werd geblokkeerd door het ontbreken van veldgegevens over de onderhavige fysische processen. Aannames zouden alleen kunnen worden vervangen door feiten wanneer dergelijke gegevens beschikbaar zouden komen.

Klaarblijkelijk heeft men nooit stilgestaan bij het complexe karakter van de fysische processen welke zich in en nabij omhullingsmaterialen afspelen. Daarom heeft het verzamelen van gegevens te velde nooit de gewenste hoge prioriteit gekregen. Zo is de mate van inzanding in draineerbuizen zelden nauwkeurig waargenomen; resultaten van incidentele opgravingen werden geacht representatief te zijn voor grote drainlengtes. In het midden van de jaren tachtig stopte men met het waarnemen van drukhoogteverliezen nabij draineerbuizen omdat nauwkeurige waarneming te bewerkelijk en te duur werd gevonden. De metingen die verricht werden waren qua aantal ontoereikend, gegeven het heterogene stromingspatroon in de buurt van de buizen.

Met behulp van analoge modellen is veel observationeel onderzoek verricht, maar de resultaten zijn nooit goed vergeleken met veldwaarnemingen. In deze studie werd een dergelijke vergelijking voor het eerst gemaakt waarbij werd vastgesteld dat analoge modellen niet geschikt zijn wanneer men te maken heeft met zwak-cohesieve gronden. De redenen hiervoor zijn: a) het mechanisme van inzanding in draineerbuizen in het veld verschilt van hetgeen in analoge modelproeven wordt waargenomen; b) de afmetingen van de analoge modellen zijn te klein om de voornaamste watervoerende heterogeniteiten in de buurt van draineerbuizen volledig te kunnen omvatten, en c) de gecompliceerde wisselwerking tussen zwak-cohesieve gronden en omhullingsmaterialen is, zowel qua ruimte als qua tijd, in dergelijke modellen aan de waarneming onttrokken. Daarom mogen de resultaten van analoge modelproeven, uitgevoerd met zwak-cohesieve gronden, niet naar veldomstandigheden worden geëxtrapoleerd en moet aan de praktische waarde van dergelijke proefnemingen sterk worden getwijfeld. Voortzetting van analoge modelproeven is derhalve ongewenst.

Een andere complicerende factor is de houding ten opzichte van observationeel onderzoek in het veld en in het laboratorium. De neiging bestaat om dit onderzoek aan te wenden als instrument om heersende aannames bevestigd te krijgen. Zijn proefuitkomsten in overeenstemming met dergelijke aannames dan worden zij geaccepteerd; resultaten die dat niet zijn worden verworpen of genegeerd. Veldonderzoek waarvan de uitkomsten onduidelijk zijn omdat onderling sterk verschillende omhullingsmaterialen een vergelijkbaar effect hebben op de drainageweerstand worden zonder meer verworpen, niet alleen door fabrikanten maar ook door onderzoekers, terwijl uitkomsten, waarin verschillen tussen omhullingsmaterialen worden vastgesteld, doorgaans worden geaccepteerd. Tegelijkertijd wordt het effect van installatieomstandigheden op de levensduur van een drainagesysteem stelselmatig genegeerd, hoewel men zich van dit effect zeer wel bewust is.

De waargenomen korrelgrootteverdelingen van grond nabij de overgangszône met omhullingsmaterialen en de aanwezigheid van driedimensionale (3D) structuurkenmerken rond draineerbuizen indiceren dat de waterstroming rond deze buizen volgens sterk heterogene patronen verloopt. De stroming geschiedt grotendeels door gebieden met hoge hydraulische doorlatendheden zoals de ruimten tussen bodemaggregaten in de sleufvulling en via dunne bodemlaagjes en wortelgangen in de ongestoorde ondergrond. Er werd vastgesteld dat de onderzijde van de drainsleuf veel water geleidt naar de zijkanten van de draineerbuis; de sleufvulling boven de buis was daarentegen vaak verslempt en bijgevolg slecht doorlatend. Ten gevolge van de stromingsdruk van het water worden gronddeeltjes geërodeerd, gesuspendeerd en naar de drain gevoerd, waarbij de hydraulische doorlatendheid van die gedeelten van de grond via welke het water wordt aangevoerd, verder toeneemt. Tegelijkertijd neemt de reeds lagere hydraulische doorlatendheid van de overige gedeelten van de verzadigde grond verder af ten gevolge van verslemping en dispersie bij lage stroomsnelheden. Het is aannemelijk dat het spectrum van initiële hydraulische doorlatendheden met de tijd breder wordt, met een klein aantal goed-doorlatende zônes en daartussen grotere gebieden waar de stroming verwaarloosbaar klein is. Op slechts enkele plaatsen stroomt het water de omhullingsmaterialen binnen (de geleidende plaatsen) terwijl elders het overgangsgebied tussen grond en omhullingsmateriaal in hydraulisch opzicht nagenoeg inert is. Het effect van het type omhullingsmateriaal op de ontwikkeling van deze stromingspatronen lijkt vooralsnog gering.

Resultaten van onderzoekingen, verricht met tweedimensionale (2D) wiskundige modellen waarin de hydraulische eigenschappen van omhullingsmaterialen werden gerelateerd aan de dikte van deze materialen werden niet bevestigd door veldwaarnemingen. In het merendeel van deze modellen wordt aangenomen dat de grond en het omhullingsmateriaal homogeen en isotroop zijn. Soms wordt heterogeniteit verondersteld, maar dan slechts in radiale richting. In dergelijke modellen wordt geen rekening gehouden met de gecompliceerde, driedimensionale (3D) structuurkenmerken rond draineerbuizen, via welke het water grotendeels wordt afgevoerd. Dergelijke structuurkenmerken blijken grotendeels bepaald te worden door de grond. Daarom is de grond en niet het omhullingsmateriaal de beslissende factor bij de wisselwerking tussen beide media. De enige parameter van een omhullingsmateriaal die van belang is, is de karakteristieke poriegrootte (O_{90}). Voor het overige hebben omhullingsmaterialen weinig invloed op de ontwikkeling van de stromingspatronen van het grondwater rond draineerbuizen.

Uit deze resultaten komt de conclusie naar voren dat, tenminste voor drainagesystemen in zwak-cohesieve gronden, het onderzoek op het terrein van de drainage omhullingsmaterialen op foutieve concepten gebaseerd is geweest omdat de aandacht louter gericht was op specificaties van deze materialen terwijl de eigenschappen van gronden werden onderschat. Meer aandacht moet worden besteed aan de eigenschappen van de grond die niet in een laboratoriumopstelling maar alleen in het veld kunnen worden waargenomen.

In ieder drainagesysteem is de zône rond de draineerbuis van beslissende betekenis. Het succes van drainage is niet louter afhankelijk van het buistype en de toegepaste omhulling. "Drainage" is veeleer een produkt waarbij de installatie de fysische eigenschappen van deze zône bepaalt. Indien een aannemer de buizen onder ongunstige omstandigheden legt is de kans groot dat hij cruciale eigenschappen van deze zône, zoals de hydraulische doorlatendheid, in (zeer) ongunstige zin beïnvloedt. Betrokkenen zijn zich hiervan bewust, maar wanneer een drainagesysteem later slecht voldoet is het gebruikelijk om omhullingsmaterialen de schuld te geven in plaats van onjuiste installatiepraktijken.

4 BELANGRIJKSTE GEVOLGEN VOOR DE PRAKTIJK

De uitkomsten van deze onderzoekingen hebben een aantal, voor de praktijk relevante, gevolgen:

1. Indien de karakteristieke poriediameter van een omhullingsmateriaal, O_{90}, binnen passende waarden ligt (bij benadering 300 - 1000 µm), kan dit in de meeste gevallen worden gebruikt.

2. Het gebruik van "dunne" omhullingsmaterialen (dikte < 1 mm) wordt afgeraden indien drains incidenteel worden gebruikt voor ondergrondse irrigatie, indien er sprake is van verstoppingsgevaar dat samenhangt met grondwater dan wel met bodemprofielen met een hoog ijzergehalte, en bij de aanwezigheid van verstoppingsbronnen van microbiologische aard.

3. Draineerbuizen moeten met zorg worden geïnstalleerd, en alleen wanneer de vochttoestand van de grond zulks toelaat. Overigens is, na installatie, nauwgezet onderhoud (i.c. "doorspuiten" met middelbare waterdruk) veelal gewenst maar niet vanzelfsprekend. Bij risico van biochemische en/of ijzerverstopping van vooromhulde draineerbuizen kan regelmatig onderhoud een gunstige invloed hebben op de levensduur van een drainagesysteem.

4. Gebruik van analoge modellen om de toepasbaarheid van omhullings-

materialen in zwak-cohesieve gronden te kunnen vaststellen moet worden afgeraden.

5. Deugdelijke informatie omtrent het functioneren van omhullingsmaterialen wordt alleen verkregen door middel van nauwgezette waarneming van de ontwaterende werking van draineerbuizen, omwikkeld met potentieel geschikte omhullingsmaterialen in proefvelden. Daarbij moet worden aanvaard dat deze procedure duur en tijdrovend is.

6. Bij proefnemingen te velde moeten altijd draineerbuizen worden betrokken die niet zijn voorzien van een omhullingsmateriaal; de inrichting van dergelijke proefnemingen moet zodanig zijn dat de waarnemingen op deugdelijke wijze statistisch kunnen worden bewerkt.

5 RICHTLIJNEN VOOR TOEKOMSTIGE BENADERINGEN

Na vele jaren onderzoek is er veel bekend geworden omtrent het functioneren van omhullingsmaterialen in zwak-cohesieve Nederlandse gronden. Het onderzoek is echter beperkt gebleven tot drainagesystemen, geïnstalleerd op plaatsen waar geen sprake was van microbiologische- of ijzerverstopping. De resultaten van dit onderzoek zijn daarom niet van toepassing op dergelijke plaatsen omdat microbiologische- of ijzerverstopping meestal een permanente bedreiging vormt, wat voor omhullingsmateriaal er ook gebruikt wordt. De effecten van genoemde verstopping kunnen alleen worden beheerst door toepassing van "volumineuze" omhullingsmaterialen en regelmatig onderhoud.

Het functioneren van omhullingsmaterialen is regionaal gebonden. Ondanks het feit dat elders verkregen resultaten vergelijkbaar kunnen zijn is het niet gerechtvaardigd om resultaten van proefnemingen klakkeloos naar andere regio's te extrapoleren. Dit geldt ook voor drainagesystemen in aride gebieden die worden toegepast om in geïrrigeerde percelen verzilting van de bodem tegen te gaan. Ook in deze gevallen verdient proefveldonderzoek de voorkeur, waarbij onderzoekers moeten aanvaarden dat het zoeken naar geschikte omhullingsmaterialen tijdrovend en lastig kan zijn.

10 ANNEXES

Annex 1:	**Determination of pore size distributions of voluminous envelopes as water retention curves**
Annex 2:	**Results of observations, made with an analogue laboratory model, equipped with weakly-cohesive soils**
Annex 3:	**Core sampling tools & core sampling and sealing hardware**
Annex 4:	**Theoretical analysis of the hydraulic gradient near subsurface drain pipes**
Annex 5:	**The process of computerised tomography (CT) and the reconstruction of CT scan images**
Annex 6:	**Data handling and image processing**

Annex 1 Determination of pore size distributions of voluminous envelopes as water retention curves

The purpose of this Annex is to test the assumption that a moisture retention curve of a voluminous envelope material is identical to its pore size distribution. This assumption is questionable and was investigated by means of a simple computer model. Results are provisional but they support the idea that the assumption is not sound.

Determination of a moisture retention curve is a stochastic rather than a deterministic process because the spatial distribution of envelope pores cannot be described analytically. Stochastic simulations generate output as probability density functions reflecting the uncertainty of the output due to the non-deterministic nature of the system involved, which in our case consisted of pores in an envelope.

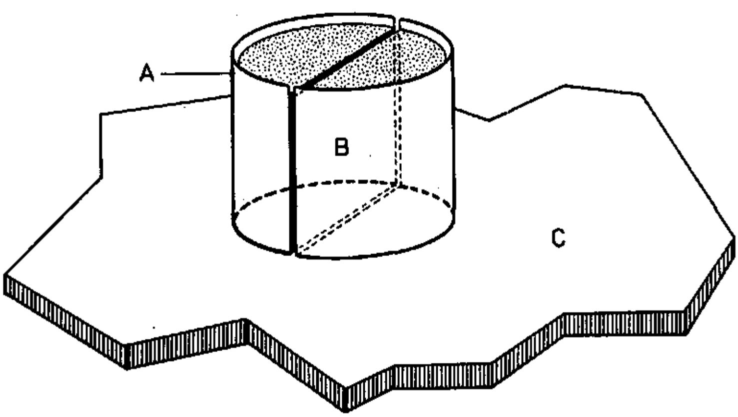

Figure 1. **A vertical cross-section through an envelope sample: A = sample, B = vertical cross-section, C = porous support plate.**

The modelling domain is a vertical cross-section through an envelope sample (Fig. 1), consisting of 1210 (min) to 24200 pores (max) with a known (input-)

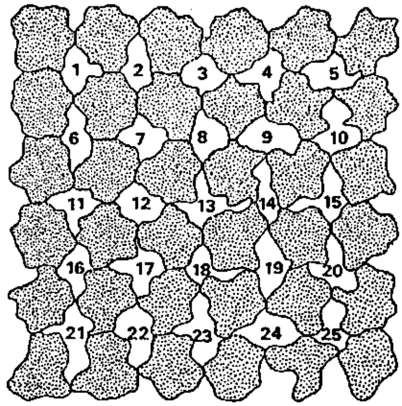

Figure 2. **Arbitrary area of the cross-section, depicted in Fig. 1. Pores have irregular shape and are labelled 1 to 25.**

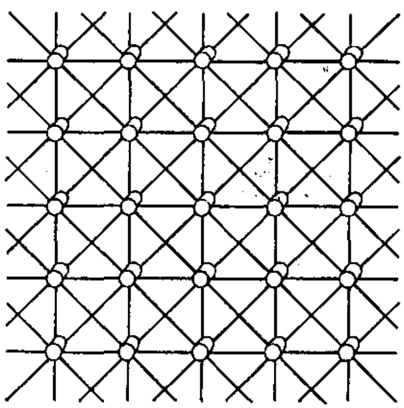

Figure 3. **"8-connectivity" between tubular pores in the cross-sectional model.**

pore size distribution. The pore size range is 10 - 2000 μm. A small part of this cross-section is shown schematically in Fig. 2. The model does not take into account differences in pore shape: all pores are considered to have a cylindrical shape and unit length. The pores are "*8-connected*": each pore is assumed to be physically connected with all its adjacent neighbours (Fig. 3). The cross-section is drained through the bottom. Air entry is possible through the upper side and (optional) through both vertical edges. Given an input pore size distribution, the model computes a corresponding moisture retention curve. It may also simulate hysteresis if a step-wise suction increase is followed by a decrease, but this is beyond the scope of this study (Stuyt, 1982).

Pore sizes of natural granular materials follow log normal probability density functions. Pore sizes of fibrous envelopes are assumed to be log normally distributed as well. The model accepts input of a pore size distribution of an envelope as a discrete, 20 class, log normal probability density function

$$P(i),\ i = 1, 2, ..., 20 \tag{1}$$

$$\text{where} \qquad P(i) \leq 1.0 \ \text{ and } \ \sum_{1}^{i} P(i) = 1.0 \ \text{ for all } i. \tag{2}$$

The average pore diameter d(i) [L] of class i is given by

$$d(i) = 10^{(1.15+0.11i)} \qquad (\mu m) \tag{3}$$

hence P(i) covers pore diameters ranging from 18 µm (d(1)) to 2232 µm (d(20)) which agrees with the range, found in voluminous drain envelopes. Assuming cylindrical pores with unit length, the relative frequency of pores n(i) in class i is calculated as

$$(p(i)\cdot d(i)^{-2}) \,/\, (\sum_{i} p(i)\cdot d(i)^{-2}) \tag{4}$$

$$\text{where } \sum_{i} n(i) = 1 \text{ and } i = 1, 2, ..., 20.$$

The median pore diameter, µ, and the standard deviation, σ, of n(i) are estimated. Next, N pseudo standard normal deviates are generated by the polar method following an algorithm by Box, Muller and Marsaglia (Knuth, 1969) where N equals the number of pores in the vertical cross-section. These standard normal deviates are converted into deviates belonging to a population following the discrete input log normal distribution, using the parameters µ and σ. Deviates beyond the size range 10 - 2000 µm are rejected and replaced by other deviates generated in an additional process. A typical set of generated pores in an envelope cross-section is schematically depicted in Fig. 4. From saturation, the water suction

$$pF(k) = {}^{10}\log(2960\cdot D(k)^{-1}) \tag{5}$$

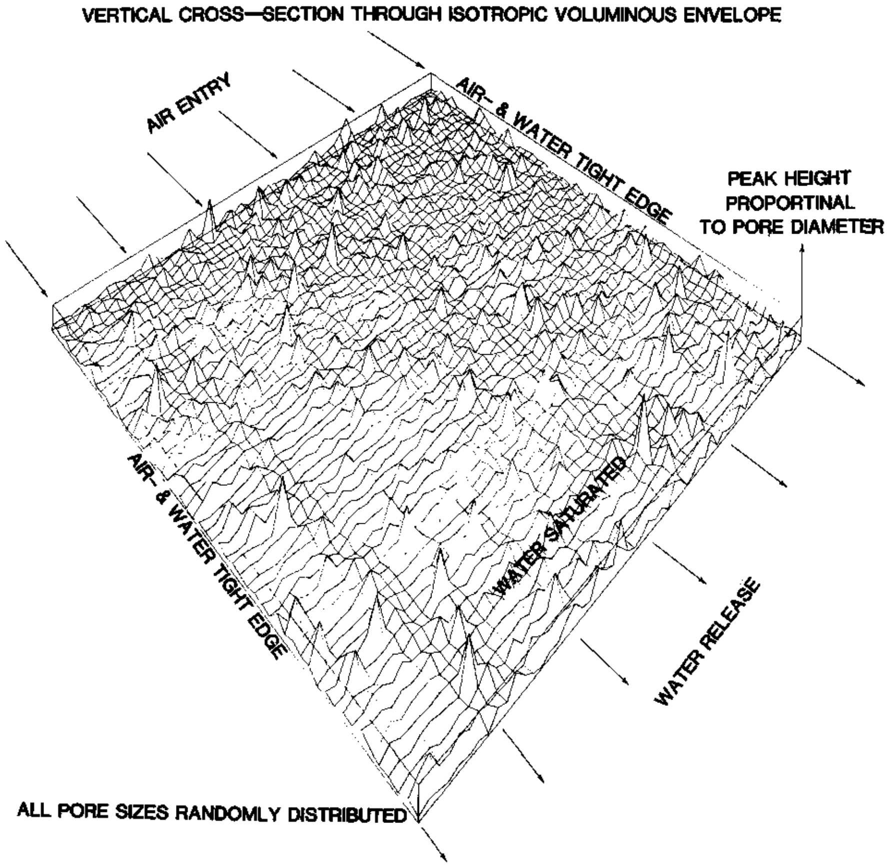

Figure 4. Schematic view of pore diameters, displayed as peak heights, generated from an input pore size distribution.

is increased in k=100 steps with f(D) = 1.00, 0.99, ..., 0.01, where D(k) is the pore diameter (μm), and f(D) is the cumulative log normal probability density function of the (generated) pores in the cross section.

At each suction pF (k), k = 1, 2, ..., 100, a point of the moisture retention curve is calculated by the following, heuristic procedure. The vertical cross-section, which is considered a two dimensional search space, is segmented into several classes, consisting of pores with similar properties.

A pore is considered "potentially drainable" at suction pF(k) if its diameter exceeds D(k) corresponding with the given suction pF(k). This does not mean, however, that it is actually drained, as will be explained later on. All pores with a potentially drainable diameter d(i,j), with

i = horizontal pore coordinate $1 \leq i \leq 440$

j = vertical pore coordinate $1 \leq j \leq 55$, where

j = 1 denotes pores which are adjacent to the glass sintered bottom plate

j = 55 denotes pores at the upper boundary of the envelope sample

at suction pF(k) are labelled $d_d(i,j)$. Potential drainability, however, will only lead to actual drainage if:

1. The pore is in contact with the bottom plate through a pathway of water-filled pores. If such contact is lacking, the isolated pore will continue to be filled with water at all higher suctions (evaporation is disregarded).

2. The pore is in contact with the atmosphere via a pathway of pores that have already emptied.

To simulate the **first** condition, *two dimensional region growing* is performed from the drainable pores which are connected with the bottom plate, $d_{dr}(i,1)$. Two dimensional region growing is the process of finding the set of all adjoining, labelled pores $d_{dr}(i,j)$ to the set $d_{dr}(i,1)$ from $d_d(i,j)$. In this search, each set pore $d_{dr}(i,j)$ is in turn used as a seed to find other adjoining pores from

$$d_d(I,J), \quad \text{where} \quad \begin{array}{l} I = i-1,\ i,\ i+1 \\ J = j-1,\ j,\ j+1 \end{array} \tag{6}$$

("8-connectivity"). In this region growing process, the vertical cross-section is alternately scanned in an upward and downward direction in as many cycles as necessary until no new pores are connected and the search has converged. Multi-directional scanning allows for geometrically complicated connected pore patterns to be detected. To simulate the **second** condition, an identical region growing process is started to find and label all the pores $d_{da}(i,j)$ which are 8-connected to empty pores as well as to pores which will drain at pF(k) and thus will be emptied themselves. Finally, all pores belonging to $d_{dr}(i,j)$ as well as to $d_{da}(i,j)$ are sampled as $d_{dra}(i,j)$. Because this subset obeys both con-ditions, its elements are assumed to be drained at pF(k). The number of pores and the released water volume are calculated. After completion of all suction increase steps, the volume of residual water is calculated from all saturated pores $d_{dr}(i,j)$. Simulated air breakthrough patterns for four suction steps are depicted in Fig. 5.

The model was run to evaluate the influence of envelope sample dimensions (diameter and height) and the corresponding varying air exchange boundary conditions on the simulated water retention curve. Four different sample diameters were considered (110, 220, 330 and 440 pores) and five sample heights (11, 22, 33, 44 and 55 pores). These dimensions were constrained by the computing time available in 1982. Starting from a suction at which 95% of the total pore space was still filled with water, the required suction increase to reduce this percentage to 20 was calculated. No repetitions of the computations were made.

Figure 5. Typical output of the model. Air penetrates downward into the envelope sample (four suction steps shown, increasing from top to bottom).

In Fig. 6, the influence of the sample height on the required suction increase is shown, for two cases: air-permeable sample edges (dashed line) and air-tight edges (continuous line). Both curves indicate that the required suction increase is inversely proportional to sample height. Apparently, when the water suction increases, the pattern of drained pores has more room to proceed growing in various directions in a relatively tall sample disc. Hence, the probability that a pore will be drained due to favourable air entry and outflow conditions is larger. If air can freely enter the vertical sample edges there is an increased risk of development of isolated clusters of pores filled with residual water due to the geometrically enhanced air entry area. Higher suctions are then needed to drain the sample out to 20% water-filled pores. In Fig. 7, the effect of the sample diameter is shown. No significant trend in required suction increase was found.

In Fig. 8, a typical simulated moisture retention curve is shown, together with the (discrete, 20 class) input pore size distribution and the corresponding continuous distribution. The number of generated pores was 24200. The generated pore size distribution is slightly offset from the input distribution due to the rejection of generated pores > 2000 µm. Still, this inaccuracy of the model does not affect the conclusion that the actual moisture retention curve is very different from the pore size distribution. The suction curve is much "steeper" than the generated pore size distribution curve and is located at much smaller pore diameters. This is mainly due to reduced air entry possibilities within a sample. The model also calculated the amount of residual water after completion of the determination of the retention curve (14%). This is not considered in the laboratory test. The simulated moisture retention curve (D_{60}/D_{10}=1.26) and the curves which were recorded on envelope sample discs with relatively large diameter pores in the laboratory show some similarity, cf. Fig. 15 on page 38.

The results must be considered qualitative rather than quantitative because

1. the model has not been calibrated,

2. the model was run only once for each case,

3. the model simulates a two dimensional cross-section only, leading to steep simulated moisture retention curves due to unrealistic, limited air entry possibilities,

4. modelled sample dimensions and the number of pores are small in comparison with real samples.

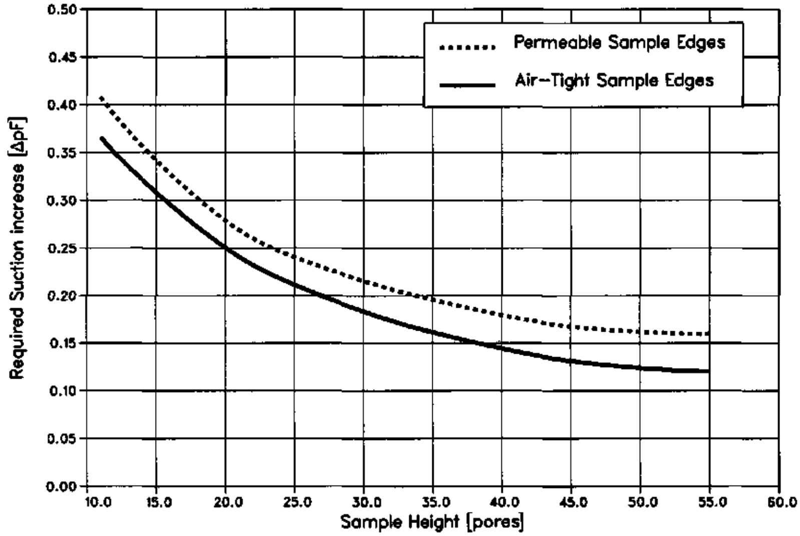

Figure 6. The influence of the height of an envelope sample disc on the suction increase required to lower the percentage of water-filled pore space from 95% to 20%.

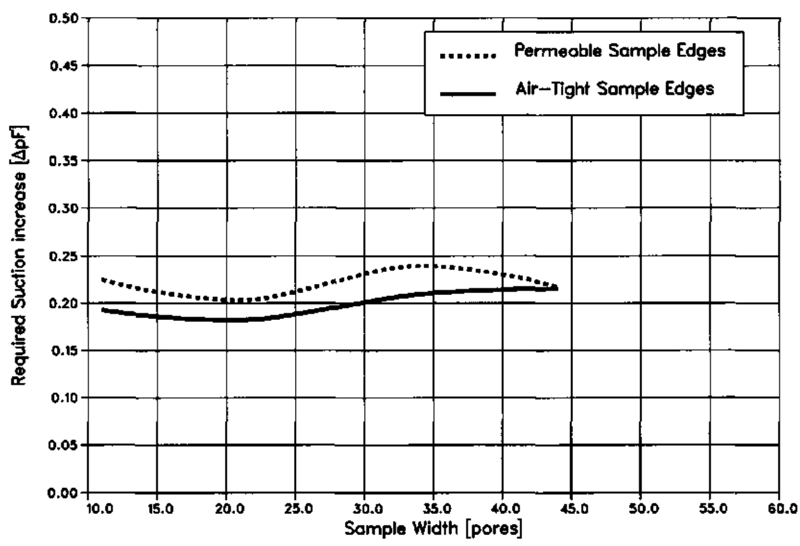

Figure 7. The influence of the width of an envelope sample disc on the suction increase required to lower the precentage of water-filled pore space from 95% to 20%.

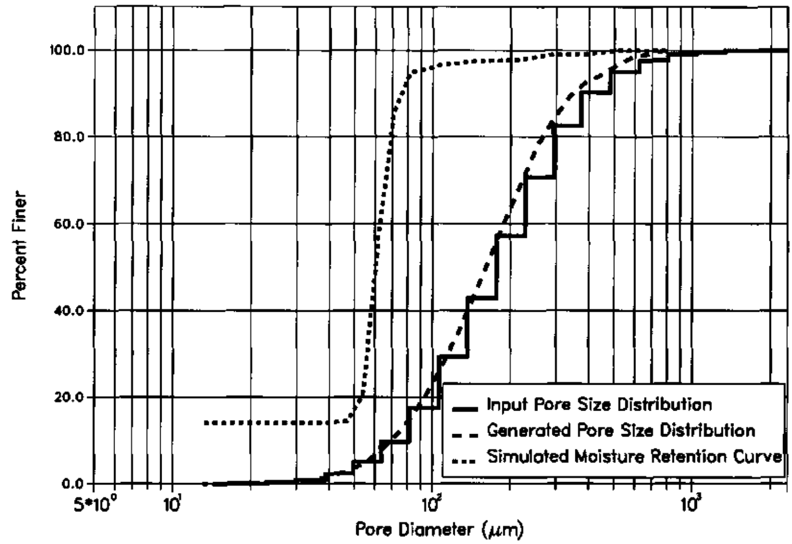

Figure 8. **Simulated moisture retention curve from input pore size distribution (see text).**

Still, there appears to be a fundamental and systematic difference between a pore size distribution curve and a corresponding moisture retention curve. Any retention curve is likely to be offset from the size distribution curve toward smaller pore diameters. The generally assumed relation between these curves is ill-defined and dependent on pore heterogeneity and sample dimensions. The extent of this problem can only be assessed after a thorough study with an improved, three-dimensional version of the model. Such a model could not be developed in 1982 due to limited computing power. Furthermore, such an investigation should be supported by other pore size distribution techniques like wet or dry sieving. In the meantime, the use of the "suction method" is not recommended. □

REFERENCES

Stuyt, L.C.P.M. 1982. Stochastische simulatie van de bepaling van een pF-curve van grofkorrelige materialen (Stochastic simulation of the determination of a suction curve of coarse-textured granular materials). Nota 1336, ICW, Wageningen, The Netherlands (in Dutch).

Knuth, D.E. 1969. The Art of Computer Programming. Vol. 2. Addison Wesley, pp. 105, 113.

Annex 2 Results of observations, made with an analogue laboratory model, equipped with weakly-cohesive soils

Estimated initial and ultimate hydraulic conductivities ($m.d^{-1}$), cumulative discharges during the flow tests (mm), equivalent sediment layer height in a 60 mm drain (mm) and Envelope Suitability Indexes (ESI)(-) (see Chapter 3).

No. Raw material or brand name	Soil sample	Flow Permeameter No.		
	1	2	3	4
1 Plain	Lelystad			
initial hydraulic conductivity ($m.d^{-1}$)	0.7	0.9	0.8	0.5
ultimate hydraulic conductivity ($m.d^{-1}$)	0.8	1.2	11.0	0.9
cumulative discharge (mm)	237	248	772	158
pipe deposit layer height (mm)	23.0	23.0	60.0	24.0
Envelope Suitability Index (ESI) (-)	1.74	1.76	1.22	1.53
2 Plain	Uithuizermeeden			
initial hydraulic conductivity ($m.d^{-1}$)	0.01	0.07	0.01	0.01
ultimate hydraulic conductivity ($m.d^{-1}$)	57.0	70.0	0.01	0.01
cumulative discharge (mm)	1840	2333	1	1
pipe deposit layer height (mm)	28.0	30.0	31.0	26.0
Envelope Suitability Index (ESI) (-)	2.48	2.53	-0.86	-0.72
3 Plain	Valthermond			
initial hydraulic conductivity ($m.d^{-1}$)	0.85	1.2	1.2	0.6
ultimate hydraulic conductivity ($m.d^{-1}$)	0.75	0.85	2.1	1.0
cumulative discharge (mm)	288	342	731	350
pipe deposit layer height (mm)	16.0	9.0	24.0	6.0
Envelope Suitability Index (ESI) (-)	2.01	2.28	2.20	2.38
4 Plain	Willemstad			
initial hydraulic conductivity ($m.d^{-1}$)	6.0	11.0	5.0	5.0
ultimate hydraulic conductivity ($m.d^{-1}$)	50.0	100.0	51.0	41.0
cumulative discharge (mm)	3663	4156	4096	3269
pipe deposit layer height (mm)	3.0	3.0	4.0	2.0
Envelope Suitability Index (ESI) (-)	3.48	3.53	3.50	3.46
5 Coconut fibres 750 $gr.m^{-2}$	Valthermond			
initial hydraulic conductivity ($m.d^{-1}$)	0.13	2.1	1.0	2.0
ultimate hydraulic conductivity ($m.d^{-1}$)	2.8	3.8	3.8	41.0
cumulative discharge (mm)	2411	3596	3218	6483
pipe deposit layer height (mm)	1.0	2.0	5.0	28.0
Envelope Suitability Index (ESI) (-)	3.35	3.50	3.37	3.08

No. Raw material or brand name	Soil sample	Flow Permeameter No.		
	1	2	3	4
6 Oltmanns polyprop/cocos mix	Lelystad			
initial hydraulic conductivity (m.d^{-1})	2.0	1 .3	900.0	2.7
ultimate hydraulic conductivity (m.d^{-1})	28.0	42.0	270.0	35.0
cumulative discharge (mm)	3617	2124	11179	2839
pipe deposit layer height (mm)	27.0	51.0	33.0	41.0
Envelope Suitability Index (ESI) (-)	2.81	1.91	3.13	2.31
7 Peat fibres "FL 86"	Valthermond			
initial hydraulic conductivity (m.d^{-1})	0.01	0.6	0.8	0.8
ultimate hydraulic conductivity (m.d^{-1})	1.0	1.3	3.0	1.0
cumulative discharge (mm)	1060	1398	2161	1346
pipe deposit layer height (mm)	0.1	0.1	0.1	0.1
Envelope Suitability Index (ESI) (-)	3.02	3.15	3.33	3.13
8 Peat fibres "Garden"	Uithuizermeeden			
initial hydraulic conductivity (m.d^{-1})	3.0	15.0	0.4	1.0
ultimate hydraulic conductivity (m.d^{-1})	3.3	22.0	13.0	6.1
cumulative discharge (mm)	506	1215	855	589
pipe deposit layer height (mm)	5.0	24.0	23.0	12.0
Envelope Suitability Index (ESI) (-)	2.57	2.42	2.29	2.44
9 Peat fibres "Flevo F"	Lelystad			
initial hydraulic conductivity (m.d^{-1})	0.8	2.0	1.7	0.1
ultimate hydraulic conductivity (m.d^{-1})	0.7	0.7	0.7	0.1
cumulative discharge (mm)	399	443	384	150
pipe deposit layer height (mm)	0.1	0.1	0.1	0.1
Envelope Suitability Index (ESI) (-)	2.60	2.65	2.58	2.18
10 Peat/Cocos mixture	Uithuizermeeden			
initial hydraulic conductivity (m.d^{-1})	8.0	0.01	32.0	13.0
ultimate hydraulic conductivity (m.d^{-1})	8.5	3.1	20.0	6.5
cumulative discharge (mm)	2269	1605	7497	2368
pipe deposit layer height (mm)	15.0	0.1	23.0	12.0
Envelope Suitability Index (ESI) (-)	2.94	3.21	3.24	3.04

No. Raw material or brand name	Soil sample	Flow Permeameter No.		
	1	2	3	4
11 "Polva"	Uithuizermeeden			
initial hydraulic conductivity (m.d^{-1})	0.01	0.01	0.01	10.0
ultimate hydraulic conductivity (m.d^{-1})	0.06	2.0	3.0	12.0
cumulative discharge (mm)	22	299	456	9010
pipe deposit layer height (mm)	4.0	19.0	11.0	25.0
Envelope Suitability Index (ESI) (-)	1.23	1.95	2.35	3.26
12 Polypropylene fibres "450"	Uithuizermeeden			
initial hydraulic conductivity (m.d^{-1})	0.01	40.0	0.01	0.01
ultimate hydraulic conductivity (m.d^{-1})	0.01	110.0	100.0	0.01
cumulative discharge (mm)	0	10126	7925	0
pipe deposit layer height (mm)	0.1	55.0	42.0	0
Envelope Suitability Index (ESI) (-)	0.00	2.48	2.73	0.00
13 Polypropylene fibres "700"	Valthermond			
initial hydraulic conductivity (m.d^{-1})	12.0	2.2	2.3	1.9
ultimate hydraulic conductivity (m.d-1)	*110.0*	*81.0*	*2.0*	*160.0*
cumulative discharge (mm)	10341	1371	682	4990
pipe deposit layer height (mm)	13.0	33.0	56.0	38.0
Envelope Suitability Index (ESI) (-)	3.65	2.22	1.28	2.64
14 Polypropylene f. "700"/5 mm	Valthermond			
initial hydraulic conductivity (m.d^{-1})	0.1	0.3	0.8	0.8
ultimate hydraulic conductivity (m.d^{-1})	105.0	12.0	4.8	88.0
cumulative discharge (mm)	3722	6808	1059	3122
pipe deposit layer height (mm)	34.0	53.0	0.1	37.0
Envelope Suitability Index (ESI) (-)	2.63	2.36	3.02	2.47
15 Polypropylene fibres "A"	Lelystad			
initial hydraulic conductivity (m.d^{-1})	1.0	1.6	1.0	1.0
ultimate hydraulic conductivity (m.d^{-1})	13.0	1.1	0.9	190.0
cumulative discharge (mm)	5863	1354	1098	8363
pipe deposit layer height (mm)	27.0	1.0	0.1	29.0
Envelope Suitability Index (ESI) (-)	3.02	3.10	3.04	3.12

No. Raw material or brand name	Soil sample	Flow Permeameter No.		
	1	2	3	4
16 Polypropylene fibres "B"	Lelystad			
initial hydraulic conductivity (m.d^{-1})	0.6	0.6	0.6	0.6
ultimate hydraulic conductivity (m.d^{-1})	1.8	2.3	2.3	2.0
cumulative discharge (mm)	2983	2953	3157	2827
pipe deposit layer height (mm)	1.0	0.1	2.0	2.0
Envelope Suitability Index (ESI) (-)	3.45	3.47	3.44	3.40
17 Polypropylene fibres "C"	Valthermond			
initial hydraulic conductivity (m.d^{-1})	0.2	0.5	0.3	0.01
ultimate hydraulic conductivity (m.d^{-1})	2.9	1.7	1.7	6.8
cumulative discharge (mm)	2505	1838	1854	5631
pipe deposit layer height (mm)	0.1	0.1	0.1	0.1
Envelope Suitability Index (ESI) (-)	3.40	3.26	3.27	3.75
18 "PSL"	Lelystad			
initial hydraulic conductivity (m.d^{-1})	52.0	60.0	70.0	210.0
ultimate hydraulic conductivity (m.d^{-1})	130.0	110.0	200.0	180.0
cumulative discharge (mm)	8855	9122	8294	8129
pipe deposit layer height (mm)	26.0	22.0	33.0	32.0
Envelope Suitability Index (ESI) (-)	3.22	3.35	3.00	3.02
19 "PSL"	Valthermond			
initial hydraulic conductivity (m.d^{-1})	1.2	0.7	1.2	1.0
ultimate hydraulic conductivity (m.d^{-1})	4.3	4.3	4.3	4.3
cumulative discharge (mm)	1417	1359	1310	1268
pipe deposit layer height (mm)	16.0	15.0	11.0	11.0
Envelope Suitability Index (ESI) (-)	2.71	2.72	2.81	2.80
20 "PSL"	Willemstad			
initial hydraulic conductivity (m.d^{-1})	40.0	60.0	40.0	60.0
ultimate hydraulic conductivity (m.d^{-1})	110.0	67.0	80.0	90.0
cumulative discharge (mm)	914	4769	6611	8944
pipe deposit layer height (mm)	7.0	24.0	35.0	19.0
Envelope Suitability Index (ESI) (-)	2.77	3.01	2.85	3.42

No. Raw material or brand name	Soil sample	Flow Permeameter No.		
	1	2	3	4
21 "PS-LDPE"	Lelystad			
initial hydraulic conductivity ($m.d^{-1}$)	15.0	1.3	1.3	1.3
ultimate hydraulic conductivity ($m.d^{-1}$)	7.0	5.5	2.8	2.3
cumulative discharge (mm)	2111	1528	964	1125
pipe deposit layer height (mm)	27.0	14.0	7.0	10.0
Envelope Suitability Index (ESI) (-)	2.57	2.80	2.79	2.77
22 "PS-LDPE" (winter 1986)	Valthermond			
initial hydraulic conductivity ($m.d^{-1}$)	0.01	0.01	0.01	0.01
ultimate hydraulic conductivity ($m.d^{-1}$)	0.3	0.9	2.7	0.1
cumulative discharge (mm)	211	379	1065	130
pipe deposit layer height (mm)	1.0	1.0	1.0	1.0
Envelope Suitability Index (ESI) (-)	2.30	2.55	3.00	2.09
23 "PS-LDPE" (spring 1987)	Valthermond			
initial hydraulic conductivity ($m.d^{-1}$)	5.0	7.0	6.5	6.0
ultimate hydraulic conductivity ($m.d^{-1}$)	2.1	3.4	22.0	3.0
cumulative discharge (mm)	1428	1923	4183	1732
pipe deposit layer height (mm)	60.0	60.0	60.0	9.0
Envelope Suitability Index (ESI) (-)	1.49	1.62	1.95	2.99
24 "PS-LDPE"	Uithuizermeeden			
initial hydraulic conductivity ($m.d^{-1}$)	52.0	0.01	0.01	32.0
ultimate hydraulic conductivity ($m.d^{-1}$)	120.0	0.01	73.0	102.0
cumulative discharge (mm)	10406	14	747	1013
pipe deposit layer height (mm)	26.0	0.1	25.0	39.0
Envelope Suitability Index (ESI) (-)	3.30	1.15	2.18	1.92
25 Acrylic fibres	Uithuizermeeden			
initial hydraulic conductivity ($m.d^{-1}$)	32.0	0.01	0.01	40.0
ultimate hydraulic conductivity ($m.d^{-1}$)	130.0	210.0	100.0	100.0
cumulative discharge (mm)	8399	7833	6014	6227
pipe deposit layer height (mm)	31.0	30.0	26.0	28.0
Envelope Suitability Index (ESI) (-)	3.06	3.06	3.17	3.02

No. Raw material or brand name	Soil sample	Flow Permeameter No.		
	1	2	3	4
26 "Big 'O'" standard 150 dtex	Valthermond			
initial hydraulic conductivity (m.d^{-1})	0.01	1.8	1.8	21.0
ultimate hydraulic conductivity (m.d^{-1})	0.5	1.0	52.0	20.0
cumulative discharge (mm)	288	840	1857	9411
pipe deposit layer height (mm)	0.1	0.1	25.0	24.0
Envelope Suitability Index (ESI) (-)	2.46	2.92	2.57	2.60
27 "Big 'O'" Heavy Pile #2	Uithuizermeeden			
initial hydraulic conductivity (m.d^{-1})	0.1	0.3	0.2	0.1
ultimate hydraulic conductivity (m.d^{-1})	18.0	2.1	52.0	2.1
cumulative discharge (mm)	2436	463	4652	399
pipe deposit layer height (mm)	16.0	8.0	14.0	4.0
Envelope Suitability Index (ESI) (-)	2.94	2.44	3.28	2.49
28 "Big 'O'" standard 150 dtex	Uithuizermeeden			
initial hydraulic conductivity (m.d^{-1})	0.8	1.1	2.0	1.1
ultimate hydraulic conductivity (m.d^{-1})	1.0	1.0	1.0	1.0
cumulative discharge (mm)	674	484	782	994
pipe deposit layer height (mm)	1.0	3.0	2.0	3.0
Envelope Suitability Index (ESI) (-)	2.80	2.60	2.84	2.91
29 "Cerex" (N-25)	Willemstad			
initial hydraulic conductivity (m.d^{-1})	27.0	12.0	7.0	23.0
ultimate hydraulic conductivity (m.d^{-1})	35.0	28.0	23.0	40.0
cumulative discharge (mm)	1350	1309	979	1298
pipe deposit layer height (mm)	0.1	0.1	0.1	0.1
Envelope Suitability Index (ESI) (-)	3.13	3.12	2.99	3.11
30 "Colback"	Lelystad			
initial hydraulic conductivity (m.d^{-1})	1.0	1.3	1.2	1.0
ultimate hydraulic conductivity (m.d^{-1})	1.1	1.1	1.3	1.5
cumulative discharge (mm)	618	689	803	834
pipe deposit layer height (mm)	0.1	0.1	0.1	0.1
Envelope Suitability Index (ESI) (-)	2.79	2.84	2.90	2.92

No. Raw material or brand name	Soil sample	Flow Permeameter No.		
	1	2	3	4
31 "Colbond" TSF 175	Willemstad			
initial hydraulic conductivity ($m.d^{-1}$)	0.15	0.6	0.5	0.5
ultimate hydraulic conductivity ($m.d^{-1}$)	11.0	51.0	95.0	51.0
cumulative discharge (mm)	2928	7004	9312	6364
pipe deposit layer height (mm)	7.0	14.0	17.0	8.0
Envelope Suitability Index (ESI) (-)	3.27	3.46	3.50	3.58
32 "Coltron"	Uithuizermeeden			
initial hydraulic conductivity ($m.d^{-1}$)	0.01	0.01	0.01	0.01
ultimate hydraulic conductivity ($m.d^{-1}$)	2.0	2.0	1.4	1.0
cumulative discharge (mm)	1109	1190	841	637
pipe deposit layer height (mm)	0.1	0.1	0.1	0.1
Envelope Suitability Index (ESI) (-)	3.04	3.08	2.92	2.80
33 Glass fibre sheet "Isover"	Willemstad			
initial hydraulic conductivity ($m.d^{-1}$)	6.0	10.0	8.0	9.0
ultimate hydraulic conductivity ($m.d^{-1}$)	28.0	36.0	12.0	59.0
cumulative discharge (mm)	2239	3035	2470	1905
pipe deposit layer height (mm)	0.1	0.1	0.1	0.1
Envelope Suitability Index (ESI) (-)	3.35	3.48	3.39	3.28
34 "Romian" fabric	Valthermond			
initial hydraulic conductivity ($m.d^{-1}$)	2.0	2.2	2.2	2.0
ultimate hydraulic conductivity ($m.d^{-1}$)	4.0	3.8	3.8	5.2
cumulative discharge (mm)	883	898	822	999
pipe deposit layer height (mm)	0.1	0.1	0.1	0.1
Envelope Suitability Index (ESI) (-)	2.95	2.95	2.91	3.00
35 "Typar" 3207	Valthermond			
initial hydraulic conductivity ($m.d^{-1}$)	0.01	1.1	0.8	0.8
ultimate hydraulic conductivity ($m.d^{-1}$)	10.0	2.7	2.9	4.0
cumulative discharge (mm)	2604	2613	2792	3459
pipe deposit layer height (mm)	31.0	0.1	0.1	0.1
Envelope Suitability Index (ESI) (-)	2.55	3.42	3.45	3.54

No. Raw material or brand name	Soil sample	Flow Permeameter No.		
	1	2	3	4
36 "Typar" 3267	Willemstad			
initial hydraulic conductivity (m.d^{-1})	6.0	15.0	10.0	13.0
ultimate hydraulic conductivity (m.d^{-1})	8.0	17.0	14.0	9.4
cumulative discharge (mm)	3286	4190	4224	2828
pipe deposit layer height (mm)	0.1	0.1	0.1	0.1
Envelope Suitability Index (ESI) (-)	3.52	3.62	3.63	3.45
37 "Typar" T-135	Lelystad			
initial hydraulic conductivity (m.d^{-1})	8.0	9.3	1.0	38.0
ultimate hydraulic conductivity (m.d^{-1})	2.0	0.7	0.7	2.0
cumulative discharge (mm)	1582	794	442	1950
pipe deposit layer height (mm)	0.1	1.0	0.1	6.0
Envelope Suitability Index (ESI) (-)	3.20	2.87	2.65	3.29

□

Annex 3 Core sampling tools & core sampling and sealing hardware

Readily available items, required for sampling of drain sections, were the following:

Core sampling tools: spade, hydraulic (oil) ram with extension sections hydraulic (oil) hand pump with steel support plate, a heavy duty hammer, a water baler, a spray can with lubricant, a measuring tape (short; 1 m), a heavy duty measuring tape (long; 15 m), a set of rubber stoppers of various diameters (55-65 mm), 2 spatulas, 2 sharp knifes, a steel brush, 2 small hacksaws, a water resistant level, at least 300 mm long. Optional: an electricity generator (petrol), a 5 litre jerrycan (petrol), a water resistant 500 w halogen lamp.

Core sampling and sealing hardware: adhesive water resistant tape, a portable gas burner and gas lighter, a pair of scissors, several water resistant markers, 2 clamps. Auxiliary: a four wheel barrow with wide pneumatic tyres, 45 sections of unperforated corrugated pipe, 2 m long and 90 pipe joints for repair of sampled drain sections and a note pad with water resistant plastic cover. □

Annex 4 Theoretical analysis of the hydraulic gradient near subsurface drain pipes

A drain may be likened to a horizontal well, hence there exists an analogy between radial flow toward a well and flow into a drain. If h [L] is the hydraulic head and R [L] the distance from the drain, the head about an "ideal" drain in a homogeneous and isotropic medium is given by

$$h = (q \cdot \ln R)/(2\pi \cdot k) \qquad (m) \qquad (1)$$

where
- h = hydraulic head (m)
- q = flow per unit length of drain ($m^2.d^{-1}$)
- k = hydraulic conductivity ($m.d^{-1}$)
- R = distance to the centre of the drain (m)

The hydraulic head loss, Δhr [L], is given by

$$\Delta h_r = (q/(2\pi \cdot k)) \ln (R.R_0^{-1}) \qquad R \geq R_0 \qquad (m) \qquad (2)$$

where
- Δh_r = hydraulic head loss (m)
- R = distance to the centre of the drain (m)
- R_0 = radius of the drain (m)

The hydraulic gradient is obtained through differentiation of the head loss with respect to the distance to the centre of the drain, R:

$$i = d\Delta h_r/dR = q/(2\pi \cdot k \cdot R) \qquad R \geq R_0 \qquad (-) \qquad (3)$$

□

Annex 5 The process of computerised tomography (CT) and the reconstruction of CT scan images

A CT scanner is a complicated instrument which measures density differences in a cross-section through a volume of material, ranging from 1½ to 12 mm in thickness, the CT scan or "slice". The suitability of CT in core analysis in this research is its non-destructive and non-invasive nature and its ability to view features near a drain in its natural surroundings. CT produces digital image data which are suitable for further processing, allowing for subsequent analyses related to the spatial distribution of soil and envelope density which are not provided by other means. In this annex, the fundamentals of CT are summarized. A thorough discussion of CT is found in Herman (1980).

For a homogeneous material of thickness D, Beer's law expresses the attenuated intensity I of a monoenergetic x-ray beam which is the intensity remaining after passing through this material in terms of the incident x-ray intensity I_0, (Fig. 1):

$$I = I_o \exp(-\mu D) \tag{1}$$

where μ is the average linear attenuation coefficient: the fractional decrease in x-ray intensity per unit length of material. It is the basic quantity measured in radiological imaging. The linear attenuation coefficient is determined by the atomic number (electron density) of the irradiated material, its packing density and the photon energy of the x-ray beam, expressed as x-ray tube voltage (80-140 kV typical) times anode current (10-300 mA typical). Application of eq. 1 to an x-ray beam passing through n elements of equal length d along a line of interest through an nonhomogeneous material like soil yields (Morgan and Phil, 1983):

$$I = I_0 \exp\left(-d \sum_{i=0}^{n} \mu_i\right) \tag{2}$$

This equation describes the x-ray attenuation rate in terms of a sum of small absorbances, where d determines the resolution in a CT image (Fig. 1). Estimation of the values of the attenuation coefficient μ_i in eq. 2 is the central concept of computerised tomography. The distribution of the attenuation coefficients in a two-

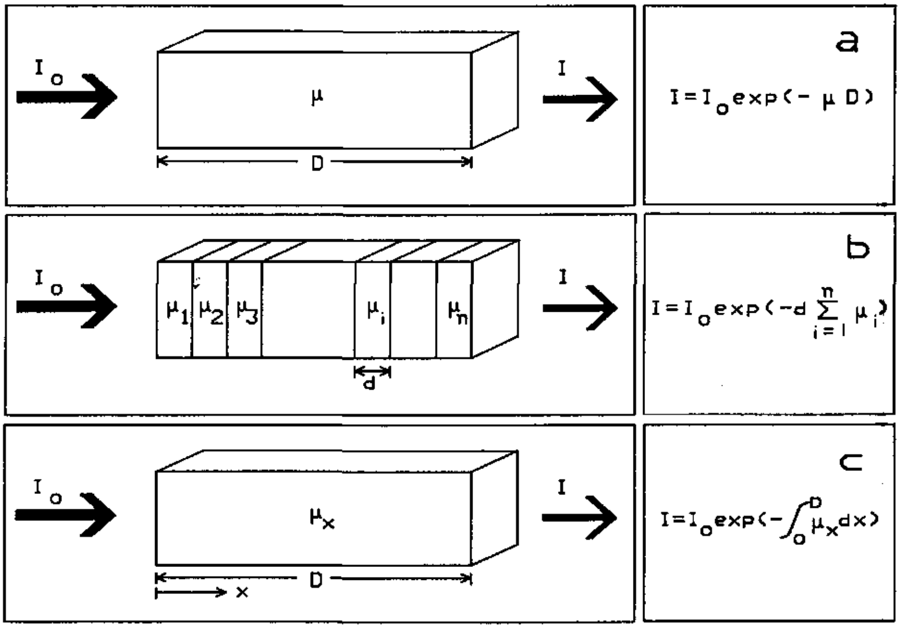

Figure 1. **Schematic representation of the attenuation of an x-ray beam of initial intensity I_0 through an object of thickness D and (a) a constant attenuation coefficient μ, (b) various attenuation coefficients μ_i for discrete units of thickness d, and (c) an attenuation coefficient μ_x which varies with distance from the x-ray source, x (after Anderson et al., 1988).**

dimensional area of interest or cross-section through an object cannot be estimated when only a single beam is attenuated and monitored, yet if many beams are passed through a sample at various angles (0-180°), the distribution of the density within a soil core can be determined or "reconstructed" at discrete points (Fig. 2). In order to reconstruct a CT image, many thousands of x-ray measurements must be made.

Usually, knowledge of the distributions of linear attenuation coefficients in an object is not the desired end product in using CT. Instead, information about the density distribution is required. In soils, this information is obtained by using an empirical relationship between the linear attenuation coefficients and a parameter of interest, soil macroporosity (Phogat & Aylmore, 1989).

The local region of interest in a CT scan is often called a "voxel" ΔV: the

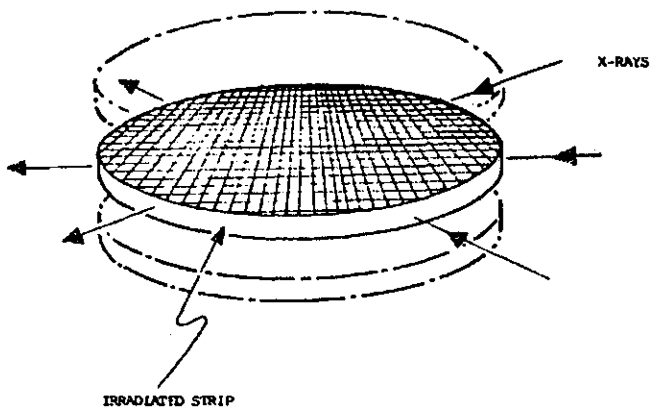

Figure 2. **Paths of x-rays are confined to a slice and pass through the imaginary elements ("voxels") of a mesh in straight lines (after Hounsfield, 1980).**

volume element represented by the product of the matrix of pixel size in the slice, $\Delta x \Delta y$, times Δz, the slice thickness, ($\Delta V = \Delta x \Delta y \Delta z$). An imaged slice consists of an n x n matrix of voxels. For multi-component voxels, i.e., containing mineral particles, pores and water, electron densities of each component are weighed by its volume fraction (*partial volume effect*). Thus the composition and density of the material(s) in a voxel will determine its linear attenuation coefficient. The average linear attenuation of x-rays in a voxel is commonly expressed as a so-called CT number or Hounsfield unit (H.U.). Hounsfield units range from -1000 to over 3000. By definition, the CT number of air is -1000 and the CT number of water is zero. The measured linear attenuation coefficient, μ, is normalized to that of water so that each CT number or Hounsfield Unit is equivalent to 0.1% of the attenuation of water (Crestana et al., 1986):

$$\text{CT number} = (\mu_{\text{material}} - \mu_{\text{water}})/(\mu_{\text{water}}) \cdot 1000 \qquad (3)$$

CT numbers (H.U.) of soils range from 500 to 2200. The response of a CT scanner to increasing density in glass-bead spheres and soils is linear (Fig. 3).

In brief, the process of CT consists of four consecutive steps:

1. **X-ray production.** An x-ray tube radiates the x-ray beam which has the shape a narrow fan and this determines the plane ("slice") of the CT image.

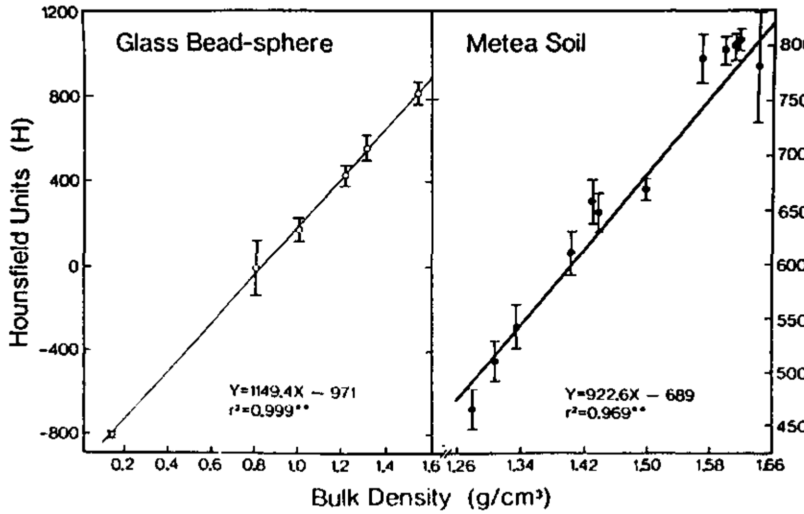

Figure 3. **The influence of increasing bulk density of a soil and glass-bead spheres on CT numbers or Hounsfield Units (H.U.) (after Petrovic et al., 1982).**

2. **Data acquisition.** Many detectors collect x-ray attenuation data along discrete lines through the slice. These measurements are referred to as projection data. During scanning, the x-ray source and detectors rotate about the object of interest, allowing acquisition of projection data along many lines from different directions.

3. **Image reconstruction.** This step involves estimation of the attenuation coefficients for all the imaginary volume elements in the slice along the lines between the x-ray source and the detector. Radon (1917) developed the mathematical foundations for image reconstruction from projection data.

4. **Image display and processing.** Images are displayed at the operator's console while scanning, and are written onto tape. Further processing is done on remote systems, i.e. on a VAX mainframe computer and a Silicon Graphics "*Personal Iris*" 3D graphics workstation.

The CT scanner used in this study is a third generation (rotate/rotate) Philips Tomoscan 350 with the following specifications or machine settings. Fan angle: 43.2 degrees, 576 Xenon ionization detectors, slice thickness: 3 mm, slice pitch: 3 mm, yoke rotation: 440 degrees, scan angle: 360 degrees, scan time: 9.6 seconds, x-ray generation: 120 kV, pulse width: 2 ms (typical), pulse repetition rate: 125/s, number of pulses or projections: 1200, number of measurements: 691200, reconstruction algorithm: filtered back-projection, reconstructed field of view: 220 mm, image reconstruction matrix: 256 x 256 pixels, pictorial resolution in the scanning plane: 0.86 mm, attenuation scale: -1000 to +3095 Hounsfield units, computer: Philips P857-128k16, image processing: array processor, data storage: 1600 BPI data density magnetic tape unit, ½ in., 9 track IBM and ANSI compatible.

The Tomoscan 350 has a "variable geometric enlargement" feature: the reconstructed "field of view" may be adjusted to the size of the scanned object such that the full x-ray beam width and hence the full range of detector channels are used. This feature was used to "enlarge" the cross-sectional images to the maximum possible size, allowing most of the set number of pixels in the reconstructed image to be occupied by the sample rather than by the plexiglass rims and the air surrounding it, resulting in maximum possible pictorial spatial resolution. □

REFERENCES

Anderson, S.H. and C.J. Gantzer. 1989. Determination of soil water content by X-ray computed tomography and magnetic resonance imaging. Irrig. Sci 10:63-71.

Crestana, S., R. Cesareo and S. Mascarenhas. 1986. Using a Computed Tomography Miniscanner in Soil Science. Soil Sci. 142 1:56-61.

Herman, G.T. 1980. Image Reconstruction from Projections, the Fundamentals of Computerized Tomography. Computer Science and Applied Mathematics, A series of Monographs and Textbooks. Academic Press, New York, N.Y.

Hounsfield, G.N. 1980. Computed medical imaging. Med. Phys. 7(4)283-290, Jul./Aug. 1980.

Morgan, C.L. and M. Phil. 1983. Basic principles of computed tomography. University Park Press, Baltimore, USA, 342 pp.

Petrovic, A.M., J.E. Siebert and P.E. Rieke. 1982. Soil bulk density analysis in three dimensions by computed tomography scanning. Soil Sci. Soc. Amer. Journ. 46(3): 445-450.

Phogat, V.K. and L.A.G. Aylmore. 1989. Evaluation of Soil Structure by using

Computer Assisted Tomography. Aust. J. Soil. Res. 27:313-323.
Radon, J. 1917. Ueber die Bestimmung von Funktionen durch ihre Integralwerte langs gewisser Mannigfaltigkeiten (About the determination of functions through their integrated values along various directions). Ber. Verb. Saechs. Akad. Wiss., Leipzig, Math. Phys. Kl. (69) 262-277 (in German).

Annex 6 Data handling and image processing

CT Examination of each sample produced 53 images (50 scans through the sample, 2 scans through the reference disc and one lateral scanogram (="traditional type" x-ray image covering the entire core, produced for reference purposes) that were recorded onto ½ in. magnetic tape in the scanning laboratory. A multi-imager supplied 50 of the 53 images on 8 x 10 in. film format. Data on tape were encoded in 12 bit figures as (Hounsfield unit + 1000), and ranged from 0 to 4095. The images were written in "T350" format and were only readable on Tomoscan "stand alone" viewing consoles and -systems. The "Scanner Science CT (SSCT)" unit of Philips Medical Systems, Best, The Netherlands provided VAX/VMS compatible software which reads "T350" formatted images from tape and converts these into unformatted 16-bit encoded sequential data files in 512 byte records. This software was run on a VAX 750 computer. Neither image ID's nor headers are converted, however, so all (14) tapes were scanned for this information separately (VAX/VMS "dump" program). Not all the required information could be recovered in this way. Most of the remaining data was printed in the single image display layouts that were provided on film. The contents of the tapes could be recovered only by combining data produced by the "dump" program, printed on film and the files produced by the Philips software together. The converted image files were stored on 3 tapes (6250 BPI data density). A series of 50 images requires 6.4Mbyte of storage (16-bit).

The data of each core were sequentially processed on two computer systems: a VAX 3600 and a Personal Iris 4D/20 Workstation by Silicon Graphics, basically designed for visual computing purposes (10 mips, 0.9 mflops, 760 Mbyte disk, IRIX operating system). The reason for processing data on two computers was that the Personal Iris was not yet available when processing started. Both systems were linked to an ethernet system. A software package, written in FORTRAN-77 was developed for image processing on the VAX while processing on the Personal Iris was done almost exclusively through commercially available 3D software, written in C.

The software, running on the VAX, performed the following 2D and 3D image processing tasks:

1. *Print 2D CT scan images* on non-graphical devices like a TTY screen or a

printer,

2. *Remove image artifacts* caused by Compton scatter,

3. *Perform calculations*, described in sections 3.2 (recognition and quantification of pipe and envelope parameters), 3.3 (determination of regions of interest) and 3.4 (sampling of macroporosity statistics near the drain) of Chapter 7,

4. Perform 2D geometric *image transformation*,

5. *Convert image data* and *create image disk files.*

These processing tasks are discussed below.

1. Print CT-images on a TTY screen or a printer

When processing of images was needed, no image processing computer system was available. Because a fast way of viewing images was required for software development, an algorithm was developed which plots a CT image on a alphanumeric terminal screen or provides a hardcopy plot on a printer. The image is proportionally resized from 256 to 20-130 columns and from 256 to 20-80 rows through 2D interpolation of pixel values. Window width settings are selected in the range -1000 to +2200 Hounsfield units. Grey values are printed as 10 alphanumeric characters. Image processing information like geometric image segmentation boundaries is superimposed in reverse grey values (Fig. 1). The remainder of the 2D software which runs on VAX/VMS was developed exclusively with this display facility.

2. Remove image artifacts caused by Compton scatter

In computerised tomography, scans are calculated from projection data of the attenuation of x-rays, measured in a number of different directions. Errors occurring in the measurements may therefore spread out over a large part of the reconstructed images in an intricate manner, yielding image artifacts, particularly if errors are data-dependent as is the case with photon scatter. Image artifacts will seriously affect image analysis results and must therefore be removed.

Ray-paths of x-ray photons are assumed to be straight lines. In practice, a path

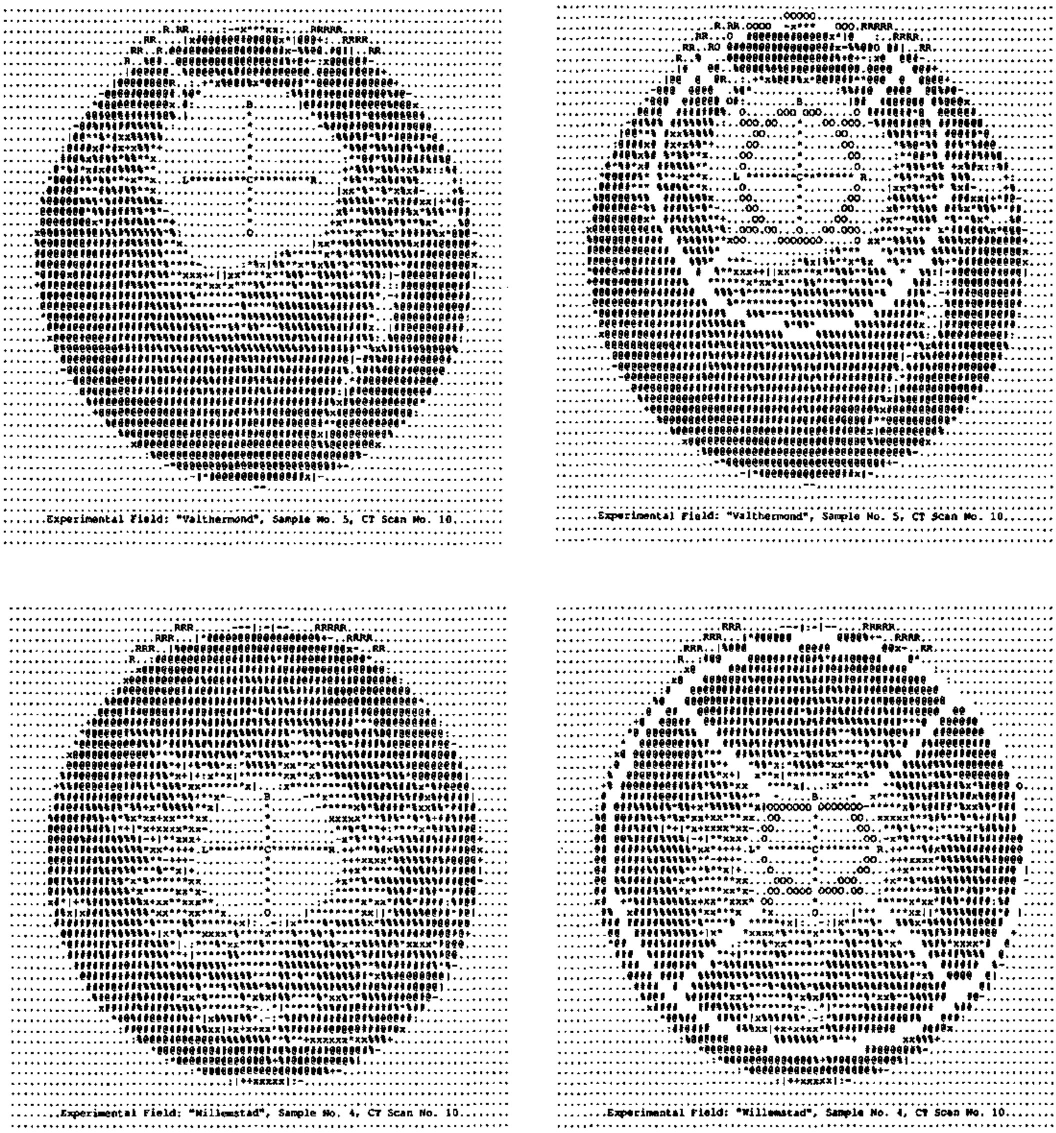

Figure 1. **Examples of CT images, printed as line printer output with and without 2D areas of interest. Top: sample No. V05 from "Valthermond" and bottom: sample No. W04 from "Willemstad". These images have not been corrected for Compton scatter, hence soil density at the sample rims appears higher than near the drain ("cupping" effect).**

of a photon may be altered while it traverses an object due to interactions with matter (i.e. electrons) in such objects. This mechanism is known as Compton scattering. As a result, a substantial scatter flux may exit from the core sample with photon trajectories nearly parallel to the primary beam. This leads to an inadequacy of measurements because scattered or secondary photons are registered along with primary photons causing distortions of the reconstructed images. These distortions are generally referred to as reconstruction artifacts. Compton scatter artifacts are similar in nature to polychromaticy ("beam hardening") artifacts (Herman, 1980). The Compton scatter artifact in the drainage sample cores consists of a lowering of density values in the central area of images, producing a "cupping" effect (Fig. 2). This artifact was found in all images and correction was required afterwards.

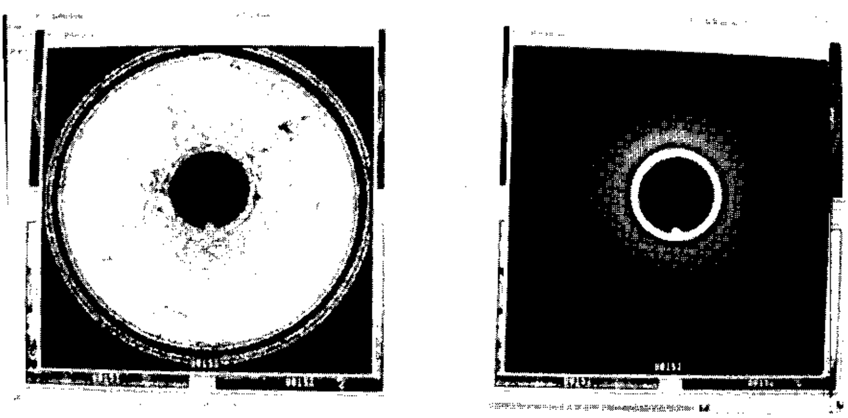

Figure 2. **Examples of image artifacts, caused by "Compton" scatter. Images appear brighter near the sample core edges (left). The image artifact is maximum near the drain (maximum brightness) (right).**

Glover (1982) found that reconstruction artifacts caused by Compton scatter are reduced by self-attenuation of scattered photons near the centre of scanned objects. In the drainage samples, however, the rate of self-absorption of scattered photons near the centre of the objects is low because of the air-filled drain.

The fundamentals of the scatter correction, applied in this study, are summarized as follows. Philips Medical Systems have removed scatter artifacts from one representative CT slice, $ri_{PH}(i,j)$, of each set of 50 slices, yielding a matching corrected slice, $ci_{PH}(i,j)$. The remaining slices, ($ri_n(i,j)$, n=1, ..., 49) were corrected by an approximative procedure, based on a linear regression analysis of Hounsfield values in the corrected slice, $ci_{PH}(i,j)$, and the matching uncorrected one, $ri_{PH}(i,j)$, yielding a series of approximatively corrected CT slices ($ci_n(i,j)$, n=1, ..., 49).

Visual comparison of an uncorrected CT scan with a corrected one suggested that the image artifact was maximum near the pipe wall and decreased in outward direction with radial symmetry. Hence, it was decided to correct the n CT scans in *k adjacent, concentric, circular regions of interest* $csc_{n,k}(i,j)$ in $ri_n(i,j)$ and $ci_n(i,j)$ with centres $(i_{0,n},j_{0,n})$ and radii r_k:

$$(i-i_{0,n})^2 + (j-j_{0,n})^2 - r_k^2 = 0 \qquad (1)$$

where n = sequence number of the CT scan, and

$$r_k=25+k,\ k=0,1,2,\ ...,\ k_{max} \qquad \text{(pixels)} \quad (2)$$

In (5), k_{max} is the shortest perpendicular distance from $(i_{0,n},j_{0,n})$ to the inside edge of the rim of the plexiglass sample core container. It is found from the perimeter of the smallest possible circle $csc_{n,k}(i,j)$ which "touches" this edge, i.e. the perimeter of the circle $csc_{n,k}(i,j)$ with the shortest possible radius (25+k) which traverses at least 15 consecutive pixel values ≤ -700 Hounsfield Units. The number of rows and columns in the correctable area of a CT slice was limited due to the lateral displacement of $(i_{0,n},j_{0,n})$ in this slice relative to the centre of the regions of interest in ri_{PH} and ci_{PH}, $(i_{0,c},j_{0,c})$. Subject to this limitation, corrections were made to the values of all pixels in the circular regions of interest $csc_{n,k}(i,j)$ in $ri_{n,k}$ (i,j):

$$(i-i_{0,n})^2 + (j-j_{0,n})^2 - r_k^2 = 0, \qquad r_k=25,r_{corr} \qquad (3)$$

where $r_{corr}=k_{max}-6$, such that each pixel value in circular region (1) is replaced by a corrected value with linear regression parameters

$$A_k,\ B_k,\ k = 25,r_{corr} \qquad (4)$$

which are computed from all pixels in the circular regions of interest

$$(i-i_0)^2 + (j-j_0)^2 - r_{reg}^2 = 0, \qquad r_{reg} = r_{k-2}, ...,r_{k+2} \qquad (5)$$

in the representative image, $ri_{PH}(i,j)$ and the matching regions in the corrected image, $ci_{PH}(i,j)$.

3. Perform geometric image transformation

Visual perception of internal soil erosion patterns near pipe drains and mineral clogging patterns inside voluminous envelopes is hindered because of the elliptic cylindrical shape of the drain. Not a single orientation in 3D space allows for global visual examination because some areas will be hidden, regardless the position of the eye. As a result, dynamic images like rotational sequences must be used to fully perceive filter clogging features and internal erosion patterns around pipe drains. To be able to examine these features and patterns from still pictures, the coordinates of the elliptic regions of interest ($ep(x,y)$, $1 \leq x \leq 256$, $1 \leq y \leq 256$) in an original CT image are geometrically transformed or mapped into coordinates, located on horizontal lines in a transformed image ($tep(u,v)$, $1 \leq u \leq 256$, $1 \leq v \leq 256$) in the uv plane. The *smallest* elliptical area of interest, covering an interior pipe area near the pipe wall (A-B-C-D-A) is *rectified and magnified into the bottom section* of the uv plane. The *largest* elliptical area of interest (E-F-G-H-E) is *rectified and reduced into the top section* of the uv plane (Fig. 3). All other regions of interest are mapped accordingly (Fig. 4).

In 3D space, a series of 50 transformed images combine into a transformed object space in which the envelope is basically flat and can be globally examined. Notwithstanding serious image deformation, judgement of mineral clogging and internal erosion features is made easier provided that adequate captions are included to elucidate the geometry of the transformed images (Fig. 5).

4. Convert image data and create image disk files

Processed image files are saved on disk in two file formats.

1. A format which is supported by 2D image processing software "TCL-Image" (TNO, 1988).

   The first 32 words of "TCL-Image" files are used as file headers and contain information about the data in the file (pixel encoding, sample etc.). Pixel values of "TCL-Image" files are scaled from Hounsfield Units (-1000 - +2200) to a lower gray scale resolution (256 gray values) because this software is used for point operations like contrast stretch and histogram equalisation which require the pixel values to range from 0 to 255.

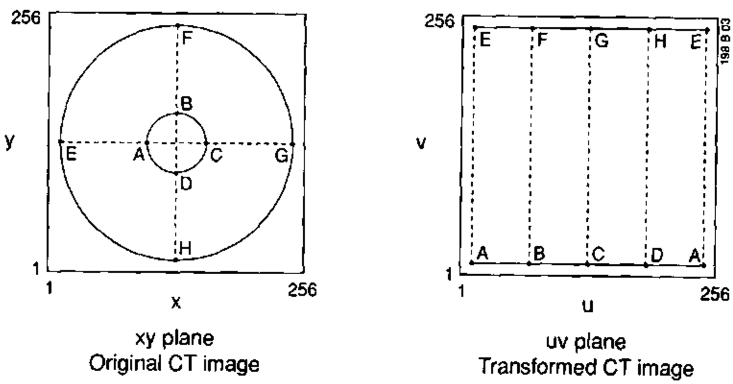

Figure 3. **Principle of geometric image transformation. Original image (left) and matching transformed image (right).**

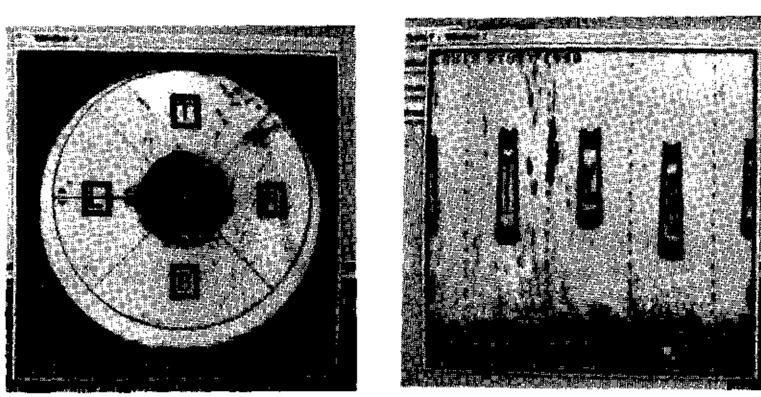

Figure 4. **Example of geometric image transformation. Original image (left) and matching transformed image (right).**

2. A format, required for subsequent 3D image processing, supported by medical image processing software "Analyze" (Robb & Barillot, 1989; Mayo Foundation, 1989[1]).

"Analyze" files do not contain header information; instead, separate header files must be created. Voxel values are not rescaled but "byte swapping" (exchange of low and high bytes) of the 16-bit encoded voxel data was required.

Computational efficiency. Processing image data from one sample took 18 hours CPU on average on a VAX 3600 computer, ranging from 13 hours to 22 hours CPU, depending on the size of the examined area of interest around the drain. While these times are given for the sake of completeness, they must not be taken too seriously. The framework of computer programs was designed for experimental use and hence was not by necessity as efficient as individual programs specially written for specific tasks. Thus the absolute values of computer times may be misleading.

5. 3D image processing (Personal Iris)

Contemporary image processing tools are used for (a) display of 3D data ("*3D Imaging*") and (b) calculations in the regions of interest that are segmented from the 3D space ("*visual computing*").

1. **3D Imaging.** The 3D data from CT are displayed in a way closely related to natural perception. 3D imaging provides tools for a natural way of looking at objects, minimizing the risk that useful information is missed, particularly in the case of geometrically complex features as found in soils and clogged envelopes around drains. The size, location, shape and orientation of features in these media, as well as their mutual relationships, are visualized in a comprehensive and natural way. 3D imaging cannot replace information provided by individual CT scan images; rather it supplements it with information on aspects that are otherwise less or not obvious. In this study, a multidimensional biomedical image display and analysis software package, called "Analyze", was used for 3D imaging (Robb & Barillot, 1989).

---

[1]ANALYZE Copyright © 1986-1991, Biotechnology Computer Resource, Mayo Foundation, Minnesota, USA.

2. **Visual Computing**. The "Analyze" software was used to perform three-dimensional region growing which is the main component of the calculation of the water acceptance of drains; see section 3.5.3 of Chapter 7.

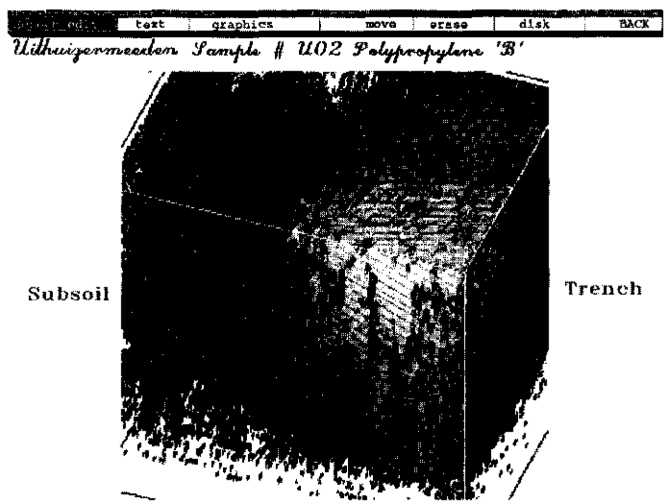

Figure 5. **Example of a transformed 3D image. The envelope is located in the bottom of the cube. Its voxels are not displayed at the chosen density window which is optimized to depict subtle density differences in the soil. In this sample, the density of the greater part of the trench backfill (bright colour; right side of the cube) exceeds that of the subsoil (darker; left side).**

REFERENCES

Herman, G.T. 1980. Image Reconstruction from Projections, the Fundamentals of Computerized Tomography. Computer Science and Applied Mathematics, A series of Monographs and Textbooks. Academic Press, New York, N.Y.

Hunt, P.K. and P. Engler. 1987. Computed Tomography as a Core Analysis Tool: applications and Artifact Reduction Techniques. Soc. Petrol. Engin. SPE 16952. Dallas, Sept. 27-30, 8 pp.

Mayo Foundation, 1989. Analyze User's Manual. Mayo Medical Ventures (Mayo

Foundation for medical education and research, Rochester, Minnesota 55905 USA.

Robb, R.A. and C. Barillot. 1989. Interactive Display and Analysis of 3-D Medical Images. IEEE Transact. on Medical Imaging 8(3):217-226.

TNO, 1988. TCL-Image User's Manual. Multihouse TSI BV/TNO Institute of Applied Physics, Delft, The Netherlands.

LIST OF USED SYMBOLS

Symbol	Interpretation	Units	Dimension
A	■ Cross-sectional area of pipe drain, filled with sediment	m^2	L^2
	■ surface area of bottom plate of laboratory permeameter	m^2	L^2
A_k	Coefficient of linear regression model	1	-
a_0	Semi-major ellipse axis or horizontal inside pipe radius of drain	m	L
a_n	Coefficient of multiple linear regression model	1	-
B_k	Coefficient of linear regression model	1	-
b_0	Semi-minor ellipse axis or vertical inside pipe radius of drain	m	L
CD	Cumulative discharge, recorded during a test made with an analogue soil tank model ('permeameter')	m	L
$csc_{n,k}$	Circular region of interest in CT image, used for correction of image artifacts caused by photon scatter	...	...
$ci_{n,k}$	CT-image, approximately corrected for image artifacts, caused by photon scatter	...	...
ci_{PH}	Representative CT-image, corrected for image artifacts, caused by photon scatter	...	...
D	Pore size (diameter) of envelope	m	L
D_{50}	Median pore size of envelope; median size of soil particle	m	L

Symbol	Interpretation	Units	Dimension
D_{60}/D_{10}	Uniformity coefficient of moisture retention curve of envelope	1	-
d	Diameter of pipe drain	m	L
d	Height of drain pipe above impermeable layer	m	L
d (i)	Average pore diameter of class i of the discrete pore size distribution of an envelope	m	L
d (i,j)	Diameter of the pore located at coordinate (i,j) in a vertical cross-section through an envelope	m	L
d_d (i,j)	Diameter of the pore located at coordinate (i,j) in a vertical cross-section through an envelope and potentially drainable at a particular water suction	m	L
d_{da} (i,j)	Diameter of a potentially drainable pore located at coordinate (i,j) in a vertical cross-section through an envelope and connected to the atmosphere through a pathway of empty pores	m	L
d_{dr} (i,j)	Diameter of a potentially drainable pore located at coordinate (i,j) in a vertical cross-section through an envelope and connected to an outlet through a pathway of water-filled pores	m	L
d_{dra} (i,j)	Diameter of a potentially drainable pore located at coordinate (i,j) in a vertical cross-section through an envelope where ddra = dda $\cap$ ddr	m	L
en (x,y)	Mappings of cross sections of envelopes in CT images	...	...

Symbol	Interpretation	Units	Dimension
ep_0	Ellipse, fitted to a cross-section of a drain pipe in a CT image	...	...
ep, ep_n	Elliptical region of interest adjacent to pipe drain	...	...
ESI	Envelope Suitability Index: qualitative indicator in which cumulative discharge through the envelope during an analogue model test (CD) and the pipe clogging rate after completion of such a test (PC) are incorporated	1	-
	$ESI = {}^{10}\log CD - PC/36$		
F_s (d)	Fitted weight fraction of the particle size distribution of a soil at distance d from a soil/envelope interface	1	-
f (D)	Cumulative pore size distribution of envelope, generated from discrete size distribution P (i)	1	-
fr_s (d)	Observed weight fraction of the particle size distribution of a soil at distance d from a soil/envelope interface	1	-
g	Gravitational acceleration (g = 9.813)	$m.s^{-2}$	$L.t^{-2}$
H	Height of sediment layer inside drain pipe	m	L
HI	Heterogeneity indicator	m	L

Symbol	Interpretation	Units	Dimension
H.U.	Hounsfield Unit; used to express the x-ray attenuation rate, μ, of an object. Also referred to as 'CT Number'	1	-
	$$\text{H.U.} = \frac{\mu_{material} - \mu_{water}}{\mu_{water}} * 1000$$		
h	■ Suction of water	m	L
	■ Height of sediment layer inside drain pipe	m	L
	■ Height indicator of sediment layer in drain pipe, used to interpret video images of the interior of a drain pipe	1	-
h_0	Water table height, with respect to drain level, above the drain	m	L
h_m	Water table height, with respect to drain level, midway between drains	m	L
I	Attenuated intensity of monoenergetic x-ray beam	$kg.m^2.s^{-3}$	$M.L^2.T^{-3}$
I_0	Incident intensity of monoenergetic x-ray beam	$kg.m^2.s^{-3}$	$M.L^2.T^{-3}$
K_e	Hydraulic conductivity of envelope	$m.d^{-1}$	$L.t^{-1}$
K_s, k	Hydraulic conductivity of soil	$m.d^{-1}$	$L.t^{-1}$
K_r	Component of hydraulic conductivity in radial direction relative to a drain	$m.d^{-1}$	$L.t^{-1}$

Symbol	Interpretation	Units	Dimension
L	Drain spacing	m	L
LMP	Limiting macroporosity	1	-
MP	Macroporosity of soil regions adjacent to pipe drain	1	-
MP_{ss}	Average macroporosity in subsoil	1	-
MP_{tr}	Average macroporosity in drain trench	1	-
N_i	Shape functions, used in finite element analysis	1	-
n (i)	Relative frequency of pores in class i of the discrete pore size distribution of an envelope	1	-
n_1, n_2	Porosity of a soil	1	-
O_{90}	Effective opening size of envelope pores; corresponds with the average diameter of soil particles of the soil fraction of which 10% falls through the envelope during a sieving test	m	L
P	Pore size distribution of envelope, expressed as a discrete probability density function	1	-
	p(i), i = 1, 2, ..., 20		
p	Groundwater pressure	$kg.m^{-1}.s^{-2}$	$M.L^{-1}.T^{-2}$
p (i,j,k)	X-ray attenuation rate in a volume element or 'voxel', located at coordinate (i,j,k) in a three dimensional (3D) CT image	1	-

Symbol	Interpretation	Units	Dimension
PC	Pipe clogging rate, expressed as a sediment layer height in a 60 mm pipe drain after completion of a test with an analogue sand tank model ('permeameter')	m	L
p_i	Weight fraction of soil fraction with $d \leq d_i$, where d = particle diameter	1	-
Q	Outflow rate from laboratory permeameter	$m^3.d^{-1}$	$L^3.t^{-1}$
q	Outflow rate from drain, recharge rate	$m.d^{-1}$	$L.t^{-1}$
q_l, q	Outflow rate per running metre of drain	$m^2.d^{-1}$	$L^2.t^{-1}$
R	Distance to the centre of a pipe drain	m	L
R_0	Radius of a pipe drain	m	L
r	Radius of a soil pore; radius of a pipe drain	m	L
$ri_{n,k}$	CT-image, selected to be corrected approximately for image artifacts, caused by photon scatter	...	...
ri_{PH}	Representative CT-image, selected to be corrected for image artifacts, caused by photon scatter	...	...
s	■ Surface tension of water	$kg.s^{-2}$	$L.t^{-2}$
	■ Fraction of particle size distribution of a soil	1	-
tep	Geometrically transformed region of interest in transformed CT-image	...	...

Symbol	Interpretation	Units	Dimension
U	Uniformity coefficient (D_{60}/D_{10}) of the particle size distribution of a soil	1	-
v	Volume of region of interest of a sampled core	m^3	L^3
W	Mass of wet sediment, trapped after completion of a flow test ($W \leq 0.52$)	kg	M
W_i	Entrance resistance of pipe drain	$d.m^{-1}$	$T.L^{-1}$
x_n	Predictor variable of multiple linear regression model	1	-
z	Elevation from impermeable layer	m	L
α	Liquid/solid contact angle	1	-
α_i	Entrance resistance factor, expressing resistance to water flow into pipe drain	1	-
ε	Eccentricity of a drain pipe	1	-
γ	Drainage resistance	d	T
θ	Angle required to calculate the height of a sediment layer, h, inside a pipe drain with radius r from the area, A, of the inside pipe segment which is filled with sediment $\left.\begin{array}{l} A = \frac{1}{2}r^2 (\theta - \sin\theta) \\ h = r - r\cos(\theta/2) \end{array}\right\}$	1	-
μ	X-ray attenuation rate	m^{-1}	L^{-1}
ρ	Density of water	$kg.m^{-3}$	$M.L^{-3}$
ϕ	Hydraulic head	m	L

ABOUT THE AUTHOR

Lodewijk Constantijn Paul Marie Stuyt was born in The Hague, The Netherlands on 29 April 1953. After attending secondary school in The Hague and in Nijmegen he acquired the diploma 'HBS B' in 1971. After a three-month stay in Israel in 1972 he began studies at the Agricultural University in Wageningen, The Netherlands. Following a nine month period in 1977 studying Catchment Hydrology at the Institute of Hydrology in Wallingford, U.K., in 1980, he graduated with honours in Hydraulics, Catchment Hydrology and Geology, with Land and Water Use and Mathematics as subsidiaries. Since graduating he has been employed as a research officer at the Institute for Land and Water Management Research (ICW) in Wageningen, now incorporated into the Winand Staring Centre for integrated Land, Soil and Water Research (SC-DLO). He is married and has two sons.

STEREOSCOPIC PLATES

Stereoscopic pictures of wrapped drain sections and structural features of surrounding soils printed stereographically by the anaglyph method

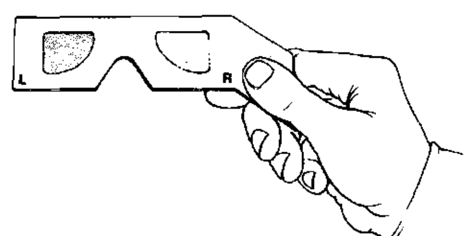

Plate 1. Example of a layered subsoil. Parts of the plexiglass rims of both the sample container and the sample holder of the scanner were cut away by image processing techniques. Experimental field: Uithuizermeeden, envelope material: "Cerex" nonwoven, sample No. U14.

Plate 2. Example of a subsoil with vertically oriented macropores, assumingly developed as a result of plant roots. Experimental field: Valthermond, envelope material: "Typar" nonwoven, sample No. V01.

Plate 3. Image areas containing all voxels with Limiting Macroporosity LMP $\geq$ 34%. Water in a permeable subsurface layer reaches the lower drain area through 2 concentrated conducts which have developed between this layer and the drain. Experimental field: Uithuizermeeden, envelope material: Big 'O' fabric, sample No. U12.

Plate 4. Image areas containing all voxels with Limiting Macroporosity LMP $\geq$ 37%. Subtle banding is evident under the drain. The trench containes some geometrically complex areas. Experimental field: Uithuizermeeden, envelope material: "Cerex" nonwoven, sample No. U14.

Plate 5. Image areas containing all voxels with Limiting Macroporosity LMP $\geq$ 37%. This drain was installed in a soil layer with a relatively high conductivity. Water flow through the trench is restricted at this LMP, possibly due to structural deterioration of the backfill material. Experimental field: Willemstad, envelope material: Polystyrene beads "PS-LDPE", sample No. W06.

Plate 6. Image areas containing all voxels with Limiting Macroporosity LMP $\geq$ 35%. Water enters this drain through a complicated system of soil layers underneath an through one side of the trench. Experimental field: Willemstad, envelope material: "Cerex" nonwoven, sample No. W07.

Plate 7. Image areas containing all voxels with Limiting Macroporosity LMP $\geq$ 41%. Water access to this drain proceeds through a series of parallell vertically oriented macropores. Not all macropores are involved at this LMP, however, see Plate 2. Experimental field: Valthermond, envelope material: "Typar" nonwoven, sample No. V01.

Plate 8. Image areas containing all voxels where the most permeable envelope areas are mapped. The envelope is mainly clogged at the interface area with the trench. Experimental field: Willemstad, envelope material: Peat/Coconut fibre mixture, sample No. W09.

Experimental Field: Valthermond   Envelope: "Typar" Nonwoven

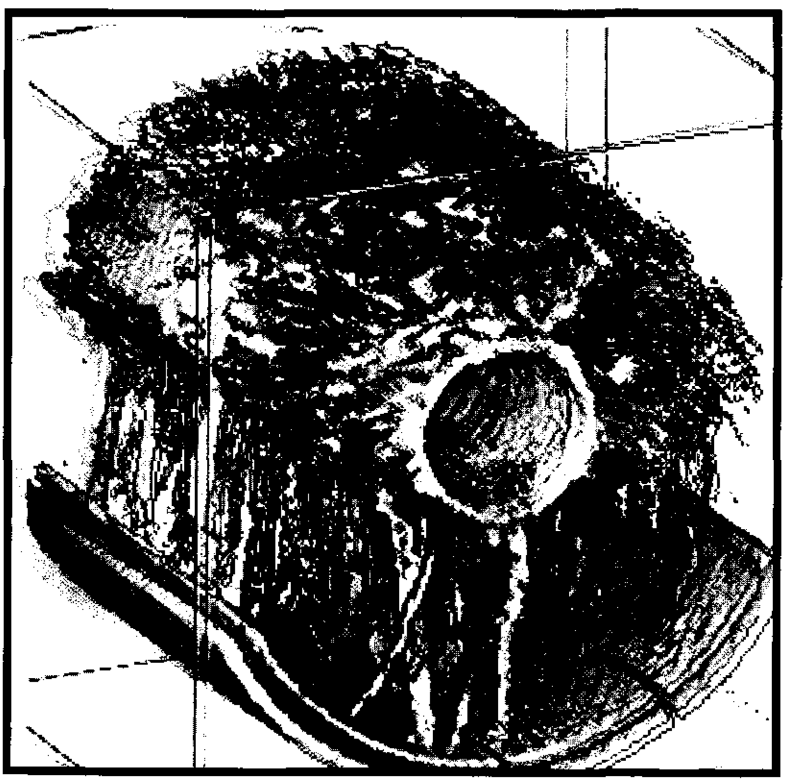

Sample No. V01   Original 3D Data; Macropores Shown

Experimental Field: Uithuizermeeden Envelope: Big 'O' Fabric

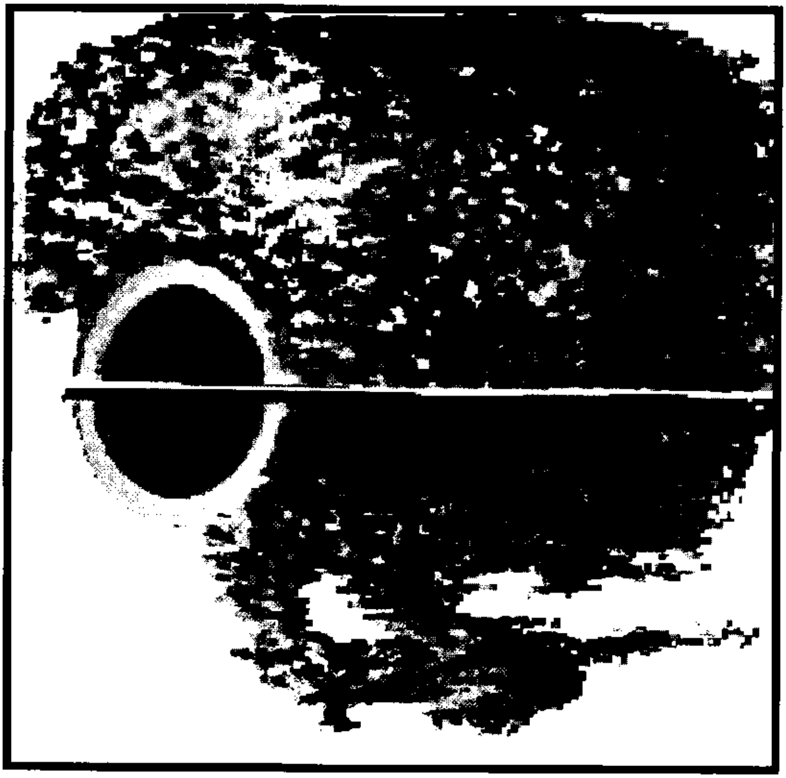

Sample No. U12 Limiting Macroporosity [LMP] = 34

Experimental Field: Uithuizermeeden Envelope: "Cerex" Nonwoven

Sample No. U14 Limiting Macroporosity [LMP] = 37

Experimental Field: Willemstad Envelope: Polystyrene–LDPE

Sample No. W06 Limiting Macroporosity [LMP] = 37

Experimental Field: Willemstad Envelope: "Cerex" Nonwoven

Sample No. W07 Limiting Macroporosity [LMP] = 35

Experimental Field: Valthermond Envelope: "Typar" Nonwoven

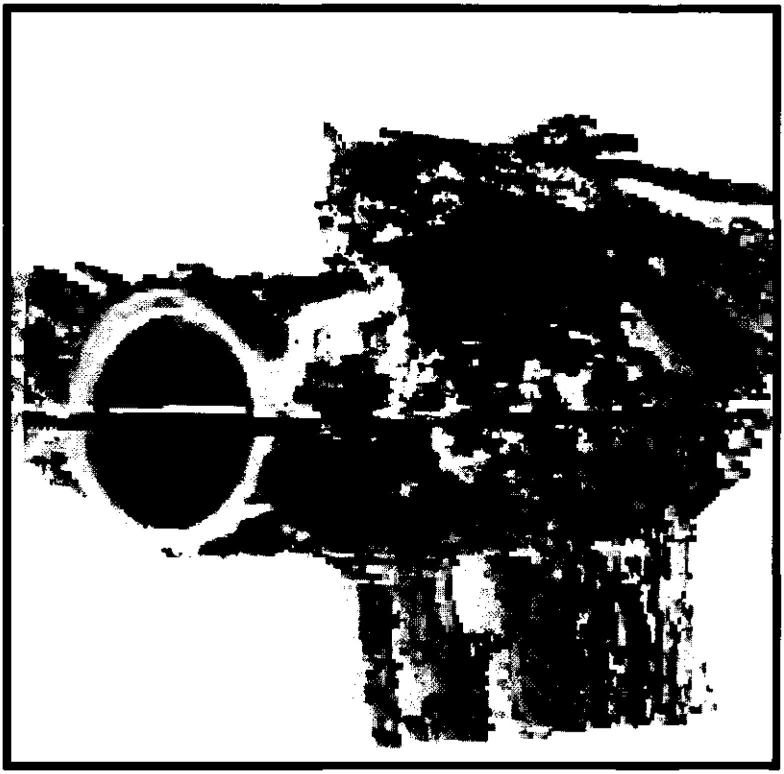

Sample No. V01 Limiting Macroporosity [LMP] = 41

Experimental Field: Willemstad Envelope: Peat/Coconut Fibres

Sample No. W09 Permeable Envelope Areas